

RCA Engineer

Vol. 18 No. 3 Oct. Nov. 1972

Einstein's Theory of Relativity

Tables of Functions

Some Mathematical Methods of Physics Goertzel & Trull

LAKSHAN LUTHER WILKES
APPLIED NUMERICAL METHODS

RAIN AUGUSTIN THEORY:
MACHINES AND LANGUAGES

Modern Mathematics for the Engineer Beckenbach editor \$3.45

THIRD EDITION
Mathematical
McGR

CALCULUS
KLINE

COMMUNICATION, TRANSMISSION,
AND TRANSPORTATION NETWORKS
FRANK FRISCH
ADDISON WESLEY

Feedback Systems
Cruz

Mathematics for Science & Engineering Alger \$2.95

John B. Peatman

The Design of Digital Systems

Toward a computerized society

"The Plan for an Information Society—a National Goal Toward Year 2000"—a recent "white paper" published by a blue-ribbon committee of Japan's Computer Usage Development Institute proposes that Japan move toward "a society that brings about a general flourishing state of human intellectual creativity." Our present industrialized society with its emphasis on material things is seen as necessarily shifting to an information society with emphasis on software, utilizing information and knowledge to advance the essential components of our social system. The committee envisions the reorientation of people from hardware to software with the "establishment of (the) computer mind" as an intermediate target.

The problems are, of course, not unique to Japan. They are brought about by increasing population in urban areas, economic depression, increasing proportion of aged in the population, depletion of natural resources, and so on.

It is not my intent to outline the proposed plan or to evaluate it. However, the requirement is real. Although the pathways we find to influence the direction of our society will undoubtedly vary with the particular area of the world involved and the traditions of the local society, that capability must come, if we are to continue operating. Parts of some of the closer-in elements of such a computerized society are already active programs in RCA. They include community information systems, automated supermarket check-out, automated vehicle control systems, and data communications systems. Other technically achievable aspects of the information society involve health care, computer-aided education, and pollution control. The alternatives are varied and the opportunities are abundant.

It seems clear that whatever course these alternatives take there will be an increasing dependence on software-oriented people and, in turn, on scientists and engineers with a solid understanding of the mathematics on which these software systems will be based. This is, of course, in addition to the applications of mathematics in the traditional engineering and scientific activities with which we have long been familiar. In the long run, I can see no way but up for the significance of "math" both in RCA and in society as a whole.

Howard Rosenthal

Howard Rosenthal
Staff Vice President
Engineering
Research and Engineering
Princeton, N.J.



RCA Engineer Staff

W. O. Hadlock Editor
J. C. Phillips Associate Editor
J. P. Dunn Art Editor
Mrs. Diane Ahearn Editorial Secretary
Mrs. Julianne Clifton Subscriptions

Consulting Editors

D. A. Meyer Technical Publications Adm.,
Electronic Components
C. W. Sall Technical Publications Adm.,
Laboratories
F. J. Strobl Technical Publications Adm.,
Corporate Engineering Services

Editorial Advisory Board

R. M. Cohen Mgr., Quality and Reliability
Assurance, Solid State Div.
F. L. Flemming VP, Engineering, NBC
Television Network
C. C. Foster Mgr., Technical Information
Services, RCA Laboratories
M. G. Gander Manager, Consumer Products
Adm., RCA Service Co.
W. R. Isont Chief Engineer,
Record Division
L. R. Kirkwood Chief Technical Advisor,
Consumer Electronics
C. H. Lane Div. VP, Technical Planning
Electronic Components
H. Rosenthal Staff VP, Engineering
P. Schneider Exec. VP, Leased Facilities
and Engineering,
Global Communications, Inc.
F. W. Widmann Manager, Engineering
Professional Development
Dr. H. J. Wolf Division VP,
Government Engineering

Our Cover

... symbolizes concentration, intuition, and study—all essential to a firm grasp of Mathematics, the language of science and technology and the theme of this issue. Fulvio Oliveto of the Missile and Surface Radar Division appears in the cover photo. **Cover design:** Joan Dunn; **Photo credit:** Ken Kleindienst of Missile and Surface Radar Division

RCA Engineer

A technical journal published by
 RCA Corporate Engineering Services 2-8,
 Camden, N.J.

RCA Engineer articles are indexed
 annually in the April-May Issue and
 in the "Index to RCA Technical Papers."

• To disseminate to RCA engineers technical information of professional value • To publish in an appropriate manner important technical developments at RCA, and the role of the engineer • To serve as a medium of interchange of technical information between various groups at RCA • To create a community of engineering interest within the company by stressing the interrelated nature of all technical contributions • To help publicize engineering

achievements in a manner that will promote the interests and reputation of RCA in the engineering field • To provide a convenient means by which the RCA engineer may review his professional work before associates and engineering management • To announce outstanding and unusual achievements of RCA engineers in a manner most likely to enhance their prestige and professional status.

Contents

Editorial input	Technology and the '72 campaign	2
Engineer and the Corporation	Test automation in G&CS manufacturing	F. Pfifferling 5
Division Profile	The Hertz Corporation—a profile	J. C. Phillips 8
Mathematics	Mathematics in communications systems research	Dr. L. Schiff 14
	Methodology and techniques of operations research	Dr. A. K. Nigam 20
	Evaluation of microcircuit packaging concepts using digital computer simulation	R. M. Engler 25
	Solution of differential and integral equations with Walsh functions	M. S. Corrington 28
	Dynamic characteristics of several algorithms for real-time digital processing	R. C. Blanchard 34
	Image enhancement techniques	D. B. Gennery 38
	Digital correlator with partial summation and received data foldover	H. A. Ulrich 45
	NMODES computer program	R. C. Bauder C. H. McKee 48
	Computer-designed microwave-integrated-circuit program	W. L. Bailey R. E. Kleppinger 50
	RCA-DYNA: a large structural dynamics computer program	Dr. R. J. Pschunder 54
	Bayesian statistics	F. E. Oliveto 57
Other papers	Apollo 15 and 16 ground commanded television assembly	B. M. Soltoff 62
	Thermal steady-state spacecraft simulation	R. A. Lauer M. K. Theus 68
	Simulation of nuclear blast effects on communication cables	E. Van Keuren 72
	Propulsion for geostationary spacecraft	Y. Brill R. Lake J. Mavrogenis 75
	High-performance television receiver experiment	D. H. Pritchard A. C. Schroeder W. G. Gibson 80
Engineering and Research Notes	Scribing and dicing of processed silicon-on-sapphire wafers	R. L. Loper 85
	Magnetic tweezers	W. A. Mülle 85
	The meaning of crosscorrelation functions	M. S. Corrington 86
Departments	Pen and Podium	87
	Dates and Deadlines	89
	Patents	91
	News and Highlights	92

technology and the '72 campaign

Among the many issues being discussed in the 1972 Presidential campaign, the reorientation of national resources toward the solution of our more pressing civil problems is of particular interest to the engineering community. Recently, twelve questions on related technical issues were posed to President Nixon and Senator McGovern by twelve professional societies representing 460,000 members of the Nation's engineering community. The questions and answers are given below, in their entirety.

Questions and answers

In recent years the nation has seen an emerging consensus on the need to reorient national priorities and reallocate national resources toward solving a number of pressing civil problems. The engineering societies believe their memberships are uniquely qualified to play an important role in this effort. The Federal Government, which has mobilized technology so effectively in the past, should act as a catalyst to mobilize available engineering manpower on a priority basis to meet today's crises. Accordingly, the societies address a number of questions intended to clarify the candidates' positions and to focus attention on how best to solve these pressing problems.

If you are elected President of the United States:

Assuming that you will support the early expansion of Federal Government engineering programs to stimulate the attack on the critical problems of health care, poverty, public safety, pollution, unemployment, productivity, international trade, housing, education, transportation, nutrition, communications, and energy resources, how would you proceed to implement programs and what specific vehicles would you employ to achieve the goals?

Nixon: Coherent R&D programs resulting from careful policy studies and Presidential decisions have already been formulated with respect to transportation, education, energy, health care delivery, environmental control, and other areas of domestic concern. These have been outlined in the President's Energy Message of June 4, 1971; his Health Messages of February 18, 1971 and March 2, 1972; and his Science and Technology Message of March 16, 1972. Many, if not all, have important engineering components. The overall direction for these efforts emanates from the Executive Office of the President. The actual research, development, testing and evaluation, however, is being carried out in individual or joint efforts by the appropriate government agencies; for example, joint programs in transportation between NASA and the Department of Transportation, programs in environmental technology and measurement carried out jointly by AEC and NSF, and programs

Editor's note: *Regretably, this issue will reach our readers after election day. However, the questions and answers included in these pages will still be valuable reading, since they clarify the position of the next President with regard to technology and its use in solving some major civil problems.*

in energy by AEC and the Department of the Interior. When the President's reorganization plan is implemented, it will provide an improved organizational structure for these civilian sector efforts thus leading to expanded engineering programs for the solution of national problems. While awaiting the passage of the reorganization proposals, the Administration has, since 1969, increased R&D for civilian needs by 65%—to \$5.4 billion. And for FY 1973 alone, the Administration asked Congress for the following increases:

- 47% more for fast, safe and pollution-free transportation
- 22% more for abundant electrical power without pollution
- 39% more educational R&D
- 46% more for reduction of loss of life and property from natural disasters
- 32% more for studies on the health effects of pollution
- 37% more for R&D on urban problems

McGovern: Except for transitional problems, these vehicles already exist in present governmental agencies. However, the funding authority approved by the Nixon Administration has been desperately thin. As President, I will work with America's technical community to develop new programs aimed at eradicating many of the social ills enumerated in your question. Indeed, I was sorry that a meeting with America's technical community could not have been scheduled as I feel such a dialogue could serve as the beginning of a cooperative effort to solve some of these pressing domestic problems.

The transition period will be greatly aided by passage of S.32, the Kennedy-McGovern conversion bill. This legislation, supported by most major American engineering societies, yet strongly opposed by the Nixon Administration, will provide 41,000 jobs for highly skilled scientists and engineers. This, in turn, could well mean 450,000 jobs on civilian production lines, and an opportunity to respond to America's domestic needs. Moreover, this legislation establishes a Civil Science Administration designed to concentrate America's scientific and engineering genius in the pursuit of domestic betterment. If elected, I will urge massive federal spending through this Administration in an effort to make America a better place for all of us to live.

To what extent will you support a national policy in which engineering concepts, judgments, and analyses will be used to obtain optimum results from the expenditures of public funds to provide the environment, transportation, water, structures, power and communications to meet the needs of people and nature?

Nixon: The use of engineering concepts, judgments, and analyses for policy making and program planning is already an important part of government. I expect to see these techniques more widely used as models are refined and more representative data are developed from current programs. Engineering concepts are already becoming increasingly vital as government-wide decision-making becomes more analytically-oriented.

McGovern: To obtain optimum results from expenditure of public funds requires a more refined consideration of costs and benefits than has been the rule under the Nixon Administration. Many of the disbenefits, e.g., in the form of pollution, that heretofore have been neglected in consideration of public and private projects must now be included in cost benefit analyses. Engineers, particularly those concerned with engineering economies, will be needed to further such pursuits. And I will insist that they operate not only at the federal level in deciding on resource allocation, but at the state and local level and in industry, in documenting costs and benefits of projects for which federal assistance is sought.

To what extent will you support the continued allocation of funds to the problems of our civil society and economy at an increasing percentage of the GNP until an adequate level is reached?

Nixon: Levels of funding hinge upon program content and scheduling. Because our major capabilities in science and technology are too valuable a resource to be wasted, it is imperative to match technical capabilities with rational funding levels which carry projects ahead on a sound engineering basis. The Administration's intentions are exemplified by the substantially increased funding in the civilian sector. Spending for these programs has risen from 37% to 45% of the budget, significantly more than the 32% spent for defense.

McGovern: Presently, the United States invests only 1.1% of its Gross National Product on research and development directed toward economic growth. In West Germany and Japan, this percentage is over 2.2%. Moreover, our export of technology-intensive products is only 50% greater than our import. In 1960, it was three times as great.

Under legislation I have cosponsored with Senator Kennedy—the National Science Policy and Priorities Act—the Federal Government's commitment to civilian R&D will increase as a proportion of our GNP. Similarly, this legislation—presently opposed by the Nixon Administration—calls for parity between military and civilian R&D, and an immediate investment of \$1.025 billion for new priority civilian projects—designing mass transit systems, cleaner and quieter jet engines, and new pollution abatement systems, among many others.

If elected, I shall call for an ever increasing federal commitment to new priority research and development directed toward domestic betterment. In this way, America will finally begin to use its scientific and engineering talent on domestic problems, providing greater economic security for our technical community and a better life for us all.

How will you proceed to support authoritative coordination and guidance of the government's programs to apply advanced technology to these critical civil problems, and by what methods will you insure an

authoritative approach to execute such coordination?

Nixon: The reorientation of the R&D enterprise is being guided by the executive branch through the mechanisms of the Office of Science and Technology, the Office of Management and Budget and other appropriate organs. Its progress is being closely monitored, encouraged and catalyzed. There have been a number of Administration initiatives in specific fields—energy, health, international cooperation, Federal-State relations and others—and the Office of Science and Technology is coordinating them. The overall policies for science and technology were elaborated in the first Science and Technology Message sent to Congress last March.

McGovern: Existing institutions must be given more authority to work with America's technical community in solving domestic problems. For example, the Office of Management and Budget, with direct day-to-day links with President Nixon, so emasculated the OST's New Technological Opportunities Program that it was left with little more than administrative cost funding. When originally proposed the program had grand plans to spend between \$3 and \$6 billion on new priority technology. However, the President, in connection with the OMB, cut the program's budget to a mere \$40 million. A McGovern Administration will guarantee greater funding to these programs, while consulting directly with our technical community in efforts to advance the best possible programs and achieve the best possible results.

For example, I am fully in favor of establishing an Office of Technology Assessment under the guidance of Congress. Such an office—similar to the GAO, yet operating in technical areas—would have overall responsibility to assess each new technical program with an eye toward cost efficiency and effectiveness, and domestic betterment. Thus, we can avoid the boondoggles that have so plagued technical programs in the military sector while providing technical advancement consistent with domestic progress.

What problems do you foresee in supporting continued appropriations to the "mission oriented" departments and agencies to conduct their R&D programs within their primary missions without reduction by reason of funds accorded to a civil science and technology agency?

Nixon: The Administration does not see direct trade-offs among civil, military, and space R&D activities. The continued support of R&D in any agency depends upon the technical soundness of the programs proposed and upon the national needs addressed. Definitions of these needs and programs will continue to provide the criteria for funding civilian, military, and space activities.

McGovern: Past results and achievements of "mission oriented" agencies have demonstrated the great potential of concentrating highly skilled men and women, the systems approach, and fed-

eral assistance behind one goal. The results of such programs provide demonstrable evidence of the manner in which science can help mankind. In turn, these successes have led to greater and greater public support for additional "mission oriented" programs. A McGovern Administration will continue to fund such "mission oriented" agencies, changing the appointed missions of some, while continuing to fund other new priority civilian technology programs. For example, the Civil Science Administration should accept the mission of improving our domestic environment, in the same way that NASA accepted and achieved the goal of placing a man on the moon. Past success should drive us on to greater future success, using the same methods and employing much the same type of expertise.

What specific plans do you have for funding the application of known technology from nationally supported R&D programs to the state and local levels?

Nixon: There is a government-wide effort now underway under the leadership of the Office of Science and Technology to find ways and means of transferring the results of Federal R&D to State and local governments more expeditiously and effectively. The Federal Government is to identify ways to determine the States' needs, to improve their access to new technology and to find ways of aggregating State and local markets. As these avenues develop, they will supplement many existing programs in mission agencies such as NASA, Transportation, HUD and other technology-based organs of government.

The \$5.6 billion in general revenue sharing funds now being sought by the Administration would supplement present Federal R&D funding for State and local purposes and the \$11 billion being asked in the President's special revenue sharing request would help even more.

The entire effort needs assistance from the science and engineering community, particularly in the development of new beneficial partnerships between universities, industries and government, and in helping State and local governments expand their appreciation of the potential of R&D for working out problems.

McGovern: In most instances, civilian research and development should be operated on the national level—this because few domestic problems are regional in nature. However, most R&D applications are regional, relating to the varying needs of particular geographical areas. Thus, highly qualified individuals on the local level must administer the application of national R&D programs, if these programs are to be effective and cost efficient.

A McGovern Administration would reestablish the defunct State Technical Services Program to assist state and local governments in applying new civilian technology projects to their respective areas. These regional offices will function much like the Agricultural Extension program, providing local scientists and

engineers to assist in the application of new technologies, in the same way as federally supported farming experts provide information and assistance to local farmers.

I would also urge reconstruction of an Experimental Technology Incentive Program with broader funding to support new innovations in the area of science and engineering. This program could work with the Civil Science Administration and the local State services program in applying new civilian technology to new civilian priorities.

How would you propose to assure the appointment of qualified engineers to fill high level federal executive and technical positions in the Executive Branch of the government when such positions can be best served by persons able to draw upon knowledge, training and experience acquired in engineering?

Nixon: Each agency of government involved with major efforts in science and technology already has technically qualified personnel in responsible administrative positions, usually at the assistant secretary level or its equivalent. To maintain a competent force of high caliber professionals, executive recruiting is carried out by each individual agency and also by the White House. Nominations of technically qualified people, and engineers in particular, come from the Office of Science and Technology, the high-technology agencies and other sources. OST sometimes solicits suggestions from the community-at-large and from organizations such as professional societies.

McGovern: I will work closely with America's scientific and engineering community in establishing new national priorities, applying new technologies to these priorities, and placing the most capable personnel in the right technological positions. For example, I would consult with the National Academy of Sciences and the National Academy of Engineering in selecting individual scientists and engineers for selected positions of responsibility. Moreover, the various technical societies could be of great help in outlining both new priority technologies and persons capable of applying these technologies to ever growing domestic problems. Industrial organizations, colleges and universities will also be consulted in finding the right person for the right position.

Unfortunately, the Nixon Administration has not made effective use of highly skilled scientists and engineers in top Administration positions. I would request that selected industries, universities and organizations allow qualified individuals to take extended leaves of absence from their posts to serve in a McGovern Administration. Drawing on the best that America's technical community has to offer will further our technological progress, advance our new priorities, and involve many innovative persons heretofore excluded from the main stream of America's science and engineering policies.

How will you support the orderly, progressive transition to new national priorities in order to minimize manpower dislocation and unemployment and to provide opportunities for retraining?

Nixon: Perhaps the most important aspect of the transition to new priorities is the creation of new jobs. The Administration's economic and budget policies which were designed to stimulate the economy are now paying off. The number of persons employed nationally has risen by 2.6 million in the last year. This has been carried out through increasing R&D budgets in domestic areas and Federally financed special activities by self-help groups and industry representatives. Some 42,000 unemployed engineers and scientists have registered under the Technical Manpower Reemployment Program and 17,000 of these have been reemployed.

McGovern: The problems of dislocation and retraining are best solved by making new opportunities and jobs available. Versatile engineers will adapt to new civilian technologies in the same way as they did to military and space technologies. Moreover, so many engineers receive on-the-job training that dislocations, once new opportunities are established, will be minimal and short lived. Again, S.32 best approaches the transition problem by providing new civilian opportunities before cutbacks in military and space programs take place. Thus we can have immediate job openings for those displaced by military cutbacks. If the Nixon Administration retracts its opposition to this legislation, the United States can finally begin an orderly, smooth conversion from military to civilian priorities. Unfortunately, the last few weeks have seen the intensity of their attacks on S.32 increase rather than diminish.

How would you propose to mobilize and maintain a balance of engineering manpower to achieve the goals of solving our critical civil problems?

Studies of our national requirements for the coming decade already indicate there will be a shortage of engineers in the late 1970's. Because engineering enrollments are continually monitored closely by NSF and the Executive Office of the President, actions within the purview of the government can be taken to help stabilize the supply and demand situation as it is affected by the government's own needs or responsive to its incentives. The National Science Foundation and the Engineering Manpower Commission help provide the data essential to overall management in a free job market economy.

McGovern: If we are to maintain a balance of engineering manpower in years to come, the United States must make effective long range plans for federal spending and manpower needs. Extended lead time must also be given to major industries so that they may best judge their ability to respond to government deadlines and contract require-

ments. These McGovern policies will further our goal of estimating accurately future engineering needs, minimizing fluctuations in demand, and adjusting the level of federal support for universities to match the output with long range projected demands.

How will you provide for active United States participation in international standardization in order to preserve the nation's competitive position in foreign trade?

Nixon: The National Bureau of Standards, in cooperation with international standards organizations and U.S. industry, has actively participated on behalf of the U.S. in international standardization efforts and these activities will continue. However, the most important recent development is the Administration's metric bill. Congressional action on this bill at the present session will go a long way toward making American products more competitive on the world markets.

McGovern: The United States had already established a national policy of converting to the Metric System during the next ten years. I supported this policy and would work to achieve it during my Administration. Similarly, I will urge the Federal Government to convert to the metric system as soon as possible—serving as a guide to private industry. Such a policy is imperative if we are to more fully compete with other technological nations, reduce our balance of trade deficit by making American tools marketable in foreign ports, and achieve technological superiority in scientific and engineering areas. I fully support international standardization as a goal worthy of our increased effort.

What Legislative and Executive actions are needed, and will be promoted by you, to insure that engineers do not forfeit their pension rights as they move from job to job in the public interest and insure early vesting and portability and otherwise protect pension rights, and what will you do to provide for pension protection by insuring adequate funding and insurance as well as proper disclosure and fiduciary standards?

Nixon: The problem of pension rights and adequate funding and insurance protection for pension funds is one which goes beyond the engineering profession. Federal regulations on pension funds to protect the pensioners are constantly being reviewed and actions to provide equity for pensioners are under active and sympathetic consideration. The Administration recognizes the need for the portability of pensions but is also aware of the extraordinary complexity of instituting the concept. Last December, the President called for a joint study of the problem by the Department of Labor and the Treasury. They are to report their findings in December (1972). The President has also proposed the following 4-point pension reform program:

1. Individual employees could set up their own tax favored retirement plans or make contributions to group plans;

2. Employer group plans would have to include a "rule of 50" vesting standard;

3. Self-employed persons would be permitted increased tax-deductible contributions to retirement plans covering themselves and their employees;

4. Standards of fiduciary responsibility would be imposed on those in charge of pension and welfare plans.

McGovern: The insecurity of pensions has long been a matter of deep concern to the working people of America. It has made old age a time of poverty and lost hopes for millions of Americans. Yet, except for modest regulation of union pension funds, it is an area which the Nixon Administration has virtually ignored. Indeed, pension reform may be dead for this year as a result of stringent Nixon Administration opposition to the Pension Reform Act presently before Congress.

Some time ago, I proposed the following National Pension Reform Policy, which, if elected, I would pursue diligently in the Congress:

1. Company pension funds should be replaced by a system in which employees would have the right to choose a government regulated and insured fund in which to invest for retirement income—to guarantee sound, responsible financial management and to provide immediate vesting of pension rights.

2. Employees should have the right to make additional voluntary contributions to their pension accounts.

3. Pension benefits should be exempted from wage controls.

4. Requirements for minimum pension contributions should be included in future minimum wage legislation, to extend private pension opportunities to all workers.

What will you do to support the concept that employed and self-employed engineers should be enabled to more responsibly provide for their own futures by making adequate tax deferred contributions to a Keogh-type pension plan?

Nixon: Self-employed people already can, with the agreement of the Internal Revenue Service, contribute to their own future pensions with tax deductions. These plans have been in effect for several years now and are constantly being reviewed to improve their effectiveness.

McGovern: I fully support the Keogh-type pension plan for employed persons, as well as for self-employed individuals.

Under the Keogh plan, a worker could invest up to \$7,500 per year in a private pension fund. This plan is fully consistent with my pension reform proposal—allowing workers to make additional payments to a pension plan of their choice in addition to the contributions made by their employers. A bill supported by the Nixon Administration would limit this additional yearly investment to \$1,500.

If we are to fully provide for the economic security and personal dignity of America's retired persons, we must provide pension plans which allow them to invest such additional funds. This policy, coupled with immediate vesting and governmental guarantees of traditional pension plans, will provide the security our retired workers so urgently require.

Engineer and the Corporation

Test automation in G&CS manufacturing

F. Pfifferling

A planned program of test automation in the manufacturing plants of Government and Commercial Systems (G&CS) has resulted in substantial savings in manufacturing cost during the last several years. Multi-purpose automatic test equipments are installed and operating in the G&CS plants in Camden, Moorestown, and Hightstown, N.J., as well as in the Van Nuys, Cal., Burlington, Mass., and Meadow Lands, Pa. facilities. This paper describes the nature of available equipment, provides examples of joint Engineering/Manufacturing efforts to design low cost products, and gives an indication of savings to date.

DURING THE LAST SEVERAL YEARS, G&CS divisional representatives from design engineering and manufacturing test engineering have been meeting several times annually to plan and implement a coordinated test-automation program in the G&CS manufacturing plants. As a result, over 100,000 printed-circuit boards, sub-assemblies, and black boxes have been automatically tested in the G&CS locations. Existing equipment has proved to be cost effective even on custom low quantity engineering designs and provides a competitive edge in new business proposals.

Test automation has been applied in the manufacture of the following G&CS products:

- Systems support equipment
- Radar equipment
- Communications receivers and transmitters
- Video tape recorders
- Video displays
- Spacecraft hardware
- Commercial aviation
- Mobile radios
- Broadcast transmitters
- Message switching systems

Test capability is broad and includes the following types of electronics:

- Digital logic
- HF and UHF subassemblies
- Hybrids
- Wire-wrapped backplanes
- Cable assemblies
- Analog circuits
- Video amplifiers
- Frequency synthesizers
- MSI components
- Intermediate frequency amplifiers
- Microwave antenna phase shifters

Factors in automating manufacturing test

The capital acquisition of automatic test

equipment, as well as other capital acquisitions in RCA, requires a supportive savings analysis which is reviewed by management in accordance with corporate procedures. A cost comparison is made between manual test stations and the proposed automated equipment. Savings in test labor, processing cost, test equipment cost, and maintenance and calibration are calculated for each case. However, a decision as to whether to acquire a particular automatic test system requires the additional

Fred Pfifferling, Mgr.
Staff Manufacturing
Government and Commercial Systems
Moorestown, N.J.

received the BEE from CCNY in 1951 and the MSEE from Drexel in 1957. Mr. Pfifferling has been active as a specialist in development of test equipment and techniques for more than ten years. He has led several engineering groups in the design of computer-controlled testers for the military. His designs include launch and checkout equipment for Dynasoar, radar-test simulators for the F-102 aircraft, Atlas-missile checkout equipment, automatic depot test equipment for the Army, and test equipment for the Lunar Orbiter Spacecraft. He was a member of the Engineering Team that developed the multi-purpose test equipment and digital evaluation equipment used by the Army. In recent years Mr. Pfifferling has been directing his attention to developing cost-effective testing on the production line. He is presently responsible for test automation in all Government and Commercial Systems Divisions. He served as Professor of Electrical Engineering at the Drexel University Evening College from 1958 to 1956. Mr. Pfifferling is a member of Tau Beta Pi, Eta Kappa Nu and IEEE.

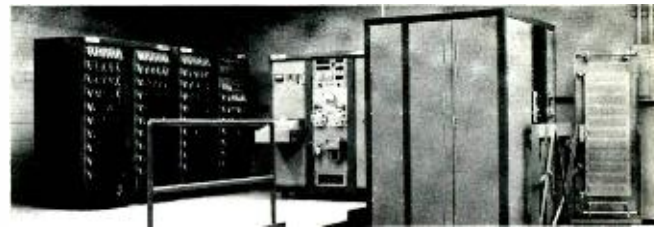


Fig. 1—Automatic continuity testing of an AEGIS backplane

consideration of the following factors which could impact the savings advantages calculated by the above method:

- 1) The automatic test equipment must be selected to be multi-purpose and have a useful life span in a changing technology. This requires a critical technical analysis of the electrical characteristics of the equipment to be tested, an examination of expected changes in the electronics industry, and a look at future business trends in the division acquiring the equipment.
- 2) The automated test equipment must help to lower bid prices on new business solicitations. Thus, a conference with the Marketing Department is usually required when determining automation needs.
- 3) In some instances, the technology of the delivered product rules out the practicality of manual test. Examples of these are antenna phase shifters and densely-packed wire-wrapped backplanes.
- 4) The cost-saving elements are not always quantifiable. For example, it is difficult to determine the effect on product rework cost when instant identification of a design problem, supported by reliable test data from an automatic test system, is made available for management action.
- 5) In spite of all that has been said about automation, successful implementation cannot succeed without the people using it wanting it to succeed. It is sometimes prudent to compromise on the system configuration if the compromise will result in a positive and enthusiastic user attitude.
- 6) Test automation improves the technical expertise of the Manufacturing Engineer and precipitates a closer relationship with the design engineer. Product cost reduction is substantial when this is done effectively.

Existing automatic test equipment

A broad range of automatic test capability exists in the G&CS divisions. The test equipment consists of

- Automatic continuity testers for testing cable harnesses and wire wrapped backplanes.
- In-circuit component verification testers for checking assembly quality of printed circuit boards.
- Logic testers for functional testing of digital equipment.
- Analog testers for dynamic waveform testing, and
- RF and microwave testers for testing communications and radar systems.

Reprint RE-18 3-2
Final manuscript received March 21, 1972

Table I—Automatic test equipment in the G&CS manufacturing locations.

Division	Continuity testers	In-circuit component verification testers	Logic testers	Analog testers	RF testers	Microwave testers
Astro-Electronics Hightstown, N.J.	X	—	X	X	—	—
Aerospace Systems Burlington, Mass.	X	—	X	X	—	—
Communications Systems Camden, N.J.	X	X	X	X	X	—
Meadow Lands, Pa.	X	X	—	—	X	—
Electromagnetic and Aviation Systems Van Nuys, Calif.	X	X	X	X	—	—
Missile and Surface Radar Moorestown, N.J.	X	—	X	X	—	X

Notes:

The RF Tester at CSD, Meadow Lands, Pa., will be available in December, 1972.
The Analog Tester at ASD, Burlington, Mass., is tied into Spectra 70/45 in time-shared mode.
X Tester installed

The equipment complement consists of a combination of in-house developments as well as purchased systems and is programmed with either paper tape or by means of a computer. Table I lists the test capability in each of the G&CS locations.

Automatic continuity testers

These purchased paper-tape-controlled testers perform continuity and resistance measurements and are used to test cable assemblies and wire-wrapped backplanes. All G&CS divisions have this equipment with the most sophisticated version existing in Camden. Fig. 1 shows the Camden system connected to a 20,000-point (0.1-in. spacing) AEGIS backplane by means of an in-house developed fixture. Measurements are performed at the rate of 1,000



Fig. 2 (above)—In-circuit testing of a commercial aviation subassembly at Electromagnetic and Aviation Systems Division.

Fig. 3 (below)—Broadcast transmitter being tested with a locator unit at Communications Systems Division, Meadow Lands, Pa.



tests/minute, and hard-copy printout of failures is provided to facilitate repair.

In-circuit component verification testers

Missing components, orientation errors and shorted solder traces are common manufacturing errors found in assembled printed-circuit boards. This problem is industry wide and is particularly severe on densely crowded boards. In-circuit component verification testers are used in several of our divisions to identify these errors. The equipment performs guarded in-circuit measurements of resistance, capacitance, inductance, and semiconductor characteristics at the rate of 50 measurements/minute and is paper-tape controlled. Contact is made to the trace side of the printed boards by means of spring-loaded pins in a pneumatically operated fixture. Fig. 2 shows a subassembly from the Commercial Aviation product line being tested in Van Nuys, and Fig. 3 shows a broadcast transmitter being tested in our Meadow Lands plant.

Logic testers

Logic testers perform functional GO/NO-GO (truth table) testing of digital arrays, logic boards, and digital black boxes. These functional testers, acquired for each of the G&CS divisions during the past four years, are tailored to accommodate each of the divisional product lines. The most recent installation (Fig. 4) exists at AED's Space Center in Princeton, where it performs 5-MHz functional testing as well as simultaneous analog testing of spacecraft components. To aid in diagnostics and programming, several divisions are using AGAT (automatic generation of array testing), a software program which permits the automatic generation of test and diagnostic tapes directly from the logic diagram.



Fig. 4—Manufacturing automated test system (MATS) used for testing spacecraft components at Astro-Electronics Division.

Analog testers

Automatic analog testers are used to perform measurements of waveform timing and low-frequency analog transfer functions. These testers usually consist of waveform generators, audio oscillators, and an automatic sampling oscilloscope. They are primarily used to check analog modules for digital systems. A unique installation exists in Aerospace Systems Division, Burlington, where the analog tester is tied into the Plant Spectra 70/45 business computer in the time-shared mode. This tie-in takes direct advantage of the large Spectra memory capacity with negligible increase in computer running time. Fig. 5 shows the ASD analog test system.

RF testers

RF testers perform functional tests of communications receivers and transmitters and their components. An automatic communications equipment tester (ACET), see Fig. 6, capable of testing HF, VHF and UHF equipment is being used to test AN/ARC-142 radios and other components at Communications Systems Division in Camden. The test system uses a test engineering oriented language called TESTTRAN, and is controlled by an RCA 1600 Computer.

A time-shared multi-station RF test system capable of testing large quantities of beam-lead hybrid assemblies is being procured for the Meadow Lands plant. The system, which is to be operational in 1972, has the unique capability of performing automatic (no operator intervention) troubleshooting almost to the piece part, as well as GO/NO-GO production testing.

Microwave testers

A purchased computer test system is used by the Missile and Surface Radar Division for automatic phase and amplitude measurements of microwave

Fig. 5—Analog tester at Aerospace Systems Division.



devices, including h , y , z , and parameters as well as VSWR, loss, and impedance. The equipment is self-calibrating, with errors corrected by means of the computer. The Moorestown installation is used for rapid testing of AEGIS antenna phase shifters (Fig. 7) and for storage and analyses of measured data.

Designing for manufacturing-test automation

Properly implemented automatic testing realizes substantial cost savings on existing products. However, to take maximum advantage of cost reductions it is the responsibility of the design engineer to develop products compatible with the existing test automation within his plant. This requires a close working partnership between the design engineer and his manufacturing counterpart. Several examples exist in Government and Commercial Systems where design engineers have accepted this responsibility and designed products for automatic test. In CSD Camden, for example, design engineers have developed low cost HF and UHF radio equipment by incorporating the following features in their designs:

- 1) Modules and sub-assemblies have been divided into functional entities to reduce the need for simulation in the test equipment.
- 2) Additional wire traces were included on printed-circuit boards to permit installation of an edge connector. Thus access is permitted to the intermediate circuit points for automatic troubleshooting and fault isolation.
- 3) Standard component placement patterns on printed boards have been rigidly maintained to reduce cost of fixturing.
- 4) Test procedures have been jointly developed to make use of existing test equipment. Standardized test procedures have been developed which can be reused on future jobs with similar equipment.
- 5) Methods for automatic compiling and analysis of manufacturing test data have been developed. This permits almost instantaneous accurate feedback of design

Table II—Test plan for a UHF radio.

Tester	Units Tested	
DIMCO	Receiver/transmitter chassis main-frame	Harness assembly
HATH	Regulator/control, Regulator/filter, Power supply chassis.	Power supply boards, Audio amplifier
LOGIC	Decoder boards, Bit-stream-generator boards	Divide-by-N boards, Memory boards
VEE	Self-test boards, Frequency-control boards, IF/audio boards, Exciter/amplifier, Power supply	VCO & divide by K boards, Guard receiver, FM/FSK modulator, Transmitter, Receiver/transmitter

deficiencies to the design engineer for corrective action.

- 6) A test connector has been included to permit automatic test and troubleshooting at the black-box level as well as at the sub-module level.
- 7) Jointly developed test plans have been implemented for machine testing of the entire product.

Fig. 8 shows a typical radio and its sub-assemblies; Table II is a test plan for machine testing of a UHF radio; and Fig. 9 shows a printed board and the traces designed in for the edge connector.

Cost reductions

The test-speed advantage of automatic testing versus manual testing ranges between 5 and 50 to one. In addition to test time savings, even more substantial gains have been realized in reduced requirements for special test equipment, test maintenance and calibration, and test procedure preparation.

Future plans

The last several years has produced significant advances in the state of the art of automatic test-equipment hardware. The future will require corresponding development of compatible software systems. Software routines for fault diagnosis to reduce troubleshooting time will be developed. Automatic testing, probing, and diagnosis of hybrid modules will be implemented. Progress will be made in the acquisition of data from remote terminals to monitor production flow and compile defect data, and automatic test systems will be integrated into broader manufacturing systems to control processes and product quality in real time.

Conclusion

Automatic testing has proven to be cost effective in the factory. A potential for even greater cost reduction exists and remains to be exercised by you—the design engineer. By joining in an active partnership with your manufacturing counterpart, and guided by the requirements of our customers we can together build a stronger Corporation.

References

1. Hellman, H., "Automatic generation of tests for combinatorial logic," RCA reprint RE-14-5-25.
2. McAleer, H.J., "A look at automatic testing," *IEEE Spectrum* Vol. 8, No. 5 (May 1971)
3. Dale, B.V., "What automatic testing means to the engineers," RCA reprint RE-14-2-14.
4. Pfifferling, F., and Williamson, D.H., "Automatic communications equipment tester," RCA reprint RE-17-5-19.

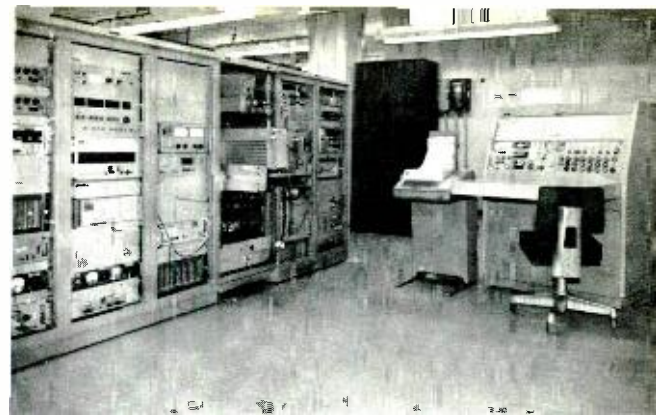


Fig. 6—ACET system at Communications Systems Division in Camden testing an AN/ARC 142 Transceiver.

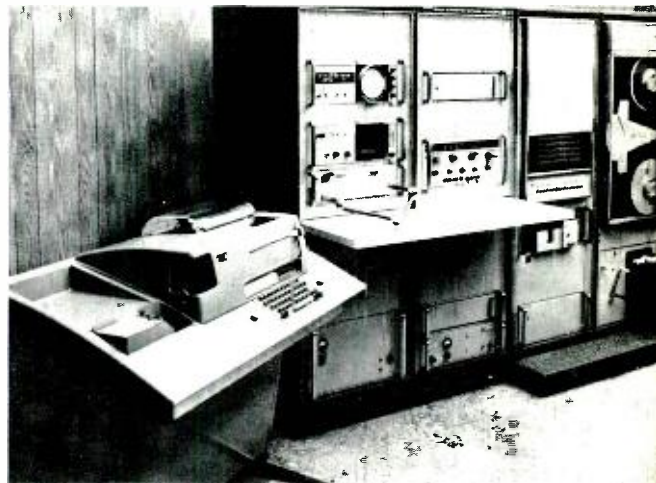


Fig. 7—Computer-controlled microwave test system used to test AEGIS antenna phase shifters at Moorestown.

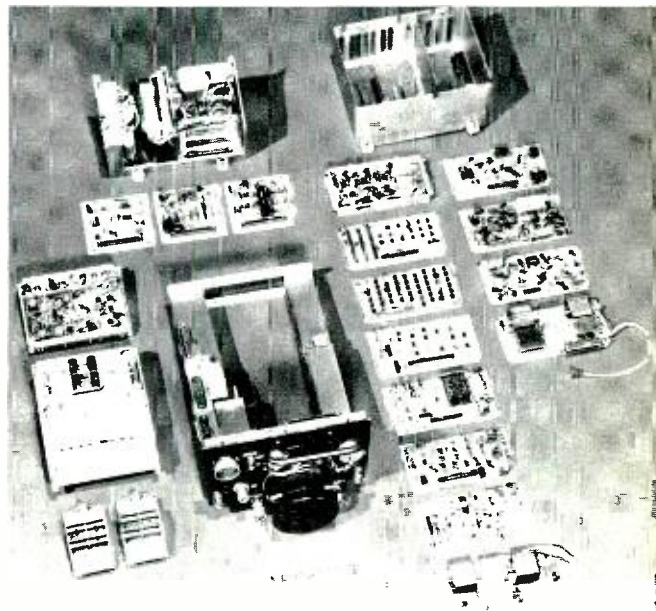
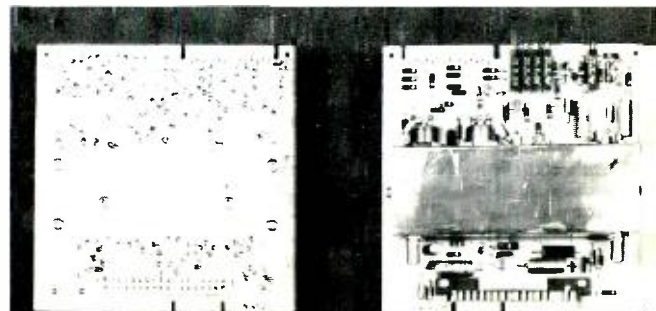


Fig. 8 (above)—Typical UHF radio and its sub-assemblies. Fig. 9 (below)—Printed board from an HF radio showing traces designed for an edge connector.



The Hertz Corporation— a profile

J. C. Phillips, Associate Editor

Renting and leasing services form an important part of the mushrooming service sector of the nation's economy. RCA is engaged in this activity through The Hertz Corporation, the world's leading vehicle renting and leasing organization. Hertz also provides service in a variety of other markets by engaging in the businesses of construction equipment rental, parking, exposition services, and hotel-motel management.

WHEN RCA WAS FORMED on October 17, 1919, Walter L. Jacobs had already been in the rent-a-car business for more than a year, providing Model T Fords from his Chicago side-street garage. But in those days, the growth of radio was meteoric compared to that of the rental car business.

Automobiles were rented from out-of-the-way garages—always for cash—and cars had to be returned to the original rental point. Actually, there was no prestige involved in renting a car; a person would rent when he couldn't afford to buy.

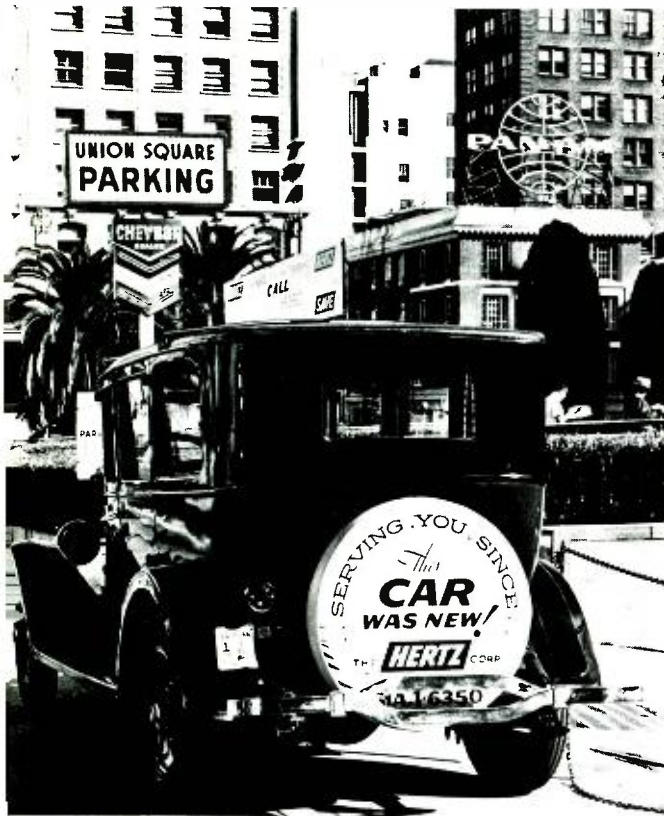
But, Mr. Jacobs' car rental business did grow somewhat, and in 1923, it attracted the attention of John Hertz who purchased the firm as part of his Yellow Truck and Coach Manufacturing Company. Hertz owned the business for only two years. In 1925, he sold certain properties including the Hertz Drive-Ur-Self System to General Motors, who primarily wanted the truck manufacturing facilities. These plants subsequently formed the nucleus of today's GMC Truck Division.

Hertz Drive-Ur-Self system—vintage 1925-26.

The original Hertz Drive-Ur-Self properties operated as a GM subsidiary until 1953, when they were sold to the Omnibus Corporation, which until then had been a holding company for bus operations, primarily in Chicago and New York. Omnibus then divested itself of bus interests and became The Hertz Corporation, concentrating on car and truck renting and leasing.

It was at this point in time that Hertz started its own meteoric rise. And since 1954, Hertz has become a leading force in the renting and leasing industry, the most successful of the rapidly expanding service industries. Some of the elements underlying this outstanding growth are

- Changes in consumer attitudes—today, increasing numbers of organizations and individuals want the temporary use of all kinds of equipment without the responsibilities of ownership.
- Strong merchandising strategies that use network television, newspapers, and magazines to good advantage.
- Introduction of modern, convenient credit plans.





Hertz' upward progress through the years can be plotted in uniform hemlines. Starting top left, to bottom center: the boxy, long-lined 1946-56 version; the more feminine 1956-62 uniform; the casual suit introduced in 1963; and the three-piece ensemble adopted in early 1968. The present Hertz uniform at right was introduced in 1971. Hertz "skirts" the issues of both hemline and business by saying the dress length is a girl's own decision and the hem is deep enough so she can change her mind.

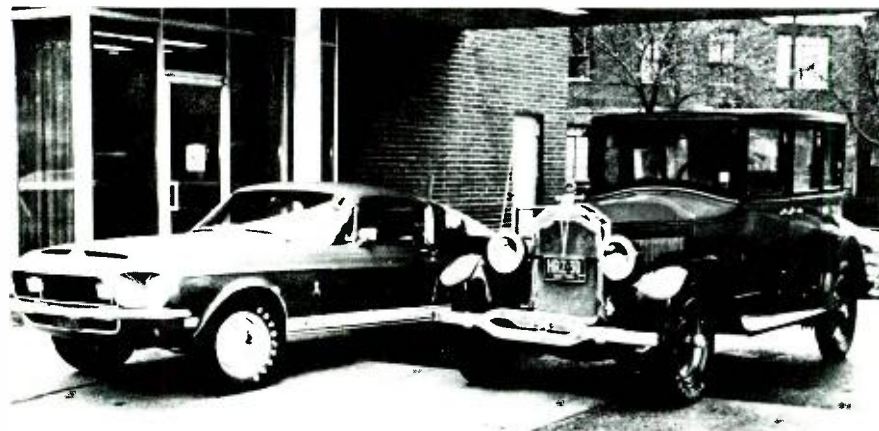
- Growing mobility in our society—with greater emphasis on air travel.
- Hertz' own emphasis on improved and expanded services.
- Establishment of services on a broad geographic scale—domestically and internationally—via owned and franchised operations.

Today, some 18,000 employees of The Hertz Corporation, exclusive of licensees, provide about 150,000 vehicles from more than 4,500 locations around the world.

A pioneer in the industry

Through more than a half century of renting and leasing, Hertz has held a

Symbolizing the changes that have taken place in the car rental field is this photograph taken on the occasion of Hertz' 50th anniversary. The two Hertz cars are a Shelby Cobra GT 350 (left) and a Hertz-built car from the mid 1920's.



position of leadership in the industry.

Hertz was first to provide late-model cars in many sizes and makes from which a renter could choose a vehicle to fit his needs—a bold move at the time.

Hertz also opened many modern main-street and airport locations.

In 1957, Hertz introduced nationwide "rent it here—leave it there" service as an innovation in the industry.

Another daring first was the extension of personal credit. Traditionally, car rental had been on a cash-in-advance basis. Hertz issued letters of credit as early as 1925, and now extends charge privileges to more than 1.8 million motorists who hold its charge card. Hertz also recognizes many other established charge cards.

Another significant activity pioneered by Hertz in the early days of auto renting was its development of "fly-drive" car rentals. By establishing accessible rent-a-car locations within hundreds of airports, Hertz has made fly-drive convenient for large numbers of businessmen and vacationers. To further stimulate fly-drive business, Hertz offers a commission plan to travel agents who book Hertz car rental reservations. This commission plan was recently extended to all airlines in North America handling car rental reservations.

These innovations brought the car rental industry out of the back-street garages of the early twenties to the present day network of airport and "main street" locations coast-to-coast and overseas.



Frank A. Olson,
Vice President
and General
Manager, Rent-
A-Car Division.



**Stephen
Russell,** Vice
President and
General Manager,
Truck Division.



Hubert Ryan,
Vice President
and General
Manager, Car
Leasing Division.



Peter W. Hofmann,
President, Hertz
International, Ltd.



Edward J. Andrie,
President, Hertz
Equipment
Rental Corp.



Ronald J. Lenney,
President,
Meyers
Parking System.



Samuel Katz,
President,
United Exposition
Service Co.



Garth Colling,
Managing Director,
Silcock
and Colling, Ltd.



Robert F. Thurston,
Vice President,
Hertz Skycenter, Inc.



Hudson Hatcher,
President,
Hertz Commercial
Leasing Corp.

The Hertz Corporation

The Hertz Corporation today embraces ten functional organizations:

- Rent-A-Car Division
- Truck Division
- Car Leasing Division
- Hertz International, Ltd.
- Hertz Equipment Rental Corp.
- Meyers Bros. Parking System, Inc.*
- United Exposition Service Co.
- Silcock and Colling, Ltd.
- Hertz Skycenter, Inc.
- Hertz Commercial Leasing Corp.

*As we go to press, Hertz has reached an agreement in principle to sell Meyers Bros. Parking System, Inc.

Rent-A-Car Division

Hertz is best known for its rent-a-car activity which represents about one-third of its business. Frank Olson became Vice President and General Manager of this division in 1970 after serving with Hertz since 1964. Hertz Rent-A-Car, which employs about 6,200 people, provides some 50,000 late-model autos on a short-term rental basis—daily, weekly, or monthly—at airports and in midtown and suburban business centers, residential areas, and resort locales in the United States.

The Rent-A-Car Division is the oldest Hertz activity.



Truck Division

Truck renting and leasing is Hertz' second most senior business. From the 1920's onward, Hertz provided trucks on short-term and long-term leases. In 1955, before Rent-A-Car started its phenomenal growth, revenues from truck rentals actually exceeded those of car rentals by about 50%. It was not until 1958 that the truck business was surpassed by Rent-A-Car.

The business grew steadily along two lines: leasing and short-term rental. The lease activity provided trucks of virtually any size or model to various companies which painted and lettered



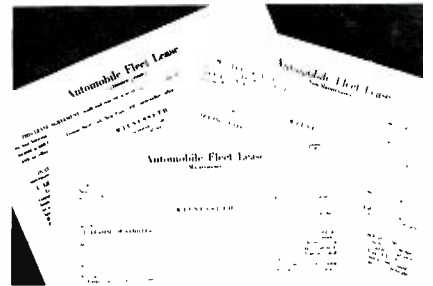
Photos at left (top to bottom) show some of the wide ranging activities of the Rent-A-Car Division: vehicles at convenient airport locations... special services... special vehicles, such as the Hertzmobile (bottom) being used by Henry Fonda at the recent TRANSCO' 72 convention.

The Truck Division's services (above) are likewise wide ranging—from trucks for do-it-yourself movers (top) to custom truck fleets for special purposes (center and bottom). Under full-service leasing, Hertz provides vehicles and most of the services and materials needed in operating them. Full-service lease trucks are painted and lettered to the customer's specifications, providing the customer with a "rolling billboard."

them to their own specifications. These trucks could be leased singly or in fleets as large as required.

The rental part of the truck business has always appealed primarily to individuals who require large vehicles for short periods of time, such as filling gaps in an established leased or owned fleet for peak periods of use, or one-time jobs.

Today, the Truck Division provides about 27,000 vehicles from some 2,600 locations in the United States, many of which are the gas station "agency" type. Total employment of the Truck Division is about 2,800. Stephen Russell is Vice President and General Manager of the Truck Division, having served previously as Vice President of Financial Analysis for RCA.



Hertz provides cars on long-term lease to companies whose needs vary from five to hundreds of autos on a nationwide basis. A wide variety of lease plans are available.

Car Leasing Division

Hertz entered the long-term auto leasing activity in 1955. At that time, Hubert Ryan became Vice President and General Manager of the new Hertz division. This operating unit concentrates on the long-term leasing of cars—generally 2 years. It leases about 28,000 vehicles through 8 locations in the United States and employs approximately 175 people.

This service appeals to companies whose needs vary from five autos to hundreds on a nationwide basis.

Two types of service are provided, or any combination of features between the two. Under a full-maintenance lease, for example, Hertz provides all services except fuel and lubrication, even including registration and insurance. Under a finance lease, Hertz buys the vehicle and, at the end of the lease, disposes of it. The lessee handles all other matters himself and absorbs the gain or loss on disposition of the car.



The Hertz logo in the Cyrillic alphabet has been used in Russia since 1969.

Hertz International, Ltd.

Hertz International, Ltd. provides car and truck rental services in over 100 countries outside the United States. At present, International owns and operates about 29,000 vehicles, mostly cars, through a network of some 1,100 locations and employs about 5,000 people. This unit conducts corporate operations in 29 countries and territories; it also handles licensee operations in 76 countries and territories. Peter W. Hofmann, President of Hertz International, joined Hertz this year after serving as Staff Vice President of International Finance for RCA. He has been with RCA since 1948.

As far back as its incorporation in 1953, Hertz had a few overseas operations, but it was not until 1957 that a joint venture with American Express was established to enter and expand the international renting and leasing market. In 1966, Hertz acquired full ownership of International by giving Hertz stock for American Express interest in International.

The company primarily rents locally manufactured cars and employs local citizens of the countries it serves. None of the country managers are American, except the manager in Spain—and he is located in Spain, not in the U.S. Hertz International Ltd. does do some truck renting, but the vast bulk of its revenue is derived from self-drive car rentals.

Like the domestic rent-a-car business, many Hertz International rentals take place at airports—again the fly-drive characteristic. As International's car rental is broadening in scope and size, however, it is finding that most of its business comes not so much from Americans traveling abroad as from nationals of other countries in their own and other lands. Thus, this part of Hertz service can be said to be a truly international business.



Hertz Equipment Rental Corporation

In recent years, growing numbers of building contractors, as well as public and private organizations which do their own construction and maintenance, have been obtaining the use of equipment conveniently and economically through renting. In 1965, Hertz entered the business of renting construction-type equipment to contractors and industrial firms.

Through Hertz Equipment Rental Corporation, a subsidiary, Hertz rents a wide variety of construction equipment, ranging from hand-operated power tools to air compressors and large cranes. This service is provided through 40 locations in the U.S. with a staff of about 750 people. Edward J. Andrie recently became President of Hertz Equipment Rental Corp. after serving as Staff Vice President of Corporate Planning for The Hertz Corporation.



Hertz rents a wide variety of equipment, ranging from hand-operated power tools to the special-purpose equipment shown in the photographs above and left.



One of the Meyers Bros. Parking System locations.

Meyers Bros. Parking System

In 1964, Hertz acquired one of the world's leading parking organizations—Meyers Bros. Parking System, Inc., established in 1923. Ronald J. Lenney is President of the System. Meyers operates about 170 parking locations throughout the United States and Puerto Rico and employs over 800. The parking locations include many multi-storied installations with modern electronic and mechanical equipment.

Meyers has also achieved nationwide prominence for its parking consultation activities with community planners, civic officials, engineers and architects related to the building of parking facilities, either separately or in connection with hotels, apartment houses, office structures and larger developments.



1)



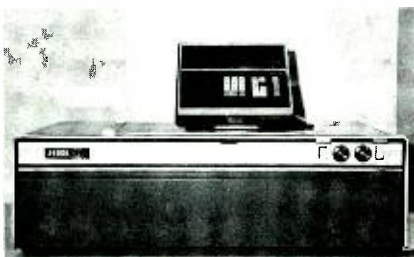
2)



3)



4)



5)

Left, from top:

1) Silcock and Colling road transporter capable of carrying six to eight cars;

2) The Hertz Skycenter at Huntsville, Ala., jetport which includes a 152-room luxury hotel and office, banking and convention facilities, and gourmet restaurants—all in one building with the terminal;

3) The Huntsville Skycenter also features a variety of special services and facilities for businessmen, including private offices, telephone answering and secretarial service, and duplicating work;

4) Architectural rendering of the new Hertz Skycenter at Jacksonville, Fla.;

5) Hertz Commercial Leasing Corp. makes available a wide selection of commercial and industrial equipment such as this office equipment.

United Exposition Service Co.

In 1967, Hertz entered yet another service activity. Its subsidiary, United Exposition Service Co., provides trade shows, conventions and expositions with three types of service: drayage, delivering exhibitors' equipment to the site; and personnel to install and dismantle exhibits. The company also designs and builds displays. Samuel Katz, President of United, was elected a Director of The Hertz Corporation at that time.

The combined activities use seven locations in the U.S. and employ about 180.

Silcock and Colling, Ltd.

Hertz in 1969 bought the British concern of Silcock and Colling, a major transporter of new autos throughout Great Britain. The company has 6 locations and employs about 1,000. Its Managing Director, Garth Colling has been with the company since 1963.

The company uses three methods of vehicle delivery—by road, driven individually; by rail on two-tiered "cartics" to a distribution point and then by road; and by road transporter, carrying 6 or 8 cars.

In March, Silcock and Colling expanded its operations to the Continent.

It plans to develop the business on the Continent as the European Economic Community's market broadens.

Hertz Skycenter, Inc.

In late 1968, Hertz unveiled an unusual service for air travelers with the official opening of the new Skycenter at the Huntsville, Alabama, jetport. A pioneering air travel complex, regarded as a model for airport centers of the future, the Skycenter features a "city-within-a-city" plan. Included under one roof are facilities for transportation, lodging, business, banking and recreation.

Through a subsidiary, Hertz Skycenter, Inc., the company runs all the terminal service facilities (other than those related to air traffic control) including a hotel, restaurants, office and secretarial services, a large parking lot and in-flight food service. A swimming pool and golf course are also part of the complex.

Located in the fast-growing Huntsville industrial area, the Skycenter serves the travel needs of the NASA and Army aerospace centers in and around nearby Redstone Arsenal. Hertz plans to open the second of its Skycenters at the new Jacksonville, Florida, jetport in mid-October.

Robert Thurston, Vice President and General Manager of Hertz Skycenter, Inc., has headed this program since its inception. He had prior background as a Vice President for the Ramada Inn organization.

Hertz Commercial Leasing Corporation

Business machines, office equipment, airplanes, skylifts, turkey brooders—these are only a few of the items available under long-term finance lease from Hertz Commercial Leasing Corporation, a subsidiary of The Hertz Corporation.

Companies in 46 states and Puerto Rico are currently using machinery or equipment leased from this subsidiary. Hertz buys the equipment and leases it to the user on a three-year basis, or longer. The customer can renew the lease or buy the equipment, if he chooses, at the end of the lease period. The user pays insurance, maintenance, operating and other costs during the lease.

Hudson Hatcher, Vice President and General Manager of Hertz Commercial Leasing, has headed the company since its inception in late 1959.

Corporate activities

The Corporate offices at 660 Madison Avenue in New York provide a range of support services to the wide-ranging Hertz network. These include such services as personnel, accounting, legal purchasing, advertising, marketing, and public relations. In addition, the Hertz Data Center in Oklahoma City, Oklahoma, provides accounting, billing, reservations, and other data processing services—primarily in support of the Rent-A-Car activity.

The Oklahoma Data Center—a 100,000-square-foot office complex with approximately 400 employees—was opened in early 1971. Operating as the nerve-center for the Rent-A-Car Charge Card, Credit and Collection, Reservations, and Data Processing Departments of the Rent-A-Car Division, the Center represents another major step in Hertz' continuing drive to improve customer service worldwide.

In fact, the Center plays a key role in two of Hertz' most recent innovations in the service field: the Hertz Number One Club and a new computer-based system for car control.

No. 1 Club

The Number One Club is a major step in bringing automation directly to customers of a service industry. Under this system, adopted in April of this year, car rental information on hundreds of thousands of regular and high-volume car renters, both individual and corporate, are fed into a computer data bank for instant retrieval. This eliminates the need for frequent customers to repeat routine information each time they rent a vehicle.

The routine rental information is filled in on the rental agreement before the "Hertz Number One Club" customer arrives at the rental counter. The customer need only produce his driver's license and the credit card he wishes to use, sign the rental agreement, and be on his way.

Customer reaction to the Number One system has been very positive.

Automated car control

An innovative, nationwide, computer system providing renters with improved service is presently being tested in two high-volume locations. Eventually, it will be integrated with the nationwide reservation and data center. The new system will print time, date, proper rates, and description of the vehicle as well as calculating accurate rental charges in a matter of seconds.

The system uses an on-line computer terminal to enter vehicle number, vehicle mileage, and rate plan selected. This information is printed on the rental agreement.

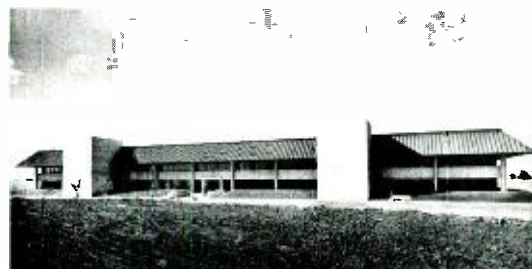
The on-line computer stores the transaction and maintains an updated status of every vehicle in the pool. Reports are periodically generated showing number of vehicles at each location, maintenance history, and various business statistics. The computer system improves fleet utilization, minimizes rental calculation errors, and also proves useful in tracing stolen vehicles and identifying customers responsible for traffic tickets. Upon customer return, the check-in mileage is entered through the terminal, and the amount due is calculated by the computer for printing on the rental agreement.

Hertz and the future

As the leading and most diversified of the companies in the renting and leasing industry, Hertz has benefited from the significant trends toward increased use of its industry's services.

The same forces in society—mobility, convenience and effective utilization—that shaped the broad expansion in use of renting and leasing services to date, remain strongly in effect. This holds true both for domestic and international markets for Hertz services.

In common with other burgeoning service industries, all signs in the field of renting and leasing point to further healthy development in the years ahead. The outlook is bright for the continued growth of Hertz, for expanded opportunities for its people, and for greater service to its many customers in the United States and abroad.



The Hertz Data Center in Oklahoma City is the nerve center of the Rent-A-Car Charge Card, Credit and Collection, and Data Processing Departments of the Rent-A-Car Division.



When calling for a reservation, Number One Club members just give their membership number and the time and place of their reservation. When they arrive, the rental agreement is pre-filled out and they need only show their driver's license, sign the agreement and be on their way.



Inside the Oklahoma Data Center.



The Hertz Booth at the recent TRANSCO '72.

Mathematics in communications systems research

Dr. L. Schiff

The mathematical examples in this paper are suggested by actual problems encountered in planning different communications systems. They have been selected for their simplicity and somewhat off-beat flavor. This is particularly true of the last example where the concern is the communications capacity of a cellular communications system. The mathematical technique needed for the solution is identical to the technique needed to solve a classic problem in recreational mathematics—how many ways are there of placing j rooks on a chessboard so that none can take any other?

Dr. Leonard Schiff
Communications Research Laboratory
RCA Laboratories
Princeton, N.J.
received the BEE from City College of New York, in 1960, the MSEE from New York University, New York, N.Y., in 1962, and the PhD from the Polytechnic Institute of Brooklyn, Brooklyn, N.Y., in 1968. From 1960 to 1966, he was employed by Bell Telephone Laboratories, Inc., Murray Hill, N.J., where he was concerned with various aspects of electronic switching systems. Since 1967, he has been employed by RCA Laboratories, Princeton, N.J. He has been concerned with data transmission systems and various types of vehicle location systems. He has also worked on various system aspects of mobile radio especially techniques for making these systems more spectrally efficient and more efficient in their traffic carry capacity. He has authored a number of technical papers in these areas. Dr. Schiff is a member of Eta Kappa Nu, Tau Beta Pi, and Sigma Xi.

MOST ENGINEERS are aware that mathematics plays an important role in communication systems analysis and design. The branches of mathematics that tend to come to mind are Fourier analysis, probability theory, statistical decision theory, theory of random processes, etc. These are the typical "textbook" applications of mathematics to communications systems. Actually there are hardly any branches of mathematics that have not been profitably applied to the analysis of communications systems. Rather than try to write an essay on what branches of mathematics can be applied to what types of communications problem (which is surely beyond the knowledge of any one author) a number of examples are given to try to illustrate the diversity of mathematical tools that can usefully be applied to communications systems.

Example 1

The first example comes from a system for vehicle location of the signpost type. In this type of system, many locations in an urban area are equipped with electronic signposts that continuously broadcast (over a very small area) a unique digital code that identifies the signpost. Vehicles are equipped with special receivers to pick up the signpost signals and store the result in a register. This register is then updated every time a new signpost is passed. When the vehicle is interrogated from a central base

station via its mobile radio, it will send back the contents of the register, thus identifying the last signpost the vehicle passed. This interrogate-respond operation can be done digitally without the driver's cooperation or knowledge.

Consider the following special receiver to pick up the signpost signals (this is a simplified version of a receiver built and described by G. S. Kaplan¹). The modulation is FSK and the message is N bits long. After the RF is stripped off, the N -bit FSK signal is passed through both a "mark" and "space" filter (matched to the two FSK frequencies respectively). If at any time, one and not both of the filters has an output level above a preset threshold, the frequency corresponding to that filter is said to be received and the circuit arranges itself to sample both filters, exactly T seconds later (where T is the time to send one bit). For the sampling, performed T seconds later, the above operation is repeated. The sampling continues until N bits are decided on at which time the process starts all over. This is illustrated in the state diagram shown in Fig. 1. The system is in state i if i bits sequentially have been regis-

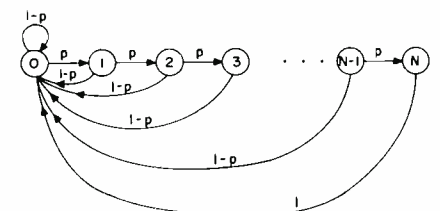
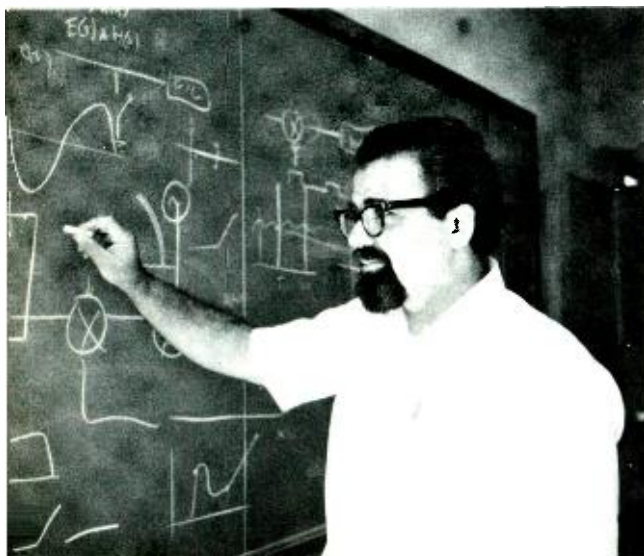


Fig. 1—State transition diagram.

Reprint RE-18-3-13
Final manuscript received June 27, 1972



tered (with no samples below threshold intervening). Every T seconds the system moves either to a higher state or to the 0 state. The exceptions are state 0 and state N . If the system moves to state N , it immediately returns to state 0. If the system is in state 0, it does not have to move on to state 1 a multiple of T later (rather it moves only when the threshold is first exceeded). Our interest here is in making sure that when the receiver is not near a signpost, the noise does not induce false messages into the register. To this end, the threshold must be made much higher than the RMS noise level. Nevertheless there is a finite probability, p , of moving into a higher state and we wish to calculate the mean time between failures where a failure is defined as entry of the system to state N . Since immediately upon entering state N the system returns to state 0, the question is equivalent to asking the mean time to reach state N , for the first time, starting from state 0. Transitions occur every T seconds except for transitions from state 0 which can occur at any time. However, if the mark and space filters are properly matched, their bandwidths are made just large enough to allow the signal to change its full-scale value in T seconds (*i.e.*, the output level goes from above threshold to close to zero in T seconds). Hence the filters can be considered to have enough inertia so that their outputs can be considered to change only every T seconds. With this final approximation, the mathematical model is complete. Transitions take place every T seconds and as shown in the state diagram in Fig. 1.

The mean time to reach state N is computed as follows. Let τ_n be the mean time to reach state n from state 0. If the system is in state n , it will, with probability p , reach state $n+1$ in T seconds. On the other hand, with probability $1-p$, the system will return to state 0 in T seconds, and the system will require, on average, another τ_{n+1} seconds to reach state $n+1$. We then have

$$\begin{aligned} \text{Average time to reach} \\ \text{state } n+1 \text{ from state } n &= \\ pT + (1-p)(T + \tau_{n+1}) & \quad (1) \end{aligned}$$

However, the average time to reach state n from state 0 is τ_n . It therefore follows that

$$\tau_{n+1} = \tau_n + pT + (1-p)(T + \tau_{n+1})$$

or

$$p\tau_{n+1} - \tau_n = T \quad n=1, 2, \dots \quad (2)$$

This is a first-order difference equation. Just as in the solution for a differential equation one first finds the solution of the homogeneous equation (with the right-hand side set equal to zero) and adds it to the steady-state solution and finds the unknown constant from the initial conditions. By direct substitution, one finds that the solution of the homogeneous equation is of the form p^{-n} and the steady-state solution is $\tau_n = -T/(1-p)$. Hence the solution is of the form

$$\tau_n = A p^{-n} - [T/(1-p)] \quad (3)$$

where A is an unknown constant which must be found by knowing some initial condition. This condition can be obtained by substituting for $n=1$ in Eq. 1 and realizing that the average time to reach state 1 from state 0 is indeed τ_1 . This gives the initial condition $\tau_1 = (T/p)$, and substituting in Eq. 3:

$$\begin{aligned} \tau_n &= [T/(1+p)] [p^{-n} - 1] \\ \tau_N &= [T/(1-p)] [p^{-N} - 1] \end{aligned} \quad (4)$$

This is the solution for the mean time between failures in the system as a function of p , the transition probability. It can be shown¹ that the transition probability is exponentially decreasing in the square of the threshold-to-noise ratio.

Example 2—vehicle locator with vehicle transmitter

The above example is for a vehicle-location circuit in which the signposts are low-power transmitters and the vehicles have receivers to receive the signpost messages. It is also possible to have a complementary system in which the participating vehicles all have low power transmitters (continuously transmitting their vehicles identity) and the signposts have receivers that pick up these messages and store them in a local signpost memory. Signposts are then interrogated periodically and the contents of their registers destructively read out by a central facility. The central facility is then aware of the last vehicles to pass a given location. The problem is that a given signpost can be in range of many vehicles even when the range is small. Each vehicle sends

a message for τ seconds every T seconds nominally. Since the vehicle transmitters are not synchronized, two messages can come in simultaneously and mutilate each other. It is evident that as the ratio τ/T becomes small, the probability of this happening becomes reduced because the sources are unsynchronized. However, because of bandwidth limitations or circuitry speed limitations, there is a limit to how small τ can be set. There is likewise an upper limit on T , the repetition time; namely, T must be small enough so that even if the vehicle passes the signpost at its maximum speed it will get off at least one transmission during the time the signpost is within its range. Hence, there is a certain minimum value τ/T can be set. The question we pose is "should T be set equal to its maximum value or a *much* smaller value?" If T is set equal to its maximum value, the probability of mutilation on any given transmission is minimized. If T is larger, the probability of a given transmission being successful is lower, but there are more transmissions. We assume here that the variations in T from one vehicle to the next are sufficiently large (compared to τ) due to clock frequency drifts and tolerances that if two vehicles have their transmissions overlap, they will not overlap on the next cycle (although the next transmissions may overlap the transmission of other vehicles).

To answer the question we try to model the process of message arrivals as a Poisson process (random arrivals). If each source transmits at a rate $1/T$ times per second and gets, on average, one message off while it is within range and, on average, there are m vehicles within range of the signpost, the average arrival rate at the signpost is $\lambda = m/T$ arrivals per second. To get a message of τ seconds through requires a blank time between arrivals of 2τ . If a new arrival occurs between zero and τ seconds after a message is started, it will mutilate the message. If it arrived between $-\tau$ and zero, the starting message will mutilate it and hence itself be mutilated. A well known result for Poisson processes is that the probability of finding a blank time of 2τ is $e^{-\lambda 2\tau}$. Hence the probability of failure, p_f is given by

$$p_f = 1 - \exp[-2m\tau/T] \quad (5)$$

Now consider the possibility of transmitting at that rate n/T for each source (*i.e.*, increasing the clock rate by a

factor n). The rate λ is then increased by a factor n , and the probability of failure on any one transmission is $1 - \exp[-2nm\tau/T]$ but since there are now n essentially independent trails

$$p_f = \{1 - \exp[-2mn\tau/T]\}^n \quad (6)$$

This function is plotted in Fig. 2 for various values of n . As can be seen the optimum value of n depends on the value of $m\tau/T$. Further, one can plot the lower envelope (*i.e.* the curve which is the greatest lower bound for all n) and hence derive the value of failure probability for the optimum value of repetition rate.

Example 3—large number of digital terminals

We now consider a communications system not at all related to a vehicle location but which does have a relation to the previous problem. Consider a system in which there are a large number of terminals each of which generates digital messages at random times and of variable lengths intended for transmission to a central point (*i.e.*, terminals do not communicate with each other but only with a central point). The terminals send to the central point either by wire or radio over a common channel (*i.e.*, party line). Assume further that there exists a reverse channel by which the central point can send messages to the terminals. Each terminal may receive the messages generated by the central source but since each message has appended to it

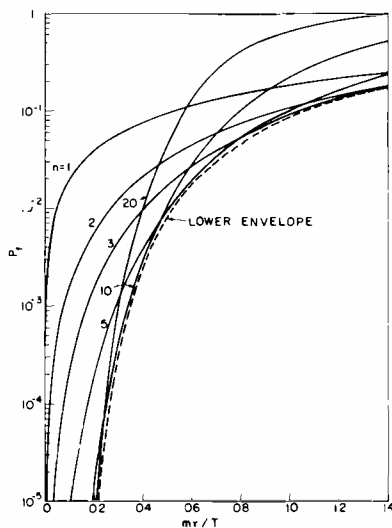


Fig. 2—Probability of failure for various values of n .

the unique number of the terminal for which it is intended, terminals “filter out” only the messages intended for them. We shall not be concerned with this reverse channel since the central point can organize messages generated by it sequentially in an orderly way. Our concern is with the forward channel; for that purpose, assume that a message that is successfully transmitted by a terminal is essentially instantly acknowledged via the reverse channel, and that if the transmission is garbled, no reverse signal is sent at all (thereby informing the terminal the message was not received by default).

There are many ways to construct such a transmission system. One obvious way is to divide the channel up among the various terminals by giving each its own frequency slot (frequency-division multiplex) or time slot (time-division multiplex). However, if there are m terminals, each terminal is forced to signal at $1/m^{\text{th}}$ the maximum channel speed. If most terminals are inactive at any one time (as, for example, might be the case if this system were used for two-way capability on a CATV system), the channel is not efficiently used. One can restore the efficiency by dividing the time into a smaller number of slots per frame such that the number of slots is equal to, or slightly above, the average number that are active at any one time (or the busiest time) and poll infrequently to see which terminal gets assigned which slot. In other words, turn the party line into a concentrator. All this requires the terminals to be mutually synchronized and have the logic to bid for slots and recognize slot assignments, etc. There exists, however, an alternative that is attractive in its simplicity and can sometimes be more economical.²

In this scheme, each terminal has a small local memory. A message is formed in memory as it is generated. When it is complete, (the terminal operator pressing the appropriate key) the message is immediately sent. If an acknowledge signal is returned, the message is erased from memory and the subscriber can generate new messages. If no acknowledge signal is returned, the terminal idles for a time (T seconds) and then retries. It keeps retrying every T seconds until the message is acknowledged.

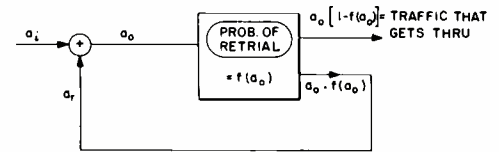


Fig. 3—Traffic flow diagram.

Just as in the previous example, messages that have their messages overlap, mutually mutilate each other and neither is acknowledged. Each terminal has a slightly different repetition cycle so that if two terminals interfere on one transmission they will not on the next cycle.

We now try to form a mathematical model for this system. An assumption must be made about the statistics of message length. It is assumed here that the duration of messages are exponentially distributed with mean τ . This is typical of many systems with non-constant transmission time (with short messages more likely than long ones). The new messages generated by all the terminals is λ_i messages per second. Now the dimensionless quantity $a_i = \lambda_i \tau$ (given the units “erlangs” in telecommunications traffic engineering parlance) is the “load” placed on the system. Clearly no single channel can carry more than one erlang, or messages build up faster than they can be sent out. In this system, the limit is lower than unity since the channel carries not only the initiated load a_i but also the retransmitted load $a_r = \lambda_r \tau$. The rate λ_r is the rate at which retrials or mutilation occur. The total load offered the party line is then $a_o = \lambda_o \tau = a_r + a_i = (\lambda_r + \lambda_i) \tau$. A flow diagram of this is shown in Fig. 3.

Our aim is to find the maximum traffic a_i this system can handle and how the quality of service depends on a_i . An immediate result from the diagram is

$$a_o = a_i + a_r = a_i + a_o \cdot f(a_o)$$

or

$$a_i = a_o [1 - f(a_o)] \quad (7)$$

What remains is to find f explicitly as a function of a_o . For simplicity, assume the arrival process on the line (λ_o) is Poisson (arrivals at random). The probability that a given arriving message is successfully transmitted (without a retrial) is $1 - f(a_o)$ and

$$1 - f = \left[\begin{array}{l} \text{Probability the line is} \\ \text{unoccupied when the} \\ \text{message arrives} \end{array} \right] \times \left[\begin{array}{l} \text{Probability no new} \\ \text{message arrives while} \\ \text{this message is on the} \\ \text{line} \end{array} \right]$$

(8)

Now, a well known result in the theory of Poisson processes is that if messages arrive at random at a mean rate λ_o and last for a time θ , where θ is exponentially distributed with mean τ , the probability that the line is unoccupied at any given time is $\exp[-\lambda_o\tau] = \exp[-a_o]$. This is the first factor on the righthand side of Eq. 8. To find the second factor simply note that, as pointed out in the previous example, for a Poisson process of rate λ_o , the probability of no new arrival for θ seconds is simply $\exp[-\lambda_o\theta]$. Of course, θ is a random variable so this result must be averaged over the statistics of message length. Since the message length, θ , is exponentially distributed with mean τ , the second factor in the righthand side of Eq. 8 is

$$\int_0^{\infty} \exp(-\lambda_o\theta) [\tau^{-1} \exp(-\theta/\tau)] d\theta = [1 + \lambda_o\tau]^{-1} = [1 + a_o]^{-1}$$

Substituting these results into Eq. 8 and Eq. 8 into Eq. 7 gives

$$a_i = \frac{a_o}{1 + a_o} \exp(-a_o) \quad (9)$$

This equation relates the initiated load (new traffic) to the total offered traffic (new traffic plus retrials) in a one-to-one manner. Formally there are two values of a_i for every value of a_o , but the larger value of a_i is physically unrealizable—corresponding to non-equilibrium situations. One way to measure the quality of the service is to define the quantity $\xi = a_o/a_i$. Since a_o is the total of new plus reoriginated traffic, ξ is the average number of transmission per message. Using that definition and Eq. 9), one can plot (Fig. 4) ξ as a function of initiated traffic a_i . For low values of a_i , the average number of transmissions is only slightly greater than unity (*i.e.*, very few are blocked and retransmitted). When a_i reaches about 0.15, however, the number of retransmissions starts to increase very rapidly as traffic increases. The maximum initial load the system can sustain before running away is slightly greater than 0.2. While this limit is only 20% of the maximum ideal capacity, it is achieved with extremely simple terminals.

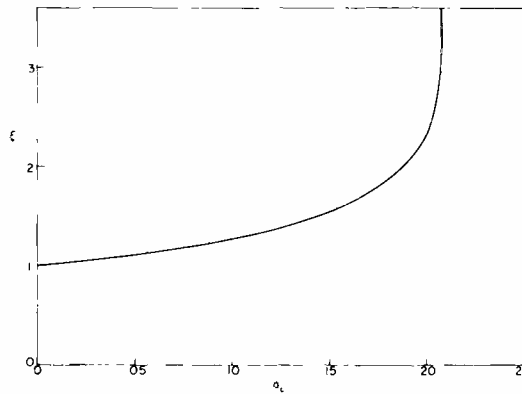


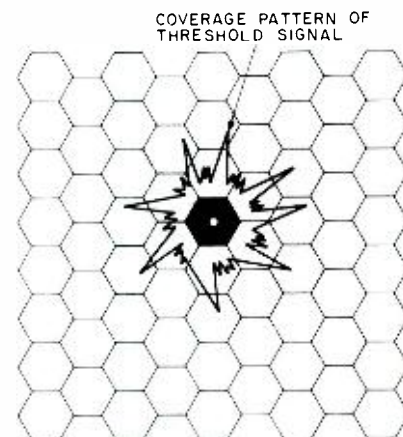
Fig. 4—Average number of trials as a function of initiated load.

Example 4—dispersed-array mobile radio system

We conclude with an example of some topical interest. Because of spectrum congestion in the land-mobile radio service, a new block of frequencies in the 900-MHz region will soon be set aside for land-mobile use. Because of the rapid growth of mobile radio much emphasis is being placed on efficient use of this new spectrum. In turn, this has led to much discussion of cellular systems. One such system called the dispersed-array has been described in a previous *RCA Engineer*.³ The following is a brief description of the way such a system would function.

The urban area to be covered by the dispersed-array, common-user, mobile-radio system is divided into a number of non-overlapping cells or zones. In the center of each zone is a fixed base station, and mobile units in the zone can communicate with this local base station. All these base stations are connected to a central processing unit (CPU) by leased land lines (or by SHF short-range, point-to-point radio links). Each of the non-mobile subscribers (or dispatchers) to the system is also connected, by leased line, to this CPU. This allows for a complete connection between any mobile unit and any fixed subscriber. [In this simple form, the system makes no provision for mobile-to-mobile communication; but from the configuration described above, it is obvious that this too can be done.] The CPU is, in effect, a switching center, switching dispatcher calls to the proper local base station. To do this, the CPU must be aware of the location of the mobile unit so that the call can be switched to the correct base station. This shows one use of a vehicle-location system.

Because of interference, two adjacent zones cannot use the same frequency channel simultaneously. If a base station (designed to give a nominally circular plane pattern in free space) is used with enough power to reliably cover its zone, its radiation pattern will probably spill over to cover major portions of adjacent zones and at least some portions of zones beyond those. Fig. 5 shows a typical pattern that might result; the zones in this drawing are hexagonal in shape. Based on some experimental data, it is felt that essentially interference-free communication can be provided if a "two-ring" buffer is placed around any active base station. That is, the same frequency cannot be used at the same time in any of the zones forming two rings about the central zone. This amounts to 18 hexagonal zones "blocked out" for any given frequency. Using square zones, the corresponding result is 24 zones. For this reason, the zones are designed to be nominally hexagonal. This buffering will still allow a frequency to be used



SHADED AREA IS FOR ZONES ON WHICH REUSE OF FREQUENCY USED IN DARKER ZONE IS FORBIDDEN

Fig. 5—Typical coverage from any one zonal transmitter.

simultaneously in many different parts of a metropolitan area.

One method of assuring this buffering of 18 zones around an active base station is to provide adjacent base stations with different frequency channels. However, from Fig. 6 it can be seen that the minimum number of frequency channels to do this is 7. This implies that each mobile unit must have capability on at least 7 frequency channels to insure communications capability in all zones. In this system, however, a different approach is used—called dynamic frequency assignment. The switching and location update facilities at the CPU are assumed to be computer controlled. This computer can also keep track of what frequencies are being used in each zone and refuse to use a base station on a frequency that is simultaneously in use in one of the 18 surrounding zones. Each base station is thereby equipped to communicate on all frequency channels assigned to a given metropolitan area, but mobile units need only be given capability on one channel. This is especially important since the major cost of the system is for mobile units. While mobile units need only be equipped for one channel, they may also be equipped for more. The desirability of this multi-channel access is well known. For a constant traffic per channel, multi-channel capability gives a better grade of service; alternately, for a given grade of service, the traffic load per channel can be

increased. Further, complete flexibility can be had by offering units with one or more channel capability. A customer can then purchase or rent a more expensive unit to provide better service.

Since the entire system is computer controlled, a number of desirable features can be implemented rather easily; e.g., giving vehicle location (i.e., what zone) on request. It must also be pointed out that many interconnections accomplished via land lines can also be done with point-to-point radio links.

The question we ask here is "How much is performance improved over the traditional mobile radio mode of one-zone operation?" One way of answering is to calculate the number of times a frequency is reused over the entire area served by the system. While this number depends on the traffic load and history, it is possible to give upper and lower bounds for the number of reuses by using simple arguments (rather similar, in principle, to "close packing" bounds in information theory).

To establish an upper bound observe that Fig. 6 gives the tightest packing so that a frequency is repeated every 7th cell or, if there are N cells, at most $N/7$ reuses are possible. That tightest packing is obtained for a repeat every 7th cell is easy to prove. Obviously, the number is not greater than 7, for a repeat every 7th satisfies the buffering rules. On the other hand, a number less than 7 would imply that, in Fig. 6, there

is a way of numbering the cells with numbers between 1 and 6 so that no cell with a given number is ever in the two ring buffer of a cell with the same number. This is not true! To show this, consider any 7 cell cluster of a center cell and the ring (made up of 6 cells) around it. Since only 6 numbers are used, one of the numbers must repeat in the group of 7 and therefore violate the 2-ring buffer rule. Hence 6 or lower is not possible. It follows that $N/7$ is an upper bound to the number of reuses.

Can a lower bound be found, and does it make sense to talk about one? It does if the question is asked in the following way—What is the smallest number of reuses such that no more reuses can be made without violating the buffering rules?—this question can be answered as follows. If a single cell is used (or occupied), neither that cell nor the 18 cells in the 2-ring buffer can be used. Hence at most 19 cells are taken away from use (if the cell is near an edge, less are taken away). Of the cells that remain, the second use can again take away a maximum of 19 cells. (It can take less if some of the cells in the 2-ring buffer of the first use are the same as some of the cells in the 2-ring buffer of the second). In fact, each cell that is occupied "takes away" at most 19. Hence as long as the number of occupancies multiplied by 19 is less than the total number, N , of cells another occupancy is possible. The lower bound on the number of reuses is then $N/19$ (to be more precise, the next highest integer to $N/19$ if $N/19$ is not an integer). And this cellular arrangement results in an improvement between $N/7$ and $N/19$.

While the above serves to give an idea of the improvement, a more exact picture can be given. Basically, we want to know what the probability of blocking, P_b , is for a given traffic density. If λ is the number of mobile calls per second in any one cell, and τ is the average length of a call so that the traffic per cell is $a = \lambda\tau$, it can be shown that P_b (i.e., the probability that an initiated call can only be completed by violating the 2-ring buffer rule and hence is not completed) is given by⁴

$$P_b = 1 - \frac{a}{N} \left[\frac{\left(\frac{dS(a)}{da} \right)}{S(a)} \right] \quad (10)$$

where $S(y)$ is a polynomial in the dummy variable y given by

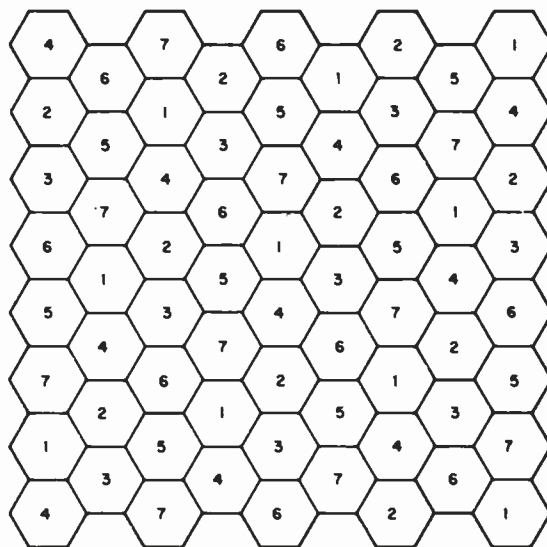


Fig. 6—Repetition pattern for tightest packing.

$$S(y) = \sum_{j=0}^{j_{max}} N_j y^j \quad (11)$$

and N_j is the total number of ways (combinations) of fitting j occupancies in the group of N cells. Hence this traffic theory problem reduces to the combinatorial analysis problem of finding the polynomial $S(y)$. The coefficients of $S(y)$ are the number of ways of having j occupancies of a group of cells where occupancy of any cell precludes occupancy of that cell and certain others in a systematic pattern (2-ring buffer). Now consider the classic problem of recreational mathematics—How many ways are there of placing j non-taking rooks on a chessboard? The similarities in the two problems are obvious. In one case, the board is an 8×8 -array of squares; in the other case, a honeycomb arrangement of N hexagons. In one case, the occupancies forbidden by occupancy of a cell are all other cells in the same column or row; in the other case, all other cells in a 2-ring belt around the occupied cell. Not surprisingly both can be solved in the same manner.

For obvious reasons, we call $S(y)$ the rook polynomial. Consider only one cell in the group of N . The number of ways j occupancies can occur is divided into those in which that cell is occupied and those in which it is not, giving

N_j = number of ways j occupancies occur in the group of $N-1$ cells obtained by deleting this particular cell.

+ number of ways $j-1$ occupancies occur in the group of cells obtained by deleting this particular cell plus all cells in a 2-ring buffer around this cell.

Using the notation $S(y;c)$ as the polynomial corresponding to a cluster of cells c , the corresponding expression for the polynomial is

$$S(y;c) = S(y;c_1) + yS(y;c_2) \quad (12)$$

where c_1 is the cluster of cells obtained by striking out any one particular cell and c_2 is the cluster obtained by striking out that cell plus all cells in a 2-ring buffer around the cell. Note that c_1 and c_2 are both smaller clusters of cells and the polynomials for each of these can be factored again.

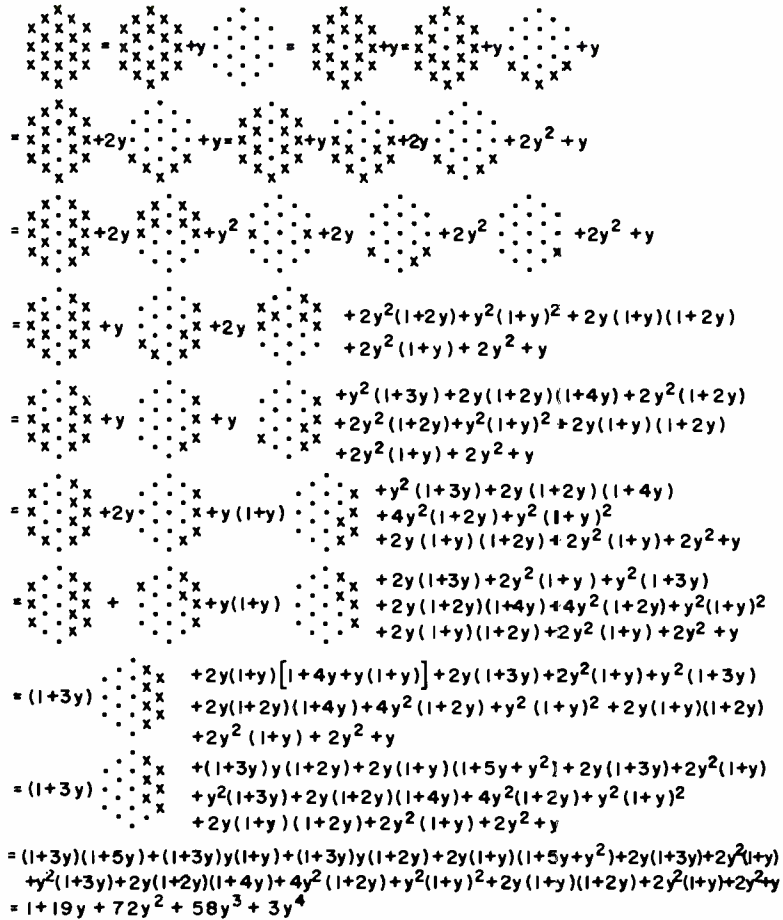


Fig. 7—Calculation of "rook polynomial" for a cluster of 19 cells.

This process can be continued until a cluster is arrived at for which the polynomial is obvious.

Fig. 7 demonstrates the method for a cluster of $N=19$ cells. Dots indicate the center of the cells. Crosses (superimposed on dots) indicate cells that are permitted to be occupied. The picture of the cluster is used to represent the polynomial itself. Note that all pictures that are the same after a rotation represent the same polynomial and are combined. Note also that any cluster with no crosses has polynomial equal to unity (there is one way of putting zero occupancies in). A cluster with one cross has polynomial $1+y$, etc. Also note the obvious result: when there are two clusters of crosses at opposite ends of the group of 19 such that occupancies in one cluster don't affect occupancies in the other, the polynomial is the product of the polynomials of the separate clusters of crosses.

The formalism allows one to proceed systematically and arrive at all coefficients N_j of the polynomial in one cal-

ulation.

Conclusion

In these examples, which portray actual problems encountered in communications systems, many branches of mathematics come into play. These examples, while elementary, help to indicate the wide variety of disciplines—from the theory of probability and difference equations to Poisson processes and traffic theory. Finally, the last example, which leads one into combinatorial analysis, best illustrates the fact that even methods of analysis which seem far removed from use in communications can be invaluable.

References

1. Kaplan, G. S., "Analysis of an Electronic Fence Element for a Vehicle Location System"; *IEEE Trans. on Veh. Tech.*, VT 20, No. 2 (May 1971) pp. 26-34.
2. Abramson, N., "The Aloha System"; *1970 Fall Joint Computer Conference Record*, pp. 281-285.
3. Staras, H. and Schiff, L., "A Dispersed Array Mobile-Radio System"; RCA reprint, *Microwave Technology*, PE-452; *RCA Engineer*, vol. 15, no. 3 (Oct.-Nov. 1969) pp. 48-51.
4. Schiff, L., "Traffic Capacity of Three Types of Common-User Mobile Radio Communications Systems"; *IEEE J. of Comm. Tech.*, vol. COM-18, no. 1 (Feb. 1970) pp. 12-21.

Methodology and techniques of operations research

Dr. A. K. Nigam

The purpose of this article is to acquaint the reader with the general nature of Operations Research. The characteristics of Operations Research are examined along with the general methodological framework in which typical problems are attacked and solved. Special emphasis is placed on the techniques used in finding solutions to problems. The techniques Linear Programming, Dynamic Programming, Network Flow Theory, Queueing Theory, Inventory Theory, and Game Theory are discussed in some detail.

SINCE THE ADVENT OF THE INDUSTRIAL REVOLUTION, there has been a tremendous growth in the size and complexity of organizations. This growth has led to spectacular results but has also created new problems. An integral part of this growth has been in the division of labor and segmentation of management responsibilities. Managers of production, marketing, finance, personnel, and the like appeared—each with their own objectives and value systems. As the complexity and specialization in an organization increased, it became easier for these managers to lose sight of the overall objectives, and at the same time it became difficult for the top management to allocate the available resources to the various activities in a way that was most effective for the organization as

a whole. Problems like these provided the environment for emergence of Operations Research.

What is Operations Research?

Instead of trying to give a definition, perhaps the best way to explain the unique nature of Operations Research is to examine its outstanding characteristics. As the very name implies, Operations Research involves “research on operations.” Operations Research is applied to problems that concern how to conduct and coordinate the activities within an organization. The nature of the organization is essen-

Reprint RE-18-3-10
Final manuscript received June 14, 1972.

Dr. Avadhesh K. Nigam

Operations Research
RCA Laboratories
Princeton, New Jersey

received the B Tech with highest distinction in Mechanical Engineering from Indian Institute of Technology, Kanpur, India in 1965 and the MS in Industrial Engineering from UC Berkeley in 1966. He joined Collins Radio Company in 1966 and worked on production planning and control aspects for one year. He reentered UC Berkeley in 1967 and received the PhD in Operations Research in 1970 and since that time has been with RCA. His responsibilities here have encompassed study of rental situations, market penetration and profitability analyses, design of experiments, and the general area of business measurements. He is a member of ORSA and TIMS.



tially immaterial; hence, the breadth of application is unusually wide. The approach of Operations Research is that of the scientific method. The essence of the process, which is discussed later, consists of formulating the problem, constructing a scientific (usually mathematical) model and obtaining results from it after verification by suitable experimentation. Thus, Operations Research involves creative scientific research into the fundamental properties of operations. However, because of its very practical orientation, in order to be successful, it must also provide positive and understandable conclusions to the decision maker.

Another characteristic of Operations Research is its broad viewpoint. An objective of Operations Research is to provide managers with a scientific basis for solving problems involving the interaction of components of the organization in the best interest of the organization as a whole. It is evident that because of the scope of applicability of Operations Research as well as the breadth of techniques available, no one individual can function well in all problem situations. Hence, it is usually necessary to use a team approach. The team would also need to have the experience and breadth of skills required to give due consideration to the many ramifications of the problem throughout the organization and to execute effectively all of the diverse phases of the Operations Research study.

As an introduction to Operations Research, this paper presents a general coverage of its methodology and techniques. The first part briefly introduces the basic methodology of the field and the way in which it adapts the scientific method to the study of operational problems. The second part reviews some of the fundamental techniques upon which Operations Research is based.

Methodology

Basically, the major phases of a typical Operations Research study^{2,7} are

- 1) Formulating the problem,
- 2) Constructing a mathematical model,
- 3) Deriving a solution from the model,
- 4) Testing the model and solution,
- 5) Establishing control over the solution, and
- 6) Implementation.

Formulating the problem

Most practical problems are initially communicated to the Operations Research team in a vague, imprecise way. Therefore, the first order of business is usually to study the relevant system and develop a well-defined statement of the problem. In formulating the problem, consideration has to be given to the objectives, the constraints that exist, the variables that are controllable and the ones that are not, the interrelationship between the area to be studied and other areas of the organization and alternative courses of action. What we earlier called the broad viewpoint of Operations Research is closely connected with the attempt to define objectives. The decision maker must be clearly identified, and all of his pertinent objectives noted. The objectives used in the study should be as specific as they can be while encompassing the main goals of the decision maker and still maintaining a reasonable degree of consistency with the higher-level objectives of the organization. This process of problem formulation is a very crucial one, since it determines how relevant the conclusions of the study will be. This does not imply that this phase is a one-shot process. Actually, the initial formulation needs to be continuously re-examined in the light of new insights obtained during the later phases.

Constructing a mathematical model

After formulating the decision maker's problem, the next phase is to reformulate it in a form that is amenable to analysis. Many of the questions to be resolved at this reformulation are very critical and determine the scope of the study. It is at this stage that we have to decide whether a static model will suffice or whether time dynamics have to be brought in. Also, whether the problem should be modeled as a deterministic system or include probabilistic effects. And, finally, whether a closed-form solution should be sought or a simulation of the system be used. The answers are not easy to come by, but the important point is that the essence of the problem should be captured by the model; that is, the model should be a valid representation of the problem.

The typical mathematical model in Operations Research problems has three characteristics. If there are n quantifiable decisions to be made, they are represented as decision vari-

ables (say x_1, x_2, \dots, x_n) whose values are to be determined. The composite measure of effectiveness is then expressed as a function of these decision variables (e.g., Effectiveness = $x_1 + 2x_2 + \dots - 5x_n$). This function is called the objective function. Any restriction on the values that can be assigned to these decision variables are expressed, usually, by inequalities (e.g., $x_1 \cdot x_2 \leq 3$). Such restrictions are called constraints. The problem in its mathematical context thus reduces to choosing the values of the decision variables so as to maximize (or minimize) the objective function subject to the given constraints.

As mentioned earlier, constructing the objective function is a complex task. It requires developing a quantitative measure of effectiveness relative to each variable. Furthermore, if there is more than one desired objective, then it is necessary to transform and combine the respective measures into a composite measure of effectiveness.

Deriving a solution from the model

After formulating a mathematical model for the problem under study, the next phase is to derive a solution from this model. The next section discusses, in detail, the subject of how to obtain solutions for various important types of mathematical models. Here we will discuss the nature of such procedures and the solutions obtained.

There are essentially two types of procedures for deriving a solution from a model: analytical and numerical. Analytical procedures generally end up using one of the mathematical techniques or a variation thereof. Numerical procedures essentially try various values of control variables in the model, analyze the results obtained, and select that set of values of control variables which yield the best solution. This may involve several iterations. Sometimes when the probabilistic nature of the variables involved is important, Monte Carlo technique may be required.

The discussion so far may have implied that an Operations Research study seeks to find the optimal solution. In fact, this is often not the case. Actually, with every solution obtained, improvements are made in the model, input data, solution procedure and then a new solution is obtained. This process is

continued until the expected improvement in solution becomes too small to warrant continuation.

Testing the model and solution

As has been mentioned before, a model is never more than a partial representation of reality. The crucial question always is: Has the model captured the essence of the situation without becoming cluttered with inconsequential details? A model is deemed good if, in spite of its incompleteness and approximations, it can yield reasonable and useful results. Confidence in the model can be acquired by testing its results over a wide range of input data and checking if the output from the model behaves in a plausible manner. These evaluations can also be performed retrospectively by the use of past data or by running it in parallel depending on the circumstances involved.

Establishing control over the solution

It is evident that a solution derived from a model remains a valid solution for the real problem only as long as this specific model remains valid. That is, as long as the uncontrollable variables retain their values and the relationships between the variables remain the same. Thus, in order to establish control over the solution, one must develop tools for determining when significant changes occur and must make provision for adjusting the solution and consequent course of action whenever such a change is detected.

Implementation

A very important aspect of an Operations Research study is to implement the solution as approved by the decision maker. This involves translating the solution into a set of operating procedures capable of being understood and applied by the personnel who will be responsible for their use. The success of the implementation depends a great deal on the support of both the top and operating management. Therefore, it is always critical to have their active participation in formulation of the problem and evaluation of the solution. It is also very valuable in its own right for identifying relevant special considerations and thereby avoiding potential pitfalls during all phases.

It should be emphasized that the steps

enumerated above are seldom, if ever, conducted in the order presented. By its very nature, Operations Research requires considerable ingenuity and innovation and hence any one set of rules or procedures will always be inadequate. Rather, the above may be viewed as a model to be used in conducting an Operations Research study.

Techniques

As might be suspected, there are certain types of problems which arise frequently. Considerable work has been done in developing techniques that make use of the special nature of these characteristic problems to obtain their solution. In this section, we will briefly survey the techniques and the related problems for which they were developed.

Linear programming

This is used to solve the general class of problems when there are a number of competing activities to be performed and when insufficient resources are available to perform each activity in its most effective way.^{3, 5} The problem is, thus, essentially one of allocating scarce resources to activities in an optimal manner. Over and above this, a primary requirement of linear programming is that the objective function and every constraint be a linear function and that the decision variables be continuous.

The most commonly used procedure to solve linear programming problems is the simplex method. It can be shown that the region in which all the feasible solutions (for which all of the constraints are satisfied) lie is a convex polyhedron in n -dimensional space, and that the optimal solution corresponds to a vertex of this polyhedron. The simplex procedure first finds a vertex of this convex polyhedron and then proceeds to examine a neighboring vertex for optimality. Since the number of vertices is finite, the optimal solution is found in a finite number of steps. If no feasible solution exists, the simplex method detects that too.

Linear programming has been applied to a wide variety of problems. For example, its application has included allocation of production facilities to products, allocation of bombers to targets, selection of shipping patterns, determining blending of feed for cattle, production scheduling, and assignment of

machines to jobs. Even though the simplex method is powerful enough to solve all these problems, there are special sub-classes of problems for which still more efficient solution procedures have been developed. These are the transportation problem, the transshipment problem, and the assignment problem. These are covered in detail in any general Operations Research book.^{3, 5, 7}

The linear programming model can be generalized in several ways by removing certain of the underlying assumptions stated earlier. For example, the linearity assumptions could be removed so that the constraints and the objective function can be non-linear. This leads to the general area of non-linear programming and no satisfactory procedure for solving the general problem exists. A second case, integer programming, occurs when the decision variables are allowed to have only integral values. Solution procedures have been developed for this case, but they are computationally feasible only for relatively small problems. Finally, if the deterministic assumption is dropped and some or all of the parameters allowed to be random variables, then this leads to the general area of linear programming under uncertainty. Several reasonable approaches are available for formulating such problems and for solving special cases.

Dynamic programming

This technique is very useful for problems which involve a sequence of inter-related decisions.¹ The problems where dynamic programming can be applied are usually characterized as consisting of several stages—each stage having several possible states associated with it. In general, the states are the various possible conditions in which the system might find itself at that stage. A policy decision is required at each stage, and this serves to transform the current state into a state associated with the next stage (possibly according to a probability distribution). In the process of this transformation (going from one state to the other) the system incurs a contribution to its objective function and the task is to find the sequence of decisions which will lead us to optimize the objective function.

Another required characteristic is the Markov property. That is, given the current state of the system, the optimal policy for the remaining stages should

be independent of the policy adopted in previous stages. Thus, the only information required at any stage is the state the system is in. The technique starts by finding the optimal policy for a one-stage version of the problem. It finds the optimal policy for each state of the last stage. Then, it considers a two-stage problem and finds the optimal policy for all states when the last two stages remain. A recursive functional relationship is usually developed which relates the optimal policy for each state with m stages remaining to the optimal policy for each state with $m-1$ stages remaining. When all the stages have been covered, the optimal decision for all states is known. The technique derives its name from the fact that it is dynamic over the stages. Dynamic programming has been used very successfully in feedback control and servomechanism problems, determination of trajectories, inventory and scheduling processes, allocation of resources, finding shortest paths, etc.

Network flow theory

This technique is concerned mainly with problems that have a network character.⁴ In the theory of graphs, a graph consists of a set of junction points called nodes, with certain pairs of nodes joined by arcs. A network is considered to be a graph with a flow of some type along its arcs. The arcs, in general, could be directed (they can be traversed only in a certain direction) or capacitated (they can take no more than a certain amount of flow). The law of conservation of flow is usually assumed to hold at the nodes. This implies that the net flow into a node equals the net outflow from that node. Examples of problems where these characteristics hold include the road network of a city with vehicles flowing between the intersections, and machine shop with work centers where jobs flow over material-handling routes from one center to the other.

The technique of network flows is used to find solutions to such problems as the maximal flow problem. In a connected network having a single source and sink, this problem involves finding the maximum flow that can take place from the source to the sink, subject to the capacity limitation of the arcs. Although the maximal flow problem can be formulated as a linear programming problem, network theory takes full advantage of the graph structure to

solve it more efficiently. The exact solution procedure is based on the max-flow min-cut theorem. Another problem in graph-like situations is to find the shortest path between two given nodes of the network when the arcs represent the distances between the nodes.

One of the most important offshoots of network flow theory is PERT (program evaluation and review technique). It is used to evaluate schedules and measure and control progress on projects that have a graph characteristic (*e.g.* construction programs, maintenance planning, preparation of proposals). In these cases, the nodes are used to represent an event that is a specific definable accomplishment recognizable at a particular instant in time, and each arc represents an activity that is one of the tasks required by the project. Each task has an associated maximum and minimum completion time, and the cost of doing the task is assumed to vary linearly at a given rate between the two extremes. PERT can be used to find the least-cost solution given a desired completion time. It also finds the critical path of the project; *i.e.*, it identifies the tasks that cause bottlenecks in the project. And finally, it comes up with the earliest and the latest starting time for each task so that the project can be completed on schedule.

Queueing theory

This technique, as the name implies, deals with queues or waiting lines.⁹ A queue or waiting line is formed when customers arrive at a facility and demand services that exceed the current capacity of the facility to provide the service. Queueing theory problems are characterized by an input mechanism, a queue discipline, and a service mechanism. The input mechanism describes the way customers arrive and join the system. The number of customers may be finite or infinite and they may arrive either individually or in groups. The probability distribution for the arrival pattern also needs to be known. The queue discipline determines the formation of the queue and the manner of the customers' behavior while waiting. The disciplines that have been treated in detail include first-come-first-served and various priority procedures. The service mechanism describes the arrangement for serving the customers. The number of servers along with the service time distribution

(distribution of time elapsed from the commencement of service to its completion) needs to be known.

Queueing theory is, in general, concerned primarily with steady-state results, although the differential equations governing the transient case have been developed in many cases. It attempts to answer such questions as the expected waiting time in the queue as well as in the system for a customer, average number of customers in the queue and in the system at any given time, probability distribution for number of customers in the system, probability that a customer comes in to find the system busy, and average idle time for the service facility. By providing these answers, queueing theory helps the decision maker balance the cost of service with the cost associated with waiting for that service, and arrive at decisions regarding the optimal number of servers to have.

Queueing theory has been applied to a wide variety of waiting-line situations. It has helped in analyzing traffic delays at toll booths, processing of jobs on a computer, storage of water at a dam, maintenance of machines, etc.

Inventory theory

This technique deals with determining inventory policies.⁶ There are many reasons why organizations need to maintain an inventory of goods. The fundamental reason for doing so is that it is either physically impossible or economically unsound to have goods arrive in a given system precisely when demands for them occur. Inventory must be carried so that customers don't have to wait for long periods of time. There are, nonetheless, other reasons for holding inventories. For example, the price of some raw material used by a manufacturer may exhibit considerable seasonal fluctuation, and hence the manufacturer may buy it at the appropriate time and keep it in inventory to take advantage of the price changes.

Inventory problems usually involve a stock of some kind on which demands are placed. The stock is depleted on meeting these demands and can be replenished from time to time. Two fundamental questions that must be answered in controlling the inventory are when to replenish the inventory and how much to order for replenishment. In general, it is assumed that the inven-

tory system has no control over the demands for the items which it stocks. Inventory theory attempts to obtain the answers by considering the overall costs to the system. The relevant costs usually turn out to be the cost of procuring the unit, cost of carrying the unit in inventory, cost associated with unsatisfied demand (or stockout cost), salvage cost, and revenue from selling the unit. Other factors that also play a part are costs of operating the inventory system, lead time associated with procuring the unit, discount rate, etc. The problem is complex because each of the cost components has its own characteristic nature. For example, in procurement costs and in revenue derived from sale of units, quantity discounts come in to complicate the situation.

The two basic inventory situations that have been treated quite extensively in the literature are the transaction reporting and the periodic review systems. The inventory is said to be using transaction reporting when all transactions are recorded as they occur and the information is immediately available to the decision maker. Thus, it is possible to make a decision as to whether or not to place an order each time a demand occurs. The policy that has been found optimal in a wide variety of such situations is the (s, S) policy, which is to order an amount $S - s$ whenever the inventory level drops to s . The order quantity is thus fixed, and the time the order is placed is a variable. The inventory is said to be using a periodic review system when the state of the inventory is examined only at discrete, usually equally spaced, points in time. The policy that has been found optimal in a wide variety of such situations is the (R, T) policy, which is to place an order every time T so that the inventory level is raised to R . The time at which the order is placed is thus fixed but the order quantity is variable.

Inventory theory techniques have been applied to many inventory problems, capacity expansion problems, and to some water storage in a dam situations.

Game theory

This technique is concerned mainly with competitive situations where the effectiveness of decisions by one party is dependent on decisions by another party.⁸ This technique has gained

popular recognition because it grew in the context of parlor games. The problems to which this technique can be applied can be characterized by n persons in a competitive situation. Starting from a given point, there is a series of personal moves; at each move the players choose from among several strategies. Depending on the moves chosen, there is a payoff from one player to another. The game could then terminate or start anew from this end position. Games like chess, bridge, roulette fall in this category. A primary objective of game theory is to develop rational criteria for selecting a strategy. It is assumed that all players are rational and that each will attempt to do as well as possible relative to his opponent; that is, all are actively trying to promote their own welfare in opposition to that of the opponent.

The bulk of the research in game theory has been on 2-person zero-sum games. As the name implies, these games involve two adversaries and one player wins whatever the other one loses (*i.e.*, the sum of all the payoffs is zero). In such games, game theory uses the minimax criterion for selecting the optimal strategies for players. In terms of payoff, it implies that the player who receives the payoff should try to maximize the minimum payoff and that the player who pays the payoff should try to minimize the maximum payoff. If the value of the payoff, as determined under these two rules, is the same, the game is said to have a saddle point and the optimal solution is a stable one. When such a saddle point does not exist, players must resort to mixed strategies. It can be shown that such problems can also be formulated as linear programming problems and hence solved by the simplex method.

One generalization of this game is to allow more than two persons to participate in the game. Another is the non-zero sum game where the sum of the payoffs to the players need not be zero. For example, the advertising strategies of competing companies can effect not only how they will split the market but also the total size of the market itself. Since mutual gain is possible, non-zero sum games are further classified in terms of the degree to which the players are permitted to cooperate.

It is quite apparent that the general problem of how to make decisions in

a competitive environment is a very important one. However, game theory has so far succeeded in analyzing only very simple competitive situations and hence its application has been rather limited.

Other techniques

The elements of statistical decision theory are similar to those of the game theory. The major difference between it and game theory is that in statistical decision theory the decision maker is assumed to be playing against a passive opponent, nature, which is not trying to maximize its winnings or minimize its losses. That is, a criterion of rational behavior for the opponent does not exist, or if it does, the decision maker has no knowledge of it.

Sequencing theory deals with the order or sequence in which service is provided to available units by a series of service points. Queueing theory, in contrast, deals with controlling the times of arrivals or the number of servers. In sequencing theory the facilities are fixed and the problem is to sequence the arrivals to optimize the objective. This technique is usually combinatorial in nature and has been used in n -job m -machine problems, line balancing, and traveling salesman problems.

The theory of reliability is concerned with life testing, structural reliability and redundancy considerations, machine maintenance and replacement problems. The theory of stochastic processes concerns itself with sequences of events governed by probabilistic laws. Of special interest are Markov processes and branching processes. In addition, Operations Research borrows standard techniques from several areas such as Statistics, Mathematics, and Electrical Engineering.

References

1. Bellman, R. E., and S. E. Dreyfus. *Applied Dynamic Programming* (Princeton University Press; 1966).
2. Churchman, C. W., R. L. Ackoff and E. L. Arnoff. *Introduction to Operations Research* (John Wiley; 1957).
3. Dantzig, G. B., *Linear Programming and Extensions* (Princeton University Press; 1966).
4. Ford, L. R. and D. R. Fulkerson. *Flows in Networks* (Princeton University Press; 1962).
5. Hadley, G., *Linear Programming* (Addison-Wesley; 1963).
6. Hadley, G. and T. M. Whitin. *Analysis of Inventory Systems* (Prentice Hall; 1970).
7. Hillier, F. S. and G. J. Lieberman, *Introduction to Operations Research* (Holden-Day, Inc.; 1968).
8. Owen, G., *Game Theory* (W. B. Saunders & Co.; 1968).
9. Prabhu, N. U., *Queues and Inventories* (John Wiley; 1965).
10. Saaty, T. L., *Mathematical Methods of Operations Research* (McGraw-Hill; 1959).

Evaluation of microcircuit packaging concepts using digital computer simulation

R. M. Engler

A major portion of the final cost of standard packaged microcircuits is the cost of packaging, not the cost of the integrated circuits themselves. The function of the package is to provide electrical continuity between the microleads on the integrated circuit and the macroleads of a package suitable for mounting on a printed circuit board. At the same time, the package provides mechanical and environmental protection for the circuit as well as paths for the dissipation of internally generated heat. Although a packaging concept can always be found that can provide a solution to these functional requirements and satisfy the additional important constraints of size, weight, and cost, it is easy to see that the comparison of packaging concepts on the basis of these functional requirements (to say nothing of reliability, marketability, availability of component parts, flexibility to change, etc.) is a monumental task.

IN THE CONSUMER-GOODS INDUSTRY, the size-weight constraints are usually relaxed in favor of heavy emphasis on cost. Because final sales price generally reflects the direct-production unit cost, a fruitful area of study for both vendor and user is the effect of wages, component costs, yields, and production volume on unit production cost. The vendor wants to study these factors to achieve an optimum unit cost that will afford him a competitive edge in providing a given packaged microcircuit function. The user should also study the effect of these factors on various packaging-

production concepts so that he may bargain effectively on unit selling price and mesh his future production requirements with the concept that provides him with a competitive edge. To both these groups—vendor and user—the evaluation of package-production unit costs by digital computer simulation offers a great benefit.

The simulation system

The simulation system discussed in this article is IBM's General Purpose Simu-

Reprint RE-18-3-11
Final manuscript received June 29, 1972



Ralph M. Engler
Packaged Circuit Functions
Solid State Division
Somerville, N.J.

received the BSME from Lehigh University in 1962 and the MSME from Rensselaer Polytechnic Institute, Hartford Graduate Center, in 1966. Mr. Engler was employed for five years by United Aircraft where he designed and developed equipment and procedures for microcircuit fabrication. Subsequently, he joined the Central Research Laboratory of Singer Company as a senior engineer in the design and development of custom microcircuits for consumer and industrial products. In January 1969, Mr. Engler transferred to the Kearfott Division of Singer where he continued work on custom monolithic and hybrid circuits for airborne-computer applications. In January 1970, Mr. Engler was engaged by the Power Hybrid Group of the Solid State Division at Somerville. Since that time, he has been engaged as a product-design engineer in the design and production of power-hybrid modules. Mr. Engler is a member of ISHM, Tau Beta Pi, and Pi Tau Sigma, and is co-author of one technical paper.

lation System, GPSS/360.¹ This system consists of a packaged program that has its own block-oriented language. The internal programming of the simulator has already been done and the user has merely to learn this general block language to construct the model of his system. No previous computer-programming experience is necessary to become a competent GPSS "programmer." However, the user must be able to define the precise sequential steps of his process and the logical decision points at which certain tests determine the next step. Each sequential step of the process is simulated by a specific block type and is physically represented by a single IBM card. These cards are assembled sequentially into a deck that then represents the operation of the user's system. To this deck are added cards that define symbols used in the program to control input-output data, and a few general control cards supplied by the computer system programmer to enable the computer to recognize the user's deck and perform the required simulation. Data input generally takes the form of functional definitions and initialization of specific easily addressable memory locations. Data output is provided by matrix savevalues (an x - y lattice of memory elements), tables, and certain standard statistics on queues, storages, and equipment.

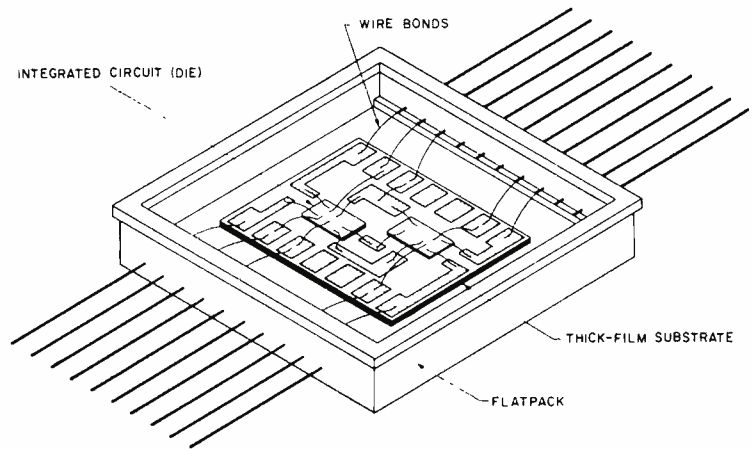


Fig. 1—Chip-and-wire package.

It is quite possible that models can be built with sufficient documentation of the required inputs and the furnished outputs to enable management and engineering personnel having no knowledge of GPSS programming to perform studies of various operating or manufacturing strategies. Some systems could be reduced to a "fill in the blanks and read the answers" level of simplicity.

An example

An actual example of a previously modeled microcircuit packaging-production

concept is the "chip-and-wire hybrid." The basic package might appear as shown in Fig. 1. The packaging-production process is described in the flow-chart, Fig. 2. In the usual manner, oval blocks indicate inputs and outputs to the system, diamond-shaped blocks indicate decision points, and rectangular blocks indicate processing steps. The primary flow of parts (no repair) is: die bond, wire bond from die to sub-assembly of substrate to flatpack, epoxy cure, wire bond from substrate to package, assembly of lid to flatpack,

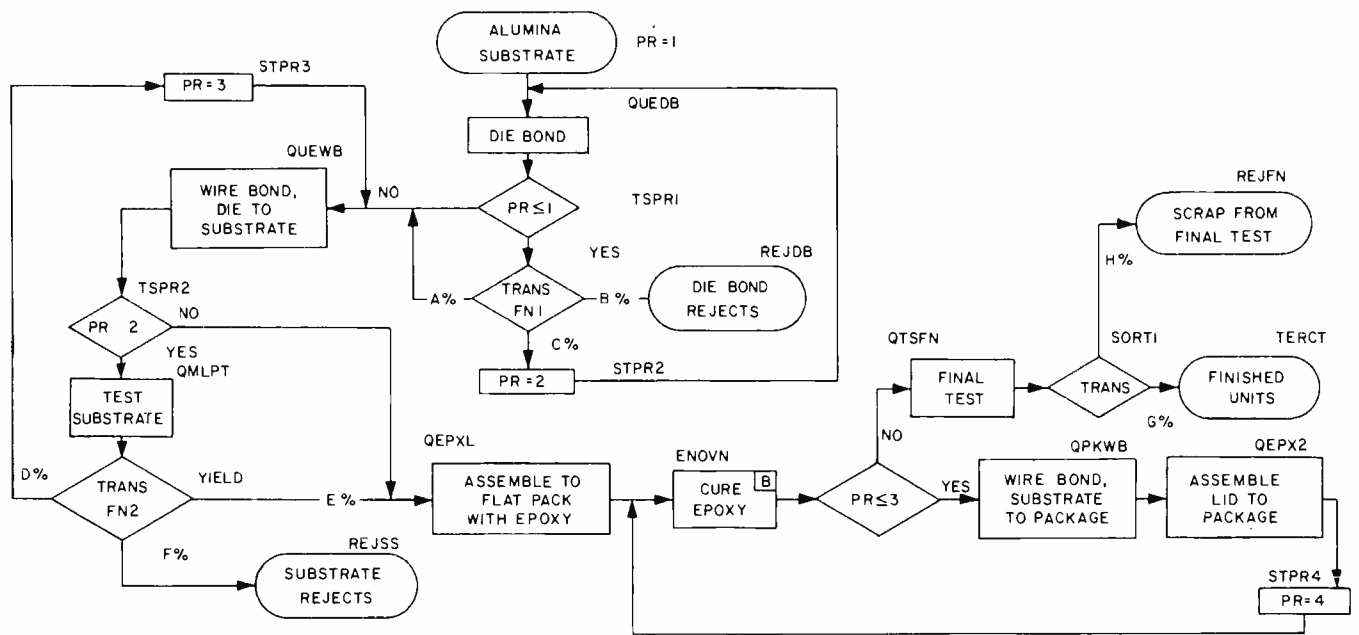


Fig. 2—Chip-and-wire production-process flowchart.

Table I—Comparison of chip-and-wire package concept with several others.

Column No.	1	2	3	4	5	6	7	8	9	10	11
Model	Avg. No Syst/Day	Avg. No Syst/Year	Unit cost = % Avg. cost	Tot. val. rejects = % No. rej.	Tot. val. rejects = % No. rej.	Avg. val.	Capital utilization = % Capital equipment	No tech	Avg. unit cost incl tech ovhd	Yearly operating cost	
A chip-and-wire	5.68	1362	\$13.15 \$35.49	37.1	\$760 168	4.52	\$ 9003 \$23500	38.3	4	\$57.19	\$77800
	B	5.68	1362	9.57 29.62	32.3	540 168	3.21 23500	38.3	4	51.32	70200
A Concept #2	13.85	3320	5.41 18.10	29.7	244 45	5.42	5072 31500	16.1	3	26.60	88200
	B	47.3	11350	1.08 5.15	20.3	57 52	1.10 31500	11.8	3	7.64	86700
A Concept #3	4.97	1192	6.17 21.02	29.4	402 77	5.22	6557 37100	17.7	2	36.82	43800
	B	4.97	1192	2.67 14.30	18.7	122 77	1.58 37100	17.7	2	30.10	35900
A Concept #4	7.10	1700	13.47 23.35	57.7	230 28	8.22	5201 26300	19.8	3	39.95	68000
	B	7.10	1700	9.97 18.66	53.5	133 28	4.75 26300	19.8	3	35.26	60000

epoxy cure, and final test. It is interesting to note the two repair loops in evidence for die bonding and wire bonding and the dual function of the epoxy curing oven. The letter **B** in the upper right-hand corner of the CURE EPOXY block indicates a batch-processing station as opposed to a facility station capable of processing one unit at a time. The capital-letter labels adjacent to some blocks indicate symbolic addresses used within the model. Units rejected and considered repairable are assigned increasing priorities because, in reality, they were started first and are probably scheduled to be finished first. The effect of introducing repairs into a processing station and the decision to repair or scrap a subassembly are other possible questions that may be investigated by the use of the GPSS.

Quite often, a package depends for its economic viability on the percentage yield (ratio of number of good units to number processed) at various process steps. In lieu of factual precedents, yields are assumed that add to or detract from the desirability of the package. Even in this simple example, small variation of yields **A** through **H** can produce wide variations in the combined results. Thus, digital simulation can provide a means for comparing differing assumptions, and, indeed, can pinpoint quantitatively the most sensitive assumptions for more detailed experimental evaluation.

In addition to the question of yield, the time-cost ratio associated with each process step may be a very complex

function depending upon such things as operator skill, equipment investment, quality control on incoming parts, and even time of day. Although this model makes no extensive provisions for such contingencies, the degree to which digital simulation can realistically model such factors is limited only by the imagination of the simulator.

The example under discussion was coded and run on an IBM model 360/50 and 360/30 as part of a general comparison of a new package concept against some conventional concepts. The time unit chosen was 0.001 hour; the simulation was carried to completion for 100 units. A typical simulation run of this type simulates 14 days of operation in two minutes on the model 360/50. The cost of the simulation (purchased computer time) might be \$8.00.

The results of the comparison of the "chip-and-wire" package with several others are shown in Table I. This table is included as a demonstration of some of the outputs available from such a simulation. The answers output from the model are always a function of the question under study. Through the use of variable statements (both arithmetic and Boolean) and functional definitions, the simulator can construct a virtually unlimited number of answer algorithms. The GPSS itself makes heavy use of standard statistical techniques and provides an easy means of obtaining semi-processed data in the form of tabulations involving frequency distributions (the unit of which may, in turn, be an event dependent upon a complex

algorithm) and utilization levels. There is also easy access to print-plot graphic outputs to facilitate communication of results.

Extension into other uses

Although the type of application discussed in this paper is useful for engineering/management evaluation of technical concepts on a relative, quantitative basis, digital simulation has meaning far beyond this sphere of interest. In its ability to simulate any process capable of definition as a series of steps in time, the method should become a powerful tool for manufacturing engineers in the improvement of production processes. Personnel involved in the specific areas of quality-control testing and production control should also be able to make key decisions based upon the simulated results of several alternative operating strategies. Just as the military has for years utilized digital simulation in the form of computer-based war games² to enable officers to test battle strategies, corporation management should find extensive use for a model of their business that would respond to changes in operating strategies in hours instead of months.

Conclusions

Although the type of evaluation under discussion could be carried forward without a computer, the use of computer-based simulation has some distinct advantages. Among the advantages are the speed of obtaining answers, the ease of change of data, the relatively low cost, and the ease of adaptation of results to statistical digestion. There are disadvantages in the false sense of security too often generated by the "sacred" numbers issuing forth from the computer, and in the usual difficulty in obtaining an exact model of the physical system. However, these two problems are not strangers to the user of engineering-mathematical approaches to problem solution, and, in general, the relative ease and speed of obtaining results, coupled with the quantitative nature of these results, justifies increased use of these techniques by both engineering and production disciplines.

References

1. *General Purpose Simulation System*; Application Description, H20-0186-2; Introductory User's Manual, H20-0304-0; User's Manual, H20-0326-0 (IBM; 1967).
2. McMillan and Gonzales, *Systems Analysis* (Irwin; 1966).

Solution of differential and integral equations with Walsh functions

M. S. Corrington

Differential and integral equations can be solved using Walsh functions. Such functions are particularly suited to studies of nonlinear systems.

WALSH FUNCTIONS¹ are now widely used to analyze communication systems² since they have most of the properties of Fourier series but are more suited to nonlinear studies.³ The notation used for the Walsh functions by various authors is not standard, so will now be developed.

Rademacher functions

An incomplete set of periodic rectangular orthonormal functions was developed by Hans Rademacher⁴ in 1922. The first five are shown by Fig. 1. The first one, $r_0(t)$, is equal to unity for $0 \leq t$. The next one, $r_1(t)$, is a square wave of unit height with a period equal 2^{k-1} . The functions are periodic, so $r_k(t+n) = r_k(t)$, where $n = \pm 1, \pm 2, \pm 3, \dots$

All of the Rademacher functions have odd symmetry about $t=0$ and $t=1/2$. This means that the set is incomplete since the sum of any number of them will have odd symmetry about these two points. It is not possible to expand a function which has even symmetry about $t=0$ or $t=1/2$ in a series of $r_k(t)$.

Walsh functions

The Rademacher functions have been combined by Walsh¹ to form a complete orthonormal set of rectangular waves. The notation used here is not the same as given by Walsh, but the functions have the same shape.

Let $b_n \dots b_2 b_1$ be an n -digit binary number, where the b_i are each 0 or 1 and $b_n = 1$. The Walsh functions will be defined as the product of the n Rademacher functions

$$\psi_{b_n \dots b_2 b_1}(t) = [r_n(t)]^{b_n} \dots [r_2(t)]^{b_2} [r_1(t)]^{b_1} \quad (1)$$

Thus

$$\psi_0(t) = r_0(t) \quad (2)$$

$$\psi_1(t) = r_1(t) \quad (3)$$

$$\psi_{10}(t) = r_2(t) \quad (4)$$

$$\psi_{11}(t) = r_2(t) r_1(t) \quad (5)$$

$$\psi_{100}(t) = r_3(t) \quad (6)$$

$$\psi_{101}(t) = r_3(t) r_1(t) \quad (7)$$

Murlan S. Corrington, Ldr.,
Computer Applications Group,
Applied Computer Systems Laboratory
Advanced Technology Laboratories
Camden, New Jersey
received the BSEE (highest honors) in 1934 from the South Dakota School of Mines and Technology and the MSc in 1936 from Ohio State University. From 1935 to 1937 he was a graduate assistant in the Physics Department of Ohio State University where he specialized in mathematical physics. In 1937 he joined the Rochester Institute of Technology where he taught mathematics, mechanics, and related subjects. In 1942 he joined the Television Division of RCA where he performed mathematical engineering on FM, loudspeakers, circuit theory, transient analysis, distortion in phonograph records, etc. In 1953 he became a manager of the Advanced Development Section with responsibility for audio, acoustics, receiving antennas, radiation measurements, and theoretical work. In 1959 he transferred to Advanced Technology Laboratories as a leader in the Signal-Processing Group. Work there included nonlinear signal processing, applications of Hilbert transforms, statistical theory of noise, Monte Carlo methods and numerical analysis. He is now responsible for work on design automation, precision artwork generation, numerical and mathematical analysis, circuit theory, computer simulation of communication systems, digital filtering, image processing, and computer programming. Mr. Corrington is a Fellow of the Acoustical Society of America, a Fellow of the IEEE, and a member of the Society for Industrial and Applied Mathematics, Sigma Pi Sigma, and Sigma Xi. He has been active on many national and local IEEE committees, has been a member of the Administrative committees of two IEEE groups of the Solid-State Circuits Council, has helped write many industry-wide standards, and has won two national IEEE awards for his work in audio and electroacoustics. He is listed in *Who's Who in the East*, *American Men of Science*, and *Who's Who in Engineering*. He has published over 65 technical articles on frequency modulation, circuit theory, mathematics, transients, and cone motion in loudspeakers, distortions in phonograph records, evaluation of integrals, nonlinear analysis, digital filtering, computer simulation, and transients in filters. He is the author of textbooks on applied mathematics and machine shop practice, and holds eight United States patents.

Reprint RE-18-3-14
Final manuscript received July 20, 1972.



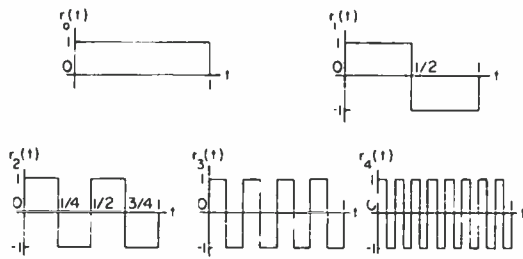


Fig. 1—Rademacher functions

In the discussion that follows the binary-digit subscript will usually be used to identify the Walsh functions, but occasionally a letter equivalent will be used for convenience. The first sixteen of these functions are shown by Fig. 2. The ones in the left column have even symmetry about the origin, and the ones in the right column have odd symmetry.

Multiplication

If two Walsh functions

$$\psi_{b_n \dots b_2 b_1}(t) = [r_n(t)]^{b_n} \dots [r_2(t)]^{b_2} [r_1(t)]^{b_1} \quad (8)$$

and

$$\psi_{a_m \dots a_2 a_1}(t) = [r_m(t)]^{a_m} \dots [r_2(t)]^{a_2} [r_1(t)]^{a_1} \quad (9)$$

are multiplied together, the product can be obtained by modulo two addition of the binary digits, since the square of any Rademacher function in the product of Eqs. 8 and 9 is unity. The Walsh functions thus form a closed set under multiplication.

Example: Multiply $\psi_{110}(t)$ by $\psi_{11}(t)$.

By modulo two addition of the binary digits,

$$\psi_{110}(t)\psi_{11}(t) = \psi(t).$$

This can be checked by Fig. 2.

Orthonormality

It has been proved^{5,6} that the Walsh functions form an orthonormal system in $0 \leq t < 1$. Thus

$$\int_0^1 \psi_m(t) \psi_n(t) dt = \begin{cases} 0 & (m \neq n) \\ 1 & (m = n). \end{cases} \quad (10)$$

Walsh series

Every function $f(t)$ which is absolutely integrable in the interval $0 \leq t < 1$ can be

expanded formally in a series of the form

$$f(t) = \sum_{n=0}^{\infty} C_n \psi_n(t) \quad (11)$$

where the constants C_n are obtained from

$$C_n = \int_0^1 f(t) \psi_n(t) dt \quad (n=0, 1, 2, \dots) \quad (12)$$

Convergence

The convergence conditions are given by Walsh¹, Paley⁵, and Fine⁶. If $f(t)$ is continuous in $0 \leq t < 1$, the series (Eq. 11) converges uniformly to the value $f(t)$, if the terms are grouped so that each group contains all of the Walsh functions designated by a given number

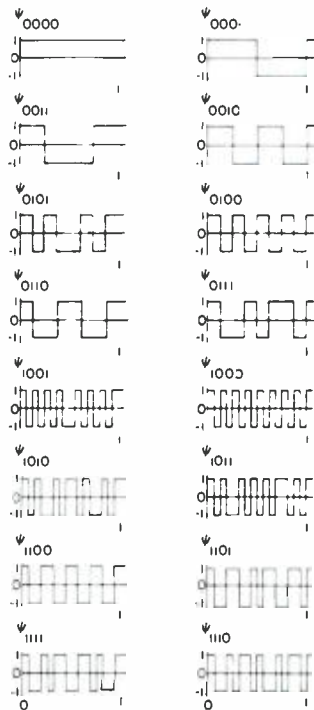


Fig. 2—Walsh functions.

of binary digits. If $f(t)$ is not continuous, there is convergence in the mean. If the Walsh series is truncated at the end of a group represented by all of the terms given by n binary digits, the partial sum of the first 2^n terms of the series will equal the average value of the function in each subinterval of length 2^{-n} .

Walsh series for $t^m, 2 \leq t < 1, m=1, 0, \dots$

The Walsh series for $f(t)=t^m, 0 \leq t < 1, m=0, 1, 2, \dots$,

$$f(t) = \sum_{n=0}^{\infty} D_n(m) \psi_n(t) \quad (13)$$

is obtained from

$$D_n(m) = \int_0^1 t^m \psi_n(t) dt. \quad (14)$$

To find a given $D_n(m)$, the integral for the desired Walsh coefficient can be evaluated easily by integrating by parts. *Example:* Derive a formula for $D_{10}(m)$ using integration by parts.

$$\begin{aligned} D_{10}(m) &= \int_0^1 t^m \psi_{10}(t) dt \\ &= \frac{t^{m+1}}{m+1} \psi_{10}(t) \Big|_0^1 \\ &\quad - \int_0^1 \frac{t^{m+1}}{m+1} \left(\frac{d \psi_{10}(t)}{dt} \right) dt \\ &= - \int_0^1 \frac{t^{m+1}}{m+1} [\delta(t) - 2\delta(t-1/4) \\ &\quad + 2\delta(t-1/2) - 2\delta(t-3/4) + \delta(t-1)] dt \\ &= [2/4^{m+1}(m+1)] [1 - 2^{m+1} + 3^{m+1} \\ &\quad - \frac{1}{2} 4^{m+1}] \end{aligned} \quad (15)$$

where $\delta(t)$ is the unit-impulse function. By this process the constants of Table I can be derived.

Table I can be used to expand a polynomial in $t, 0 \leq t < 1$, in a series of Walsh functions by expanding each power of t in a Walsh series and adding the results, after multiplication by the coefficients in the polynomial.

Integration of Walsh functions

The indefinite integrals of the first four Walsh functions are shown by Fig. 3. Thus

$$I_0(x) = \int_0^x \psi_0(t) dt = x \quad (0 \leq x < 1)$$

$$= \frac{1}{2} \psi_0(x) - \frac{1}{4} \psi_1(x) - \frac{1}{8} \psi_{10}(x) - \frac{1}{16} \psi_{100}(x) - \dots \quad (16)$$

by Table I. Similarly

$$I_1(x) = \int_0^x \psi_1(t) dt = x \quad (0 \leq x \leq \frac{1}{2})$$

$$= i - x \quad (\frac{1}{2} \leq x < 1)$$

$$= \frac{1}{2} x [\psi_0(x) + \psi_1(x)] + \frac{1}{2} (1-x) [\psi_0(x) - \psi_1(x)]$$

$$= \frac{1}{2} \psi_0(x) - \frac{1}{2} \psi_1(x) + x \psi_1(x)$$

$$= \frac{1}{4} \psi_0(x) - \frac{1}{8} \psi_{11}(x) - \frac{1}{16} \psi_{101}(x) - \frac{1}{32} \psi_{1001}(x) - \dots \quad (17)$$

Each integral can be expressed by a series

$$\int_0^x \psi_n(t) dt = \sum_{m=0}^{\infty} E_n(m) \psi_m(x) \quad (18)$$

where the $E_n(m)$ are given by Table II.

Solution of differential equations with Walsh functions

When Walsh functions are differentiated, the result is a series of Dirac delta functions, one for each discontinuity, with alternating signs. Second and higher-order derivatives lead to higher-order singularity functions. A

Table I — Coefficients of Walsh series

		$D_n(m) = \int_0^1 t^m \psi_n(t) dt$								$t^m = \sum_{n=0}^{\infty} D_n(m) \psi_n(t)$		
		$m=0$	1	2	3	4	5	6	7	8		
$n=$	0	1	$\frac{1}{2}$	$\frac{1}{3}$	$\frac{1}{4}$	$\frac{1}{5}$	$\frac{1}{6}$	$\frac{1}{7}$	$\frac{1}{8}$	$\frac{1}{9}$		
	1	0	$-\frac{1}{4}$	$-\frac{1}{4}$	$-\frac{7}{32}$	$-\frac{3}{16}$	$-\frac{31}{192}$	$-\frac{9}{64}$	$-\frac{127}{1024}$	$-\frac{85}{768}$		
	10	0	$-\frac{1}{8}$	$-\frac{1}{8}$	$-\frac{31}{256}$	$-\frac{15}{128}$	$-\frac{691}{6144}$	$-\frac{219}{2048}$	$-\frac{13231}{131072}$	$-\frac{9325}{98304}$		
	11	0	0	$\frac{1}{16}$	$\frac{3}{32}$	$\frac{27}{256}$	$\frac{55}{512}$	$\frac{429}{4096}$	$\frac{819}{8192}$	$\frac{18565}{196608}$		
	100	0	$-\frac{1}{16}$	$-\frac{1}{16}$	$-\frac{127}{2048}$	$-\frac{63}{1024}$	$-\frac{11971}{196608}$	$-\frac{3939}{65536}$	$-\frac{993007}{16777216}$	$-\frac{731725}{12582912}$		
	101	0	0	$\frac{1}{32}$	$\frac{3}{64}$	$\frac{111}{2048}$	$\frac{235}{4096}$	$\frac{7659}{131072}$	$\frac{15309}{262144}$	$\frac{1454125}{25165824}$		
	110	0	0	$\frac{1}{64}$	$-\frac{3}{128}$	$\frac{123}{4096}$	$\frac{295}{8192}$	$\frac{10749}{262144}$	$\frac{23499}{524288}$	$\frac{2390725}{50331648}$		
	111	0	0	0	$-\frac{3}{256}$	$-\frac{3}{128}$	$-\frac{535}{16384}$	$-\frac{645}{16384}$	$-\frac{46179}{1048576}$	$-\frac{37065}{786432}$		
	1000	0	$-\frac{1}{32}$	$-\frac{1}{32}$	$-\frac{511}{16384}$	$-\frac{255}{8192}$	$-\frac{195331}{6291456}$	$-\frac{64899}{2097152}$	$-\frac{66198511}{2147483648}$	$-\frac{49424845}{1610612736}$		

Table II — Coefficients for integrating Walsh functions, $E_n(m)$, Eq. 18.

$n=$	$m=0$	1	2	3	4	5	6	7	8	9	10	11	12	13	14	15
0	$\frac{1}{2}$	$-\frac{1}{4}$	$-\frac{1}{8}$	0	$-\frac{1}{16}$	0	0	0	$-\frac{1}{32}$	0	0	0	0	0	0	0
1	$\frac{1}{4}$	0	0	$-\frac{1}{8}$	0	$-\frac{1}{16}$	0	0	0	$-\frac{1}{32}$	0	0	0	0	0	0
10	$\frac{1}{8}$	0	0	0	0	0	$-\frac{1}{16}$	0	0	0	$-\frac{1}{32}$	0	0	0	0	0
11	0	$\frac{1}{8}$	0	0	0	0	0	$-\frac{1}{16}$	0	0	0	$-\frac{1}{32}$	0	0	0	0
100	$\frac{1}{16}$	0	0	0	0	0	0	0	0	0	0	0	$-\frac{1}{32}$	0	0	0
101	0	$\frac{1}{16}$	0	0	0	0	0	0	0	0	0	0	0	$-\frac{1}{32}$	0	0
110	0	0	$\frac{1}{16}$	0	0	0	0	0	0	0	0	0	0	0	$-\frac{1}{32}$	0
111	0	0	0	$\frac{1}{16}$	0	0	0	0	0	0	0	0	0	0	0	$-\frac{1}{32}$
1000	$\frac{1}{32}$	0	0	0	0	0	0	0	0	0	0	0	0	0	0	0
1001	0	$\frac{1}{32}$	0	0	0	0	0	0	0	0	0	0	0	0	0	0
1010	0	0	$\frac{1}{32}$	0	0	0	0	0	0	0	0	0	0	0	0	0
1011	0	0	0	$\frac{1}{32}$	0	0	0	0	0	0	0	0	0	0	0	0
1100	0	0	0	0	$\frac{1}{32}$	0	0	0	0	0	0	0	0	0	0	0
1101	0	0	0	0	0	$\frac{1}{32}$	0	0	0	0	0	0	0	0	0	0
1110	0	0	0	0	0	0	$\frac{1}{32}$	0	0	0	0	0	0	0	0	0
1111	0	0	0	0	0	0	0	$\frac{1}{32}$	0	0	0	0	0	0	0	0

careful study of these functions has shown that such series are not very useful in solving differential equations since the resulting series are usually divergent.

If the Walsh functions are integrated, the discontinuities are removed, as shown by Fig. 3. Successive integrals smooth the functions even more. Table II gives the coefficients, $E_n(m)$, for performing the integration of a given Walsh series.

The differential equations will be solved for the highest derivative first. This result will then be integrated successively the required number of times to give the solution to the differential equation.

Integral representation of derivatives

Consider the differential equation

$$\frac{d^n y}{dx^n} + a_1(x) \frac{d^{n-1} y}{dx^{n-1}} + \dots + a_n(x) y = f(x) \quad (19)$$

where it will be assumed that the a 's are well behaved at the origin. Let the highest derivative be

$$\frac{d^n y}{dx^n} = u(x) \quad (20)$$

Then

$$\frac{d^{n-1} y}{dx^{n-1}} = \int_0^x u(t) dt + C_1 \quad (21)$$

where C_1 is the constant of integration. Integrating again gives

$$\frac{d^{n-2} y}{dx^{n-2}} = \int_0^x ds \int_0^s u(t) dt + C_1 x + C_2 \quad (22)$$

where C_2 is a second integration constant. Interchange the order of integration to give

$$\begin{aligned} \frac{d^{n-2} y}{dx^{n-2}} &= \int_0^x u(t) dt \int_t^x ds + C_1 x + C_2 \\ &= \int_0^x (x-t) u(t) dt + C_1 x + C_2 \end{aligned} \quad (23)$$

This process may be continued to give

$$y = \frac{1}{(n-1)!} \int_0^x (x-t)^{n-1} u(t) dt + \sum_{k=0}^{n-1} C_{n-k} \left(\frac{x^k}{k!} \right) \quad (24)$$

If the integral representations for the derivatives—Eqs. 21, 23, and 24—are substituted into the differential equation (19), the result is

$$\begin{aligned} u(x) + \int_0^x \left[a_1(x) + a_2(x)(x-t) + a_3(x) \frac{(x-t)^2}{2!} + \dots + a_n(x) \frac{(x-t)^{n-1}}{(n-1)!} \right] u(t) dt \\ = f(x) - a_1(x) C_{1-} a_2(x) [C_1 x + C_2] \\ - \dots - a_n(x) \sum_{k=0}^{n-1} C_{n-k} \left(\frac{x^k}{k!} \right) \end{aligned} \quad (25)$$

or

$$\begin{aligned} u(x) + \sum_{k=1}^n \frac{a_k(x)}{(k-1)!} \int_0^x (x-t)^{k-1} u(t) dt \\ = g(x) \end{aligned} \quad (26)$$

where

$$g(x) = f(x) - \sum_{k=1}^n a_k(x) \sum_{j=0}^{k-1} C_{n-j} \frac{x^j}{j!} \quad (27)$$

Solution of integral equation using Walsh functions

Eq. 26 is Volterra's linear integral equation of the second kind (Ref. 7, p.3). For it to have a solution it is necessary that the C 's have definite values. These are determined by the boundary conditions for the differential equation.

The solution is obtained by the method of successive substitutions (Ref. 7, Chap. 2). Assume $a_k(x) \neq 0$ and $g(x) \neq 0$ are real and continuous in $0 \leq x < 1$. To start the solution let

$$\begin{aligned} u_1(x) &= g(x) \\ &- \sum_{k=1}^n \frac{a_k(x)}{(k-1)!} \int_0^x (x-t)^{k-1} u_0(t) dt \end{aligned} \quad (28)$$

and assume an approximation to the desired result, $u_0(x)$. Substitute this in Eq. 28 and find $u_1(x)$, which is an improved result. Substitute $u_1(x)$ into the integral (eq. 28) and find a new approximation, $u_2(x)$. The process of iteration is continued until the result is as accurate as desired. The sequence of partial sums converges absolutely whenever the integrand is well behaved.

The initial approximation can be one or two terms of a Walsh series. The solution requires the expansion of integrals of type

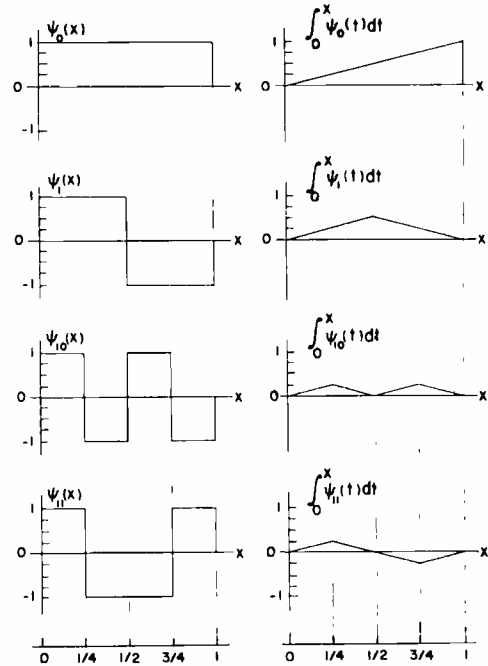


Fig. 3—Integrals of Walsh functions.

$$\frac{1}{k!} \int_0^x (x-t)^k \psi_n(t) dt \quad (k=0, 1, 2, \dots)$$

in a Walsh series. The case for $k=0$ has already been solved and the series coefficients, $E_n(m)$, are given in Table II. The series for higher values of k will now be derived.

Evaluation of weighted integrals

Expand the weighted indefinite integrals of $\psi_n(x)$ used to solve Volterra's integral equation in a Walsh series. Then

$$\begin{aligned} \frac{1}{\Gamma(m+1)} \int_0^x (x-t)^m \psi_n(t) dt \\ = \sum_{r=0}^{\infty} F_r(m, n) \psi_r(x) \end{aligned} \quad (29)$$

Multiply both sides by $\psi_r(x) dx$ and integrate from 0 to 1. The Walsh series coefficients are given by

$$\begin{aligned} F_r(m, n) \\ = \frac{1}{\Gamma(m+1)} \int_0^1 \psi_r(x) dx \int_0^x (x-t)^m \psi_n(t) dt \end{aligned} \quad (30)$$

The coefficients $F_r(m, n)$ can be evaluated in the following manner.

Example: Expand the integral in a Walsh series.

$$\frac{1}{m!} \int_0^x (x-t)^m \psi_1(t) dt$$

Table IV — Table of $F_r(2,n)$.

$$\frac{1}{2!} \int_0^x (x-t)^2 \psi_n(t) dt = \sum_{r=0}^{\infty} F_r(2, n) \psi_r(x)$$

$r =$	0	1	10	11	100	101	110	111
$n = 0$	$\frac{1}{24}$	$-\frac{7}{192}$	$-\frac{31}{1536}$	$\frac{1}{64}$	$-\frac{127}{12288}$	$\frac{1}{128}$	$\frac{1}{256}$	$-\frac{1}{512}$
1	$\frac{7}{192}$	$-\frac{1}{32}$	$-\frac{1}{64}$	$\frac{17}{1536}$	$-\frac{1}{128}$	$\frac{65}{12288}$	$\frac{1}{512}$	0
10	$\frac{31}{1536}$	$-\frac{1}{64}$	$\frac{1}{128}$	$\frac{1}{256}$	$-\frac{1}{256}$	$\frac{1}{512}$	$\frac{17}{12288}$	0
11	$\frac{1}{64}$	$\frac{17}{1536}$	$-\frac{1}{256}$	0	$\frac{1}{512}$	0	0	$\frac{17}{12288}$
100	$\frac{127}{12288}$	$-\frac{1}{128}$	$-\frac{1}{256}$	$\frac{1}{512}$	$-\frac{1}{512}$	$\frac{1}{1024}$	$\frac{1}{2048}$	0
101	$\frac{1}{128}$	$\frac{65}{12288}$	$-\frac{1}{512}$	0	$\frac{1}{1024}$	0	0	$\frac{1}{2048}$
110	$\frac{1}{256}$	$\frac{17}{512}$	$\frac{1}{12288}$	0	$\frac{1}{2048}$	0	0	0
111	$\frac{1}{512}$	0	0	$\frac{17}{12288}$	0	$\frac{1}{2048}$	0	0

$$= \left(\frac{-1}{m!} \right) \left(\frac{(x-t)^{m+1}}{m+1} \right) \Big|_0^x$$

$$= \frac{x^{m+1}}{(m+1)!} \quad (0 \leq x < \frac{1}{2})$$

$$= \left(\frac{-1}{m!} \right) \left(\frac{(x-t)^{m+1}}{m+1} \right) \Big|_0^{1/2}$$

$$+ \left(\frac{1}{m!} \right) \left(\frac{(x-t)^{m+1}}{m+1} \right) \Big|_{1/2}^x$$

$$= \frac{x^{m+1} - 2(x - \frac{1}{2})^{m+1}}{(m+1)!} \quad (\frac{1}{2} \leq x < 1)$$

$$= \frac{x^{m+1}}{(m+1)!} \psi_0(x)$$

$$- \frac{(x - \frac{1}{2})^{m+1}}{(m+1)!} [\psi_0(x) - \psi_1(x)]$$

$$(0 \leq x < 1) \tag{31}$$

Expand each power of x and $x-1/2$ in Eq. 31 in a Walsh series, using the coefficients $D_n(m)$ of Table I. Multiply the Walsh functions and collect terms to give the coefficients $F_r(m, 1)$. The results for $m=1$ and 2 are given in Tables III and IV. A similar process can be used for higher values of n .

Example: Solve the differential equation $dy/dx - y = 0$ with the boundary conditions $y=1$ at $x=0$.

Let $dy/dx = u(x)$

so

$$y = \int_0^x u(t) dt + 1.$$

The integral equation is

$$u(x) = 1 + \int_0^x u(t) dt.$$

The first approximation, for small x , will be taken as the constant term on the right of the integral equation. Let $u_0(x) = \psi_0(x)$. Then

$$u_1(x) = \psi_0(x) + \int_0^x \psi_0(t) dt$$

$$= \frac{3}{2} \psi_0(x) - \frac{1}{4} \psi_1(x)$$

by Table II. The second approximation is

$$u_2(x) = \psi_0(x) + \int_0^x \left[\frac{3}{2} \psi_0(t) - \frac{1}{4} \psi_1(t) \right] dt$$

$$= \frac{27}{16} \psi_0(x) - \frac{3}{8} \psi_1(x) - \frac{3}{16} \psi_{10}(x)$$

$$+ \frac{1}{32} \psi_{11}(x) - \dots$$

by Table II. The third approximation is

$$u_3(x) = \psi_0(x) + \int_0^x \left[\frac{27}{16} \psi_0(t) - \frac{3}{8} \psi_1(t) - \frac{3}{16} \psi_{10}(t) + \frac{1}{32} \psi_{11}(t) - \dots \right] dt$$

$$= 1.7266 \psi_0(x) - 0.4180 \psi_1(x)$$

$$- 0.2109 \psi_{10}(x) + 0.0469 \psi_{11}(x)$$

$$- 0.0625 \psi_{100}(x) + 0.0234 \psi_{101}(x)$$

$$+ 0.0117 \psi_{110}(x) - 0.0020 \psi_{111}(x)$$

$$+ \dots$$

This process can be continued to give any prescribed accuracy. The final result for an eight-term approximation is

$$u(x) = \frac{dy}{dx} = e^x = 1.71828 \psi_0(x)$$

Table III — Table of $F_r(1,n)$

$$\int_0^x (x-t) \psi_n(t) dt = \sum_{r=0}^{\infty} F_r(1, n) \psi_r(x)$$

$r =$	0	1	10	11	100	101	110	111
$n = 0$	$\frac{1}{6}$	$-\frac{1}{8}$	$-\frac{1}{16}$	$\frac{1}{32}$	$-\frac{1}{32}$	$\frac{1}{64}$	$-\frac{1}{128}$	0
1	$\frac{1}{8}$	$-\frac{1}{12}$	$-\frac{1}{32}$	0	$-\frac{1}{64}$	0	0	$\frac{1}{128}$
10	$\frac{1}{16}$	$\frac{1}{32}$	$-\frac{1}{48}$	0	$-\frac{1}{128}$	0	0	0
11	$\frac{1}{32}$	0	0	$-\frac{1}{48}$	0	$-\frac{1}{128}$	0	0
100	$\frac{1}{32}$	$-\frac{1}{64}$	$-\frac{1}{128}$	0	$-\frac{1}{192}$	0	0	0
101	$\frac{1}{64}$	0	0	$-\frac{1}{128}$	0	$-\frac{1}{192}$	0	0
110	$-\frac{1}{128}$	0	0	0	0	0	$-\frac{1}{192}$	0
111	0	$\frac{1}{128}$	0	0	0	0	0	$-\frac{1}{192}$

Table V — Comparison of eight-term approximation with true value.

Range	Eight-term approximation	e^x at mid-interval
$0 - \frac{1}{8}$	1.06519	1.06449
$\frac{1}{8} - \frac{2}{8}$	1.20701	1.20623
$\frac{2}{8} - \frac{3}{8}$	1.36773	1.36684
$\frac{3}{8} - \frac{4}{8}$	1.54983	1.54883
$\frac{4}{8} - \frac{5}{8}$	1.75621	1.75505
$\frac{5}{8} - \frac{6}{8}$	1.99003	1.98874
$\frac{6}{8} - \frac{7}{8}$	2.25499	2.25353
$\frac{7}{8} - 1$	2.55525	2.55359

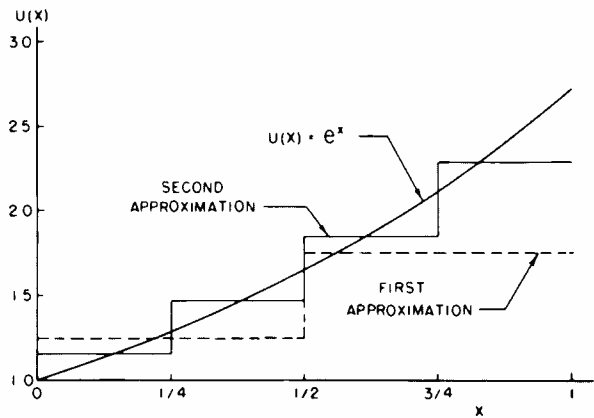


Fig. 4—First and second approximation to $u(x) = e^x$.

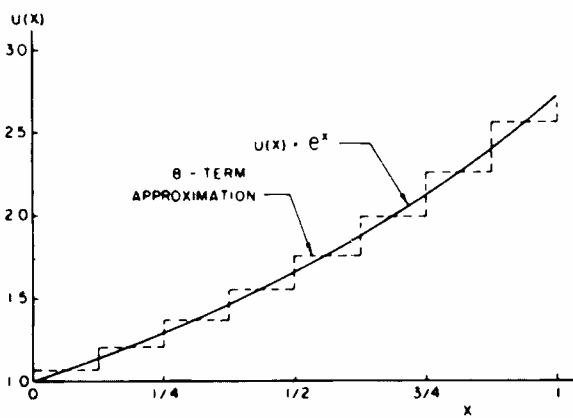


Fig. 5—Eight-term approximation to $u(x) = e^x$.

$$\begin{aligned}
 & -0.42084 \psi_1(x) - 0.21367 \psi_{10}(x) \\
 & + 0.05233 \psi_{11}(x) - 0.10725 \psi_{100}(x) \\
 & + 0.02627 \psi_{101}(x) + 0.01334 \psi_{110}(x) \\
 & - 0.00327 \psi_{111}(x) + \dots
 \end{aligned}$$

Integration, using Table II gives the value of y , since

$$y = 1 + \int_0^x u(x) dx = e^x$$

Fig. 4 shows the first and second approximations to the solution and Fig. 5 shows the eight-term approximation. If a smooth curve is drawn through the midpoint of each horizontal step, it will be very close to the correct value. Table V shows a comparison of the eight-term approximation and the true value at each mid-interval. The accuracy is very good considering that the series was truncated after the eighth term.

Effect of nonlinear operations on a Walsh series

Any well-behaved waveform can be expressed as a Walsh series over a given interval. If the series is truncated at the end of a certain group of Walsh functions of a given order, the resulting partial sum will be a staircase approximation to the desired waveform. If this staircase function has a single-valued nonlinear transformation applied to it, the result will be another staircase function with the same number of steps, but the heights of the individual steps will be changed. The new resulting series can be transformed by additional nonlinear operations if desired. The effect will always be to modify the coefficients of the given series, but the resulting series will never have any additional terms not in the groups included before the original series was truncated. It is not necessary to perform an integration to find the coefficients; they can be

obtained by simple algebraic processes.

This property can be used to solve a wide variety of nonlinear differential equations, since the successive iterations can be carried out without complicated integration procedures. Fig. 6 shows the solution to the nonlinear differential equation

$$\frac{d^2 y}{dx^2} = 2y^2$$

with the boundary conditions $x=0, y=1$, $y'=0$. The associated nonlinear integral equation is

$$u(x) = 2 \left[1 + \int_0^x (x-t) u(t) dt \right]^2$$

The accuracy is quite good, considering the limited number of terms of the Walsh series that was used.

Conclusions

Differential and integral equations can be solved using Walsh functions and previously prepared tables of coefficients. In each small interval, the approximate solution will approach the

mean value of the true solution in the same interval. The Walsh functions have simple rules for multiplication and the computation of partial sums of the series.

The solution to the differential or integral equations will be periodic, but can be extended to non-periodic functions by using the values at the end of one period as the boundary conditions for the start of the second period.

References

- Walsh, J. L., "A closed set of normal orthogonal functions," *American Journal of Mathematics*, vol. 45 (1923) pp. 5-24.
- Harmuth, Henning F., *Transmission of Information by Orthogonal Functions* (Springer-Verlag; Berlin-Heidelberg-New York; 1969). Contains extensive bibliography.
- Corrington, Murlan S., and Adams, Roy N., "Applications of Walsh functions to nonlinear analysis," Report on Contract AF30(602)2484, Rome Air Development Center, Griffiss Air Force Base, New York, AD-277-942. Contains extensive bibliography on mathematical properties.
- Rademacher, Hans, "Einige Sätze über Reihen von allgemeinen Orthogonalen Funktionen," *Mathematische Annalen*, vol. 87 (1922) pp. 112-138.
- Paley, R. E. A. C., "A remarkable series of orthogonal functions," *Proceedings of the London Mathematical Society*, second series, vol. 34 (1932) pp. 241-279.
- Fine, N. J., "On the Walsh functions," *Transactions of the American Mathematical Society*, vol. 65 (1949) pp. 372-414.
- Lovitt, William Vernon, *Linear Integral Equations*, (McGraw-Hill Book Company, Inc.; New York; 1924. Also Dover Publications, Inc.; New York; 1950).

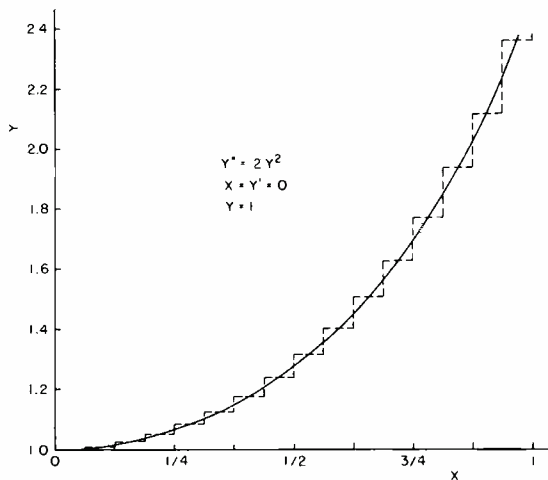


Fig. 6—Walsh-function approximation to solution of $y'' = 2y^2$.

Dynamic characteristics of several algorithms for real-time digital processing

R. C. Blanchard

The autopilot for the Space Shuttle will utilize digital processing for the servo-compensation networks. Such networks can be synthesized by any of a variety of algorithms for solving differential equations. In this paper, several of the more common types are considered, with dynamic response as the principle criterion in the form of gain-and-phase plots vs frequency while operating on a 1st-order differential equation. It is concluded that the trapezoidal integration rule and Runge-Kutta 2nd-order rule (explicit solution method) when applied to the 1st-degree equation have advantages over the other methods considered in terms of desirable attenuation characteristics for input frequencies up to 1/2 the sampling frequency.

WITH THE PROSPECTIVE use of a digital autopilot for the Space Shuttle, it is necessary to select the best technique for integrating the required equations. In this study, the dynamic lags of several techniques are compared in the frequency domain to aid in this selection. (Although many comparisons of computational algorithms have been made in the past for "batch" process solutions with accuracy as the figure-of-merit, the dynamic characteristics of the processing technique is a much neglected subject and is critical to real-time solution within a control loop).

The usual criterion of solution accuracy is not, it is felt, of importance in the operation of an autopilot because static

R. C. Blanchard
System Dynamics
Aerospace Systems Division
Burlington, Mass.

received his BSME and MSME from Massachusetts Institute of Technology in 1952 and 1953 respectively with emphasis on feedback systems. Following one year of work as a Staff Engineer at MIT, he was a member of the U.S. Army serving as an engineering specialist at Frankford Arsenal, Phila. After joining RCA in 1956, he was assigned a variety of work in system dynamics including advanced airborne fire-control, AICBM hydrofoil control systems, LM Rendezvous Radar, Stabilized Platforms, Cobra night-surveillance system, and, most recently, NASA's Space Shuttle.



inaccuracies due to computation are cancelled by loop action in the autopilot. Accordingly such typical considerations as truncation and round-off errors are not covered in this paper.

Candidate integration rules

The following integration rules have been compared for dynamic response while operating on a 1st-order differential equation.

Rectangular rule
Trapezoidal rule
Runge-Kutta 2nd-order
Runge-Kutta 4th-order
Nystrom's rule-2nd-order
Impulse-invariant algorithm

Sample equation

The following simple first-order equation was used to compare the various techniques for dynamic response and is representative of those that may be derived from higher-order equations by order-reduction techniques:

$$\frac{dy}{dt} = \frac{1}{\tau} (x[t] - y)$$

OR

$$\frac{y}{x} = \frac{1}{(\tau s + 1)}$$

General analysis method

The analysis was carried out in six steps:

- 1) Write the time-domain process equation.
- 2) Simplify the algorithm if necessary.
- 3) Transform to the Z domain.
- 4) Evaluate for $Z = \exp(-j\omega T)$.
- 5) Write computer program to generate output.
- 6) Run program and plot results.

Reprint RE-18-3-17

Final manuscript received August 29, 1972

Rectangular rule

The general rectangular integration rule is:

$$y_n = y_{n-1} + T \left(\frac{dy}{dt} \right)_{n-1}$$

where $\left(\frac{dy}{dt} \right)_{n-1} = \frac{1}{\tau} (x_{n-1} - y_{n-1})$

It is preferable to reduce dynamic lag by taking:

$$\left(\frac{dy}{dt} \right)_{n,n-1} = \frac{1}{\tau} (x_n - y_{n-1})$$

(if this is not done, a phase lag substantially exceeding that of the analytic function results);

Then, the modified rectangular rule yields:

$$y_n = y_{n-1} + \frac{T}{\tau} (x_n - y_{n-1})$$

The equivalent "z" transform is:

$$Y = Yz^{-1} + \frac{T}{\tau} (X - Yz^{-1})$$

Whence:

$$\frac{Y}{X} = \frac{T}{\tau} \left(\frac{1}{1 + z^{-1} [T/\tau - 1]} \right)$$

and

$$\frac{Y^*}{X^*} = \frac{T}{\tau} \left(\frac{1}{1 + \exp(-j\omega T) [T/\tau - 1]} \right)$$

or

$$\frac{Y^*(j\omega)}{X^*(j\omega)} =$$

$$\frac{T}{\tau} \left(\frac{1}{[1 + (T/\tau - 1) \cos(-\omega T)] - j[(T/\tau - 1) \sin \omega T]} \right)$$

where Y^* , X^* are the sampled transforms.

Evaluation of the final expression was carried out over a range of frequencies using a Telcomp program for a given choice of (T/τ) . This same approach has been applied to several additional algorithms presented in the succeeding paragraphs of this paper.

Trapezoidal rule

$$y_n = y_{n-1} + \frac{T}{\tau} \left(\frac{x_{n-1} + x_n}{2} - y_{n-1} \right)$$

Note that two values of $x(t)$ are averaged in this rule.

The Z transform is:

$$Y = Yz^{-1} + \frac{T}{\tau} \left(\frac{Xz^{-1} + X}{2} - Yz^{-1} \right)$$

or

$$\frac{Y}{X} = \frac{1}{2} \left(\frac{T}{\tau} \right) \left(\frac{z^{-1} + 1}{1 + z^{-1} [T/\tau - 1]} \right)$$

$$\frac{X^*}{X^*} = \frac{1}{2} \left(\frac{T}{\tau} \right) \left(\frac{\exp(-jT\omega) + 1}{1 + \exp(-jT\omega) [T/\tau - 1]} \right)$$

Finally:

$$\frac{Y^*}{X^*} = \frac{1}{2} \left(\frac{T}{\tau} \right)$$

$$\frac{(1 + \cos \omega T) - j (\sin \omega T)}{(1 + [T/\tau - 1] \cos \omega T) - j (T/\tau - 1) \sin(\omega T)}$$

Runge-Kutta-2nd -order rule

$$y_n = y_{n-1} + \frac{1}{2} [Tf(t_{n-1}, y_{n-1})$$

$$+ Tf(t_n, y_{n-1} + Tf[t_{n-1}, y_{n-1}])]]$$

where f denotes dy/dt

$$y_n = y_{n-1} + \frac{1}{2} \left(\frac{T}{\tau} \right)$$

$$\cdot (x_{n-1} [1 - T/\tau] - y_{n-1} [1 - T/\tau] + x_n - y_{n-1})$$

Transforming, and collecting terms:

$$\frac{Y}{X} = \frac{1/2(T/\tau)(1 + z^{-1} [1 - T/\tau])}{(1 + z^{-1} [-1 + T/\tau - 1/2(T/\tau)^2])}$$

Whence:

$$\frac{Y^*}{X^*} =$$

$$\frac{1/2(T/\tau)([1 + A \cos \omega T] - j[A \sin \omega T])}{([1 + B \cos \omega T] - j[B \sin \omega T])}$$

$$A \equiv (1 - T/\tau)$$

$$B \equiv (-1 + (T/\tau) - 1/2(T/\tau)^2)$$

Impulse-invariant algorithm

This algorithm generates a sampled output function with values identical to

those of a given Laplace transfer function at the sampling instants for an impulsive input transient.

It is implemented directly from the z-transform as derived from the Laplace transform:

$$\frac{y(s)}{x(s)} = \frac{1}{\tau s + 1} \rightarrow \frac{Y(z)}{X(z)} = \frac{1 - \exp(-T/\tau)}{1 - \exp(-T/\tau)z^{-1}}$$

where the numerator has been scaled to yield unity at zero frequency. Using, as before, $z^{-1} \exp(-j\omega T)$, we have:

$$\frac{Y(j\omega)}{X(j\omega)} = \frac{(1 - \exp(-T/\tau))}{(1 - \exp(-T/\tau)\cos \omega T) + j \exp(-T/\tau)\sin \omega T}$$

which is evaluated and plotted in Figs. 1, 2, 6, and 7. Since this method requires an identical number of computer "equivalent additions" to that of the rectangular rule, both are shown in Figs. 6 and 7 for the same sample frequency.

Nystrom algorithm

The Nystrom algorithm² is a 4th-order method applied to a 2nd-degree equation. It is very similar in this form to the Runge-Kutta algorithm and, when reduced to 2nd order, is identical to the Runge-Kutta just derived.

Results in the frequency domain

The results of the frequency domain response of the preceding four techniques (Nystrom identical to Runge-Kutta) are presented in Figs. 1 through 4 and are there compared to the precise analytical function in magnitude and phase shift.

In Figs. 1 and 2, a sample-period/time-constant ratio of 0.5 was used. This is equivalent to:

$$(sample \ frequency) = 4\pi \ (break \ frequency)$$

In Figs. 3 and 4,:

$$sample \ frequency = 10\pi \ (break \ frequency)$$

Note that the characteristics repeat for a frequency interval equal to the sample frequency. Furthermore, the amplitude characteristic is an *even* function about the Nyquist frequency ($1/2$ the sampling frequency) if plotted with a linear frequency axis; the phase is an odd function on a similar plot.

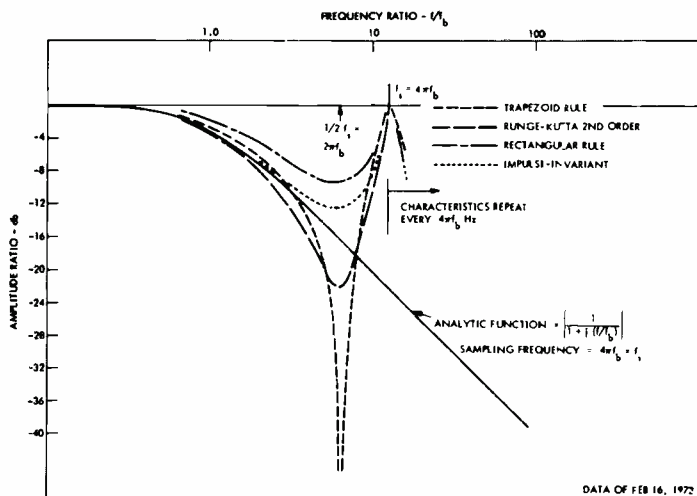


Fig. 1—Magnitude comparison of four integration rules, each acting on a 1st-degree equation—(dynamics of a zero-order hold are not included).

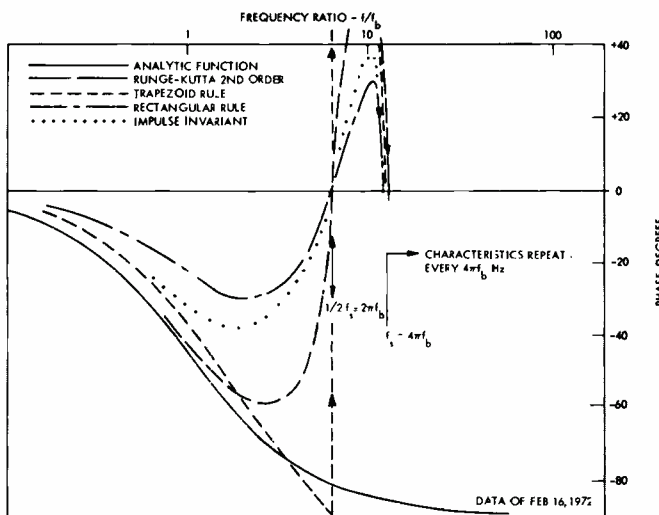


Fig. 2—Phase comparison of four integration rules, each acting on a 1st-degree equation—(dynamics of a zero-order hold are not included).

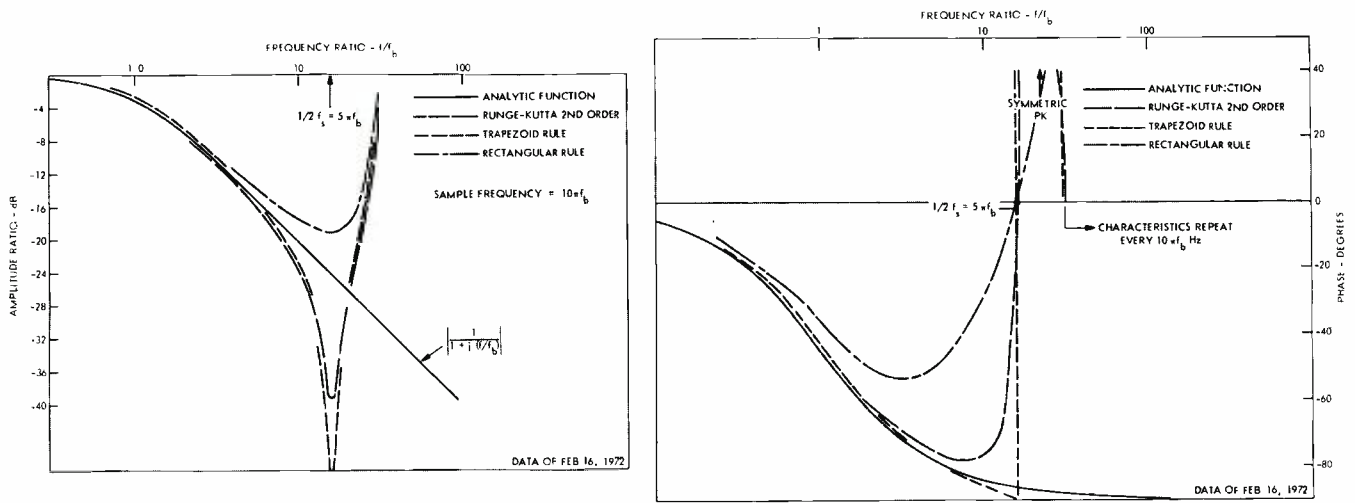


Fig. 3—(above) Magnitude comparison of three integration rules, each acting on a 1st-degree equation—(dynamics of a zero-order hold are not included. Fig. 4—(right) Phase comparison of three integration rules, each acting on a 1st-degree equation—(dynamics of a zero-order hold are not included.

The trapezoidal solutions seem to represent the best choice of those studied since the attenuation is generally greater and the phase-shift somewhat smaller than that of the analytic function.

It is important to note that these characteristics represent the values at a series of *sample instants* and that they may not be utilized as an analog output until a digital-to-analog converter, including a zero-order hold, has been introduced. The dynamic characteristics of a hold device are far from negligible as will be seen in the following section.

Runge-Kutta 4th-order solution

This algorithm is usually represented as follows:

$$y_{n+1} = y_n + \frac{1}{6} (k_0 + 2k_1 + 2k_2 + k_3)$$

$$k_0 = Tf(x_n, y_n)$$

$$k_1 = Tf(x_{n+1/2}, y_n + k_0/2)$$

$$k_2 = Tf(x_{n+1/2}, y_n + k_1/2)$$

$$k_3 = Tf(x_{n+1}, y_n + k_2)$$

Since a real-time solution cannot include future data in a current calculation (as x_{n+1}), a change in indices is required to provide for real past and present data:

$$y_n = y_{n-1} + \frac{1}{6} (k_0 + 2k_1 + 2k_2 + k_3)$$

$$k_0 = Tf(x_{n-1}, y_{n-1})$$

$$k_1 = Tf(x_{n-1/2}, y_{n-1} + k_0/2)$$

$$k_2 = Tf(x_{n-1/2}, y_{n-1} + k_1/2)$$

$$k_3 = Tf(x_n, y_{n-1} + k_2)$$

Since:

$$f(x_{n-1}, y_{n-1}) \equiv \left(\frac{dy}{dt} \right)_{n-1} = \frac{1}{T} (x_{n-1} - y_{n-1})$$

then

$$k_0 = (T/\tau)(x_{n-1} - y_{n-1})$$

$$k_1 = (T/\tau)(x_{n-1/2} - [y_{n-1/2} + k_0])$$

$$k_2 = (T/\tau)(x_{n-1/2} - [y_{n-1/2} + k_1/2])$$

$$k_3 = (T/\tau)(x_n - [y_{n-1} + k_2])$$

Because of the nesting of the above equation set, the algebra becomes tedious. The result of simplifying is:

$$\frac{Y}{X} = \frac{1/6(T/\tau)[1 + B \exp(-j\omega T) + C \exp(-j\omega T/2)]}{[1 + A \exp(-j\omega T)]}$$

$$A \equiv [-1 + T/\tau - 1/2(T/\tau)^2 + 1/6(T/\tau)^3 - 1/24(T/\tau)^4]$$

$$B \equiv [1 - T/\tau + 1/2(T/\tau)^2 - 1/4(T/\tau)^3]$$

$$C \equiv [4 - 2(T/\tau) + 1/2(T/\tau)^2]$$

It will be found that, for $j\omega T \rightarrow 0$; $(Y/X) \rightarrow 1$ as required. The frequency

response is computed from:

$$\frac{Y^*}{X^*} = 1/6(T/\tau)$$

$$\frac{\{ [1 + B \cos \omega T + C \cos(\omega T/2)] + j[-B \sin \omega T - C \sin(\omega T/2)] \}}{(1 + A \cos \omega T) - jA \sin \omega T}$$

Note that the expression contains terms in ωT and $\omega T/2$, the latter being the result of the original inter-space samples required for terms like $x_{n-1/2}$. Since samples of the input are needed at these points, the sample period should properly be called $T/2$. The corresponding sample frequency is therefore twice as high as the parameter T would indicate. On this basis, two sample frequencies were used in the dynamic response:

sample frequency = 8π (break frequency)

and
sample frequency = 20π (break frequency)

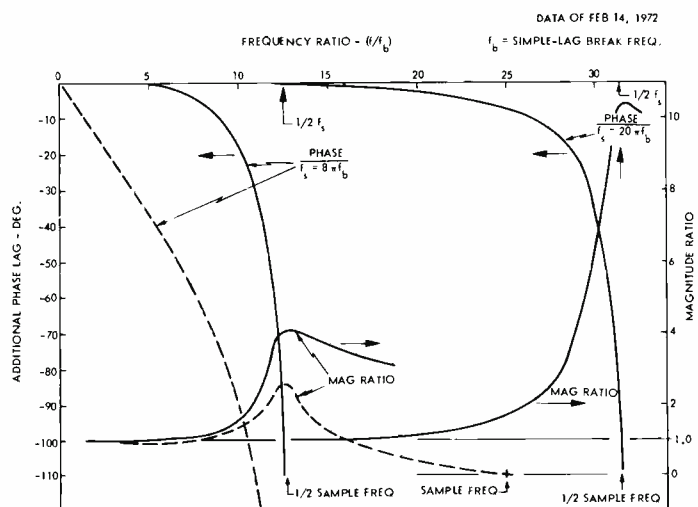


Fig. 5—4th-order Runge-Kutta on 1st-degree equation . . . additional phase lag beyond that of analytic function; magnitude divided by that of analytic function.

The plots of Fig. 5 show the results with the amplitude function plotted as:

$$\text{Magnitude function} = (\text{mag. of R-K 4}^{\text{th}}\text{-order}) / (\text{mag. of analytic function})$$

The phase function plotted is:

$$\text{Phase function} = (\text{phase of R-K 4}^{\text{th}}\text{-order}) - (\text{phase of analytic function})$$

Each phase curve is drawn only up to a frequency equal to $1/2$ the sampling frequency because the remainder of the curve ($1/2 f_s < f < f_s$) lies at large positive phase values.

The effect of a zero-order hold is dramatic when applied to the lower sampling rate case. It contributes the most significant phase lag by far compared to the Runge-Kutta solution as may be seen by the dashed curve.

Additionally, the zero-order hold's amplitude characteristic is such as to attenuate the peak in the Runge-Kutta's ratio-magnitude function, reducing it to zero at the sampling frequency.

Choice among methods

The time duration of each computation cycle must be taken into account before selection may be made as to the preferred equation solution technique. If sampling may be accomplished as often as desired, then the simpler algorithms may be computed at a higher frequency than the more complex. Accordingly, the properties of the processor under consideration as well as the equation to be solved must be considered. The analytical methods presented above may be used with whatever parameter values need to be compared.

Specifically, an estimate has been made of the number of "equivalent additions" among the several methods presented, and a separate sampling interval that is proportional to the number of such additions has been chosen. With the number so estimated normalized to unity for the trapezoidal algorithm, the corresponding sample periods come out to:

Algorithm	Sample period
Trapezoidal	1.0
Rectangular	0.562
Runge-Kutta-2 nd -order	1.0
Runge-Kutta-4 th -order	1.75
Impulse-invariant	1.0

Note that the estimates of sample period for both Runge-Kutta techniques are based on the explicit solutions pre-

sented earlier and therefore represent significantly fewer computer operations than would be required for the traditional Runge-Kutta algorithms as usually programmed. (Note that a minimum of computer operations per time slice and not a minimum of storage locations is desired in a digital autopilot).

Figs. 6 and 7 present the results of this comparison for three appropriate sampling rates. The curves of the Runge-Kutta 2nd-order are missing because they are identical to those presented in Figs. 3 and 4, and the sampling period is the same as the trapezoidal-algorithm sampling period.

Conclusions

There is an appreciable variation in dynamic characteristics among the

methods studied. When one takes into account the more frequent sample processing that is possible for the simpler algorithms in a computer of given speed, it is found that such simpler techniques offer better dynamics in terms of suitability for closed-loop control than those having more elegant structure.

Accordingly, the trapezoidal rule provides a desirable extra attenuation characteristic and excellent phase match up to a frequency close to one-half the sampling frequency and is considered the most suitable algorithm of those studied for closed-loop autopilot control.

References

1. Tou, J. T., *Digital and sampled-data control systems* (McGraw-Hill Book Co.; 1959) pp. 198-207.
2. *NASA Space Shuttle Report*, Vol. III, Section 9.6.1.2 (revised Dec. 1, 1971) p. 9.6-47.

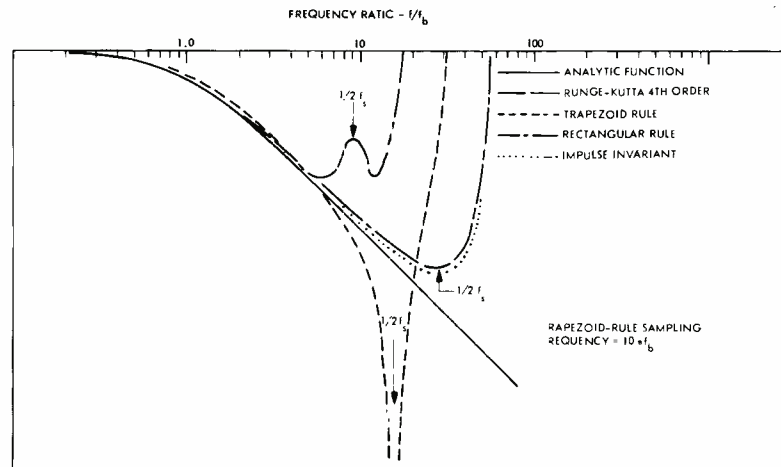


Fig. 6—Magnitude comparison with adjusted sample rates according to equivalent adds per computation period.

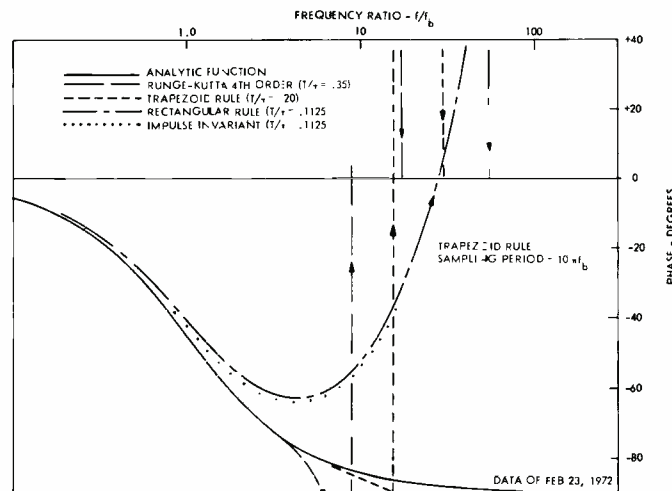


Fig. 7—Phase comparison with adjusted sample rates according to equivalent adds per computation period.

Image enhancement techniques

D. B. Gennery

This paper discusses the enhancement of images to restore detail that has been obscured by blurring. An optical analog method and several digital methods of performing this processing are discussed. Sample results from one of the digital methods are shown.

IN MANY FIELDS OF SCIENCE AND TECHNOLOGY it often happens that a photograph has been obtained in such a manner that blurring has reduced the sharpness of the image. For example, in astronomical photographs obtained by earth-based telescopes, the turbulence of the atmosphere causes a degrading of the image. Similar effects occur in underwater photography. Also, in photographs obtained from space probes, improper focus or motion during the exposure may blur the image. In medical X-rays, the resolution often is not as good as might be desired. Many other examples could be mentioned.

Reprint RE-18-3-12
Final manuscript received June 23, 1972

Donald B. Gennery
Missile Test Project
RCA Service Company
Patrick Air Force Base, Fla.

received the MS in Physics from the Florida Institute of Technology, 1969. For the past fifteen years, Mr. Gennery has been with the RCA Missile Test Project at Patrick Air Force Base, Florida, where he currently is a Senior Systems Analyst. In this position, he has developed data reduction techniques for various instrumentation systems and has done statistical studies associated with these systems. He has written several papers on the subject of digital filters. He has designed new types of digital filters which are currently used in processing Eastern Test Range data by RCA. For the past five years, he has been working in the field of image enhancement, and he has developed several computer programs for the processing of images.



In such cases, it sometimes is possible to process the image in such a way as to correct for the blurring process and thus to improve the resolution of the image. Other processing can also be performed so as to accentuate certain features of the image. As many others have pointed out¹⁻⁶, these types of processing in many cases can be performed by two-dimensional spatial filters. Both analog filters using optical techniques and digital filters using general-purpose digital computers will be discussed below.

General principles

If an image formed in noncoherent light is blurred in a constant way throughout the image plane, this smearing-out process can be described by the convolution operation, as follows:

$$z = g * \hat{z} \quad (1)$$

(The quantities z , \hat{z} , and g are all functions of the two spatial coordinates x and y in the image plane, but the functional dependence is not shown in Eq. 1.)

The convolution theorem states that a convolution in the space domain is equivalent to a multiplication in the frequency domain, and vice versa. Therefore, Eq. 1 can be transformed to the following in the frequency domain:

$$Z = G \hat{Z} \quad (2)$$

Eq. 2 can be solved for Z as follows:

$$\hat{Z} = Z/G \quad (3)$$

Thus processing the blurred image with a filter whose transfer function is $1/G$ would produce a restoration of the ideal image.

However, G may be zero at certain frequencies. Furthermore, G may be so small at some frequencies that the image content at these frequencies has dropped below the noise level in the photographic emulsion and thus cannot be restored. Therefore, instead of Eq.

3, the following procedure is used.

The optimum filter for separating a message whose power spectrum is P_m from noise whose power spectrum is P_n has the transfer function $P_m / (P_m + P_n)$ if the message and noise are uncorrelated⁷. The message, in this case, is the blurred image z , whose power spectrum is $P_z |G|^2$, where P_z is the power spectrum of the ideal image \hat{z} . Making this substitution and multiplying by $1/G$, to restore the image in the absence of noise, produces the following transfer function of the restoring filter including noise suppression:

$$H = \frac{P_z |G|^2}{P_z |G|^2 + P_n} \cdot \frac{1}{G} \quad (4)$$

This reduces to

$$H = \frac{\bar{G}}{|G|^2 + \beta^2} \quad (5)$$

where $\beta^2 = P_n / P_z$ and \bar{G} denotes the complex conjugate. (β represents the ratio of noise amplitude to signal amplitude in the intensity data. β in general is a function of the two components of spatial frequency, but it will be considered to be constant here for simplicity. Note that when $\beta=0$, $H=1/G$.) Thus, instead of Eq. 3, we have

$$\hat{Z} = HZ \quad (6)$$

In the space domain, Eq. 6 becomes

$$\hat{z} = h * z \quad (7)$$

where h is called the filter impulse response.

The filtering of an image to perform the above can be done by one of two basic methods. In the transform method, the input image, z , is transformed to the frequency domain; multiplied by the filter transfer function, H , at each frequency according to Eq. 6; and then transformed back to the space domain to produce the output image, \hat{z} . In the convolution method, the input image, z , is convolved with the filter impulse response, h , in the space domain according to Eq. 7 to produce the output image, \hat{z} .

Determination of optical transfer function

We must now discuss means of determining the optical transfer function, G , of the blurring process so that it can be used in Eq. 4 to determine the restoring filter.

Notation

a, b	arbitrary constants.	L	focal length of lens.	z	image z expressed in mixed domain.
f_x, f_y	x, y components of frequency.	m, n	arbitrary integers.	β	noise to signal ratio (parameter controlling restoring filter).
g	optical impulse response (point-spread function).	n_x, n_y	filter semi-span in x or y dimension in digital convolution method.	Δx	digital sampling interval in x dimension.
G	optical transfer function (g transformed to frequency domain).	N_x, N_y	number of columns or rows in digitized image (after being filled out to a size that can be transformed).	Δy	digital sampling interval in y dimension.
h	filter impulse response (data multipliers for digital filter).	P	power spectrum of signal (denoted by subscript).	λ	wavelength.
H	filter transfer function (h transformed to frequency domain).	T_A	amplitude transmittance of analog filter transparency.	$\hat{}$	denotes ideal image or restored image instead of observed image (used with z and u).
H	filter expressed in mixed domain.	u	intensity in image of known object.	*	convolution operation.
i	$\sqrt{-1}$.	U	image u transformed to frequency domain.	-	complex conjugate.
j_x	x frequency component integer index ($=N_x \Delta x f_x$), used modulo N_x .	x	horizontal dimension in image.		absolute value.
j_y	y frequency component integer index ($=N_y \Delta y f_y$), used modulo N_y .	y	vertical dimension in image.	arg	argument of complex quantity.
k_x	x dimension integer index ($=x/\Delta x$), used modulo N_x .	z	intensity in image to be processed.	exp	exponential function.
k_y	y dimension integer index ($=y/\Delta y$), used modulo N_y .	Z	image z transformed to frequency domain.	Re	real part of complex quantity.

In some cases, the optical transfer function can be computed from theoretical considerations. For example, if the blurring is caused by aberrations in lenses, the point spread function, g , can be computed by ray tracing, and the Fourier transform of this can be computed numerically to obtain the transfer function, G . In many cases, however, the smearing is due to some phenomenon (such as unknown inhomogeneities in the medium) whose effects cannot be predicted and thus must be measured.

If a known object can be photographed along with the object under study, its blurred image can be used to determine the optical transfer function. If the ideal image of the known object is denoted by \hat{u} and its blurred image by u , then

$$u = g * \hat{u} \quad (8)$$

$$U = G \hat{U} \quad (9)$$

Thus, G can be determined as follows, except where \hat{U} becomes so small as to be seriously contaminated by noise:

$$G = U/\hat{U} \quad (10)$$

A special case of Eq. 10 that is of some

importance occurs when the known object is a point source. Then, \hat{u} is a delta function (unit impulse), and if we assume that it is at the origin, \hat{U} is a constant. Furthermore, by normalizing U so that it is equal to unity at zero frequency, \hat{U} can be set equal to unity. Thus $G = U$ in this case. That is, the optical transfer function is equal to the two-dimensional Fourier transform (normalized to be unity at the origin) of the blurred image of a point source. An example of using a point source as a standard can occur in astronomical photography, where a star can be considered to be a point source.

There are cases in which the optical transfer function can be partially computed from theoretical considerations, so that an analytical expression is obtained containing some unknown coefficients. Such a case sometimes occurs with atmospheric turbulence, for example⁵. If a measurement of the transfer function is also obtained by using a known object as described above, the theoretical function can be fit to this measured data. That is, a least-squares (or other) solution for the unknown coefficients can be performed, and by using these values, the

theoretical transfer function can then be used. Using this adjusted theoretical function instead of the raw measured function reduces the effects of noise in the latter.

A fairly common simple case of the above use of a combination of theoretical knowledge and measured data occurs when the entire shape of the optical transfer function is known theoretically and only the frequency scale factor is unknown. In this case, just the scale factor needs to be determined in the adjustment. For example, in some cases it can be assumed with good accuracy that the optical transfer function is a Gaussian function, and only its width needs to be determined. (Due to the Central Limit Theorem in statistics, many random processes tend to produce the Gaussian function.)

If the shape of the optical transfer function is known and only its frequency scale factor needs to be determined, a trial-and-error procedure can often be used. This would be done by using the filter transfer function computed from Eq. 5 but adjusted for a series of different scale factors. When the blurred image is processed by each of these fil-

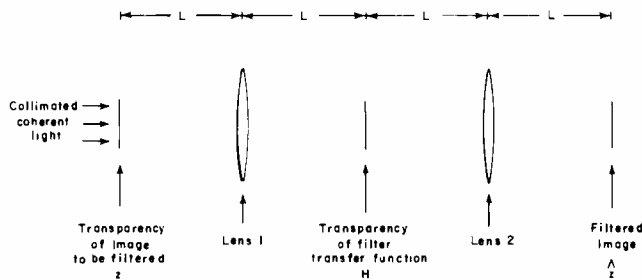


Fig. 1—Optical filtering.

ters, it should be possible to determine the best one by visual inspection. While this procedure may be time consuming, it requires no specific information about the content of the image, but is based only on general information about the presence of sharp detail or types of shapes in the ideal image.

Analog techniques

Methods of performing the above processing by means of analog computations using coherent light will now be discussed. The transform method of filtering an image will be used, as stated by Eq. 6.

The complex amplitude distribution in the back focal plane of an ideal lens is the Fourier transform of that in the front focal plane⁸. This fact is utilized to perform the two Fourier transforms needed in the transform method.

The basic configuration is shown in Fig. 1. A positive transparency of the image to be filtered is inserted into the front focal plane of lens 1 of focal length L and is illuminated with collimated coherent light. This transparency must have a gamma of 2, so that the amplitude of light passing through it is proportional to the intensity in the original image. The spatial frequencies of the original image are displayed in the back focal plane of the lens. Here a filter is positioned, whose amplitude transmittance at each position is proportional to the desired transfer function, H , at the corresponding frequency. Thus, the

multiplication called for by Eq. 6, is performed. The filter plane is also the front focal plane of a second lens of focal length L , which transforms the result back to the space domain. The resulting filtered image appears in the back focal plane of this lens. (The frequency scale factor in the back focal plane of lens 1—i.e., the ratio of spatial coordinate in the back focal plane to frequency component in the front focal plane—is $L\lambda$.)

If the function H is always positive real, the above method is satisfactory. However, if H contains imaginary parts, the filter must produce phase shift in addition to changing the amplitude. One way of doing this is to convert the phase information into amplitude information by modulating the desired transfer function H onto a carrier.

The carrier consists of a sinusoidal pattern of amplitude transmission bands proceeding in one direction across the filter. The amplitude of the carrier wave is proportional to the absolute value of H , and the phase of the carrier is determined by the phase (argument) of H . The filter transparency then is one type of hologram⁹. The carrier in the hologram acts like a diffraction grating, and the first-order light diffracted in the proper direction to produce the correct polarity of phase shift produces the desired filtered image. The undiffracted light and the light diffracted in the other direction produce unwanted images that can be ignored if they are sufficiently

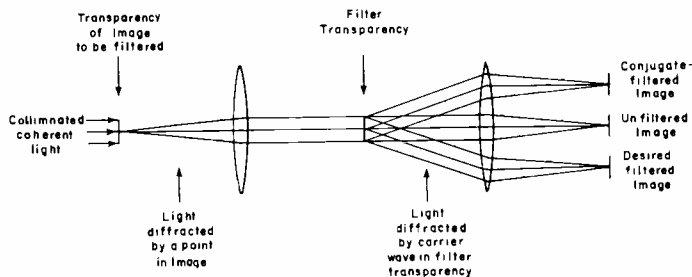


Fig. 2—Use of complex filter modulated onto carrier.

separated. Higher-order diffracted images will not exist if the carrier wave is truly sinusoidal. This entire process is illustrated in Fig. 2. The amplitude transmittance in the filter transparency as a function of the components of frequency f_x and f_y is proportional to

$$T_A(f_x, f_y) = a + 2|H(f_x, f_y)| \cos [2\pi b f_x + \arg H(f_x, f_y)] = a + 2Re[H(f_x, f_y) \exp(2\pi i b f_x)] = a + H(f_x, f_y) \exp(2\pi i b f_x) + \bar{H}(f_x, f_y) \exp(-2\pi i b f_x) \quad (11)$$

where the constant b is the "frequency" (in the frequency domain) of the carrier, and the constant a is chosen so that T_A is always positive.

It remains to discuss means of producing the hologram filter used above. A method of doing this for the case in which a point source is available for determining the optical transfer function will be discussed and is illustrated in Fig. 3.

According to the discussion following Eq. 10, the optical transfer function G is simply the Fourier transform of the image of a point source, that is, the Fourier transform of the point spread function g . The image of the point source can be transformed to G by means of a lens, as previously described.

Now consider Eq. 5. The term \bar{G} can be produced by making a hologram by causing a reference beam of collimated coherent light to interfere with the light forming G to produce interference fringes which form the carrier wave. By suitably choosing the angle of the beam, the desired carrier frequency is selected, and by suitably choosing the polarity of the angle compared to the desired diffraction direction in Fig. 2, \bar{G} is obtained instead of G .

For the moment, neglect the term β^2

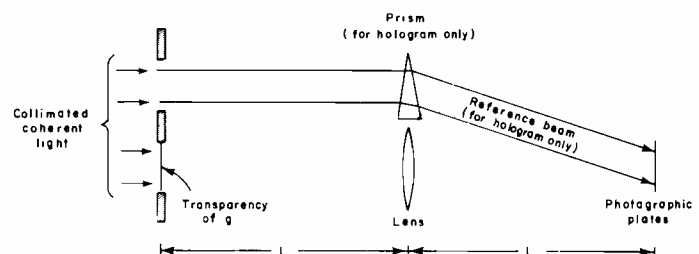


Fig. 3—Production of two plates for complex filter.

in the denominator of Eq. 5. To produce the function $1/|G|^2$, it is necessary only to expose a negative in the ordinary way to the function G and to develop it for a gamma of 2, since the transmission through a developed negative is proportional to the minus gamma power of the exposure. If the above hologram containing \bar{G} is simply stacked together with this negative containing $1/|G|^2$, the function $\bar{G}/|G|^2=1/G$ is produced. This filter transfer function would restore the image completely in the absence of noise ($\beta=0$).

To account for the presence of noise (and zeros in G) the term β^2 is inserted into the denominator of Eq. 5, as previously explained. The effect of this term can be approximated in a crude but sufficient way as follows. In making the negative for $1/|G|^2$ as described above, the exposure is adjusted so that for sufficiently small values of G the negative becomes underexposed, and thus the amplitude transmission no longer follows $1/|G|^2$, but instead approaches a constant value corresponding to $1/\beta^2$. The resulting negative is stacked with the hologram for \bar{G} as before, to produce a filter that approximates the filter transfer function H as given by Eq. 5. This filter is used as previously shown in Fig. 2.

Digital techniques

Methods of using a digital computer to perform the image processing will now be discussed. Both the convolution method and the transform method will be described, as well as the hybrid method, which is a combination of the other two.

Convolution method

In the convolution method, Eq. 7, which represents a convolution in the space domain, is used. (The filter impulse response h is here usually known as the data multipliers.) For digital data, the convolution in Eq. 7 can be written out as follows:

$$\hat{z}(k_x, k_y) = \sum_{k'_x=-n_x}^{n_x} \sum_{k'_y=-n_y}^{n_y} h(k'_x, k'_y) z(k_x - k'_x, k_y - k'_y) \quad (12)$$

where the span of the filter impulse response has been constrained to a span of $2n_x + 1$ by $2n_y + 1$ points to keep the computation time down. (n_x and

n_y must be large enough to allow all of the important effects in the desired transfer function H to be approximated sufficiently well.) In practice, the computations in Eq. 12 can sometimes be reduced by taking advantage of the symmetry, if any, of the data multipliers.

If the input image is read in and out of the computer by columns (y direction), it can be seen that it is necessary to store $2n_x + 1$ complete columns of the input image in the computer memory at any one time. To reduce the memory requirements, the following method was developed for use in the program OSIR on the IBM 7094 at the Eastern Test Range. These $2n_x + 1$ columns are stored in packed form, as 9-bit fixed-point values, four to a word. Then only the $2n_x + 1$ by $2n_y + 1$ points needed at a time in Eq. 12 are stored in normal unpacked form. Each time a new filtered point is computed, $2n_x + 1$ points are unpacked. This method is illustrated in Fig. 4.

Transform method

In the transform method, Eq. 6 is used, which represents a point-by-point multiplication in the frequency domain. The transformation of the image to the frequency domain and the transformation of the result back to the space domain after multiplication by the filter transfer function H are performed by finite discrete two-dimensional Fourier transforms, which may be defined as follows:

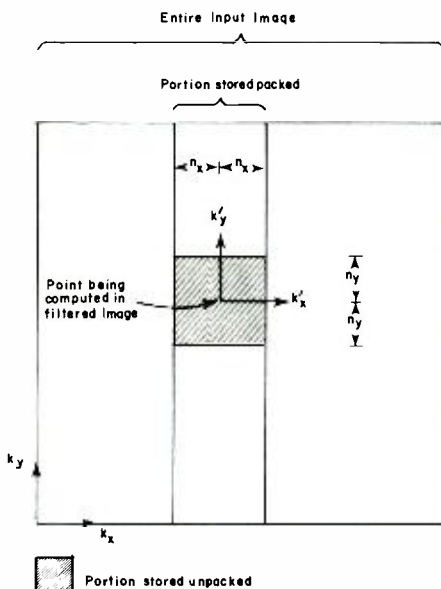


Fig. 4—Storage of data for convolution method.

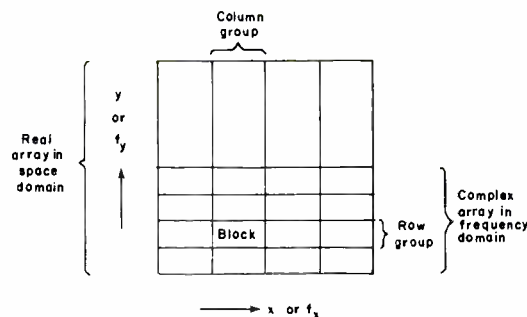


Fig. 5—Partitioning of array for transformation.

$$Z(j_x, j_y) = \sum_{k_x=0}^{N_x-1} \sum_{k_y=0}^{N_y-1} z(k_x, k_y) \exp \left[2\pi i \left(\frac{j_x k_x}{N_x} + \frac{j_y k_y}{N_y} \right) \right] \quad (13)$$

$$\hat{z}(k_x, k_y) = \frac{1}{N_x N_y} \sum_{j_x=0}^{N_x-1} \sum_{j_y=0}^{N_y-1} \hat{Z}(j_x, j_y) \exp \left[-2\pi i \left(\frac{j_x k_x}{N_x} + \frac{j_y k_y}{N_y} \right) \right] \quad (14)$$

where N_x and N_y represent the number of columns and rows, respectively, in the image.

The direct implementation of Eq. 13 and 14 would require too much computer time. Therefore, the Fast Fourier Transform developed by Cooley and Tukey¹⁰ is used. Furthermore, large images may not fit into the computer memory. Therefore, a method of partitioning the image and using disk storage was developed for use in the program OSIP on the IBM 360/65 at the Eastern Test Range. This method can be described as follows, provided that the image is available by columns (y direction).

The real array in the space domain is divided into groups of adjacent columns and groups of adjacent rows, as shown in Fig. 5, such that one entire group of columns or two entire groups of rows can fit into the main memory at one time, together with the rest of the program. Each portion of the array that is common to a particular group of columns and a particular group of rows is called a block. Each group of columns is read into memory at one time and is transformed along the y dimension only. Each block in this group is then read out separately to disk storage. After all of the groups of columns have been transformed in this way, the transforming of the rows begins. All of the blocks comprising one group of

rows are read from disk storage into memory by using the direct-access feature of the disks, these rows are transformed along the x dimension, and the result is read out to external storage (or used in subsequent processing) by rows. When all the groups of rows have been processed in this way, the two-dimensional transform of the original array is sitting in external storage, stored by rows (or has otherwise been used by rows). When an inverse transform is desired, the above operations are reversed, starting with the array stored by rows and ending with the array stored by columns. Thus the computations using the arrays can be arranged so that in the space domain any array is always stored by columns and in the frequency domain any array is always stored by rows. In the applications here, the arrays in the space domain will always be real, whereas in the frequency domain they will be complex. However, only the lower half of the array is used in the frequency domain, since, if $z(x, y)$ is real, then $Z(N_x - j_x, N_y - j_y) = \bar{Z}(j_x j_y)$.

The one-dimensional transforms along the columns or rows needed in the above method are performed by a subroutine written specifically for this task using the Fast Fourier Transform. This subroutine can handle arrays of sizes of the form $2^n \cdot 3^m$. (The image is filled out with a constant to the next larger size of this form in each dimension.) By using this subroutine and the above method of disk storage, a 1024 by 1024 array can be transformed in 10 minutes on the IBM 360/65, when 41,000 words (164,000 bytes) of main memory for data and coding for this part of the program are used.

Hybrid method

The hybrid method essentially consists of using the convolution method in one dimension and the transform method in the other dimension. That is, the image is transformed to the frequency domain along one dimension only (here assumed to be y); the result is convolved with the filter function along the other dimension (x); and this result is transformed back to the space domain along the first dimension (y). This can be stated mathematically as follows:

$$z(k_x, j_y) = \sum_{k_y=0}^{N_y-1} z(k_x, k_y) \exp\left(\frac{2\pi i j_y k_y}{N_y}\right) \quad (15)$$

$$\hat{z}(k_x, j_y) = \sum_{k'_x=-n_x}^{n_x} \mathbf{H}(k'_x, j_y) z(k_x - k'_x, j_y) \quad (16)$$

$$\hat{z}(k_x, k_y) = \frac{1}{N_y} \sum_{j_y=0}^{N_y-1} \hat{z}(k_x, j_y) \exp\left(-\frac{2\pi i j_y k_y}{N_y}\right) \quad (17)$$

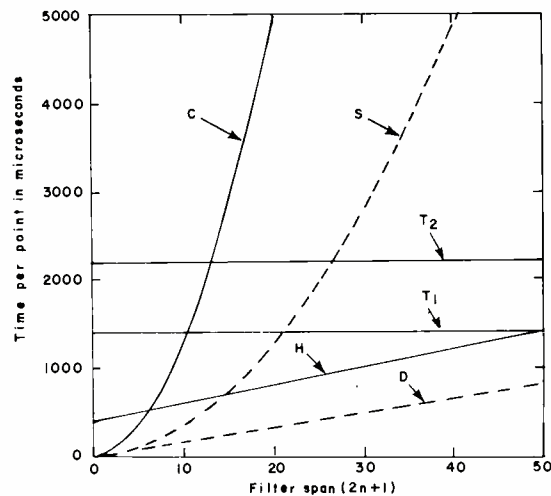
The filter function \mathbf{H} needed above could be obtained from the equivalent data multipliers that would be used in the convolution method, as follows:

$$\mathbf{H}(k_x, j_y) = \sum_{k_y=-n_y}^{n_y} h(k_x, k_y) \exp\left(\frac{2\pi i j_y k_y}{N_y}\right) \quad (18)$$

The boldface letters used in the above four equations represent quantities expressed in a mixture of the space domain (k index) and the frequency domain (j index).

The one-dimensional Fourier transforms denoted by Eq. 15, 17, and 18 would actually be performed by the Fast Fourier Transform. Furthermore, since $z(k_x, N_y - j_y) = \bar{z}(k_x, j_y)$ (and similarly for \hat{z} and \mathbf{H}), only half-sized arrays are used in the mixed domain, to save more time and storage.

Although the hybrid method has never actually been used to the author's



T₁ - transform method excluding filter computation
T₂ - transform method including filter computation
H - hybrid method

C - convolution on method
S - convolution method with circular symmetry
D - convolution using two one-dimensional symmetrical direct filters

Fig. 6—Estimated computation time on IBM 360/65.

knowledge, calculations indicate that in some cases it would require less computer time than either of the other two methods. Furthermore, the hybrid method is suitable in some cases in which the transform method is completely impractical due to the lack of disk storage and the size of the computer memory. However, for large filter spans the hybrid method requires a larger main memory than does the convolution method or the transform method with disk storage.

Computation of filter

In Fig. 6 the approximate amount of IBM 360/65 computer time required per image point to process a single image by each of the three methods is shown as a function of the span of the filter impulse response (assumed to be square). These times are rough estimates assuming efficient programming and typical conditions suitable for the method at hand. The two dashed lines show special cases in which the convolution method can be made faster. For the curve marked S, it is assumed that the desired filter transfer function H is real and is a function only of the magnitude of the frequency, and thus the impulse response also has this symmetry about the origin. For the curve marked D it is assumed that H can be factored into separate functions of f_x and f_y and that these functions are symmetrical about the origin. (While the S case is fairly common, the D case is not.)

Computation of filter

The digital techniques of performing the actual filtering of an image have just been described. However, computing the filter itself (performed before the actual filtering) involves some special considerations depending on the digital method being used and on the method of determining the optical transfer function. Here, it will be assumed that the optical transfer function is being obtained from a known object according to Eq. 10, and the particular techniques for implementing the computations for each of the three methods will be discussed.

In any of the methods, if a known object has been photographed as previously described and the results digitized, Eq. 10 can be used to compute the optical transfer function. To do this, the known image \hat{u} and its blurred form u in digital form representing intensity would each be processed as follows. The background intensity level (if any) is subtracted from each point in the image, so that the results indicate light from the known object only. The image is truncated to an area sufficiently large to include the significant information, but no larger, in order to reject as much noise as possible.

In the convolution method, the computations now proceed as follows. The truncated images u and \hat{u} are filled out with zeros to produce arrays of the size decided on for h . The finite discrete two-dimensional Fourier transforms of u and \hat{u} are then computed to obtain U and \hat{U} . The ratio of these at each point is computed to obtain the optical transfer function G , as stated by Eq. 10. Once the optical transfer function is available, the desired transfer function H' of the filter to be used is computed at each point in the frequency domain using Eq. 5. (The prime is used on H here because this transfer function may not be achieved exactly, as is explained below.) Then the inverse finite discrete two-dimensional Fourier transform of H' is computed to obtain h' . This function could be used as the impulse response h of the filter. However, since it has been necessary to limit h to a fairly small array for computation purposes, small values of the ideal h may exist outside of this array. By limiting the size of the array, these values rejected have in effect been replaced by zeros (and the values within

the array have adjusted themselves also). Thus a discontinuity has been introduced into the function h , which would cause "ringing" in the frequency domain. (That is, if h' were filled out with zeros to form an array the size of the image z and the result were transformed to the frequency domain, the resulting function H' would be identical to the function H' above at those frequencies that were defined above as points in the array. But with the full-sized array, many points of frequency have been added between these original ones, and the value of H' at these points would oscillate about a smooth curve passing through the original values.) Thus it may be desirable to multiply h' by some apodizing function, which decays gradually to zero at the edges, to obtain h , in order to remove the discontinuity.

The above computation of h does not require much computer time, especially if the Fast Fourier Transform is used, since the arrays to be transformed are small. (They are the same size as h .) The function h forms the filter data multipliers to be used in Eq. 12, as previously described.

In the transform method, one way of computing the filter transfer function H is first to compute the filter impulse response h exactly as it would be computed in the convolution method, as described above. Then h is filled out with zeros to make an array the same size as the image, and this full-sized array is transformed to the frequency domain by the same two-dimensional Fourier transform subroutine used to transform z . According to the convolution theorem, the transform method in this case would give results that are mathematically identical to those that would be obtained with the convolution method. However, it will be recalled that in the convolution method it was necessary to truncate h to a reasonably small span in order to save computation time. Since this is no longer necessary in the transform method, it may be desirable to remove this truncation. Doing so will often produce slightly more accurate results, since, even though the original point spread function g may be limited to a small span, the impulse response h needed to perform the inverse of g will usually not be so limited. Therefore, the following method of computing H may be preferable.

Starting with the truncated images u and \hat{u} previously described for the convolution method, the images u and \hat{u} are filled out with zeros to produce arrays of the size of the image z . The same two-dimensional Fourier transform subroutine used to transform the image z to the frequency domain is then used to transform u and \hat{u} to the frequency domain to obtain the arrays U and \hat{U} . (As previously explained, these arrays in the frequency domain need to be only half of the full size.) The ratio of these at each point is computed to obtain the optical transfer function G , as stated by Eq. 10. Once the optical transfer function is available, the transfer function H of the filter to be used is computed at each point in the frequency domain using Eq. 5. The resulting transfer function is used in Eq. 6, as previously described. (If the images u and \hat{u} are sufficiently small, it is possible to save computation time by transforming them both together with a single Fourier transform.)

For the hybrid method, the filter can be obtained from the corresponding filter for the convolution method by using Eq. 18, as previously described.

Example

Fig. 7 shows a test target that was photographed deliberately out of focus to produce the blurred image shown in Fig. 8. The negative from which Figure 8 was made was scanned in a microdensitometer. A sample interval of 0.1 mm was used in each dimension, with a 0.1 mm square slit. By using the characteristic curve of the emulsion, the measured density values were converted to intensity in arbitrary units such that the white areas in the scene have the approximate value 1. The resulting values were plotted using a variable intensity plot on a cathode-ray tube plotter to produce Fig. 9. No filtering was done in this case. (Fig. 9 is shown for comparison with later figures, it should look essentially the same as Figure 8.)

Threshold plots, in which every intensity above or below a certain threshold is plotted as all white or all black, respectively, were also made, for maximum contrast enhancement. The same blurred image shown in Fig. 9 is plotted at two different thresholds in Figs. 10 and 11. In none of these are the numerals readable.

409
586

Fig. 7—Original scene.



Fig. 8—Blurred photograph.



Fig. 9—Unfiltered image, variable intensity plot.



Fig. 10—Unfiltered image, threshold 0.5.



Fig. 11—Unfiltered image, threshold 0.7.

409
586

Fig. 14—Filtered image, variable intensity plot.

409
586

Fig. 15—Filtered edited image, variable intensity plot.

409
586

Fig. 16—Filtered edited image, threshold 0.5.

409
586

Fig. 17—Filtered edited image, threshold 0.7.

To determine the optical transfer function, the vertical and horizontal bars in Fig. 7 were used as known objects. The regions of the data in Fig. 9 containing these bars were used in accordance with Eq. 10 to obtain a raw estimate. Furthermore, since the blurring was caused by an out-of-focus camera, the shape of the transfer function was computed theoretically by assuming a circular aperture. The frequency scale factor of the theoretical function was obtained by adjusting it to fit the raw estimate. The resulting estimate of the optical transfer function G is shown in Fig. 12, which is assumed to apply in all directions in the two-dimensional frequency domain. This was used in Eq. 5 with $\beta=0.025$ to produce the filter transfer function H shown in Fig. 13.

The image shown in Fig. 9 was filtered by this filter using the transform method, and the result is shown in Fig. 14. The large and medium-sized numerals can now be read. The small numerals show up faintly, but in order for them to be readable a smaller sample interval than 0.1 mm would probably be required.

The circular patterns visible in the filtered image are due to specks of dirt (or other imperfections) on the original out-of-focus negative. It is possible to correct partially these erroneous points by an editing procedure before the image is filtered. The result of filtering such edited data is shown in Fig. 15. Threshold plots of this same filtered edited image are shown in Figs. 16 and 17.

Acknowledgments

This paper was adapted from a paper originally presented at the Seventh Space Congress in Cocoa Beach, Florida in April, 1970.

The analog techniques described herein were developed primarily by various others^{1,2,3,11,12}. In developing the digital techniques and in preparing the example, the author received help and programming services from many of his co-workers at RCA. Among these were Anne Exline, Dennis Johnston, Sheldon Jordan, Dave Karlson, Robert Lastra, John Rollins, Neil Walker, and Larry Wilson.

References

1. Elias, P., Grey, D. S., and Robinson, D. Z., "Fourier

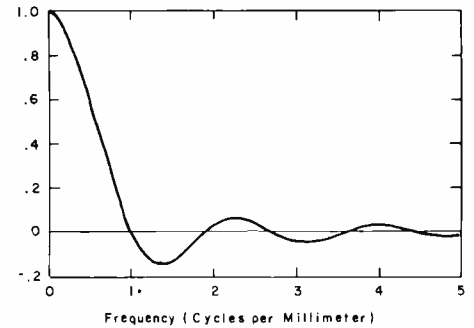


Fig. 12—Optical transfer function in example.

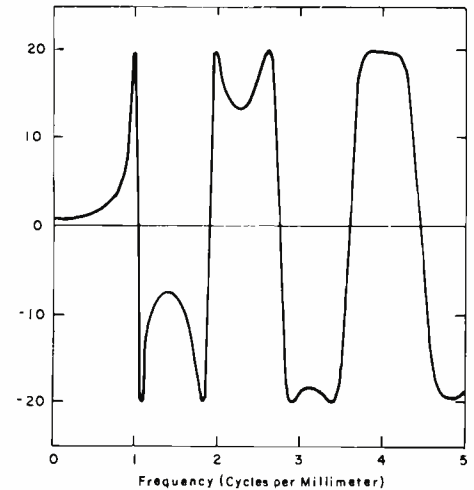


Fig. 13—Filter transfer function in example.

2. Treatment of Optical Processes," *J of Optical Soc of America*, Vol. 42, No. 2 (Feb 1952) pp. 127-134.
2. O'Neill, E. L., "Spatial Filtering in Optics," *IRE Trans on Information Theory*, Vol. IT-2, No. 2 (June 1956) pp. 56-65.
3. Cutrona, L. J., Leith, E. N., Palermo, C. J., and Porcello, L. J., "Optical Data Processing and Filtering Systems," *IRE Trans on Information Theory*, Vol. IT-6, No. 3 (June 1960) pp. 386-400.
4. Vander Lugt, A., Rotz, F. B., and Klooster, Jr., A., "Character-Reading by Optical Spatial Filtering," *Optical and Electro-Optical Information Processing*, (ed. J. T. Tippett et al.; The Massachusetts Institute of Technology Press; 1965).
5. Harris, J. L., Sr., "Image Evaluation and Restoration," *J of Optical Soc of America*, Vol. 56, No. 5 (May, 1966) pp. 569-574.
6. McGlamery, B. L., "Restoration of Turbulence-Degraded Images," *J of Optical Soc of America*, Vol. 57, No. 3 (March 1967) pp. 293-297.
7. Wainstein, L. A. and Zubakov, V. D., *Extraction of Signals from Noise*, (trans. R. A. Silverman; Prentice-Hall; 1962).
8. Preston, Jr., K., "Use of the Fourier Transformable Properties of Lenses for Signal Spectrum Analysis," *Optical and Electro-Optical Information Processing*, (ed. J. T. Tippett et al.; The Massachusetts Institute of Technology Press; 1965).
9. Leith, E. N. and Upatnieks, J., "Wavefront Reconstruction with Continuous-Tone Objects," *J of Optical Soc of America*, Vol. 53, No. 12 (Dec 1963) pp. 1377-1381.
10. Cooley, J. W. and Tukey, J. W., "An Algorithm for the Machine Calculation of Complex Fourier Series," *Mathematics of Computation*, Vol. 19, No. 90, (April 1965) pp. 297-301.
11. Leith, E. N., Kozma, A., and Upatnieks, J., "Coherent Optical Systems for Data Processing, Spatial Filtering, and Wavefront Reconstruction," *Optical and Electro-Optical Information Processing*, (ed. J. T. Tippett et al.; The Massachusetts Institute of Technology Press; 1965).
12. Stroke, G. W., Indebetouw, G., and Puech, C., "A Posteriori Holographic Sharp-Focus Image Restoration from Ordinary Blurred Photographs of Three-Dimensional Objects Photographed in Ordinary White Light," *Physics Letters*, Vol. 26A, No. 9 (25 March 1968) pp. 443-444.

Digital correlator with partial summation and received data foldover

Harold A. Ulrich

The digital correlator processor described in this paper lends itself to hardware reduction and simplification, minimization of re-clock distribution, and ease of processor expansion for any length code. This technique is presently employed by RCA on the Aegis program.

THE PULSE-COMPRESSION SYSTEM employs a transmitted waveform at a given frequency comprised of N bits of binary phase code. A pseudo-random code generator is used to generate the transmitted phase code. The received signals are phase detected into quadrature, bi-polar video components. Each video component is hard limited into a single-bit, binary signal. This single bit is sampled at a frequency, f , and the samples are then correlated with the transmitted reference phase code in a digital processor.

Harold A. E. Ulrich
Signal Processing
Missile & Surface Radar Division
Moorestown, New Jersey

received both the BE and MSEE degrees from Stevens Institute of Technology in 1963 and 1965 respectively. He joined RCA in 1965 as a Design Engineer with the Moorestown Signal Processing Engineering Department, where he has worked on the design of Digital Systems for such programs as Terrier, RDP, Site X, MPS-36, and presently the AEGIS Signal Processor. Mr. Ulrich has also served as an instructor, for several years, in the RCA After Hours Study Program.

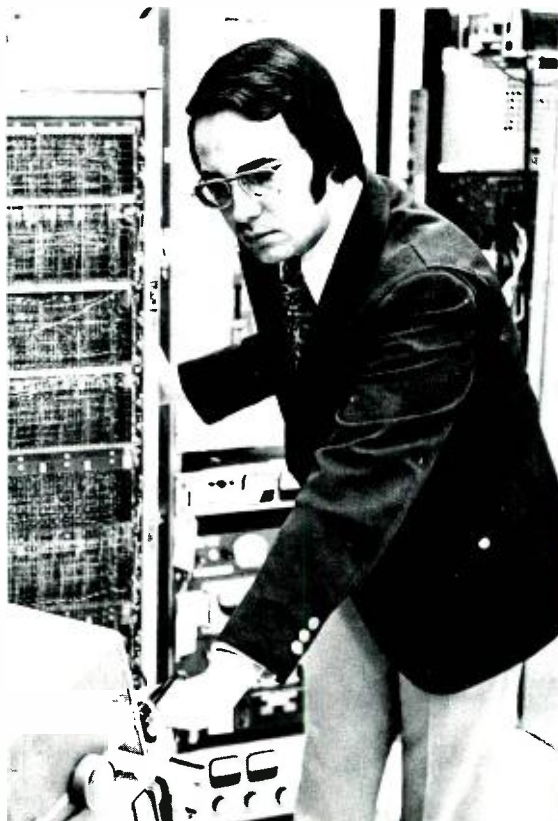
Correlation algorithm

The digital pulse compression system performs the cross-correlation between the transmitted code and returned signal as follows:

- 1) Choose the "true" sequence (transmitted code).
- 2) Arrange (quantize) the incoming data into a binary sequence of 1's and 0's.
- 3) Compare columns of true sequence and incoming data.
- 4) Form the following correlation factor, C , for the segment of time under consideration:

$$C \equiv \frac{(\# \text{ of agreements}) - (\# \text{ of disagreements})}{(\# \text{ of agreements}) + (\# \text{ of disagreements})}$$

- 5) Read out range-cell result.
- 6) Shift incoming data one bit and repeat 3) through 5)
- 7) Continue the shift and compare operation until the end of the receive interval.



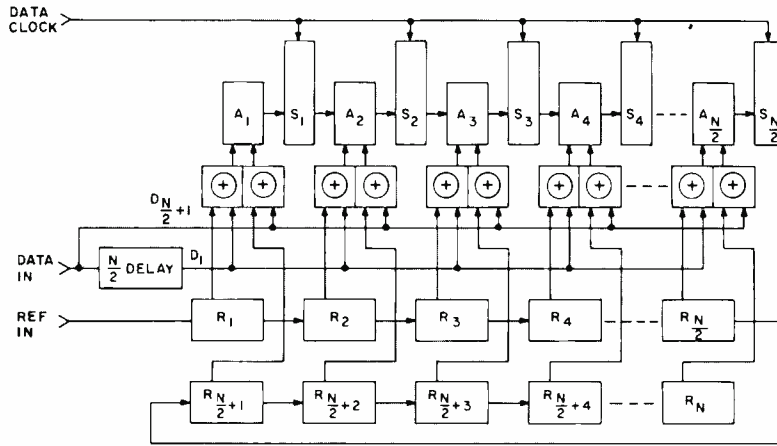


Fig. 1—Implementation of the data-foldover partial-summation technique for N -bit code.

The digital correlator performs steps 3) through 5) above yielding instantaneous target signal strength for each range cell processed. The correlator transfer function is derived as follows: Let M be the number of agreements and N be code length. Then $N - M$ is the number of disagreements.

Substituting into the correlation factor equation yields:

$$C = \frac{M - (N - M)}{M + (N - M)} = \frac{2M - N}{N}$$

$$C = \frac{2}{N} \left(M - \frac{N}{2} \right)$$

$$\text{Signal strength} = C \frac{N}{2}$$

Thus,

$$\text{Signal strength} = M - \frac{N}{2} \quad (1)$$

Note that $M=0$ corresponds to a strong out-of-phase target return; $M=N$ corresponds to a strong in-phase target return; and $M=N/2$ corresponds to the average for a noise-only environment.

Data-foldover partial-summation technique

This implementation approach is shown in Fig. 1 for the N -bit-code case. The data to be processed is divided such that one portion is fed directly into the correlation unit and the other portion is delayed in a shift register by half the code length ($N/2$ delay). When data bit D_1 appears at

the output of the $N/2$ delay register, data bit $D_{(N/2)+1}$ is at the direct input. Hence data bit $D_{(N/2)+1}$ has been folded over'' onto data bit D_1 thus allowing both bits to be processed at the same time in the correlation unit with the result that the processing length of the unit is cut in half.

The partial summation portion of the correlation unit is indicated by A_1, A_2 through $A_{N/2}$ of Fig. 1. This ripple add-store approach replaces the adder-tree requirement of the usual correlator processor.

The correlation unit operates as follows. Data bit D_1 is compared to reference code bits R_1, R_2 , through $R_{N/2}$ at the same time data bit $D_{(N/2)+1}$ is compared to reference code bits $R_{(N/2)+1}$ through R_N . The resultant comparisons of D_1 with R_1 and $D_{(N/2)+1}$ with $R_{(N/2)+1}$ (written as $D_1 + R_1$ and $D_{(N/2)+1} - R_{(N/2)+1}$) are supplied to partial adder A_1 . The other comparison results are also applied to their respective partial adders. Hence the outputs of A_1 through $A_{N/2}$ are as follows:

$$A_1 = D_1 \oplus R_1 + D_{(N/2)+1} \oplus R_{(N/2)+1}$$

$$A_2 = D_1 \oplus R_2 + D_{(N/2)+1} \oplus R_{(N/2)+2}$$

•

•

$$A_{N/2} = D_1 + R_{N/2} + D_{(N/2)+1} + R_N$$

At the next clock, the A_1 output is strobed into storage register S_1, A_2 into $S_2, \dots, A_{N/2}$ into $S_{N/2}$. This strobe also shifts data bit D_2 on line from the $N/2$ delay register and data

bit $D_{(N/2)+2}$ from the direct input. As before, D_2 is compared to R_1 through $R_{N/2}$ and $D_{(N/2)+2}$ to $R_{(N/2)+1}$ through R_N ; the resultant comparisons are then applied to their respective partial-adder inputs along with the shifting-register contents from the previous stage yielding the following adder outputs:

$$A_1 = D_2 \oplus R_1 + D_{(N/2)+2} \oplus R_{(N/2)+1}$$

$$A_2 = S_1 + D_2 \oplus R_2 + D_{(N/2)+2} \oplus R_{(N/2)+2} \\ = D_1 \oplus R_1 + D_2 \oplus R_2 + D_{(N/2)+1} \\ \oplus R_{(N/2)+1} + D_{(N/2)+2} \oplus R_{(N/2)+2}$$

•

•

•

$$A_{N/2} = S_{(N/2)-1} + D_2 \oplus R_{N/2} + D_{(N/2)+2} \oplus R_N$$

This process continues over the entire received signal interval. It takes N reclocks to obtain the following first full correlation output (there are $N/2$ shift-register stage delays in the foldover unit and $N/2$ processing delays in the correlation/partial summer unit):

$$A_{N/2} = S_{(N/2)-1} + D_{N/2} \oplus R_{N/2} + D_N \oplus R_N$$

where

$$S_{(N/2)-1} = \sum_{i=1}^{(N/2)-1} D_i + R_i + \sum_{j=(N/2)+1}^{N-1} D_j + R_j$$

Recalling from above that the range cell signal strength is equal to $M - (N/2)$. The $-(N/2)$ is achieved in this correlation technique as a simple pre-set to the input of adder A_1 .

Hardware implementation

An eight-stage correlator module is shown in Fig. 2. It is a complete unit containing storage for eight changeable reference bits, eight comparison networks, and a partial-summation network capable of handling code lengths up to 128 bits. The summation network input/output bit weighting was selected such that any code that is an even multiple of eight can be accommodated by just adding the appropriate number of modules in a series fashion as follows:

Code Length	No. of Modules Required
8	1
16	2
32	4
64	8
128	16

Fig. 3 shows the module configuration for a code length of 32.

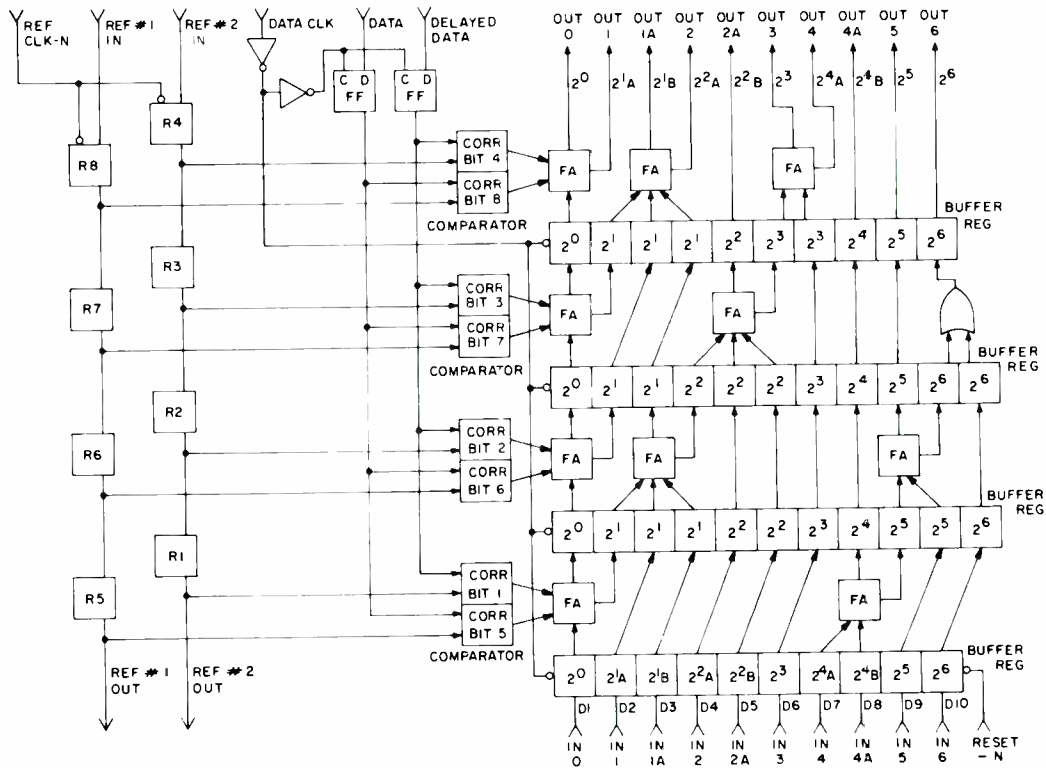


Fig. 2—Eight-stage correlator module.

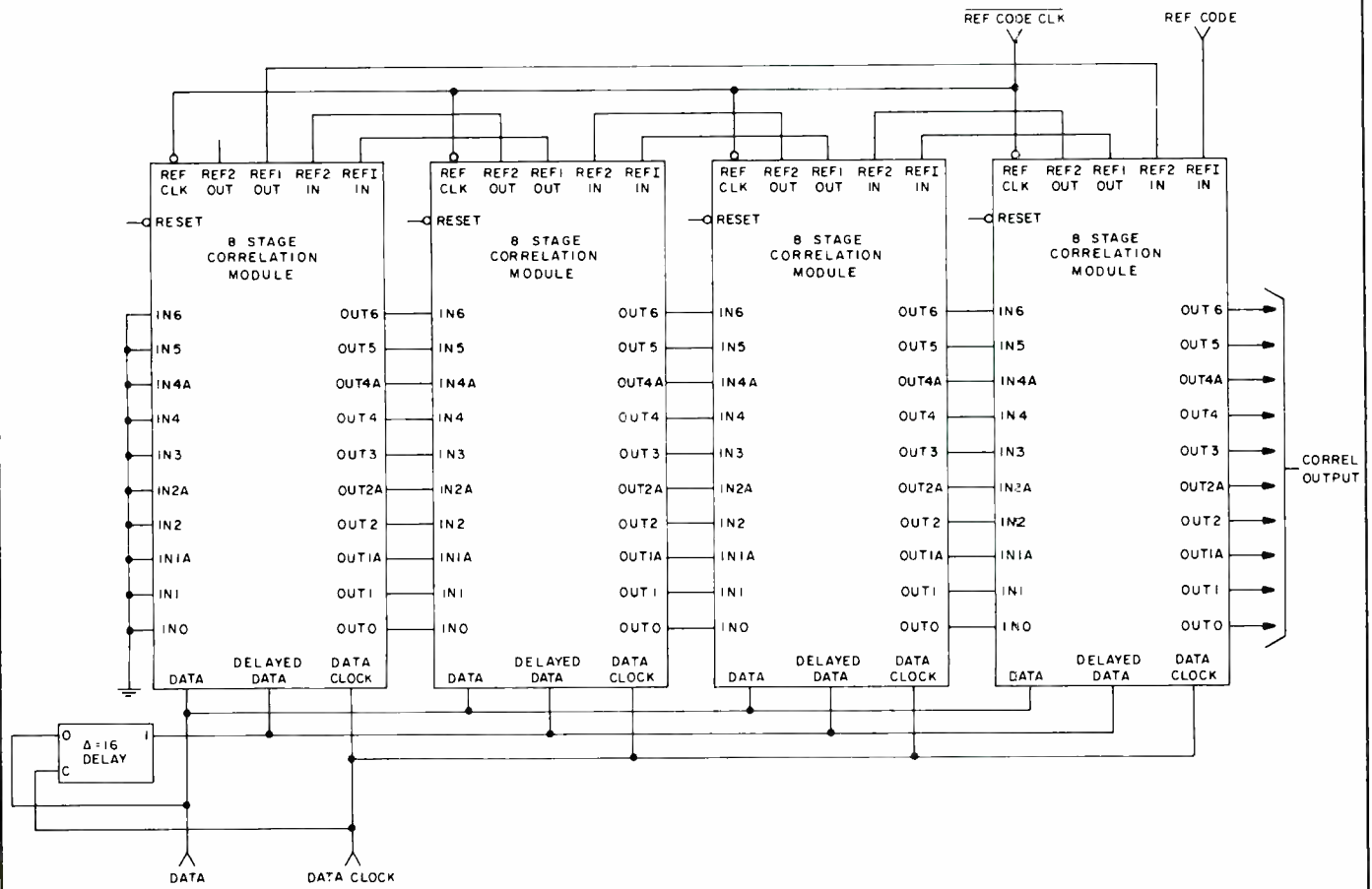


Fig. 3—Correlator for a code length of 32.

NMODES computer program

R. C. Bauder | C. H. McKee

NMODES is a mechanical design-aid computer program which calculates the free vibration and shock response of many types of structures. Understanding the free-vibration behavior of electron devices is often important. The problem approach usually used involves repeated prototype building, educated guessing, and testing. With NMODES, however, consistent mass and stiffness matrices are developed which, when applied to an eigenvalue problem solution, yield the natural frequencies and modal shapes of the structure.

THE ADVANTAGES OF THE NMODES PROGRAM, as compared to other structural computer analysis techniques such as electrical analogs and static framework techniques, are:

- NMODES deals directly with the individual beam material and section properties without recourse to electrical analogs.
- The only inputs for each structure member are density, length, modulus of elasticity, type of beam, and dimensions. There are fourteen standard beam types built into the program.
- Using simple *yes* or *no* instructions, the designer can model each member as a flexible beam with mass, a flexible beam without mass, or a rigid mass.
- The distortion of each beam segment is specified by a rotation and deflection at each end, thereby approximating a smooth polynomial. Actually, a cubic is used which implies that shear is constant and moment varies linearly over each beam segment. This technique is more accurate than mass lumping at discrete points.
- NMODES includes shear deformation to yield more accurate results when short thick beams such as the hollow cylinders used in the construction of many electron devices are involved.

Computer program

The program is available on BTSS and batch. The BTSS program will handle up to twenty degrees of freedom. The batch program will handle up to thirty degrees of freedom. Provisions are made to store the basic model to allow for subsequent model changes. The basic flow chart given in Fig. 1 does not show the "aside" options such as data display, model storage, and special inputs.

Modeling the problem

A three-element structure, shown in Fig. 2, is used to illustrate the mechanical modeling. The design engineer is usually interested in the natural frequencies and the amount of motion at these frequencies (modal shapes). To specify these motions, the absolute

displacements, U_{ij} , and absolute rotations, ω_{ij} , (as shown in Fig. 3) are used. However, because the deformation of each beam is specified by a *deflection and rotation at each end*, it is more appropriate to specify a different coordinate system (illustrated in Fig. 4) which defines the conditions at each end of the beam and joins this additional system to the absolute coordinate system by means of a joiner matrix.

Reprint RE-18-3-9
Final manuscript received May 1, 1972.

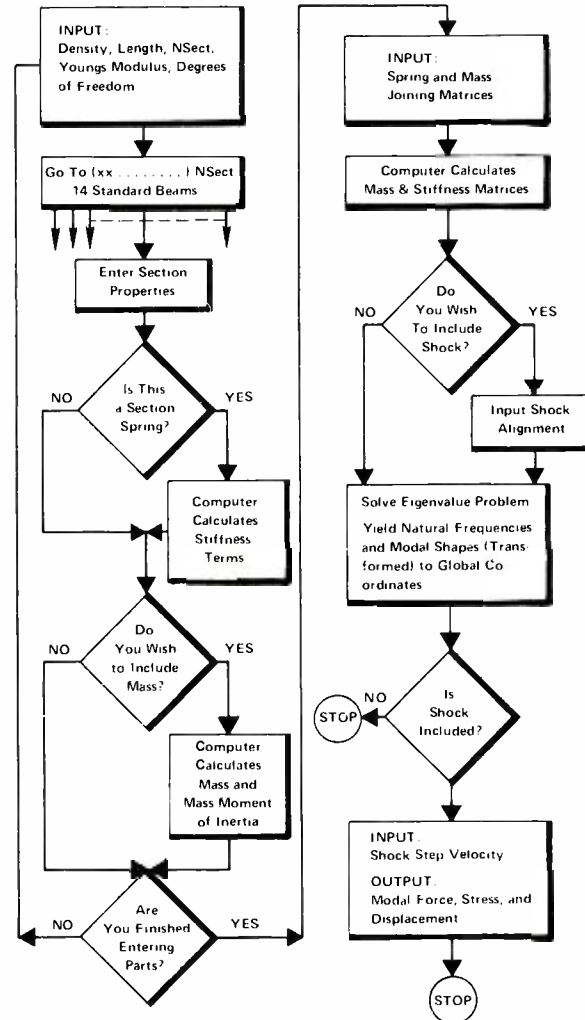


Fig. 1—Basic NMODES flow chart.

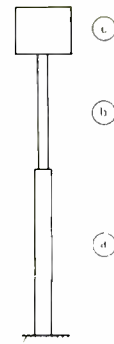


Fig. 2—Three-element model.

Thus,

$$U_{b2} = X_1 + \Theta_1 L_b + X_2 + X_0 \quad (\text{for small deflections})$$

$$U_{a2} = U_{b1} = X_1 + X_0$$

$$\psi_{a2} = \psi_{b2} = \Theta_1$$

$$\psi_{a1} = U_{a1} = 0$$

$$U_c = X_1 + (L_b + d_1) \Theta_1 + X_2 + d_1 \Theta_2 + X_0$$

$$\psi_c = \psi_{b2} = \Theta_1 + \Theta_2$$

where the subscript $a1$ refers to the lower end of element @, etc., as illus-

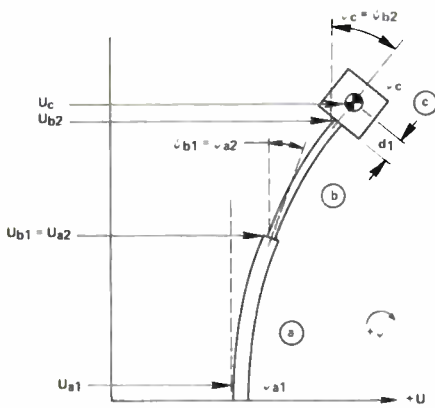


Fig. 3—Deformed model.

trated in Fig. 3. The X_1 , θ_1 , X_2 , θ_2 coordinates, shown in Fig. 4, are the system coordinates.

In the matrix form, the two coordinate systems can be joined as follows:

$$\begin{bmatrix} U_{a1} \\ \psi_{a1} \\ U_{a2} \\ \psi_{a2} \\ U_{b1} \\ \psi_{b1} \\ U_{b2} \\ \psi_{b2} \\ U_c \\ \psi_c \end{bmatrix} = \begin{bmatrix} 1 \\ 0 \\ 1 \\ 0 \\ 1 \\ 0 \\ 1 \\ 0 \\ 1 \\ 0 \end{bmatrix} [X_b] + \begin{bmatrix} 0 & 0 & 0 & 0 \\ 0 & 0 & 0 & 0 \\ 1 & 0 & 0 & 0 \\ 0 & 1 & 0 & 0 \\ 1 & 0 & 0 & 0 \\ 0 & 1 & 0 & 0 \\ 1 & L_b & 1 & 0 \\ 0 & 1 & 0 & 1 \\ 1 & (L_b + d_1) & 1 & d_1 \\ 0 & 1 & 0 & 1 \end{bmatrix}$$

$$[U] = [J_m] [X]$$

where $[J_m]$ is the mass-joining matrix. The computer program forms a consistent mass matrix from the relationship.

$$[M] = [J_m]^T [M_{unc}] [J_m]$$

where M_{unc} is the uncoupled-mass matrix which is computer-formed from the input material constants and section properties, of each structural member.

Likewise, a spring-joining matrix is formed as follows:

$$\begin{bmatrix} D_a \\ \phi_a \\ D_b \\ \phi_b \end{bmatrix} = \begin{bmatrix} 1 & 0 & 0 & 0 \\ 0 & 1 & 0 & 0 \\ 0 & 0 & 1 & 0 \\ 0 & 0 & 0 & 1 \end{bmatrix} \begin{bmatrix} X_2 \\ \theta_1 \\ X_2 \\ \theta_2 \end{bmatrix}$$

$$[D] = [J_s] [X]$$

Where D_a and D_b are the spring deflection of members a and b , respectively in Fig. 2 and 3, and θ_a and θ_b

are the spring rotation of these members.

The computer program forms a symmetric stiffness matrix.

$$[K] = [J_s]^T [K_{unc}] [J_s]$$

Where K_{unc} is the computer-formed uncoupled stiffness matrix of each spring member.

The eigenvalue problem.

$$[K][V] = \varphi [M][V][\Lambda]$$

is now solved where $[K]$ is the structure stiffness matrix; $[M]$ is the mass matrix; $[V]$ is the eigenvector (modal shape) matrix; and $[\Lambda]$ is the eigenvalue (frequency squared) matrix.

Considerations

- 1) To use this program as a design aid, the engineer must simply model the structure as an assembly of springs and masses and write the joining matrices. The assumptions involved are made through assigning stiffness and/or mass properties to the elements.
- 2) The eigenvalue problem will yield modal shapes, which are *relative displacements* (with direction). These displacements are normalized to one. Subsequently, if the actual displacement of one coordinate

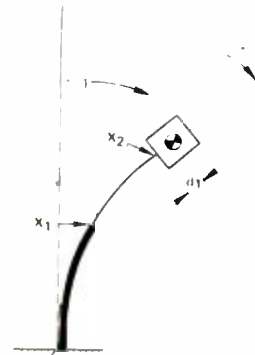


Fig. 4—System coordinates.

point is experimentally measured from a prototype test, the actual displacement of any other point is simply a matter of applying ratios to the modal shapes.

- 3) Although the program does not synthesize structures, it does provide for investigation of changes without re-entering the entire data deck. A "model tape" is preserved which contains the joining matrices and individual beam information. The theoretical structure change is executed by entering only the new data for the elements involved.
- 4) The user has the option of applying a theoretical step-velocity shock pulse and shock-alignment vector to the structure and getting actual deflection, force, and stress as output. These outputs are printed in modal form (magnitude and direction at each natural frequency).

R. C. Bauder, Environmental Engineering, Electronic Components, Lancaster, Pennsylvania, received the BS in Physics from Muhlenberg College in 1961. He then attended Franklin and Marshall College and received MS in Engineering and Science from Penn State University in 1969. Mr. Bauder joined the Special Equipment Design group at RCA Lancaster in 1962 and worked on the design of microwave test equipment for small and medium power tubes. From 1965 to 1968, he worked in Color Tube production. The major assignments here were the development of automated phosphor screening processes and the reclamation of phosphors from waste water. Since 1968, he has worked in Environmental Engineering where his primary responsibilities have been in stress analysis and the development of computer-aided structural design programs. He has published several reports on the NMODES method of predicting the dynamic behavior of structures.

C. H. McKee, Environmental Engineering, Electronic Components, Lancaster, Pennsylvania, attended Lycoming College, Williamsport, and General Motors Institute, Flint, Michigan. He holds a Professional Mechanical Engineering License in the state of Pennsylvania. In 1959, Mr. McKee joined Electronic Components Environmental Engineering section. He has been active in environmental design, stress analysis, and vibration analysis. He has written numerous computer programs and published several papers in these fields.

Authors Bauder (left) and McKee



Computer-designed microwave-integrated-circuit layouts

W. L. Bailey | R. E. Kleppinger

A system has been developed whereby the microwave-integrated-circuit designer can interact with a time-sharing computer to design microstrip and lumped-element components, determine circuit layouts, and obtain the photomasks for these circuits. Computer programs have been written for those component designs that are adequately defined. Other component designs requiring more judgment are left to the designer. A method of interlocking these design concepts to obtain the necessary circuit photomasks is described.

MICROWAVE INTEGRATED CIRCUITS (MICs) can be made by use of distributed or lumped-element circuit techniques. Distributed circuits consist of a strip conductor separated from a ground plane by a dielectric layer. Lumped-element circuits, on the other hand, are made by use of thin-film discrete resistors, capacitors, and inductors that are smaller than a quarter wavelength. Either type circuit can be made in hybrid form where individual components are mounted on a common substrate and appropriate connections made between them. However, from both economical and technical viewpoints, it is desirable to make these circuits as completely integrated as possible. This requirement is particularly true of lumped-element circuits.

To accomplish this integration goal, photomasks must be obtained before the circuits are processed. Once the electrical circuit is known, the following steps are required:

- 1) translation of the electrical data to physical component data,
- 2) determination of an acceptable physical circuit layout, and
- 3) transfer of the circuit layout to a set of photomasks.

In the past, these three steps have been done by use of nomographs and slide rules, standard mechanical drafting tools and artwork-cutting methods, and photographic reduction and step-and-repeat techniques. Considerable

effort has been expended in recent years to develop computer-generated artwork. Many individuals are also currently developing device models utilizing computers. In general, these two efforts have not yet been combined.

Robert E. Kleppinger
RF Design Engineering
Solid State Division
Somerville, N.J.

received the BSEE from the University of Nebraska in 1951 and a MS in mathematics from Stevens Institute of Technology in 1955. He joined RCA in 1951 as an engineer. In this capacity, he developed germanium alloy transistors for different frequencies and power, and low power germanium drift transistors. In 1960 he became an Engineering Leader. As such he has been responsible for the design and processing of small signal germanium and silicon transistors, rectifiers, and MOS transistors. From 1968 to 1971 he was responsible for the module processing of microwave micro-electronics. Mr. Kleppinger has one patent issued and has authored or co-authored several technical papers. He is a Senior Member of the IEEE.

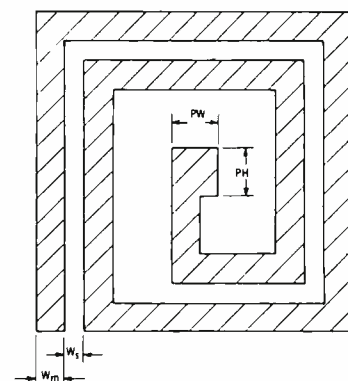


Fig. 1—Square-spiral coil.

This paper describes a system developed to obtain MIC photomasks from electrical and physical process data with appropriate use of a time-sharing computer.

Once the electrical circuit is determined, the physical sizes of individual components and their placement relative to each other must be developed. This step then must be translated into data which will operate a Mann Pattern Generator to obtain the desired circuit photomasks. Because many of these operations are repetitious and well defined, a computer can be used advantageously to perform them. However, certain component designs and layouts still require sufficient judgment that complete computer usage is questionable. Prints of the masks from the Pattern Generator are directly usable to make small numbers of circuits for quick testing. When an acceptable circuit has been made, the original layout data can be reused to obtain photomasks with large numbers of circuits for production.

Those components that currently lend themselves to complete machine design will be discussed first. The computer program aids used in designing other

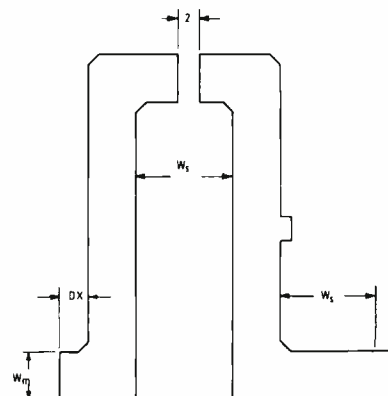


Fig. 2—Bar inductor.

Reprint RE-18-3-7 (ST-4685)
Final manuscript received October 29, 1971.

components will then be described. Next, the computer program required to transfer this data into data acceptable to the Pattern Generator computer will be discussed. Last, the method of obtaining a particular MIC photomask set will be traced through the system.

Component design

Equations to transform electrical component values to physical component parameters can be found in the literature.^{1,2} From this information, the component geometry can be chosen that is compatible with the overall circuit layout. The extent a computer is used in each of these steps depends on the degree of design flexibility required. For example, spiral and bar inductors lend themselves to designing with a time-sharing computer; tuneable metal-oxide-metal (MOM) capacitors do not, because of the numerous pattern possibilities. Resistor and microstrip line patterns can be computer designed once the geometrical translations are mathematically defined.

Because the present Mann Pattern Generator cannot produce circles, computer programs for only square or rectangular spiral coil constructions have been written. Given the desired electrical value for the square spiral coil shown in Fig. 1, a metal width and spacing can be chosen and the computer used to obtain a geometrical layout which gives a coil length within a specified amount of the value calculated from the following equation:

$$L = 0.0068 \frac{l^4/3}{w^1/3} \quad (1)$$

where L is the inductance (nH); l is the length (mils), and w is the sum of w_m and w_s , in which w_m is the metal width and w_s is the spacing between adjacent metal strips (both in mils).

The computer program gives a choice of a square or rectangular coil shape. In the case of a rectangle, the width or height is controlled to be less than a specified value. The coil length is adjusted until it is within a specified amount of the required length and the controlled side is within a specified value of that required. Because the inner pad could be near the coil end or at the opposite side of the rectangle, this choice is made available. The coil exit or end could be at any of the four corners of the square or rectangle and

/DO MIC REC		
IF SQUARE COIL TYPE S, IF RECTANGULAR TYPE R HERE=>>R		
INNER PAD SAME SIDE AS COIL EXIT OR OPPOSITE -TYPE S OR O HERE=>>O		
TYPE COIL EXIT AS TOP,BOTTOM-LEFT,RIGHT-HORIZONTAL,VERTICAL		
-FOR EXAMPLF TYPE TOP-LEFT-HORIZONTAL AS TLH HERE=>>BRV		
CORRECTION FOR UNDERCUTTING=R		
RFC=22		
WM=3		
WS=2		
PW=8		
PH=8		
MAXIMUM COIL WIDTH=48		
IF ONLY ONE LOOP TYPE 1 OTHERWISE TYPE 2 HERE=>>2		
RFCE= 25.28NH ERROR= 0.00% RECTANGLE 4R,8PBV 74.25MIL		
WM= 3.00MIL WS= 2.00MIL D= 26.25MIL		
INNER PAD 4,8PBV 8.00MIL LENGTH= 710.25MIL #BLOCKS= 21		
IF TAP DATA WANTED TYPE 0, OTHERWISE TYPE 1 HERE=>>0		
LOOP#	LENGTH	INDUCTANCE
0.5	81.00	1.39
1	137.25	2.82
1.5	212.00	5.03
2	288.25	7.97
2.5	383.00	11.06
3	479.25	14.91
3.5	594.00	19.86
4	710.25	25.28
COIL MOVED TO NEW POSITION? TYPE YES OR NO HERE=>>NO		
BOTTOM LEFT CORNER COORDINATES FOR INNER PAD ARE (20.00, 46.25) AND		
FOR COIL EXIT ARE (45.00, 1.25)		
DATA STORED IN TAPE55		
1690		

Table 1—Spiral coil design.

is specified by noting top or bottom and left or right. The coil exit direction is specified as vertical or horizontal. For example, the coil exit in Fig. 1 would be specified as bottom-left-vertical. This coil position is valuable later during construction of the passive integrated-circuit layout. The ability to correct for metal etch undercutting is provided in the program. The inner pad width, PW , and height, PH , can be zero or any value convenient for the deposited or bonded connection to be used. Included in the program is the ability to impose a one-loop restriction. Coil design data useful in later circuit-layout considerations is printed by the computer. If desired, a table showing the inductance value at each half and whole loop can be obtained. Again, for circuit layout convenience, the coil can be moved to a different coordinate posi-

tion. The last step in this program is to provide a tape file containing the block data required for the translation program. An example of the operation of this program is shown in Table 1. The underscored parts are the data supplied by the teletype operator.

Given the required electrical value for a bar or strip inductor, a metal width and thickness can be chosen and the computer used to obtain a geometrical layout. To provide more circuit versatility, a tuneable bar or strip inductor has been designed as shown in Fig. 2. Different inductance values are obtained by wire bonding across the two legs at different points.

Because the distance from the inductor to the next component may need to be very small, the ability to set this arrangement is provided in the computer

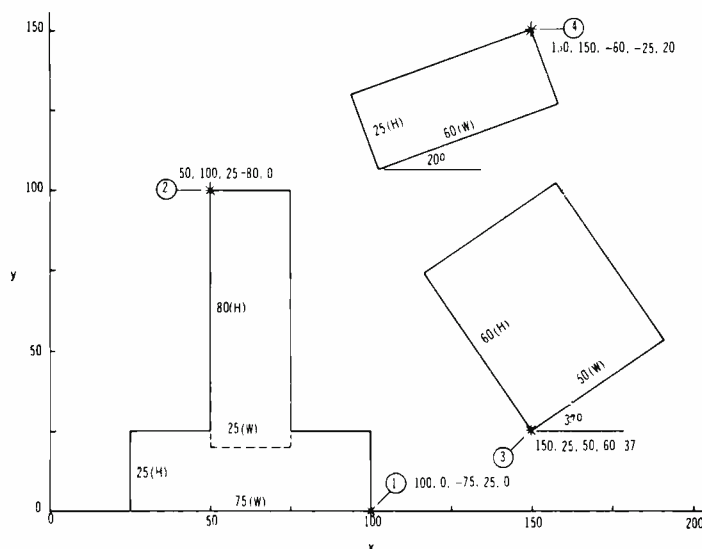


Fig. 3—A typical block pattern.

Component	Value (pF)	Area (mil ²)	Size (mil)
Capacitors	1.0	32	6 × 5.5
	0.75	24	4 × 6
	0.5	16	4 × 4
	1.5	48	4.8 × 10
	3.5	112	11 × 10
Spiral Coil	25 nH		48 × 75 see Table I
Strip Inductor	1.3-5.4		79 × 93 see Table II

Table IV—Component geometry data.

conditions, the layout method will be followed for the circuit shown in Fig. 4. In this case, there are two clusters of capacitors, a spiral coil, and a strip inductor. The sequence of steps to follow for this example is shown in Fig. 5. The first step is to obtain the electrical-physical inductor and capacitor data shown in Table IV. From the sketch shown in Fig. 6, the required capacitor, component-connection, and alignment-key-position data can be determined. These data are then placed in the computer memory and checked for correctness using the display section of the translate program. The rectangular spiral coil and strip inductor data are determined with their new coordinate positions and added to the capacitor and connector data in memory. From this step, a punched paper tape is obtained which will operate the Pattern Generator and provide a photomask from the top metal layer. By assumption that the capacitor-connector data are already stored in the computer under the file name TAPE95. The data obtained from the working sketch (Fig. 6) for the bottom metal layer and the oxide layer must be run separately through the Pattern Generator.

The complete set of photomasks for this circuit is shown in Fig. 7. Because this circuit is developmental, only six circuit patterns were reproduced directly from the Pattern Generator. The choice of three patterns in the *x*-direction ($NX=3$) and two in the *y*-direction ($NY=2$) reduces computer running times. Once the circuit is electrically acceptable, the data obtained from the working sketch and component design programs can be used to obtain reticles from the Pattern Generator. These reticles are then used to obtain photomasks with a large number of circuit patterns.

Conclusions

A system has been developed to design microstrip and lumped-element circuit

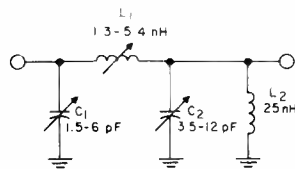


Fig. 4—MIC circuit diagram.

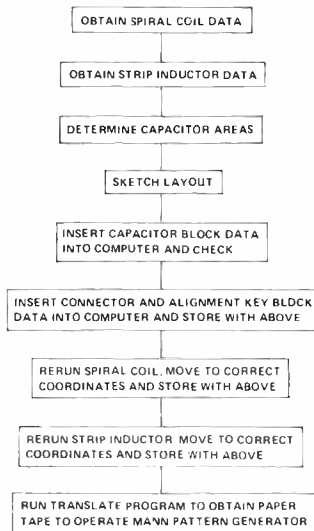


Fig. 5—IC-layout flow chart.

photomasks. This system determines component designs, microwave integrated-circuit layouts, and obtains the circuit photomasks using appropriate interaction between the designer and a time-sharing computer. Computer programs have been written for those component designs that are adequately defined. As other components become sufficiently defined for computer design, they can be readily included in the system developed. Component designs requiring considerable judgment are left to the designer with provision made to readily include these in the system to obtain the final circuit photomask. The data generated can be used to quickly obtain photomasks with a few circuit patterns for rapid electrical evaluation. Once the design is finalized, this same data can be used to generate

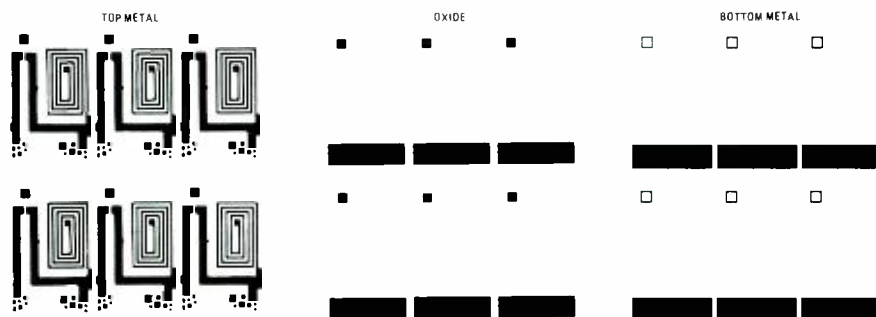


Fig. 7—Photomasks.

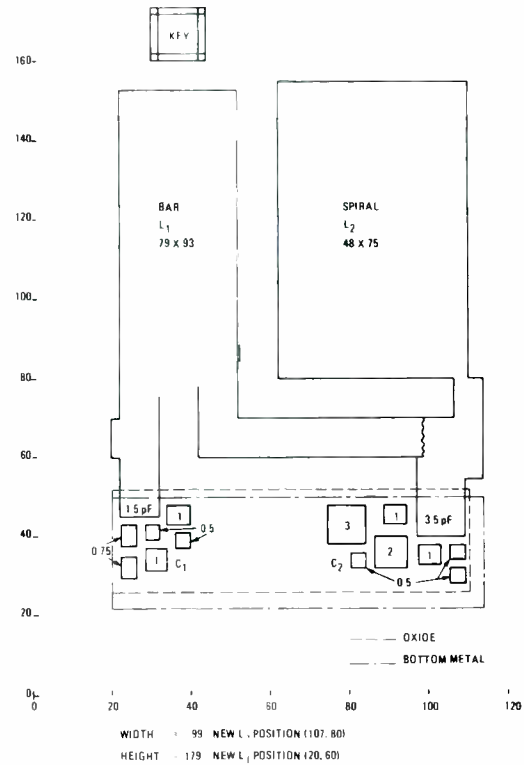


Fig. 6—IC working layout.

photomasks with large numbers of circuits for mass production. As an example, the method for obtaining a particular lumped-element circuit has been described. This same basic system has been used to obtain microstrip circuit photomasks and could be used to obtain a photomask having both microstrip lines and lumped elements in the circuit. The overall system frees the designer of much of the tedium involved with component designs, integrated circuit and microstrip circuit layouts, and reduces the overall time from concept to useful photomasks.

References

1. Sobol, H., "Technology and Design of Hybrid Microwave Integrated Circuits," *Solid State Technology* (Feb. 1970).
2. Dill, H. G., "Designing Inductors for Thin-Film Applications," *Electronic Design* (Feb. 17, 1964).

RCA-DYNA: a large structural dynamics computer program

Dr. R. J. Pschunder

The design of high performance structures to dynamic specifications requires the availability of a reliable structural dynamics computer program. Missile and Surface Radar Division, Moorestown, N.J. has acquired a basic routine and has built it into a powerful tool. RCA-DYNA is able to analyze the dynamic responses of large complex structures to any type of input.

THE SPACE AGE has greatly advanced the state of the art in structural analysis. In contrast to hand analysis, which is limited to simple structures or simplifying assumptions, computer programs can analyze complex structures with a high degree of accuracy. Safety factors, which previously had to be large to compensate for many unknown factors, are now allowed to shrink, resulting in efficient, lightweight structures. In these structures, the control of the effects of shock and vibrations becomes an important consideration. Further progress was made by extending the statics programs into the field of structural dynamics. The result is an analysis capability that a few years ago seemed unreachable.

Sophisticated customers are aware of these developments and are expecting the producer of high-performance equipment to have acquired the new technologies in structural design.

M&SR has established in-house capabilities to be responsive to all coming needs in the structural dynamics field.

Development of RCA-DYNA

Basic skills in structural dynamics were developed at M&SR for the design of the family of tracking radars, such as FPS-16, FPQ-6, TPQ-18, and FPS-49. For more complex analysis, as required by NASA for the Lunar Module landing radar, M&SR had to rely on outside consultants. The winning of the AEGIS program by M&SR released funds to acquire a basic dynamics computer program and implement in-house capabilities in structural dynamics. This resulted in a better control of the costs, schedules, extent, and reliability of the analysis.

Since then, much effort has gone into rewriting and increasing the capabilities

of the original program. The new development was named "DYNA" for Dynamic Structural Analysis System. It is fully operational to the extent described in this paper.

Capabilities of DYNA

DYNA is a large structural dynamics program that uses the finite element approach to model complex structures and normal mode theory for solving the dynamics. This program is dimensioned to work with:

2000 structural elements such as: bars, beams, triangular, rectangular and quadrilateral plates, special elements, and rigid members

2000 elastomechanics degrees of freedom

300 mass degrees of freedom

The analysis options are as follows:

- 1) Static analysis of deflections and stresses of structures.
- 2) Natural frequencies and mode shapes.
- 3) Dynamic responses to:
 - a. Sinusoidal force or base motion inputs. (Aeolian vibrations, responses to discrete frequencies.)
 - b. Sine sweeps in evenly or unevenly spaced frequency steps. (Predictions of behavior during a shaker test.)
 - c. Random vibrations, given a spectral density plot. (Calculations of random g' levels and random stresses.)
 - d. Shocks specified by a time plot. (Atomic and gun blasts, under water and ground shocks, earthquakes, driving over rough road beds, etc.)
 - e. Shock spectra on Navy vessels (NAVSHIPS-250-423-30).
 - f. Shock spectra, given by velocity or acceleration vs. frequency plots.

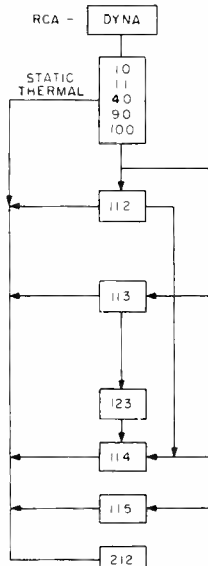


Dr. Ralph J. Pschunder
Advanced Mechanical Technology Group
Missile and Surface Radar Division
Moorestown, N.J.

received the MME in 1941 and the PhD in 1965 from the Technical University in Vienna, Austria. In Vienna, Dr. Pschunder was a research engineer for the Viennese Locomotive Works in the field of thermodynamics and stresses of steam engine boilers. For seven years, before coming to the U.S., he taught mechanical engineering and served as consultant to industry in the thermal lab attached to the school. In 1954, Dr. Pschunder worked for the N.Y. Brake Co. in Watertown, N.Y., where he was a research engineer in aircraft hydraulics. In 1959, he joined M&SR and was assigned to various structural analysis tasks. He worked on the BMEWS radomes and developed the theory and designs of the MIPR tower and foundations and, later, FPS-16's. He has spent 5 years generating the theory and computer programs for the complex cable structures of the Cobra-Mist antenna, for which he has written a number of accurate catenary and guyed tower programs. He was involved in the dynamics of ships structures (AEGIS), space structures (Apollo and Viking), and hardened structures (CAMEL). Dr. Pschunder has implemented the RCA-DYNA computer program at RCA facilities and is presently writing DYNA-2. He holds 4 U.S. patents, has written several papers, and is a Licensed Professional Engineer in the State of New Jersey.

g. Generation of shock spectra for selected mass-degrees of freedom.

- 4) Thermal stresses—The deflections and stresses caused by temperature gradients are treated as a statics problem. The thermal stress option allows a link-up between DYNA and SPTHA (Spectra-Thermal Analyzer), the thermal program that successfully calculated the thermal profiles of the Lunar Module radars during the Apollo missions. The thermal program calculates steady-state or transient temperature fields which are fed into DYNA.
- 5) Simultaneous vibrations of shocks—Several options exist to superimpose or RMS the responses to inputs coming from various directions (3 axial inputs).
- 6) Phase shift or time delay—Options permit specifying delays of the input functions reaching the mass points; thus it is possible to analyze the effects of a blast wave rolling sideways over a structure.
- 7) Damping—Options include uniform viscous damping, modal damping and individual damping between mass points.



Structural dynamics program 1972

- Input check
- Element and thermal stiffness matrices
- Global stiffness matrix
- Flexibility matrix
- Natural frequencies and mode shapes

Dynamics

1. Sinusoidal force or base motion input
2. Sine sweeps
3. Random vibrations
4. Shock inputs
5. Shock spectrum generation
6. Plots of 1, 2, 3 and 5
7. Super position of compatible runs
8. Time delay for travelling shock

Dynamics for earthquakes

1. Simultaneous shock inputs
2. Plots of selected responses
3. Data save for 123

Shock spectrum generation for 113

Response to shock spectra

Shock analysis on ships

NAVSHIPS-250-423-30/31

Stress analysis (deflections & stresses)

1. Static loading
2. Thermal loading via cards
3. Temperature fields vs time from SPTHA-thermal program
4. Dynamic loading
5. Report on maxima for each member and for total run

Fig. 1—Flow chart of various DYNA subprograms and their functions.

It is then possible to assign various damping rates to different parts of the structure.

- 8) Plotting—Inputs and responses may be presented in graphical form by on-line plotting or using a Calcomp plotter.
- 9) Report on maxima—Tables are printed that record the maximum deflections, g levels or stresses, and when they took place. The maxima tables are used for dynamic responses or transient temperature conditions. This ensures that the most important events are not missed in the bulk of the output.
- 10) Data readability—Great emphasis was put on the readability of the output formats, by providing sufficient headings that make the data understandable to those not too familiar with DYNA.

Operation of DYNA

DYNA is written in FORTRAN-4 and operational on the RCA Spectra 70/55 in M&SR. It also ran on the RCA Spectra 70/45 at RCA's Cherry Hill facility.

The flow chart in Fig. 1 shows the various subprograms and their functions. The linking of successive steps is done by a 10-tape schedule, which saves intermediate data and permits restart without having to regenerate good data.

Efficient operation, i.e., pulling through several steps in one shot, requires the availability of up to 7 tapes and one disc station. The largest memory requirement is 232 bytes.

The DYNA source decks occupy 6 boxes of cards, which are maintained by the Advanced Mechanical Technology Group at M&SR. Actual operation is done from the up-to-date DYNA systems tape or its backup.

DYNA has successfully been used on the following programs:

- AEGIS—Analysis of the MFA support structure, a welded aluminum frame, supporting a phased array radar for the Navy. It lieu of shock testing the 17,000-lb assembly, compliance to MIL-S-901C, MIL-STD-167 and other specifications was proven by this analysis.

The 6-hour net computer time on the relatively slow RCA Spectra 70/55 is typical for a large problem involving the following parameters:

- Coordinate points (209)
- Elasto-mechanics degrees of freedom (291)
- Mass-degrees of freedom (180)
- Structural elements, i.e., beams, plates, etc., (204)

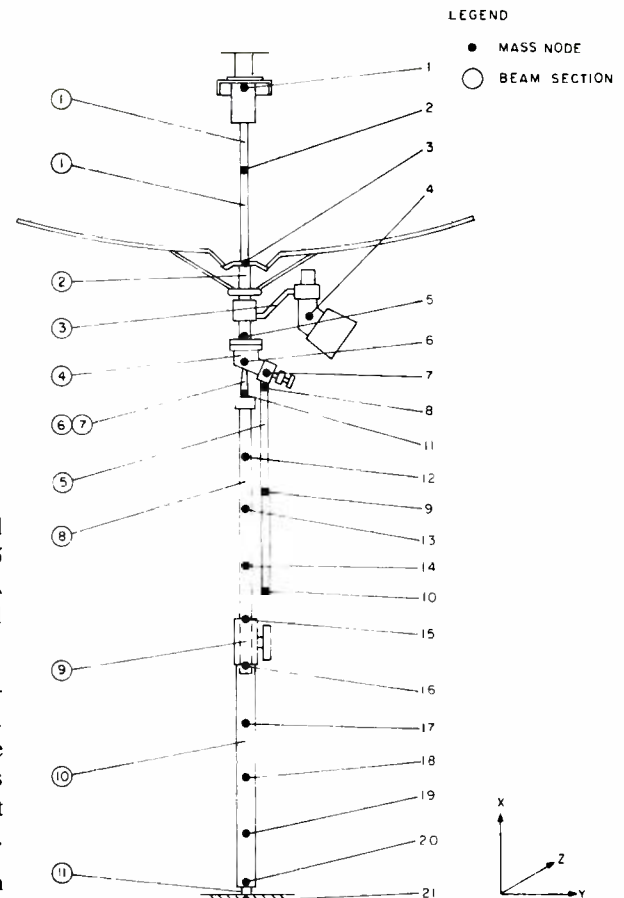


Fig. 2—Location of mass nodes on LCRU high-gain antenna structure used on Apollo.

Analysis of natural frequencies and mode shapes

3-axial shocks, atomic and gun blast (2)

25-Hz sine inputs (3)

Stresses for all conditions

Plotting of selected responses

- Apollo—Analysis of Lunar Communications Relay Unit (LCRU) high-gain antenna, used on the Lunar Rover

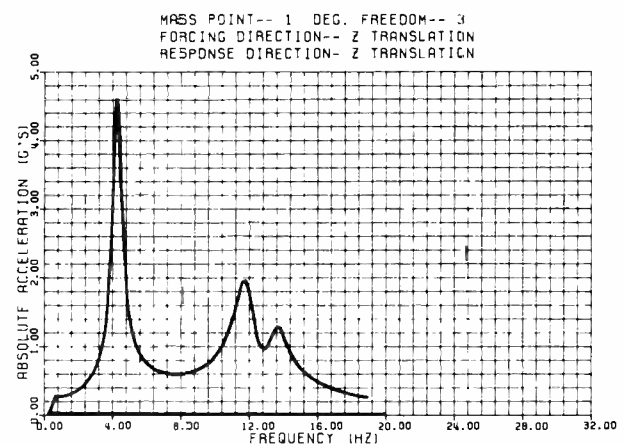


Fig. 3—LCRU high-gain antenna, sine vibration response.

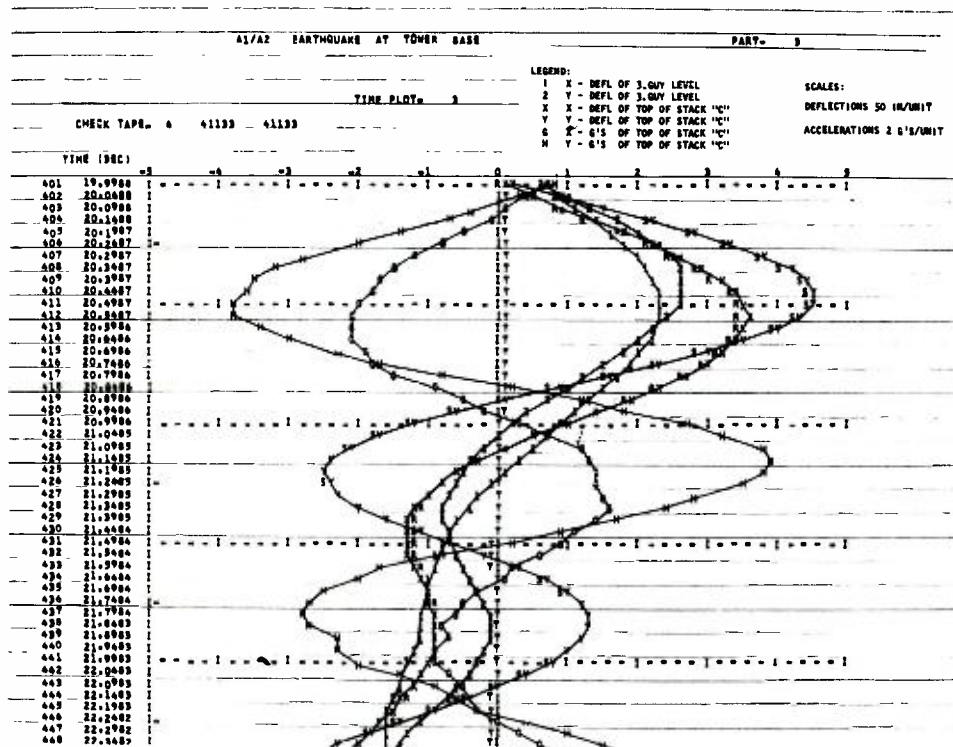


Fig. 4—Response plot of TV antenna to severe earthquake.

to transmit color TV pictures to earth. As shown in Fig. 2, the antenna consists of a supporting mast, the umbrella-type antenna, its feedhorn, and a positioning handle. The structure was modeled by 20 spring-connected masses, each having 6 degrees of freedom. The dynamic response of the feedhorn mass (point 1) to a sine sweep is presented in Fig. 3. (This work was done for the Camden facility.)

- CAMEL—Responses and stresses of a hardened phased array to atomic blast and ground shock environment.

- TV-antennas—Several TV-antennas were analyzed for RCA-Gibbsboro, deriving responses and stresses due to KARMAN vortex excitation and severe earthquakes. The response plot of a guyed structure to an 8.3 Richter earthquake is shown in Fig. 4.

- Viking mars lander high- and low-gain antennas—The analysis derives the responses and stresses to deployment and landing shocks, sine sweeps, and shock spectra.

Additionally, DYNA was used in several proposals to demonstrate RCA's structural capabilities.

To gain confidence in the results pro-

duced by the very complex operations of DYNA, the following checking and verifications procedure was followed:

- 1) All new branches and options were tested on a simple 3-mass model that still can be checked by hand analysis.
- 2) The actual MFAR structure was statically load tested to calibrate the analysis and modeling procedures. Valuable experiences were gained for the choice of the proper factors when using large shear beams.
- 3) The LCRU antenna was tested on a shaker table and gave excellent correlations with the sine sweep analysis.
- 4) On several occasions, DYNA results were compared to the results of other programs. The agreement was highly satisfactory as far as mode shape data was concerned. Dynamic response data on a 1000-time slice earthquake showed correlation in magnitude and phase.

Future improvements of DYNA

The experience with DYNA so far has been extremely gratifying. The M&SR-written dynamic response options are probably the most versatile and useful available in this country and at this time. However, possible improvements are clearly visible and several changes to DYNA are anticipated. The tentative program is as follows:

Faster routines (in preparation). As

the state-of-the-art in finite element methods progresses, the fastest and most efficient methods are established by a trial and error process. Desirable features of other programs are picked up and incorporated in DYNA to increase speed and reduce costs. Input and output formats might be changed to adapt to the practical needs of DYNA-users.

Structural elements (in preparation). The number of structural elements will be enriched to include bending plates and 3-dimensional elements. This will benefit work in the areas of radomes and waveguide windows under atomic blast and thermal conditions.

Non-linear conditions. There is a need to include the effects of backlash and elements with non-linear spring rates. This is a difficult task and will require a study of which of the theoretical possibilities is the most economical.

Thermal stresses. The inclusion of non-linear capabilities will permit analyzing the efforts of severe temperature gradients, where high temperatures drastically change the structural properties of the heated elements. The ultimate goal is the inclusion of thermal shock, where the dynamic effects of sudden expansion are considered.

DYNA is a program, unlike commercial ones, that is completely controlled by its users in M&SR; therefore, it is relatively simple to re-write and add a routine for a special purpose. This has been done on several occasions. DYN 115 is a special version of DYN 112 that calculates the affects of shock on ships according to NAVSHIPS-925-50-30 procedures, and DYN 113 was written for RCA's Gibbsboro facility to calculate the effects of long-duration earthquakes on structures.

The Advanced Mechanics Technology Group intends to have and maintain a structural dynamics program that represents the state-of-the art and is able to respond to any task in structural dynamics that RCA might need to remain competitive as a supplier of high-performance equipment.

Compared to other structural dynamics programs, DYNA can only be surpassed by NASTRAN in scope and capability. DYNA's great advantages are the simple input format, its great range of dynamic options, and the in-house capability.

Bayesian statistics

F. E. Oliveto

Probability and statistics play very important roles in almost all phases of scientific research and applications. Bayesian statistics is a relatively new scientific and engineering application of these disciplines.

MEN'S INTEREST in predicting the outcomes of events either from a need or curiosity goes back to the earliest of times. Perhaps cavemen resorted to casting lots by tossing stones to determine fairly the outcome of some questionable events. Gamblers from all ages always have tried to devise schemes to forecast the best odds in their favor so to be able to outguess their opponent, whether by tossing a pair of dice, flipping a coin, playing cards, etc.

It was Gerolamo Cardano¹ (1501-1570), also known as Jerome Cardan, an Italian Medical Doctor, a mathematical genius, and a renowned gambler who first formalized the concept of probability in the sixteenth century. In his *Book on Games of Chance*,² he

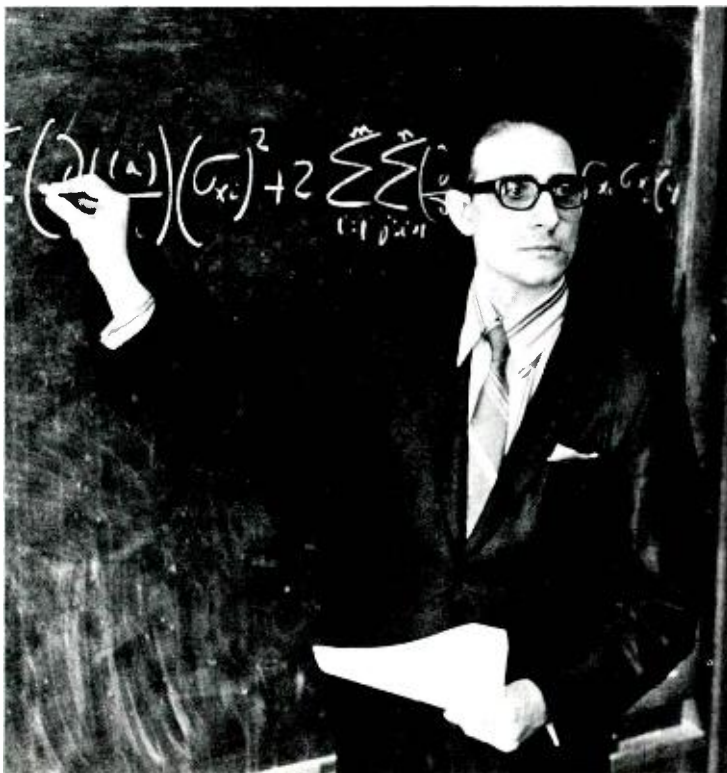
first studied the enumeration of all the different outcomes of tossing dice. He considered that if two dice are tossed and there are 36 possible ways for two distinguishable dice to fall and since six of these 36 ways produce a seven, the probability of producing a seven must be $6/36$ or $1/6$, etc.

Beginning with Cardano, the first formalized laws of classical probability theory were established, followed by later contributions of such distinguished mathematicians as Pascal, Fermat, and Bernoulli.

Definition of probability

Cardano, and the others who followed, began to formalize a more pre-

Final manuscript received September 22, 1972.
Reprint RE-18-3-20



Fulvio E. Oliveto
Technical Assurance
Missile and Surface Radar Division
Moorestown, N.J.

received the BS in Electronic Physics from St. Joseph's College in 1958, the MS in Probability and Statistics from Villanova University in 1968. He was a cooperative student at the Burroughs Research Center from 1956 to 1958. In 1958, he joined the Electronics Division of the Westinghouse Electric Corporation, as a design engineer. In 1960, he joined the RCA Communications System Division and was assigned to the Minuteman Program as a Project Engineer. In this capacity, he participated in reliability tasks and implementations, failure-mode and effects analysis, statistical and probability techniques, chaired the Design Review Program, and was especially concerned with problems of circuit stability over long intervals of time. Mr. Oliveto then joined the New Product Line Department in Computer Systems as a Senior Design Engineer where he was involved in developing the MSI and LSI circuits for the new generation of the computers. In 1970, Mr. Oliveto joined M&SR and was assigned to the Technical Assurance Department as a Senior Reliability Engineer. In this capacity, Mr. Oliveto has technical responsibility for the various reliability tasks and implementation for the AN/SPY-1 System on the AEGIS Program. Mr. Oliveto was awarded the Program Improvement Goal Certificate of Achievement for his contribution to AEGIS and the Chief Engineer's Technical Excellence Award for his outstanding technical accomplishment. Mr. Oliveto has presented and published numerous technical papers both nationally and internationally. He is a member of IEEE, Vice-chairman of System, Man and Cybernetics Society, and a group member in Reliability, Circuit, and Component parts. He is a Fellow of the Intercontinental Biographical Association.

cise concept and definition of the probability discipline and science. This concept and definition became to be known as the classical objective definition of probability:

If we let n be the number of exhaustive, mutually exclusive, and equally likely cases of an event under a given set of conditions, where n is equal to all possible outcomes and the occurrence of each of these outcomes is independent with equal probability, and if m of these outcomes are known as the event A , then the probability of event A under the given set of conditions is m/n .

For example, if one ball is to be drawn from a bag containing two white balls (w), and three red balls, (r) and each ball has an equal chance of being drawn, then the probability of drawing a white ball is $w/n=2/5$ and the probability of drawing a red ball is $r/n=3/5$.

Development of Bayesian statistics

In 1763, "An Essay Toward Solving a Problem in the Doctrine of Chance" was published in the *Philosophical Transactions of the Royal Society*.³ This Essay was written by the Reverend Thomas Bayes (1702-1761) and submitted to the Society by Bayes' friend, Richard Price, after Bayes' death.

The essay gave rise to a new form of statistical reasoning, suggesting that probability judgments based on previous experience and observation should be combined with probabilities based on relative frequencies by the use of Bayes' theorem.

The Bayesians statistical reasoning is based on the idea of a rational degree of belief or inductive probability as opposed to the classical approach in which subjective or inductive judgment has no place.

The classical statistician defines probability in terms of frequency of occurrence in repeated trials, as in games of chance. He perceives situations and, as a matter of routine, draws inference and attempts to conceive and formulate procedures that will hold in the long run. He feels that factors of belief or subjective deduction should be kept from probability theory and formulation. Although, as a statistician he is expected to use his personal judgment, he is careful not to include it in his theories.

The Bayesian statistician, on the other hand, tries to demonstrate how experience and observations should be used to alter previous concepts. His main problem is then with inferences in the presence of uncertainty; therefore, all his endeavors will be toward making his observations and opinions as precise and formal as possible.

The classical statistician enumerates the possible outcomes and predicts the probability of each event; e.g., a coin being tossed produces one of two possible outcomes—head (H) or tail (T). In classical probability theory, then, $n=2$ and the probability for either H or T is equal to H/n or $T/n=1/2$.

The Bayesian statistician, on the other hand, observes the outcomes (prior knowledge), and from these previous observations determines the prediction (posterior deduction).

The classical statistician says, "I cannot change the outcome: a coin has 50% chance of being a head and 50% of being a tail regardless of previous observation of head and tail. The Bayesian statistician says, "I cannot change the outcome of possible events, but by observation I can see the trend of a specific event." For example, if a coin is tossed 1000 times and a head occurs 80% of the time, it can be predicted that the 1001th time will have a higher probability of producing a head than a tail, even though the reason is not obvious. With a roulette wheel, the same reasoning can be applied: if by long observations, the numbers 1 to 5 come out more often than 6 to 10 (approximately by 85%), it can be predicted that on the next spin, there is a higher probability that the numbers 1 to 5 will come out.

The probabilities of the above examples could be the results of a bias in the coin, the wheel, the ball, or some other factors which somehow have influenced the outcome of a particular event.

In the real world, most people are using Bayesian reasoning in solving everyday problems or making decisions. For example: going home from work, an individual has two possible ways he can take: road A or road B . Assume the distance and the number of stops of road A or B are approximately equal; therefore, the travel times are

equal. At 5 p.m. leaving work, he must decide which road (A or B) to choose. Using classical probability theory and the above assumptions, the probability of choosing A or B is $m/n=1/2$ (two possible outcomes or 50%.) This can be accomplished by flipping a coin, tails for road A and heads for road B , etc. However, this individual has been riding road A or road B for the past year. Within this period, he observed that from 5 to 5:45 p.m., road A is very congested for the first 3 miles and, therefore, he has to wait for at least 45 minutes before it clears up, but road B , for the same period of time, is clear. After having observed this situation for a while he makes a subjective (intuitive) decision based on his past experience that if he leaves work between 5 and 5:45 p.m., he goes home by way of road B . But if he leaves work before 5 or after 5:45, he uses the classical approach of choosing either A or B .

Unfortunately, many pseudomathematicians in the early days of Bayesian popularity, misapplied Bayesian reasoning. In fact, they became a subject of ridicule among the classical objective mathematicians. Even to this day, people too frequently tend to apply Bayesian reasoning where it should not be applied, either because of the lack of proper information or other factors (not considered) which would not be applicable to the Bayesian approach.

A simple example of how Bayesian reasoning can be applied incorrectly is as follows: If there are two individuals—designated A and B ; A is 100 years old and B is 25 years old. Predict the probability of A and B surviving one more year.

Applying Bayesians theorem incorrectly.

- 1) The ages of both men are known as prior information.
- 2) Also, it is a fact that A has lived 75 years more than B .

Since A has survived 75 years more than B , intuitively A would have a higher probability of surviving one more year than B .

As a result of early misapplication, the Bayesian theory was not accepted for many years, until a recent renewal by many mathematicians who believe that Bayesian reasoning is very important

and highly useful when properly applied. Many of the works that are landmarks in the new upsurge in Bayesian theory have come within the last twenty-five years. F. P. Ramsey^{4,13} wrote an essay on truth and probability. Extensive developments were made by B. de Finetti⁵ on a personalistic view of probability and the modern theory of utility. L. J. Savage⁶ in his, "The Foundations of Statistics", develops, explains, and defends a certain abstract theory of behavior in the face of uncertainty. (The theory is based on a synthesis of the works of B. de Finetti). Also I. J. Goode,⁷ H. Jefferies,⁸ D. V. Lindley,⁹ and H. Raiffa,¹⁰ to name a few.

Bayesian theory

Briefly, the Bayesian theorem is based on conditional probability as follows:

Assuming that $P(AB) = P(BA)$:

- 1) When A and B are mutually exclusive events, then $P(A \cup B) = P(A) + P(B)$
- 2) The conditional probability of B , given A , is $P(B/A) = \frac{P(B \cap A)}{P(A)}$ ($P(A) > 0$)
- 3) When A and B are not statistically independent, then $P(BA) = P(A) P(B/A)$
- 4) When A and B are statistically independent, then $P(B/A) = P(B)$ and $P(A \cap B) = P(A) P(B)$

Let us find the probability of a joint occurrence $P(AB)$ of events A and B . The conditional probability of B , given A , is defined as:

$$P(B/A) = \frac{P(B \cap A)}{P(A)}$$

From this, the multiplication rule can be derived:

$$P(B \cap A) = P(A) P(B/A)$$

or

$$P(AB) = P(A/B) P(B)$$

From the last two expressions, we have:

$$P(B/A) = \frac{P(AB)}{P(A)}$$

But $P(AB) = P(A/B) P(B)$; therefore

$$P(B/A) = \frac{P(A/B) P(B)}{P(A)} \quad (1)$$

The terms in Eq. 1 can be explained as follows:

$P(B)$ is the prior probability (the knowledge gained before the new information A is known).

$P(A/B)$ is the possibility (how likely is the new information A , provided that the original assumption B is true).

$P(A)$ is the probability of the new information A .

$P(B/A)$ is the posterior probability of B (what is the probability of B after the new information A is now known or available).

As it is seen from the stated postulates, Bayes' theorem provides a useful technique for constant renewal of the original probability prediction due to the continual gathering of new information. Therefore, the procedure becomes straight-forward: as the new information B' is known, the new prior is $P(A/B)$, the new "posterior" is $P(A/B')$, etc.

$P(A)$ is not an easy concept to handle, but it can be represented as:

$$P(A) = \sum_{B_i} P(A/B_i) P(B_i)$$

for discrete probability

and

$$P(A) = \int P(A/B) j_p(B) dB$$

for continuous probability.

Stating Eq. 1 in general form, let B_1, B_2, \dots, B_n be n mutually exclusive and exhaustive events and at least one of them, and not more than one, must have happened, but it is not known which one. Suppose also that an event A may follow any one of the events B_k , with known probabilities, and that A is known to have happened.

What is then the probability that it was preceded by the particular event B_k ?

We suppose that the prior probabilities [$P(B_1), P(B_2), \dots, P(B_n)$] are known and also the probabilities [$P(A/B_1), P(A/B_2), \dots, P(A/B_n)$]. We have to calculate $P(B_k/A)$, the posterior probability of B_k .

Now the probability that B_k happens and is followed by A is

$$P(B_k) P(A/B_k)$$

The probability that A happens, no matter which of the B_k preceded it, is

$$\sum_{k=1}^n P(B_k) P(A/B_k)$$

Hence the probability that when A happens, it is preceded by B_k is given by

$$P(B_k/A) = \frac{P(B_k) P(A/B_k)}{\sum_{k=1}^n P(B_k) P(A/B_k)}$$

Application of the Bayes theorem

A simple example of the classical approach and the straight-forward use of the Bayes theorem is illustrated.

Suppose we have three urns containing the following balls:

- Urn I: 3 black, 2 white
- Urn II: 4 black, 7 white
- Urn III: 5 black, 4 white

An urn is selected at random and a ball is drawn from it. Given that the ball drawn is black, what is the probability that the urn chosen was Urn I?

In the classical approach, in order to find $P(U_i/B)$, it is necessary first to compute $P(U_i \cap B)$ and $P(B)$:

We have three urns; therefore, the probability of selecting any one of the three urns is $1/3$. And the probabilities of black and white balls from each urn are:

- Urn I: $P(B) = 3/5$ and $P(W) = 2/5$.
- Urn II: $P(B) = 4/11$ and $P(W) = 4/9$.
- Urn III: $P(B) = 5/9$ and $P(W) = 4/9$.

therefore, the probability that urn I is selected and a black ball drawn is $1/3 \times 3/5 = 1/5$; that is $P(U_1 \cap B) = 1/5$. Since there are three urns, we have

$$P(B) = (1/3 \times 3/5) + (1/3 \times 4/11) + (1/3 \times 5/9) = (1/3)(150.4/99)$$

and

$$P(U_1/B) = \frac{P(U_1 \cap B)}{P(B)} = \frac{1/5}{150.4/99} = \frac{297}{752}$$

Alternatively, by using Bayes' theorem (Eq. 1)

$$P(U_1/B) = \frac{P(U_1) P(B/U_1)}{\sum_{k=1}^3 P(U_k) P(B/U_k)}$$

From the preceding calculation,

$$\begin{aligned} P(U_1) &= 1/3 & P(B/U_2) &= 4/11 \\ P(U_2) &= 1/3 & P(B/U_3) &= 5/9 \\ P(B/U_1) &= 3/5 & P(U_3) &= 1/3 \end{aligned}$$

Thus,

$$P(U_1/B) = \frac{1/5}{1/5 + 4/33 + 5/27} = \frac{297}{752}$$

This same principle also can be applied in solving technical and scientific problems. Indeed, mathematicians and engineers are applying the Bayesian theorem in almost every scientific field. In reliability engineering, for example, several companies and Government agencies are doing extensive studies on the application of the Bayesian statistics to reliability.

Reliability engineering application

Time and cost are often major factors in a testing program; in many instances, they are prohibitive. Time and cost required to demonstrate conformance depend on the severity of the reliability requirements. However, testing time (hence cost) can often be reduced by application of the Bayesian concept, provided sufficient prior data is available. Thus it is of the utmost importance that all data regarding component parts and equipment be retained as potential prior data.

The well known reliability demonstration test plans and new approach to reliability testing should be investigated before decision is made on what type of test procedure will be the best suited with regard to time, cost, and applicable result to be implemented.

The test plans delineated in MIL-STD-781B are usually implemented to demonstrate reliability conformance. The parameters used in this standard are:
 β —consumer's decision risk
 α —producer's decision risk
 θ_0 —specified MTBF (mean time between failures)
 θ_1 —minimum acceptance MTBF, and
 θ_0/θ_1 —discrimination ratio.

Example of reliability demonstration test plans using MIL-STD-781B

The primary requirements for this hypothetical test are that:

- 1) The customer shall take no greater than a $\beta=10\%$ risk
- 2) The equipment will be accepted whose MTBF is less than $\theta_1=10,000$ hours, and
- 3) The producer shall take no greater than $\alpha=10\%$ risk of rejecting equipment having a true MTBF equal to or greater than $\theta_0=15,000$ hours.

Sequential type tests, rather than fixed-time tests are chosen in these examples.

Test Plan I of MIL-STD-781B meets the specified conditions. When θ_0 , the true MTBF of the equipment under test, is 15,000 hours, the expected time necessary to reach a decision is 259,500 hours. (The accept-reject criteria operating characteristic curve, and expected test time curve for this plan are on pages 19 and 62 of MIL-STD-781B).

If the specified MTBF were 20,000 hours, the discrimination ratio would be 2, and the expected time necessary to reach a decision according to Test Plan III of MIL-STD-781B is 102,000 hours (pages 21 and 64 of MIL-STD-781B).

This test time, however, can be reduced using MIL-STD-781B, in conjunction with the Bayesian approach. To reach a statistically sound decision for a reliability demonstration test using the Bayesian approach, it is necessary to have adequate prior information *applicable to the equipment being demonstrated*. At the end of a preliminary phase of a program, the producer has an excellent opportunity to apply this technique toward a cost effective demonstration test plan. In addition, once the design and development are completed and production begins, continual adjustment of the prior distribution based on previous test results and field evaluations can also serve to keep testing to an economical minimum. As a minimum, the test plan should be designed to demonstrate the required MTBF at the level of confidence required by the customer.

To put the previous discussion (Eq. 1) of Bayesian theory into the context of the reliability demonstration test problem, let A represent acceptance of the equipment by means of reliability demonstration test, and let θ be the equipment MTBF.

It follows that $P(A/\theta)$ is the probability of acceptance given an MTBF of θ , and $j_p(\theta)$ is the probability density function of θ before testing (prior density).

Then, similar to Eq. 1

$$f(\theta/A) = \frac{P(A/\theta) j_p(\theta)}{\int_0^{\infty} P(A/\theta) j_p(\theta) d\theta} \quad (2)$$

This is the basic equation for the Bayesian approach to reliability dem-

onstration tests. Such reliability demonstration tests, as delineated in MIL-STD-781B, are based on two assumptions

- 1) An equipment with a specified low reliability level has a low probability of acceptance, and
- 2) High reliability equipment will pass the test with high probability.

Application of the procedure

The first step is to determine the prior distribution as related to the MTBF for the proposed equipment. The prior distribution should then be used to develop the posterior distribution by means of the conjugate. If the posterior distribution of θ is based on an estimate, θ will be of the same form as the prior distribution: such distributions are called conjugate.

Raiffa and Schlaifer^{10,11} have worked out the theory of such distributions as follows:

- 1) If sample test data are known to be normally distributed, a normal distribution is most conveniently selected as a prior. A normal distribution will be obtained as the posterior distribution.
- 2) If sample test data is known to be exponentially (or Poisson) distributed, a Gamma distribution is most conveniently selected as a prior. A Gamma distribution will also be obtained as the posterior distribution.
- 3) If sample test data is known to be binomially distributed, a Beta distribution is most conveniently selected as a prior. A Beta distribution will then be obtained as the posterior distribution.

The main difficulty in applying the Bayesian approach is determining the operating characteristic (o.c.) of the test procedure and how it is related to the posterior distribution. The o.c. curve of a life-test sampling plan shows the probability that a submitted lot with given mean life would meet the acceptability criterion on the basis of that sampling plan. The o.c. curve or equivalent test parameters can be determined to fulfill the conditions on θ_1 , and still assure high acceptance probability of θ_0 for a given prior density.

Using the conditions stated previously:

- θ_0 —predicted (expected) MTBF = 15,000 hours
- θ_1 —acceptable MTBF = 10,000 hours
- β —consumer's risk = 10%
- α —producer's risk = 10%
- θ_0/θ_1 —discrimination ratio = 1.5

As outlined in MIL-STD-781B, the expected total test time is 259,500 hours for these conditions.

Prior and posterior probability

Since space does not permit the development of the complete set of prior distributions, the following prior probabilities for each corresponding MTBF are merely stated to illustrate the example.

MTBF (hours) (θ_i)	Prior probability (P_i)
1. 8,000	0.05
2. 10,000	0.10
3. 12,000	0.20
4. 14,000	0.25
5. 16,000	0.25
6. 18,000	0.10
7. 20,000	0.05

It should be emphasized, however, that the development of prior distributions is the key to successful application of the Bayesian approach.

Once the prior and posterior distributions have been determined, an expression for β can be developed:

$$\beta = \frac{\sum_{i=1}^k (\Pi P_i) \exp[-(\sum_{i=1}^m \lambda_i) T]}{\sum_{i=1}^n (\Pi P_i) \exp[-(\sum_{i=1}^m \lambda_i) T]} \quad (3)$$

where T is the total test time required; $\Pi P_i = P_i$ represents the prior probabilities; and $\sum \lambda_i = \theta_i$ represents the stated MTBF. Eq. 3 is based on the zero failure acceptance criteria developed by H. Balaban.^{11,12} It also assumes an exponential component-failure-time distribution.

Expanding Eq. 3 to the extent of our present example, we can solve for T as follows:

$$\beta = \frac{P_1 \exp(-T/\theta_1) + P_2 \exp(-T/\theta_2)}{P_1 \exp(-T/\theta_1) + \dots + P_7 \exp(-T/\theta_7)}$$

By substituting the values of P_i and θ_i tabulated above and using $\beta = 0.10$, we can produce a numerical solution.

Since analytical solutions do not exist for this equation, a computer program can be developed to calculate T . In this example, T was calculated to equal 11,600 hours.

To provide both the producer and the customer a high probability of passing equipment which has an MTBF of

15,000 hours the following modifications are made:

- 1) The component equipment Beta risks for a zero-failure-acceptance criterion are determined.

$$\beta'_i(\lambda_i) = \exp(-\lambda_i/T)$$

The zero-failure for $T = 11,600$ hour test for acceptance is equivalent to a beta risk for a 10,000-hour MTBF of

$$\exp\left(\frac{11,660}{10,000}\right) \approx 0.51$$

- 2) This beta risk for $\theta = 10,000$ hrs. in conjunction with a 10% α -risk associated with a 15,000-hour MTBF, provides the following test conditions:

$$\theta_n = 15,000 \quad \alpha = 0.10$$

$$\theta_1 = 10,000 \quad \beta' = 0.51$$

- 3) For the test plan conditions as specified in 2) above and by using the sequential theory formulas for the exponential case, the expected total test time is approximately 122,750 hours.

If the predicted MTBF is 20,000 hours and the discrimination ratio is 2.0, the expected total test time before a decision is reached is approximated to be 40,100 hours compared to 102,000 hours for the same plan using MIL-STD-781B.

Test time savings

From the preceding examples it is shown that the use of prior information has resulted in a potential time savings of $(259,500 - 122,750) = 136,750$ test hours. By reducing the test time by approximately 136,750 hours, the cost to perform the Reliability Demonstration Test has been reduced quite considerably over the test plan by using MIL-STD-781B.

Table I shows the corresponding total expected test time with the different original Beta requirement for a predicted MTBF of 15,000 hours.

Table I—Expected test times versus original beta risk requirement.

Original Beta risk	Revised Beta risk	Expected test time
0.100	0.317	122,750
0.105	0.368	101,550
0.110	0.411	84,280
0.115	0.465	67,600
0.120	0.522	54,850
0.125	0.589	37,850
0.130	0.657	25,150

From the Table I, it is seen that if the customer is willing to take a risk of 12% of the outgoing equipment to have an MTBF of 10,000 hours or less, the total expected test time can be re-

duced to 54,850 hours, which is a significant savings over 10% beta requirement.

Acknowledgment

The author thanks Mr. H. Balaban for consultation and adoption of the zero-defect procedure derived from the mentioned reference papers. Also, thanks are extended to R. E. Davis, R. E. Killion, and J. C. Phillips for review and suggestions on this paper.

References

1. Oystein, Ore. *Cardano, the Gambling Scholar* (Princeton University Press; 1953).
2. Cardano. Gerolamo. *Libro de Ludo Aleae*
3. Bayes, Thomas. *An Essay Towards Solving a Problem in the Doctrine of Chance, Philosophical Transactions of the Royal Society* (1763).
4. Ramsey, Frank P., *Truth and Probability Studies* (John Wiley and Sons; 1963).
5. De Finetti, Bruno, *Studies in Subjective Probability* (John Wiley and Sons; 1963).
6. Savage, L. J., *The Foundations of Statistical Inference* (John Wiley and Sons; 1963).
7. Goode, I. J., *Probability and the Weighing of Evidence* (Charles Griffin and Company; London. Hafner Publishing Company, Inc.; 1965).
8. Jeffreys, Harold, *Theory of probability* (Second Edition; Oxford University Press; London; 1948).
9. Lindley, D. V., *Introduction to Probability and Statistics from a Bayesian viewpoint. Part 2.—Inference* (Cambridge University Press; 1965).
10. Raiffa, Howard and Schlaifer, Robert, *Applied Statistical Decision theory* (Howard University Press; 1964).
11. Balaban, H., "A Bayesian Approach for Designing Component Life Tests," *Proceedings of the 1967 Annual Symposium on Reliability*. (Jan. 1967).
12. Balaban, H., "A Bayesian Approach to Reliability Demonstration", *Annual of Maintainability Symposium* (July 1969).
13. Ramsey, Frank P., *The Foundations of Mathematics and Other Logical Essays* (Humanities Press, New York, 1950).
14. Weir, W. T., *Proceedings of the Second Missile and Space Division Seminar on Bayes' Theorem and its Application to Reliability Measurement* General Electrical Co., 1967.

Bibliography

- Bellini, A., "Gerolamo Cardano e il suo tempo" *Studi di Storia della Medicina*, Vol. 8, Milan (1947).
- Bortolotti, E., "Italiani scopritori e promotori di teorie algebriche", *Annuario Universita di Modena* (1918-1919) pp. 51-149.
- Freeman, Harold, *Introduction to Statistical Inference* (Addison—Wesley Publishing Company Inc.; 1965).
- Lombroso, C., *Genio e follia in rapporto alla medicina legale, alla critica ed alla storia* (Turin: 1877).
- Luce, Duncan R., and Raiffa Howard, *Games and Decision* (Harvard University, John Wiley and Sons, Inc.; 1967).
- Martin, J., J., *Bayesian Decision problems and Markov chains* (John Wiley and Sons, Inc., 1967).
- McKinsey, J., *Introduction to the theory of games* (McGraw Hill Book Company, Inc.; 1952).
- Morgan, Bruce, W., *An Introduction to Bayesian Statistical Decision Processes* (Prentice-Hall Inc.; 1968).
- Rivari, E., *La mente di Girolamo Cardano*, Bologna (1906).

Apollo 15 and 16 ground commanded television assembly

B. M. Soltoff

The Ground Commanded Television Assembly, developed by Astro-Electronics Division for NASA, represents a new level of performance for space application television equipment. Functioning as the heart of the television system during the Apollo 15 and 16 missions, the camera provided the scientific community and the home viewer with real-time coverage of the lunar exploration. Quality of the received video was better than that of any previous missions.

Bert M. Soltoff, Design Mgr.
Camera Development
Astro-Electronics Division
Princeton, New Jersey

received the BSEE from Drexel Institute of Technology in 1956 and the MSEE from the University of Pennsylvania in 1964. In 1956, he joined the Research Division of the Philco Corporation where he worked on the development of the "Apple" color television receiver and other related television receiver systems and problems. This included the use of analog computer techniques to optimize cathode-ray tube design in 1960. Mr. Soltoff joined the Commercial Engineering Section of Philco where he was concerned with transistor applications for newly developed devices. In 1962, Mr. Soltoff joined RCA and worked in system and circuit design for the miniaturized AN/APN-155 radio altimeter. After transferring to AED in 1963, his initial assignment was the development of an automatic shading and spectral response calibrator for the AVCS cameras. He next was assigned the lead engineer responsibility for the APT cameras used on the TIROS-TOS satellites. He received the IR-100 award for development of the HAX box adapter used to process HRIR data on the Nimbus satellites. In 1968, as Manager, Camera Development, he initiated the design and development of the high-resolution Two-Inch Return Beam Vidicon cameras used for surveillance on the earth resources satellites. In the fall of 1969, he directed a task force which developed a miniature color TV camera for potential space applications. This effort was extended to development and delivery in 1971 of the Ground Commanded Color Television Assembly used on the Apollo 15 and 16 missions. During this period, he also directed the development of the video multiplexer and sequence generator for the RBV system. Mr. Soltoff played a key role in the performance of the Video Data Quality and Measurement Study for NASA. He also recently performed trade-off analyses and provided recommendations for the hardware requirements of the Space Shuttle TV System. Mr. Soltoff is a member of the IEEE and the Technical Group on Broadcast and Television Receivers, and he has published several papers in the Technical Group Journal.



Fig. 2—Ground Commanded Television Assembly (GCTA).

received at one of the four earth sites and relayed to NASA's Manned Space Center at Houston, where the field-sequential format is converted to standard NTSC video and supplied to the TV pool for network transmission.

Command control signals for the GCTA flow in the reverse direction. Generated in the mission control centers, the encoded signals are relayed to the earth sites for transmission via S-band to the LCRU. After demodulation in the LCRU, the signals are supplied to the TCU, where they are decoded to recover the original commands. These commands then activate the remote function in both the TCU and the CTV.

General description of the GCTA

Fig. 2 shows the GCTA configuration as mounted on the bumper of the Lunar Roving Vehicle (LRV). The camera system can be operated manually on the moon by an astronaut or by remote commands from earth. The assembly

Reprint RE-18-3-3

Final manuscript received April 13, 1972.

This work was performed by AED for NASA's Manned Spacecraft Center under Contract No. NAS 9-11260

THE OUTSTANDING QUALITY of the TV pictures obtained with the Ground Commanded Television Assembly (GCTA) on the Apollo 15 and 16 missions was achieved by applying to each area of camera performance the latest technical concepts. Addition of ground-command capability from the Mission Control Center permitted versatility and optimization of the TV coverage, without diverting the astronauts from their primary role of lunar exploration.

The system signal flow is shown in Fig. 1. The GCTA consists of a color television camera (CTV) and a television control unit (TCU). The CTV utilizes a field-sequential color wheel to generate color TV images. During operation on the lunar Rover, the CTV video signal is routed through the TCU where a vertical interval test signal (VIT) is inserted. Next the signal is supplied to the Lunar Communications Relay Unit (LCRU), designed by Communications Systems Division, where it modulates a 10-W, S-band transmitter. The transmitter output is beamed to earth using a 3-foot collapsible parabolic antenna developed by Missile and Surface Radar Division. The S-band signal is

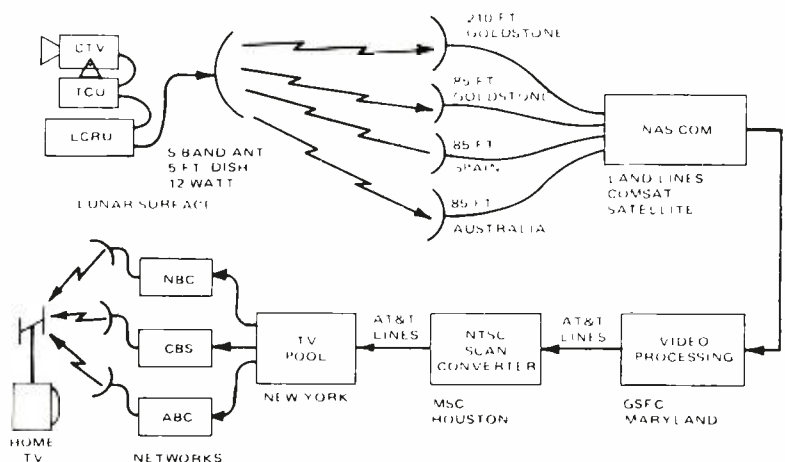
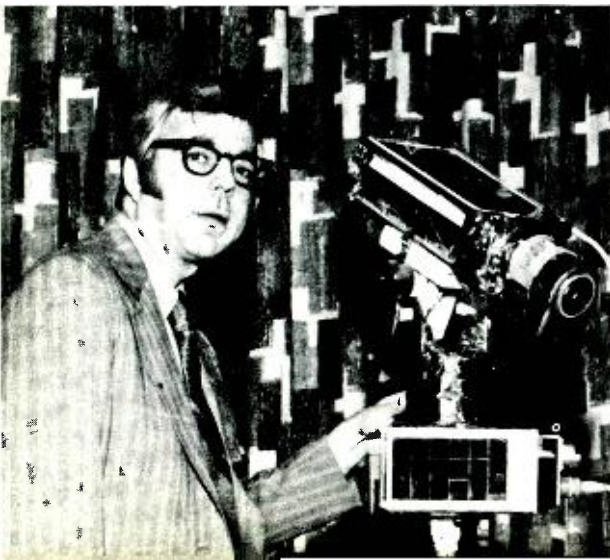


Fig. 1—Communications link for Apollo TV system.



consists of the CTV, the TCU, and a short staff at the base of the control-unit electronics box which mounts the GCTA to a fitting on the vehicle chassis. The mounting staff has a swing-away capability to allow removal of the LCRU without removing the GCTA.

The CTV is a small, lightweight unit producing high-quality, field-sequential color television at standard line and field rates. The camera uses a single silicon-intensifier-target (SIT) tube and a rotating filter wheel to generate color video data. A zoom lens is incorporated in the CTV with provisions for manual or remote control of zoom and iris settings. A coupled focus system provides focus tracking as a function of zoom setting. Automatic light control (ALC) operating on average or peak scene luminance also is incorporated. ALC may be selected manually or by remote control.

The TCU provides an azimuth/elevation mount for the color TV camera, and permits manual or ground-controlled TV coverage from the Apollo Lunar Roving Vehicle (LRV). The TCU receives a command subcarrier from the Lunar Communications Relay Unit (LCRU) mounted on the LRV and provides the electronics required for decoding and execution of remote commands for:

azimuth and elevation movement of the TCU camera cradle; CTV zoom, iris, automatic light control, and power functions; and transmitter/voice sub-carrier control within the LCRU. The TCU accepts the CTV video signal, adds a test signal, and routes the combined video to the LCRU for transmission to earth.

The CTV is initially stowed in the Lunar Module (LM) and is deployed by the astronaut during the first egress. At the start of the first extra vehicular activity, the astronaut assembles the CTV on a tripod to view the LM landing area. During these phases, video transmission is channeled through the LM communications system. After deploying the LRV, the CTV is mounted on the cradle or upper portion of the TCU, as shown in Fig. 2, and communication is accomplished by the LCRU transmitter.

degree filter segments, two each of red, blue, and green. The wheel is rotated by a hysteresis synchronous motor driven by signals from the sync generator. An optical pick-up provides motor-phase information to properly phase the segments of the color wheel with respect to the camera vertical scan.

The three primary-color video signals are sequentially transmitted at a 60-Hz field rate, with red information transmitted during the first field, blue information during the second field, and green during the third field; the sequence is repeated continuously. In addition, a special color-flag pulse is inserted during line 18 of each green field-blanking interval to permit automatic color-field phasing at the receiving site. The width of this pulse is modulated to provide telemetered temperature data during camera operation.

The CTV is capable of self-contained operation, using only a single power input (+28 VDC) to provide the composite video output signal. A DC/DC converter is used to translate the 28-V input to lower and higher voltages required for operation of the internal circuits. Critical output voltages are derived from internal voltage regulators.

CTV description

General

As shown in the block diagram of the CTV (Fig. 3), the camera employs a SIT tube as its sensor. This tube provides the required high sensitivity and immunity to image burn. The color wheel interposed between the camera lens and the SIT tube, contains six 60-

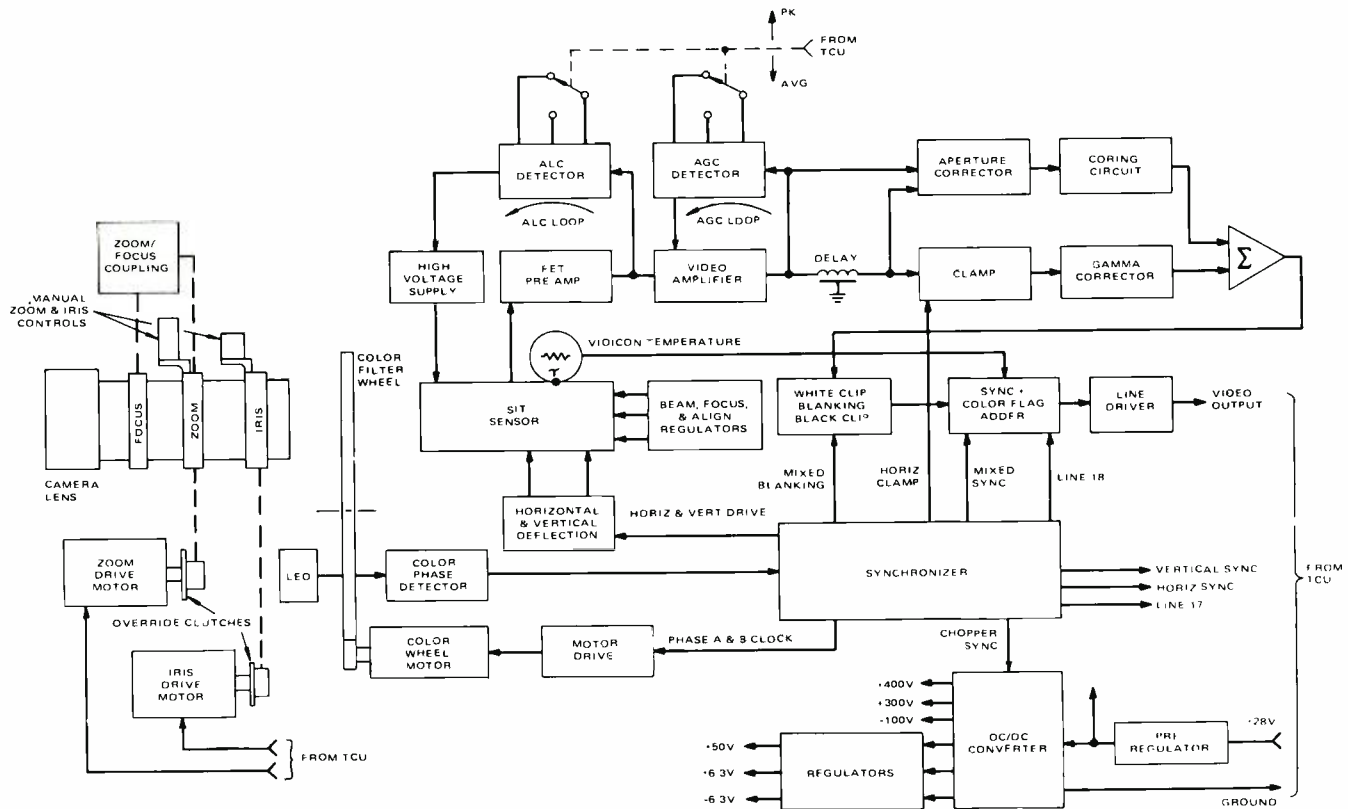


Fig. 3—Color television camera, block diagram.

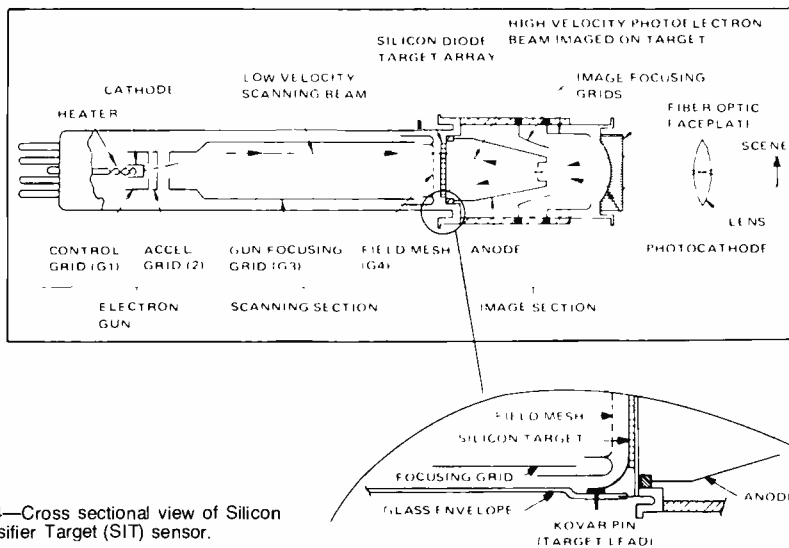


Fig. 4—Cross sectional view of Silicon Intensifier Target (SIT) sensor.

The synchronizer (sync generator) furnishes digitally derived timing pulses for use by the video and deflection circuits, and for synchronizing the operation of the DC/DC converter. It also provides timing signals required for the TCU operation.

The video circuits process the signal output of the sensor to present it in the required format. The processing includes ALC and AGC circuits, aperture and gamma correction, sync and blanking addition, and black and white clipping.

Stepping motors mounted on the lens assembly permit remote operation of the zoom and iris controls through astronaut override clutches. These motors are actuated by step pulses received from the TCU and permit exact position prediction based on command duration. Limit switches stop the remote operation at the end of normal ranges.

Electrical interfaces are routed through a 26-pin, zero-g connector whose pin assignments have been configured to permit operation through the LM link, through the TCU into the LCRU, or into the LCRU directly as a contingency mode.

Table I summarizes the performance characteristics of the GCTA system.

Sensor assembly

The sensor assembly comprises the SIT sensor, a printed circuit yoke and focus coil assembly, and an electrode divider assembly which filters the SIT control voltages. These items are secured in a magnesium sleeve that provides electrical shielding, a positive index for mounting, and good thermal conduction

to the camera baseplate.

The 16-mm SIT sensor selected for use in the camera is a ruggedized unit that features high sensitivity and broad spectral response, with a limiting resolution of 600 TV lines. A cross-section of the sensor is shown in Fig. 4. The SIT sensor uses an S-20 photocathode for conversion of photons to electrons, a silicon-diode-array target to produce gain by impact of photoelectrons, and a scanning beam to produce an output signal at the target. The silicon target can produce electron impact gains of 3000 or more. The target consists of a two-dimensional array of p-n junction diodes formed in an n-type single-crystal silicon wafer by use of planar silicon technology. The p-region of each diode faces the electron scanning beam. An insulator covers the regions between diodes to prevent the beam from reaching the n-type substrate. Due to the insulating properties of the reversed-biased p-n junction, the diodes act as elemental storage capacitors and are biased by the low-velocity scanning beam.

Operation of the target is illustrated by Fig. 5. Hole-electron pairs are produced when an energetic electron is incident on the silicon target. The holes created in the valence band diffuse through the n-region, and pass through the depletion layer to contribute to discharging the storage capacity. The output signal is generated by capacitive displacement current during recharging of each elemental capacitor by the scanning beam.

Current gain in the SIT is determined by the average energy required by a photoelectron to make a hole-electron pair. To provide a greater range of gain

Table I—GCTA performance summary

Parameter	Characteristics
Sensor	SIT camera tube
Sensitivity	Greater than 32 dB S/N at 3 fL
Resolution	80% response at 200 TV lines
ALC dynamic range	1000 to 1 (minimum)
Non-linearity	3% (maximum)
Gray scale	10 $\sqrt{2}$ steps
Video output level	1.0 volts p-p into 75 Ω ohms, full EIA sync
ALC	Peak or average detection modes
Optics:	
Zoom ratio	6:1 (12.5 mm to 75 mm)
Iris control	f/2.2 to f/22
Pan angle	+214 } degrees from front -134 }
Tilt angle	+85 } degrees from horizontal -45 }
Power @ 28V input	CTV TCU
	14.5 W 5.5 W
Weight	12.8 lb 13.5 lb

control, an additional "buffer" layer was added to the front surface of the target to absorb a portion of the electron energy. Good imaging characteristics are retained without appreciable loss of resolution occurring with low-voltage levels in the image section. This buffered design as used in the CTV camera provides gain control in excess of 300:1 by varying the accelerating voltage from 3 to 9 kV. The SIT camera tube combines traditional photocathode and electron-gun technology with the new solid-state technology, and provides high performance and resistance to very high light overloads in a compact and rugged package.

Sync generator

The sync generator comprises a master crystal oscillator and related counting and decoding circuits. All counting and decoding functions are accomplished with synchronous techniques, and are implemented with high-speed, low-power, TTL integrated-circuits.

A simplified block diagram of the sync generator is shown in Fig. 6. The sync generator supplies vertical and horizontal rate signals for deflection generation, for SIT blanking, for DC restoration in the video amplifier, and for insertion of mixed sync and blanking into the composite output video signals. It also provides timing pulses to synchronize the DC/DC converter to one-half the line rate, and a split-phase drive signal to operate the synchronously driven color-wheel motor.

The method of establishing and main-

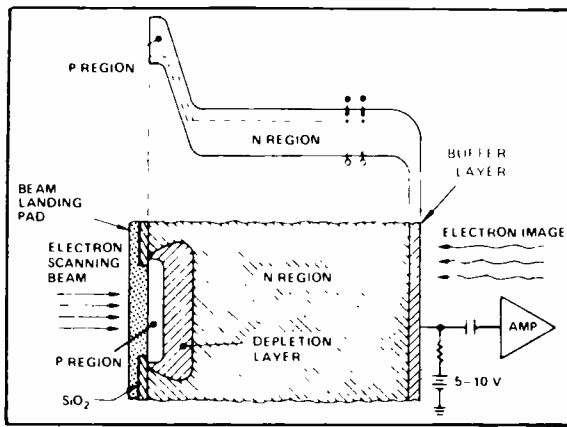


Fig. 5—Operation of silicon target in SIT tube.

taining the proper phase relationship between the color wheel and the scanning beam after power application is such that the coherence of the horizontal and vertical synchronizing pulses remain undisturbed and independent of the color wheel synchronizing operation. This permits the camera sync rates to be locked to a rubidium standard at the ground site to provide continuous information to the TV network pool. A wheel pulse is generated by an optical pickup for each one-half revolution of the color wheel.

This color wheel pulse is routed to a phase comparator that compares its timing to the vertical sync pulse. If the wheel pulse and vertical sync pulse are not in proper phase, the inhibit gate will cause the 420-Hz split-phase counter to drop one count. The result is one 420-Hz cycle which terminates 90 degrees later than normal, causing the wheel motor to change phase by 90 electrical degrees. One count is dropped for each wheel pulse that is not in proper phase with the vertical sync. Since this occurs twice for each revolution of the color wheel, the motor speed is decreased (although still running synchronously) until the flag pulses and vertical sync pulses are in proper phase. At this time, the inhibit gate allows the split-phase counter to count normally, the motor rotates the color wheel at the proper speed, and the "dead zones" between segments of the color wheel track the scanning beam. During the period when the proper phase relationship is being established between the color wheel and vertical sync, the horizontal and vertical synchronizing pulses are transmitted uninterrupted and without timing errors.

The initiating signal for the green-flag pulse is formed in the sync generator, and it is then processed further in the video amplifier. Additionally, certain

signals required by the TCU are generated by the sync generator. These are:

- Line 17 tag: Used to initiate insertion of a vertical interval test signal (VIT) into the composite video output.
- Vertical rate: A 60-Hz signal, used to provide the rate clock for the stepping motor drivers.
- Horizontal rate: Used to provide synchronizing information for the TCU DC/DC converter.

Color wheel drive

A 6300-r/min, size 11, two-phase, hysteresis synchronous motor, with provision for reduced power consumption while running, is used to drive the color wheel through a speed-reducing gear train. Each of the motor phase windings is provided with a center tap to permit changing the motor power input from "start" to "run" levels. A relay is used to switch the motor windings from "start" mode to "run" mode after synchronous speed is reached, which minimizes power requirements. The motor is driven by a saturated transistor bridge. Total motor and electronics power drain in the "run" mode is a nominal 1.8 W.

Video circuits

The video circuits accept the signal from the SIT sensor and process it into the composite video format required at the camera output. To accomplish these functions, a number of circuit refinements have been developed and incorporated into the GCTA design. These include an aperture corrector which contains a "coring" circuit to slice out excess noise in the high-frequency, low-amplitude areas of the video signal, and a gamma corrector which modifies the overall gamma of the sensor/video amplifier to approximately 0.7. Both of these circuits serve to improve the signal-to-noise ratio of the output video

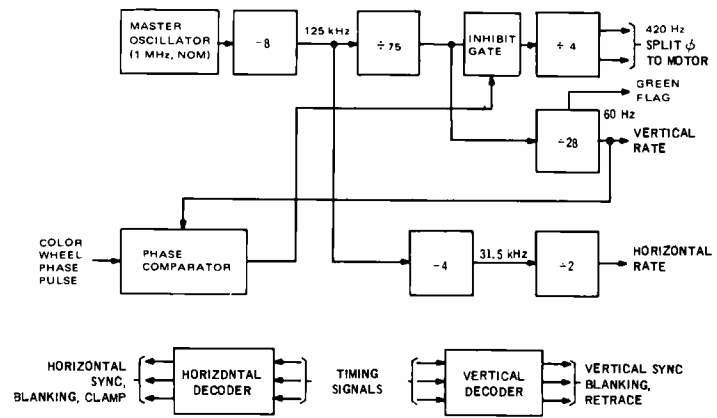


Fig. 6—Sync generator, simplified block diagram.

signal.

As shown in Fig. 3, the signal from the SIT target is first amplified in a low-noise, FET preamplifier. The preamplifier delivers two outputs: A signal to the ALC control loop and an output to a video amplifier stage which contains a feedback AGC loop.

ALC loop

Automatic light control is accomplished by a closed feedback loop from the output to the input (intensifier portion) of the SIT sensor. The loop, which comprises the SIT sensor, the preamplifier, the ALC video amplifier, the ALC detector, and the high-voltage power supply, maintains the video output constant over a range of 300:1 in the scene luminance.

The signal output of the preamplifier is fed to a fixed-gain ALC video amplifier, whose output is clamped to provide the DC reference, then detected to generate a DC control signal. The mode of detection is switched from "peak" to "average" by an external switch accessible to the astronaut, or by ground command. To prevent blooming on picture highlights, the peak mode is designed to operate on as little as 0.5% of the picture area. The DC control signal is amplified, then applied as the programming input to the high-voltage power supply. The high-voltage output, in turn, is applied to the photocathode of the SIT sensor.

As the high-voltage varies, the photoelectron energy is changed, resulting in a change in the gain of the image section of the SIT. Thus, with the feedback loop closed, the system functions to maintain a fixed output at the preamplifier output. The loop response time is designed to be slow enough to prevent color contamination by field-to-field gain changes.

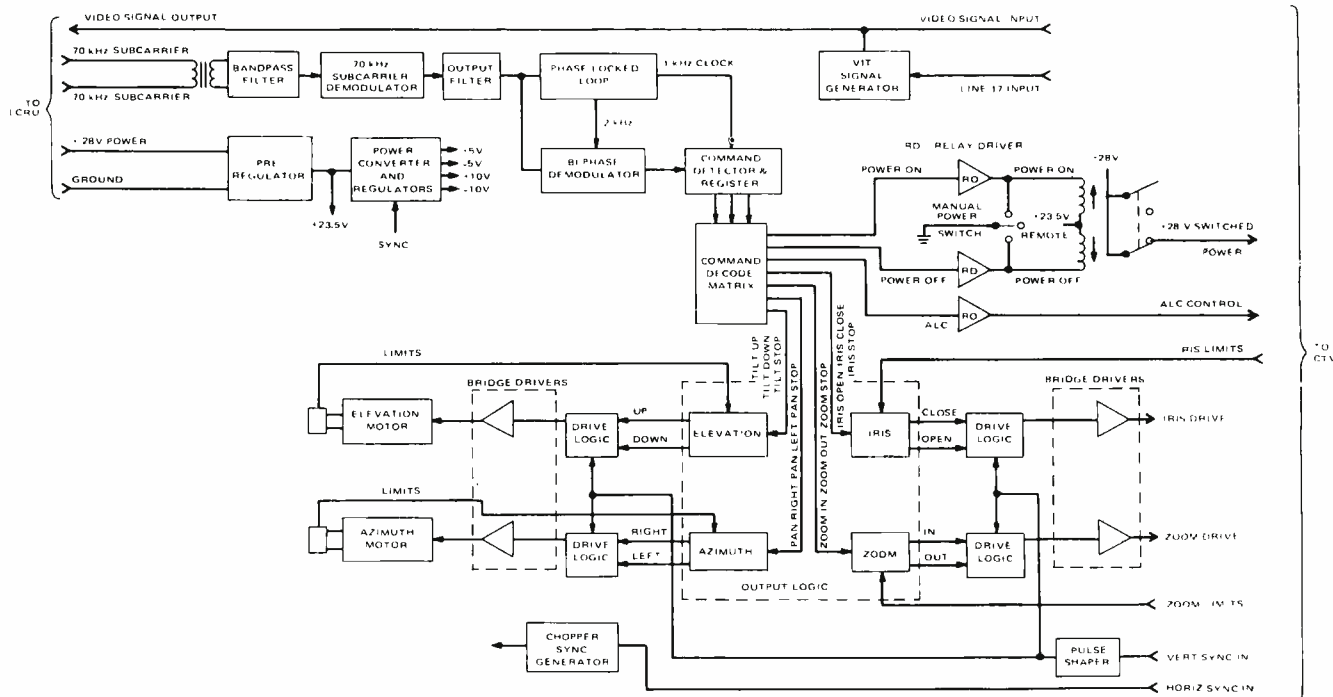


Fig. 7—Television control unit (TCU), block diagram.

AGC loop

An AGC range of 4:1 is achieved by detecting the output of the video amplifier and applying the detected level as a control signal to an FET connected as a voltage-controlled resistor in a voltage-divider circuit at the input to the video amplifier. The detection mode of the AGC circuit is switched simultaneously with the ALC.

Video processing

The video amplifier output is clamped to restore the dc component of the signal, and is routed to the gamma corrector. The gamma corrector is implemented with an integrated-circuit transistor array which provides a linear piecewise approximation to a transfer curve with a gamma of 0.7.

Gamma correction provides the following advantages to the overall Apollo TV system performance:

- Increased definition of shadowed areas of scenes. This advantage is particularly important when operating in ALC/AGC “peak” mode and viewing high-contrast scenes on the moon.
- Picture appearance is improved in the presence of noise expected in the overall system communications network.
- Color-hue tracking over the system dynamic range is more accurate.

Noise, both random and coherent, is

increased in the black region in accordance with the gamma gain. For a gamma of 0.7, the increase is 6 dB. The random noise in the system, which is predominantly photoelectron noise in the image section of the SIT tube, varies as the square root of the light level. Assuming the dynamic range is 32:1, the noise in the black region is $\sqrt{32}$, or 15 dB below the white-level noise. Thus, the gamma correction serves to redistribute the random noise more uniformly over the dynamic range. The gamma corrector generates three line segments to produce the proper curve. Gamma gain is 2.0 minimum in the black region and nominally 0.8 at white level.

The aperture corrector, located in a parallel path with the gamma corrector, utilizes a differential amplifier which takes the difference signal which appears at either end of a delay line to separate the high-frequency component of the video signal. The amplified high-frequency components then pass through a “coring” threshold circuit that clips the low-amplitude elements (noise) from the signal. Use of the cor-

ing circuit permits the SIT resolution response to be effectively doubled without increasing the noise in the low-frequency or broad areas of the scene. After coring, the aperture-correction signal is summed with the gamma-corrected low-frequency signal at the white clipper input. The white clipper removes signals and transients which exceed the specified composite video white level. Insertion of blanking and black clipping at the signal porch level are accomplished in the following stage.

Sync insertion is performed with an FET switch. A parallel FET switch inserts the color flag pulse into the composite video format during line 18.

The composite signal is then routed to a line driver with a current source output that delivers a 0- to 1-V video signal of proper format into a 75-Ω load.

TCU description

The TCU electronics functions are shown in the block diagram of Fig. 7. These include command subcarrier decoding, relay drivers, bridge-drive circuits for the four motorized functions, and the VIT pulse generation and insertion. The TCU cradle, driven in azimuth and elevation, holds the CTV for remote pointing in response to ground commands. The azimuth and elevation drives are coupled through override clutches, permitting the astronaut to assume control when desired.

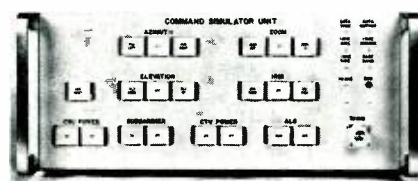


Fig. 8—Command simulator panel.

The up-link command signal relayed from the LCRU to the TCU is a 70-kHz subcarrier, frequency-modulated by a composite command signal which consists of the linear sum of a 2-kHz message subcarrier and a 1-kHz coherent synchronization tone. The message subcarrier and the synchronization tone have equal carrier-frequency deviation. Total peak deviation is ± 5 kHz.

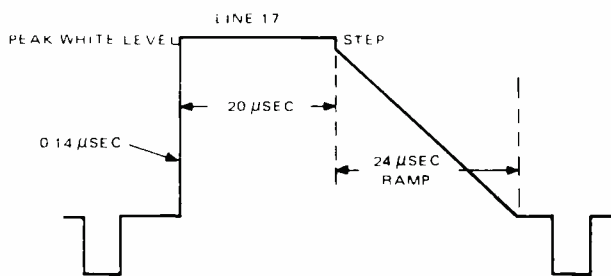
The commands are initiated in the Mission Control Center by means of individual function switches on the command simulator panel, as illustrated in Fig. 8.

Digital command information is carried by the 2-kHz message subcarrier and is phase-shift-keyed at a rate exactly one-half the rate of the subcarrier frequency. The message subcarrier is modulated by a train of binary "ones" and "zeros" (referred to as sub-bits) at a rate of 1000 per second. The train is in two-level, non-return-to-zero binary code.

A 1-kHz clock is regenerated from the demodulated subcarrier signal, and used to detect the proper sub-bit format for each of the permissible commands. Twenty-four unique commands are possible with the format used; eighteen of these are utilized in the GCTA operation.

The stepper-motor-bridge drive circuits utilize a 60-Hz clock signal supplied by the CTV vertical sync to restrain motor switching transients to the vertical blanking interval. Horizontal sync from the CTV is used to synchronize the DC/DC converter so that converter transients are contained within the horizontal blanking interval.

The VIT signal is generated within the TCU, and inserted in line 17 of each field during operation of the complete GCTA configuration. The test signal format in Fig. 9 contains:



- 1) a fast-rise leading edge to determine system bandwidth and transient performance,
- 2) a peak-white reference level for gain adjustment and measurement,
- 3) and a controlled ramp for checking system linearity. A small step also is provided at the end of the peak-white signal level and prior to the ramp to verify that the white signal has not been compressed. The step also permits oscilloscope triggering at the start of the negative-going ramp.

The rise time of the signal, T_r , has been chosen to be consistent with the bandwidth requirements of the CTV video signal at 200-line transmission. The corresponding cutoff frequency, F_c , with a linear phase-type filter is:

$$F_c = \frac{0.35}{T_r} = \frac{0.35}{0.14 \times 10^{-6}} = 2.5 \text{ MHz}$$

The block diagram in Fig. 10 shows the method by which the test signal is generated. A timing signal from the CTV sync generator (line 17 tag) identifies the start of each test signal. The test signal generator acts as a controlled-current source and is AC-coupled to the parallel CTV source and LCRU terminating impedance. The generator floats on the video line, except during insertion of the test pulse.

Thermal control

Thermal control of the CTV is achieved by the interaction of a second-surface mirror radiator on the top of the camera with the lunar surface and with deep space. The CTV rejects heat through radiation and receives heat by:

- 1) internal heat dissipation,
- 2) solar radiation incident on the mirror radiator, and
- 3) lunar-surface radiation when the radiator is tilted toward the lunar surface. A thermal insulating blanket covers the remaining surfaces of the camera to insulate against radiation from the lunar surface. The camera is cooled by orienting the second-surface mirror radiator level (horizontal) with the lunar surface. The

camera can be heated by activating the CTV electronics and by tilting the radiator toward the lunar surface.

Thermal control of the TCU is achieved through the use of side radiators on the lower housing (electronics compartment). At low sun angles, the radiators absorb sufficient solar and lunar heat in any azimuth position to prevent the unit from experiencing less than the minimum temperature limits for the assembly. The radiators also are large enough to prevent the TCU from exceeding the maximum temperature limits when the unit is operating under worst-case hot conditions. The worst-case hot condition occurs when maximum heat inputs are present due to lunar dust degradation of the TCU radiators and the TCU presents maximum projected area for solar irradiation. All other surfaces of the TCU (other surfaces of the electronics box and the entire azimuth/elevation drive unit) are thermally blanketed.

Acknowledgments

The development of the GCTA involved a dedicated team effort by members too numerous to identify individually, but whose contributions are none the less greatly appreciated. The guidance provided by L. Weinreb and his program office staff is gratefully acknowledged. A special note of thanks for S. Russell's system design, the mechanical design effort by D. Binge, the many hours of special testing by F. Hubit, and the helpful suggestions of S. Bendell of the Broadcast Systems. The program success must also be attributed to the development of the SIT sensor by Electronic Components, and the RF link design contributed by the Communications System Division. Technical guidance was provided by W. Perry, Technical Officer for NASA's Manned Spacecraft Center.

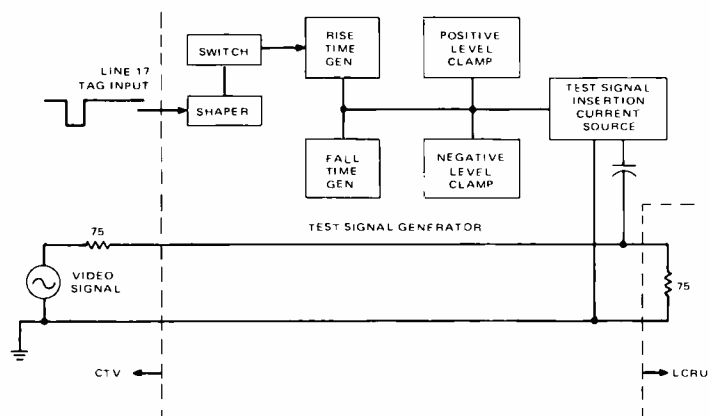


Fig. 9 (above)—Format of vertical interval test signal.
Fig. 10 (right)—Generation of vertical interval test signal.

Thermal steady-state spacecraft simulation

R. A. Lauer | M. K. Theus

Analytical prediction of the thermal characteristics of a spacecraft has been accelerated and refined in the past decade, with improved computer programs playing a dominant role. A program developed at AED uses a series of matrix manipulations of fourth order equations to directly calculate orbit average temperatures.

ORBITING SPACECRAFT (i.e., satellites) are subject to extreme temperature environments as they move from direct exposure to the sun into the shadow of the planet concerned. The heating inequity is further aggravated in more recent satellites, which no longer spin while orbiting, but maintain the same sector or side facing the planet continuously. Tests in a simulated environment to verify that the thermal design of the spacecraft maintains the temperatures of its constituent parts within the prescribed limits are time-consuming and expensive. Computer-aided analytical methods have been developed and refined to a point where accurate temperature predictions for many locations in a complex, modern satellite are possible.

Program development

The thermal steady-state computer program developed at AED is used to simulate a system of isothermal nodes. The system represents a satellite or specific components of a satellite in steady-state equilibrium from which orbit average temperatures are determined. Before transient and steady-state thermal programs were developed, the satellite was described by as few as three nodes. As the missions of spacecraft became more advanced, the components increased in number and complexity, so that the temperature variation of individual boxes became critical. It was no longer sufficient to describe a satellite system with a small number of nodes. As an

Authors Theus (left) and Lauer.

Mary K. Theus

Systems Analysis and Scientific Programming Group
Astro-Electronics Division
Princeton, New Jersey

received the BA in Mathematics from Augustama College, Rock Island, Illinois, in 1968. At that time, she joined the Research and Engineering Department of the U.S. Army Weapons Command and worked on stabilization systems, generalized vehicle/weapon simulations and cost effectiveness studies. She came to AED in 1969 and has since worked on 1) thermal analysis problems, 2) generalized magnetic closed-loop torque control simulation, 3) digital analog simulations of control systems, nutation damping systems, and a rigid, 3-body satellite simulation, and 4) a spacecraft configuration (e.g., family tree, parts list) reporting system.

Raymond A. Lauer

ITOS Project Office
Astro-Electronics Division
Princeton, New Jersey

received the BSME from Lehigh University in 1968. At that time, he joined RCA and participated in the six-month training program. His initial work included mechanical design and thermal design on several of the AED spacecraft projects. He is currently a mechanical engineer with the Integration and Test Group for the ITOS "M" and "D" series spacecraft.

Reprint RE-18-3-4

Final manuscript received March 6, 1972



alternate, actual environmental simulation was utilized to determine if the operating temperatures of certain components would be exceeded during flight.

The advantages of analytical prediction were again made available by the development of a "transient" program that described the variation in temperature until steady-state conditions were achieved. Orbit average temperatures could be derived by running the program through a steady-state orbit. Since orbit average temperature satisfied most of the requirements of the engineering analysis, it appeared inefficient to run an entire transient analysis to derive the orbit average temperatures. The steady-state computer program was developed to calculate these orbit average values directly from the mathematical equations for steady-state temperatures.

Specific problems which occur in thermal analysis of satellites in space dictated the method which was used to solve the system of equations. The three principal advantages of this approach are:

- A direct fourth solution is performed, avoiding inaccuracies in the linearization of the radiative coupling.
- The variable coupling coefficients required in active thermal control can be accommodated.
- A special interpolation routine is employed to insure convergence of the solution.

Statement of problem

The system is defined by a network of isothermal nodes, or bodies, coupled radiatively and conductively to one another and radiatively to external sinks. In this analysis, a sink is considered an isothermal node which, regardless of the amount of heat added or removed, remains at a constant temperature. One sink is usually used to represent space (considered 0 K). Other sinks can be defined to represent heat impinging on the spacecraft. If the incident heat is combined with the internally generated heat, Q_i , the same temperature predictions are obtained as when using external sinks. The analysis begins with the basic first order differential equation for temperature with nonzero capacitance (i.e., mC_p).

$$m_i C_{pi} dT_i/d\theta = Q_i + \sum_{\substack{j=1 \\ j \neq i}}^n R_{ij} (\sigma T_j^4 - T_i^4) + \sum_{\substack{j=1 \\ j \neq i}}^n K_{ij} (T_j - T_i) + \sum_{s=1}^k R_{is} (\sigma T_s^4 - T_i^4) \quad (1)$$

where n is the number of bodies, k is the number of sinks, i is the i th body, j is the j th body, m is the mass, C_p is the specific heat, Q is the internal heat generated, σ is the Stefan Boltzmann constant, T is the temperature, θ is the time, R_{ij} is the radiative coupling from body i to body j , R_{is} is the radiative coupling from body i to sink s , and K_{ij} is the conductive coupling from body i to body j .

The steady-state solution is obtained when $dT_i/d\theta = 0$, reducing Eq. 1 to:

$$\sum_{\substack{j=1 \\ j \neq i}}^n K_{ij} T_j + \sum_{\substack{j=1 \\ j \neq i}}^n R_{ij} \sigma T_j^4 + \sum_{s=1}^k R_{is} \sigma T_s^4 = Q_i + \sum_{\substack{j=1 \\ j \neq i}}^n R_{ij} \sigma T_i^4 + \sum_{\substack{j=1 \\ j \neq i}}^n K_{ij} T_j + \sum_{s=1}^k R_{is} \sigma T_s^4 \quad (2)$$

This system of equations can be solved by a matrix solution of first order simultaneous equations, or by a series of matrix manipulations of fourth order equations (which will be referred to as the σT^4 solution).

Method of solution

Since the principal application of this program involves satellites in space, the radiative couplings have a greater effect on the system than the conductive couplings, with the radiative couplings to space dominating over all. To solve for T_i by simultaneous first order equations would require the linearization of the radiative coupling terms. There are two major disadvantages to the linearization approach. First, because of the predominant effect of the radiative couplings to space, their values must be accurately calculated. The linearization would decrease the accuracy of these couplings, thus degrading the system solution. Second the radiative couplings between bodies are described in

greater detail and with more accuracy than the conductive couplings. Linearization would introduce additional error into the system as well as being laborious since, in general, more radiative couplings are present than conductive couplings.

On the other hand, the conductive couplings are generally approximations and their transformation to fourth order equivalents will not significantly affect the solution. The σT^4 solution allows the precise radiative couplings, calculated in other computer programs, to be used together with transformed conductive couplings which yield a more accurate solution than the linearization. In addition, the solution of first order simultaneous equations limits the solution to a unique value. As will be shown later, it is necessary to vary couplings as a function of temperature to accurately describe the physical system. The σT^4 iterative solution allows the couplings to vary with the temperature as it converges toward the solution.

The program calculates the orbit average solution for T_i in an iterative loop which is terminated when the temperature tolerance criteria is achieved. In the initial steps of the iterative loop, the conductive coupling terms, K_{ij} , are transformed to fourth power equivalents using the expression $1/[(T_i + T_j)(T_i^2 + T_j^2)]$. The temperatures used for the K_{ij} transformation were stored as the solution to the previous iteration. The principal section of the iterative loop uses program calls to standard matrix multiplication and inversion subroutines. The radiative and conductive couplings are summed for all bodies and the radiative couplings to sinks are combined. After this matrix is inverted, it is multiplied by the R_{is} matrix. The inverted matrix is also multiplied by the internal heat matrix, Q , which, in turn is multiplied by a column matrix describing the effective radiance of the sinks. Summing these last two matrices yields the σT^4 solution. In the final sections of the iterative loop, the fourth root of σT^4 is taken, defining the temperature. These temperatures are compared to the previous iteration temperatures to determine if the specified temperature tolerance has been achieved. If the difference of any node is greater than the tolerance, the

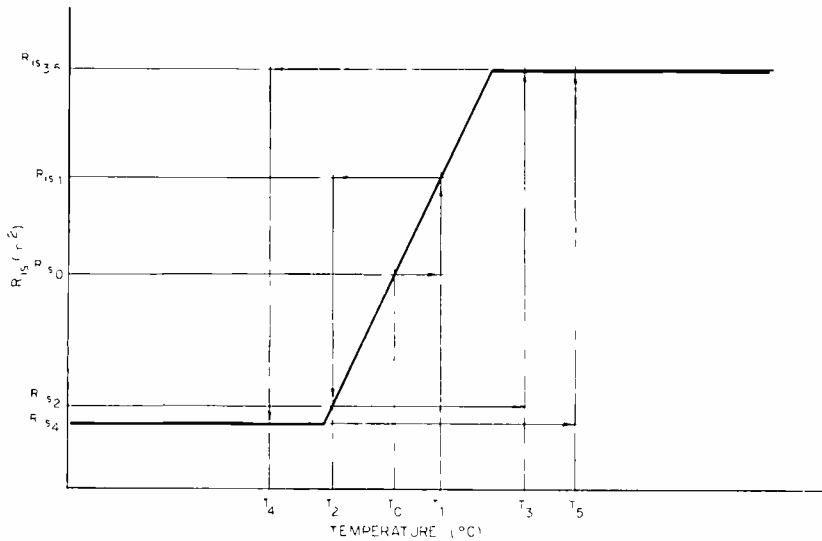


Fig. 1—Solution divergence.

present iteration temperatures are stored, and the program returns to the beginning of the iterative loop where couplings are updated and the entire iteration repeated.

As indicated above, the principal goal of this program is to calculate two successive iteration temperatures within a small temperature difference (nominally less than 0.05 degree). This is accomplished easily by the matrix solution for σT^4 , unless variable couplings must be introduced into the system. Active thermal control of a spacecraft causes variable radiative couplings between bodies. The heat inputs may also vary due to an active thermal control system. Some components, due to nature, have a varying heat dissipation as a function of their temperature. Thus the physical system is more realistically described by allowing some of the "constants" to vary and thus enhance the solution accuracy. However, these variable couplings may cause the mathematical solution to diverge, although this is physically impossible. Moreover, while in certain circumstances variable couplings will not cause the solution to diverge, they will make the convergence prohibitively slow. Therefore, to insure that convergence occurs and to minimize computation time, a temperature interpolation routine has been devised which forces the temperatures to converge rapidly.

The temperature interpolation is done for the bodies with variable couplings, if after any two successive iterations

the temperatures are not within tolerance. The temperature interpolation method is used only on R_{ij} and R_{is} curves. Curves which vary internal heat dissipation, Q_i , as a function of temperature were not included for two reasons. First, since many Q curves are double valued, there may not be a unique solution to the interpolation. Second, in general the ratio of change in Q due to the change in temperature in two successive iterations to the total heat generated in the spacecraft is sufficiently small that there is no divergence problem. In the event there is more than one dependent variable as a function of the temperature of a single body, the interpolation subroutine is called only for the first coupling encountered in the program input. Multiple calls to the same body may create divergence, since the slope for each coupling curve is used to determine the interpolated temperature. If the temperature of the independent body is changed after the slope is calculated, the next iteration will be using an inconsistent temperature value to calculate the new slope. If the temperature is determined only once and used for all successive couplings dependent on this body, no inconsistency occurs. The single call also eliminates the redundant calculation of the temperature for a single body, which would increase computation time.

Temperature divergence is caused by an instantaneous mathematical response to a change in coupling value. In the physical system the damping caused by the mass of the bodies

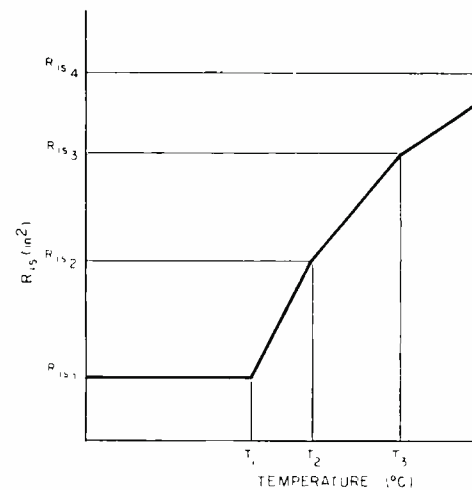


Fig. 2—Typical R_{is} curve.

would inhibit the rapid change and thus not allow divergence. An example of divergence through successive iterations is seen in Fig. 1. Even mathematically this problem only occurs when the change in the coupling value from one iteration to the next represents a significant change in the total system coupling value. Since the temperature of every body is dependent on the temperature of every other body in the system, a small change in the coupling value of one body will not force other nodes far from their solution temperature. Therefore; if the temperature of the body with the varying coupling is never allowed to change greatly, divergence will not occur. This may cause slow convergence but not divergence.

The following representation of a varying coupling was used to determine the appropriate method to use for the temperature interpolation. A set of steady-state solutions for a one body problem using different R_{is} couplings was generated. This solution curve was then compared with typical R_{is} curves to determine useful relationships. It was determined that the solution curve was a high order curve which had a unique intersection with the R_{is} curve. This intersection represents the steady-state solution. Since the solution curve is relatively linear over the defined region of the R_{is} curve, a straight line approximation may be used to determine the approximate intersection for expedience in computation. A typical R_{is} curve is shown in Fig. 2.

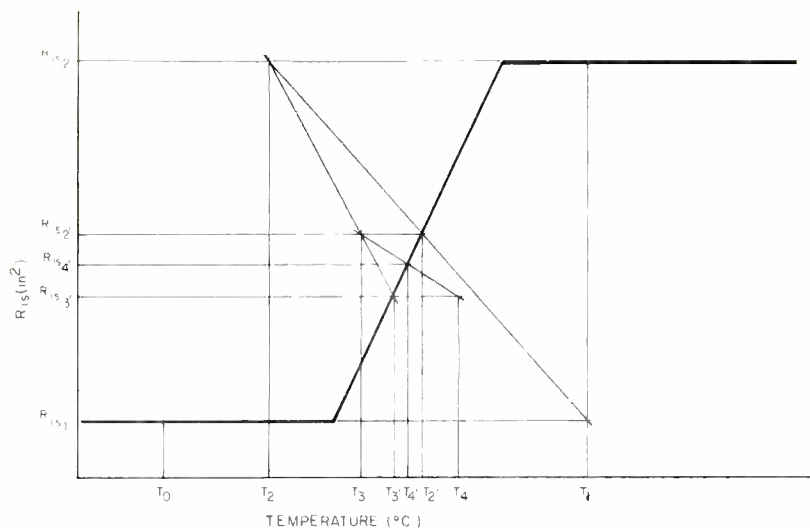
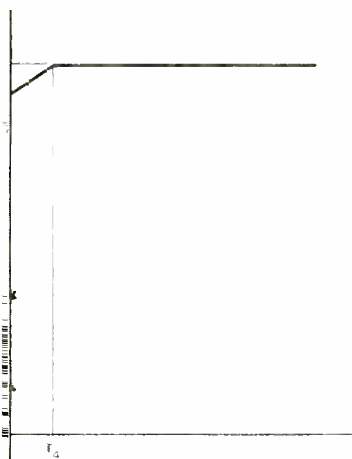


Fig. 3—Solution using interpolation

The interpolation subroutine is called as the last step of the iterative loop in the program. Two successive iteration temperatures are required to determine an intersection with the coupling curve. The subroutine first checks the difference of the successive temperatures; for a difference of less than 0.01°K , the interpolation for that temperature is discontinued, as the temperature is considered to have reached its solution. The radiative couplings calculated in the two previous iterations are stored for use when the slope must be calculated. The difference between these couplings divided by the difference of the corresponding temperatures will define the slope of the solution curve. If the slope derived has a positive value, the interpolation is abandoned for the present iteration, as a positive slope may force the interpolated temperature to diverge from the true solution. More frequently, a solution curve with a positive slope may not intersect the coupling curve in a single point. In either case, no interpolation temperature is defined. The present temperature is not stored so that in the next iteration, the slope of the solution curve will be determined by temperatures and coupling values two iterations apart. Once the slope of the solution curve is determined, the coupling intercept is also calculated. These two values, of course, define the solution line. The slope of the solution line is compared with the slope of each straight line section of the coupling curve. If both slopes have a zero value, the temperature will not change as the

coupling value lies on a constant segment of the curve. Assuming the solution slope has a non-zero value, the intersection of the solution line and the coupling curve is calculated. The temperature at this point replaces the temperature determined in the matrix solution. This updated temperature is then used in the next iteration to define all couplings which are dependent on the temperature of the body for which the interpolation was done. This interpolation will force the temperature to converge rapidly. It eliminates the possibility of the temperature oscillating around the true solution, taking many iterations to actually reach this point. After the interpolation of temperatures associated with variable couples, the new temperature values are returned to the main program.

An example of the interpolation method is shown in Fig. 3. The initial temperature values are not used in the interpolation as these input values may not resemble the solution. Frequently, all temperatures are input at zero degrees. Since most couplings are defined for positive temperature values, considering the zero point would cause a positive slope and, thus, no temperature would be calculated. After the second iteration through the program loop, the first and second iteration temperatures and corresponding coupling values are stored, assuming the temperatures exceed the tolerance. (These are T_1 and T_2 in Fig. 3). The solution slope is defined and, if negative, the solution curve intercept (T_2') is determined and used to determine the

coupling values during the next iteration. The graph in Fig. 3 shows that, through succeeding iterations, the intersections approach a solution. The graph illustrates the inherent problems caused by a positive slope of the solution curve.

Applications

The orbit average program is used in most thermal analyses. It was used for the Ground Commanded Television Assembly on Apollo 15, although the interpolation routine was not used as no variable couplings were required. The interpolation routine has been used for the ITOS B, C, D, and E satellite simulations and the Viking design. The interpolation routine appears to halve the number of iterations required to reach the solutions, according to the ITOS D&E simulations.

Summary

The simulation describes the thermal design of a spacecraft by defining a system of isothermal nodes. These bodies are coupled both radiatively to each other and to sinks, and conductively to each other. The radiative couplings may vary with respect to temperature. To insure that these variable coupling curves do not cause a divergent temperature, an interpolation routine is used to drive the temperature to its true solution rapidly. The orbit average temperatures for each of these nodes is then determined by solving the fourth order, steady-state, heat-transfer equation for σT^4 .

Simulation of nuclear blast effects on communication cables

E. Van Keuren

Communications cables which will survive in close proximity to a nuclear blast and at very high overpressures are necessary components of many military systems. High explosives can be used in various forms for simulation of blast effects on cables as well as other equipment. This article describes some of the tests which have been conducted, presents the results of testing various cables, and discusses some of the ramifications with regard to use of these cables.

WITH THE ADVENT OF STRATEGIC WEAPON SYSTEMS that are required to survive in proximity to a nuclear blast, the need arose for highly survivable communications networks to interconnect weapon sites and other survivable (hardened) facilities. The Minuteman system, which uses cables for both pre- and post-attack communications in five of its six wings, is one of the best known examples. A major effort was devoted to the study of advanced system nuclear-hardening

Edward Van Keuren, Ldr.
Systems Engineering
Government Commercial Systems
Camden, New Jersey

received the AS in Engineering from University of Bridgeport in 1948 and the BS from Rutgers and the MBA from Drexel Institute of Technology in 1963 and 1968, respectively. He joined RCA in 1948 and was assigned shortly thereafter to experimental UHF station KC2XAK. Subsequently he was assigned to what is now Consumer Electronics, first with the Resident Engineering Department in Indianapolis and later as a radio and high fidelity equipment design engineer at Cherry Hill. He has been with Government and Commercial Systems since 1961. During this latter period, his primary responsibilities have been in systems engineering related to the Minuteman and other programs. Since 1965, his responsibilities have included weapon system survivability/vulnerability analysis and consultation. In this capacity his evaluations have included the Hard Rock Silo Program, Minuteman, the Status Authentication System, the Airborne Launch Control Center, and the URC-78 Radio.

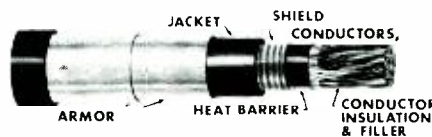


Fig. 1—Armored cable configuration.

approaches which were ultimately consolidated into the Hard Rock Silo program. Hard Rock has since been cancelled; however, the technology on which it was based and the results of the tests are applicable to future systems such as SANGUINE, Safeguard, Minuteman Defense, and others yet to be conceived.

Armored cable designs

In October 1967, Anaconda Wire and Cable Co., which was a member of the RCA Hard Rock team, introduced a new armored cable intended to survive extremely high nuclear overpressure pulses. In this cable, tension and compression strength is provided by two layers of counterwrapped steel armor, which also provides shear and impact protection. The core of the cable was completely filled with a polyethylene compatible wax to furnish internal and external pressure balancing and to improve the overpressure resistance. In later configurations, the steel armor was copper plated to minimize corrosion and improve EMP shielding; an outer protective jacket also was added. This configuration is shown in Fig. 1.

The original design was based on a completely filled, twisted-pair core, but it soon became apparent that coaxial configurations would be desirable for transmission of RF and wideband data. Although it was originally felt that a

completely filled cable would be required for high overpressure survivability, subsequent preliminary analysis indicated that the steel armor alone might have adequate strength to protect an air-core or foam-filled cable. Based on this analysis, coreless samples were constructed to simulate an air dielectric cable. These samples were exposed to overpressures up to 4200 lbf/in² during Blast On Structures (BOSS) tests conducted by Physics International at their Tracy, Calif. explosive test site. These tests, as described later in the article, demonstrated that a hollow cable could survive.

High explosive simulation testing

As used here, the term high explosive simulation testing (HEST) refers to a specific series of blast effect tests conducted by the Air Force to evaluate the survivability of various constituents of the Minuteman and other weapon systems. The series began with small-scale "sand box" types of tests on short sections of cable and various types of splice cases used in the Minuteman system. These tests demonstrated that, with moderate physical damage which did not impair electrical performance, the cable system would survive a first shot at design overpressure. As the size of the tests increased, other components such as hardened antennas and some actual Minuteman facilities were included.

More recent HEST tests, such as Rock Test I which was used to evaluate a variety of equipments and facilities destined for the Hard Rock program, cover an area of approximately a city block, i.e., in the order of 300 feet on a side. The samples are installed within the boundaries of this area and a steel supporting structure is erected as shown in Fig. 2. A platform is laid over this structure with the explosive charge in the form of primacord covering the platform. The entire installation is then covered with a large mound of earth to provide momentary containment of the blast pressure.

When ignited, the primacord burns across the test area, thereby providing an approximation of a blast wave passing across the surface. The photo in Fig. 3, taken a short time after ignition and just after the earthen cover has been breached, illustrates this phenomenon.

Reprint RE-18-3-6
Final manuscript received May 15, 1972





Fig. 2—HEST structure.



Fig. 3—HEST explosion.



Fig. 7—BOSS test configuration showing containment duct.

Rock Test I

Samples of the armored cable and the Minuteman type currently in use were tested in Rock Test I. This test was fired near Albuquerque, N.M., and was the first attempt to measure blast effects on cables and other facilities installed in competent granite rock rather than in soil. The cable samples were installed in trenches which were pre-cut into the rock. Cable burial depths ranged from a few inches to a foot, and the samples were covered with a concrete cap. Some of the samples included splice cases which had been pre-installed at the Anaconda plant; all sections of the cable were rigidly restrained. The measured peak overpressure that was achieved in the vicinity of the cable samples was somewhat over 3000 lbf/in².

Fig. 4 shows a comparison between the pre- and post-test condition of the armored cable. The salient point to note is that there is essentially no compression in the sample which was tested at the 3000 lbf/in² value.



Fig. 4—Pre and Post-test condition of armored cable.



Fig. 5—Pre and Post-test condition of Minuteman cable.

Fig. 5 shows a comparison between the pre- and post-test condition of the Minuteman cable. The key point to note

in this picture is the amount of compression at the measured overpressure since this is used as a check point for other measured overpressures discussed later. In this test, overpressure far exceeded Minuteman criteria and, although the Minuteman cable was severely compressed, no electrical failures resulted. Thus, the probability of survival at and even well above Minuteman-specified overpressure would be extremely high.

Rock Test II

Rock Test II was fired at Cedar City, Utah. This test included the first attempt to simulate the combined effect of overpressure and direct-blast-induced earth and rock motion. Previously, all large-scale high-explosive simulation testing had been limited to overpressure only. In Rock Test II, buried charges were included with the overhead charges. Detonation of the buried charges was time phased with respect to the overhead charge, so as to cause the resultant earth motion to occur at the samples in the proper relationship with the overpressure pulse.

To achieve competency, soil and weathered rock were scraped away until a layer was reached that was relatively hard and had a minimum of faults in the test area. The cable samples were installed in trenches cut into the rock, at depths down to a foot, and covered with a concrete cap. This test was fired

Fig. 6—Armored cables and "Y" splice case.



in March 1970 and the samples excavated in May. The picture in Fig., 6 taken when the cables were uncovered, shows the generally undamaged condition of the cables and "Y" splice cases. Damage to the armored cable in both Rock Tests I and II was so slight that a relative comparison is difficult.

Presumably, one of the worst effects on a cable installed in rock would be the shearing effect produced by the relative displacement in adjacent rock strata caused by direct induced motion. However, no effects of this type were apparent, either in the rock itself or in damage to the cable.

Blast on structures simulation testing

Blast on structures (BOSS) testing is a technique for overpressure testing developed by Physics International of San Leandro, California. In this concept, the blast wave is generated by an explosively driven flyer plate and transmitted down a long duct. The overpressure pulse characteristics, amplitude, duration, etc., are determined by the size of the charge and the configuration of the duct.

BOSS test configuration

Due to RCA's involvement in various programs which require the use of survivable cables, RCA arranged for samples of three types of cables to be constructed and delivered to Physics International for testing. These samples included the filled armored cable, the air-core armored cable, and the Minuteman cable. With the permission of the Navy, the cables were included by Physics International in a test of other devices. The long duct technique used by Physics International was ideal for testing of a blast wave propagating along the cable.

Fig. 7 shows the duct in the process installation. The duct has been enclosed in a large wooden trough filled with wet (saturated) sand to help in momentarily containing the pressure. The entire



Fig. 8—Cable compression at 3000 lbf/in².

structure is ultimately covered with additional sand as shown at the right half of the picture. The explosive chamber and filling port are located at the extreme right. The filling port is left uncovered so that the explosive can be added at the last possible moment, thus providing a high degree of safety during construction of the test.

The cable samples were eventually installed under and in close proximity to the duct, at roughly the mid point. Fifteen-foot samples of each type were located along the duct, longitudinal to the blast wave; and two-foot samples were located across the duct, transverse to the blast wave. The ends of all samples were tightly capped to prevent the pressure pulse from entering the cable and creating a pressure-balanced condition. This was particularly important in the case of the hollow cable. The low-pressure end of the longitudinal samples was located at what was calculated by Physics International to be the 3000 lbf/in² point. This calculation subsequently proved to be highly accurate. Measurements showed that the high-pressure end of the longitudinal samples and the transverse samples were located at the 4200 lbf/in² point.

In this BOSS test, the explosive charge consisted of 1000 pounds of liquid nitro methane. The combination of the duct configuration, the sand enclosure, and this explosive charge, produced an overpressure pulse which, in the 3000 to 4000 lbf/in² region, had a duration and shape similar to that which would result from a blast of roughly 20-kilotons.

Test results

Fig. 8 shows a cross section of the three samples that were placed at the 3000 lbf/in² point. Note the similarity between the compression of the Minuteman cable shown at the left in



Fig. 9—Cable compression at 4200 lbf/in².

this picture and that shown by the HEST test sample in Fig. 5. It was originally felt that variations in pulse width between Rock Test I and the BOSS test might produce totally different results; however, the high degree of similarity between the effects on the Rock Test I and BOSS samples of Minuteman tends to indicate one of two things: either the pulse widths were similar, which is the most likely—or the cable is not pulse width sensitive, which is rather unlikely. Based on this, the conclusions drawn from the BOSS test results are assumed to be valid and relateable to Rock Test I.

The key point in Fig. 8 is the absence of damage to the hollow sample shown on the right. Prior to this test, it was thought that the armored cable's completely filled core provided the overpressure resistance. This presumably provided pressure balancing and prevented flattening. Pre-design analysis of the cable indicated the possibility that the bridging capability of the armor might provide adequate overpressure resistance; hence, a sample constructed with the same armor but with a hollow core, was included in the BOSS test. As noted previously, the hollow sample retained equal integrity with the filled sample, thus showing the capacity of an air or soft-core dielectric wideband cable to withstand severe overpressures.

Fig. 9 shows a cross section of the three cables taken from the longitudinal samples near the 4200 lbf/in² end. Again, the samples of the armored cable were essentially undamaged. At this overpressure, the Minuteman cable displayed a teardrop shape, with most of the compression on one side, rather than an overall flattening. Fig. 10 is a cross-section view of the transverse samples which were exposed to a force of 4200 lbf/in². These samples were too

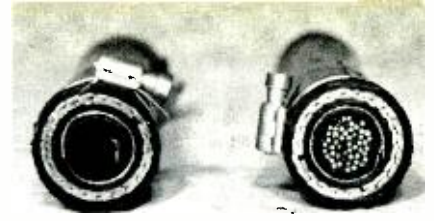


Fig. 10—Cross section of transverse samples at 4200 lbf/in².

short to support a broad conclusion; however, the tendency to resist damage is evident.

Fig. 11 depicts the result of a severe dent in the cable. This dent was located close to the 3000 lbf/in² end but was not a result of overpressure. The dent appeared to result from buckling of the duct. The force at this point, although unmeasured, was probably well over 10,000 pounds. Again, the similarity in the effects on the filled and hollow cable should be noted since they reinforce the conclusion that the bulk of the strength is in the armor. If an inner conductor had been present and insulated enough to prevent a direct short, the cable would have retained usable transmission characteristics even though its performance would have been altered.

With Hard Rock in abeyance at the time that the tests discussed in this article were concluded, the most likely program for application of hardened cables appeared to be the Safeguard Communications Agency (SAFCA) which had a wide-band data transmission requirement. The author constructed several samples containing a combination of three wideband coaxial tubes and nine twisted pairs as shown in Fig. 12 and presented these for SAFCA consideration. This cable construction technique was well received, and the program turned over to Anaconda to pursue further. A subsequent sample, as shown in Fig. 13, was constructed by Anaconda to meet specific Safeguard requirements.

This cable has subsequently been subjected to rigorous evaluation by SAFCA and an order placed for the quantity required for the first Safeguard wing. Evaluations are also being performed by other agencies for future uses such as the Minuteman Defense (Hard Site) Program.

Fig. 11—Severe dent due to impact of duct.

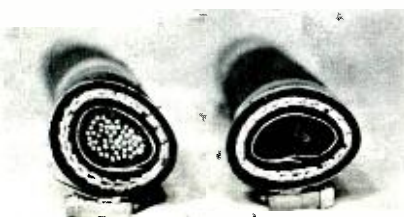


Fig. 12—Demonstration sample, wide/narrow band cable.

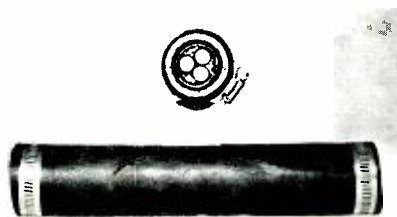


Fig. 13—Safeguard cable.



Propulsion for Geostationary Spacecraft

Y. Brill | R. Lake | J. Mavrogenis

A dual-thrust-level hydrazine propulsion system offers significant, cost, weight, and simplicity advantages for geostationary spacecraft missions lasting up to ten years. A flight-weight dual-thrust-level hydrazine system was fabricated and tested at Astro-Electronics Division. A nominal 4.1-lbf-thrust-level hydrazine/Shell 405 thruster was coupled with a 0.030-lbf hydrazine electrothermal decomposition thruster. System performance was characterized in steady-state and pulsed operation representative of synchronous mission requirements. Testing of the model propulsion system has provided the confidence that such systems are ready for flight application.

AN EARTH SYNCHRONOUS or geostationary orbit is a circular orbit in the equatorial plane with an orbital period of one sidereal day. Satellites in a synchronous orbit typically perform missions as communication relays, navigation aids, and meteorological observers. Use of a geostationary orbit provides unique operational advantages to a spacecraft because highly directional and continuous coverage of a given theatre becomes possible with only a limited number of spacecraft—in the limit one—provided it has eclipse capability.

This paper examines the on-board propulsion requirements of typical geostationary spacecraft, compares propulsion system weights for orbit maintenance and attitude control, and identifies a dual-thrust-level hydrazine propulsion system which has distinct

advantages for geostationary mission application. Also, the fabrication and testing of a flight-weight model dual-thrust-level hydrazine system is described.

Mission analysis and propulsion system comparison

The propulsion subsystem for a typical geostationary spacecraft consists of a solid-propellant apogee kick motor and an on-board reaction control system. The kick motor is used to transfer the spacecraft from the booster low-altitude parking orbit to the desired synchronous altitude. The on-board reaction control system is integral with the spacecraft and used to control the spacecraft during the transfer, to trim the resultant injection orbit, and to provide on-orbit station keeping and momentum control.

Authors (left to right) Mavrogenis, Lake, and Brill.

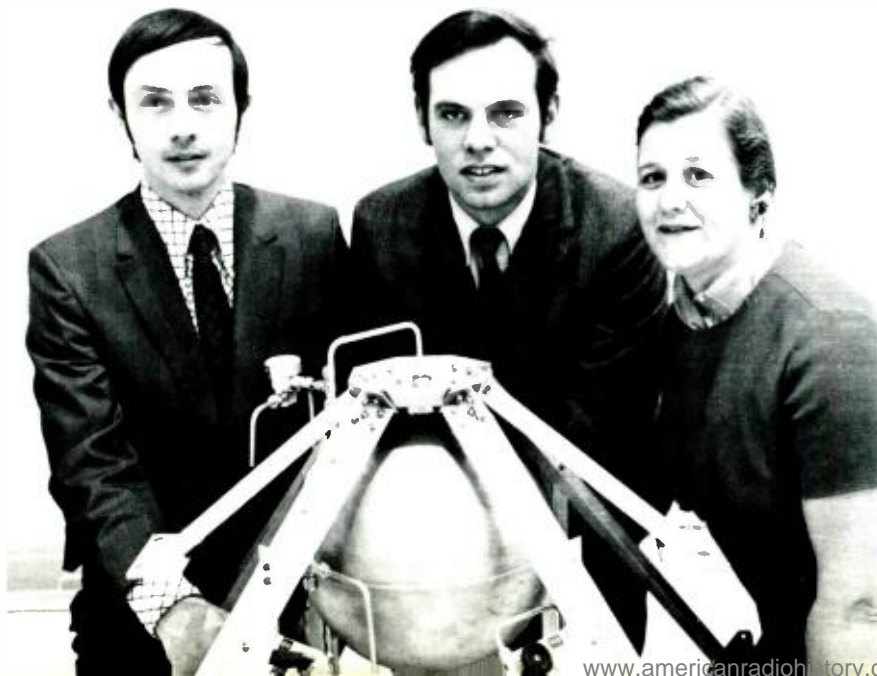


Table I—Velocity increment requirements.

Source of perturbation	ΔV velocity increment (ft/s)		
	1 year	5 year	7 year
Correct booster dispersions and station acquisition	[THOR/DELTA LITAN 3C]	200 140	One time only
Station keeping*			
Lunar and solar (N-S)	150	75	1050
Tesseral harmonic (E-W)	6	30	42

*Assumes continuous correction for inclination and longitudinal drift due to earth-moon and triaxial perturbations.

Velocity correction requirements which must be provided by the on-board propulsion system are summarized in Table I for 1-, 5- and 7-year orbital lifetime. Maintenance of orbital position to within 0.1 degree in both latitude and longitude is assumed. In addition to these requirements, propulsive capa-

Jim Mavrogenis

Propulsion Systems Group
Astro-Electronics Division
Princeton, New Jersey

received the BSME degree from the University of Wisconsin in 1963 and has done postgraduate work at Washington University and at UCLA. Before joining AED in December 1970 he was associated with the TRW Systems Group, as an assistant manager for the propulsion system of the Vega Satellite program. At AED he was lead engineer on the Dual-Thrust Propulsion Program (from which this paper is drawn) and presently is associated with the Atmosphere Explorer Program as the senior propulsion systems engineer.

Ralph Lake

Propulsion Systems Group
Astro-Electronics Division
Princeton, New Jersey

received the BME degree in 1969 from City College of New York. After graduation he joined the Spacecraft Design Group of AED, where he was engaged in the mechanical and structural design of spacecraft components. At present his primary function is design of spacecraft auxiliary propulsion systems with emphasis on research and development of advanced propulsion technology. Recent projects involved capillary propellant management systems and simulation of low-gravity fluid behavior in an earth-based experiment, using liquid neutral-buoyancy techniques.

Yvonne Brill

Propulsion Systems Group
Astro-Electronics Division
Princeton, New Jersey

received the MS in Chemistry from the University of Southern California. She joined the RCA Astro-Electronics Division in 1966 as a member of the technical staff, Propulsion Systems. Since joining RCA, she has been responsible for the analysis and design of a number of spacecraft propulsion systems, including those for several broadcast and communication satellites, and the proposed station-keeping systems for the Atmosphere Explorer and ITOS spacecraft. Her prior experience has been in analysis and on research and development programs in rocket engines, ramjets, and advanced turbojets at Wright Aeronautical, United Aircraft Research Labs, Marquardt, and the Rand Corporation. She has coauthored six published papers and is a member of AIAA and Sigma Xi. She was the recipient of an AED Engineering Excellence Award in 1970.

Reprint RE-18-3-1

Final manuscript received January 22, 1972

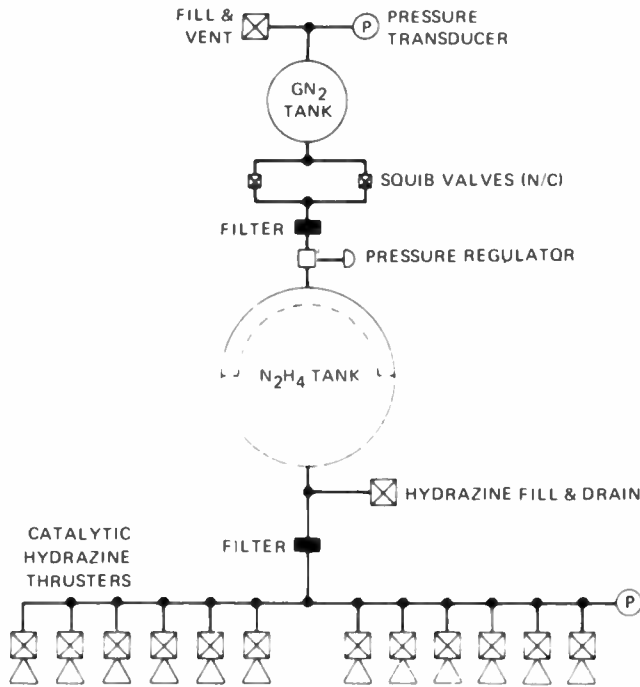


Fig. 1—Hydrazine/Shell 405 spacecraft propulsion system.

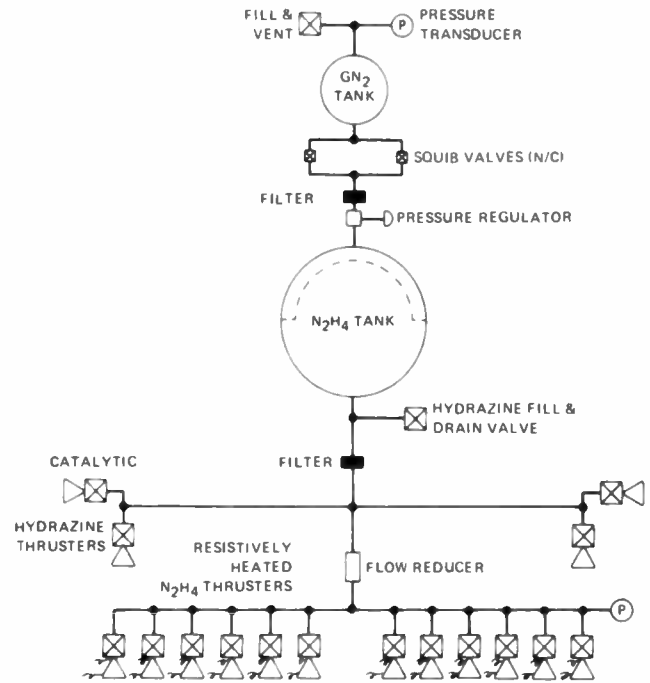


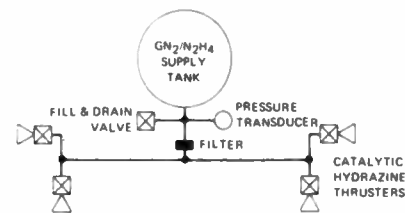
Fig. 2—Dual-thrust-level hydrazine spacecraft propulsion system.

bility is necessary for spacecraft attitude stabilization. For the mission discussed, requirements for this function are based on assuming active three-axis stabilization such as provided by an Astro-Electronics Division "Stabilite" attitude control system which employs a single-axis flywheel or momentum wheel to provide two-axis control (roll and yaw) by utilizing the gyroscopic stiffness property of spinning bodies. Control of the third axis (pitch) is obtained by modulation of the wheel speed. Propellant requirements for attitude control, therefore, are modest relative to a pure jet system or reaction wheel types of attitude stabilization.

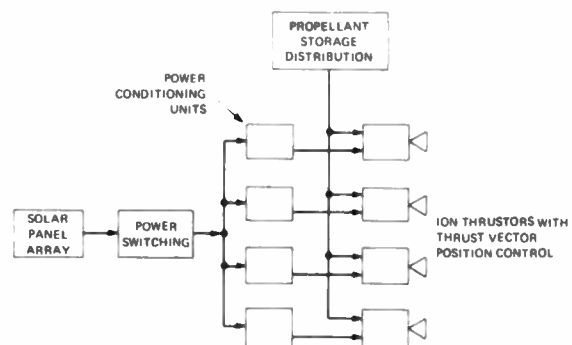
Propulsion systems were sized and weights determined for spacecraft weights of 700, 1500, 3000, and 4500 lb for 1-, 5-, and 7-year orbital life. Table II lists the pertinent propulsion system types analyzed. Selection and limitation of types for study is based on results of a previous broad-based propulsion system tradeoff analysis for a two-year geostationary mission.² The referenced study indicated that although electrostatic (ion) engines are characterized by high specific impulses, ($I_{sp} > 3000$ s), which make them attractive for station keeping on long-term missions, they are extremely complex and, of necessity, are constrained to low thrust levels. This makes them impractical for use in the satellite orbit acquisition phase or

any maneuver in which a relatively large impulse bit is required in a short period of time. Thus, use of an ion engine for station keeping additionally requires a chemical system for the other functions. Optimization of propulsion system weight for synchronous missions, therefore, is bounded by the weight penalty due to acceptance of either the higher propellant weight associated with use of total chemical system or the higher hardware weight and greater complexity associated with the use of a higher performance chemical / ion system.

In addition to typical catalytic hydrazine systems and hydrazine/ion systems, Table II identifies a dual-thrust-level propulsion system which is capable of satisfying both the high- and low-impulse bit rate demands of synchronous missions. This system combines the moderate thrust capability of a catalytic hydrazine thruster (typically 1.0 to 5.0 lb_f) to provide the initial velocity demand of station acquisition, with efficient low-level thrusting of a hydrazine resistojet to provide long-term station-keeping and



(a) HYDRAZINE/SHELL 405 PROPULSION SYSTEM FOR STATION ACQUISITION



(b) ELECTRIC PROPULSION SYSTEM FOR LONG TERM STATIONKEEPING (IHg BOMBARDMENT ION)

Fig. 3—Chemical/ion spacecraft propulsion system.

attitude control. Choice of hydrazine as the propellant enables utilization of a single propellant storage and feed system and offers a steady-state vacuum I_{sp} of 230 s for the higher thrust portions of the mission and a potential I_{sp} of 340 s for the low thrust portions. (This value is predicted by Marquardt based on 8000 hour life test data for 100 millipound resistojet thrusters operated at 2200 K gas temperatures.⁶) The greater I_{sp} is achieved by augmenting the enthalpy of hydrazine decomposition products by application of electrically supplied heat. The distinct advantage that hydrazine enjoys over other resistojet propellants is that it yields a high specific impulse as a monopropellant, while as a resistojet propellant it requires less power input than other common working fluids to achieve the same final operating temperature. This is because part of the necessary thermal input is supplied by its exothermic chemical decomposition.

Propulsion system schematics for each of the systems studied are presented in Figs. 1, 2, and 3. Each propulsion system type is configured to provide two completely redundant half systems with thrusters arranged to accomplish all required maneuvers with either system. An outline of a typical three-axis stabilized spacecraft showing the locations of the thrusters for a hydrazine system is shown in Fig. 4. Hydrazine (chemical) system weights assume high-pressure storage, regulated nitrogen gas pressurization, and positive expulsion tankage. The hydrazine systems are

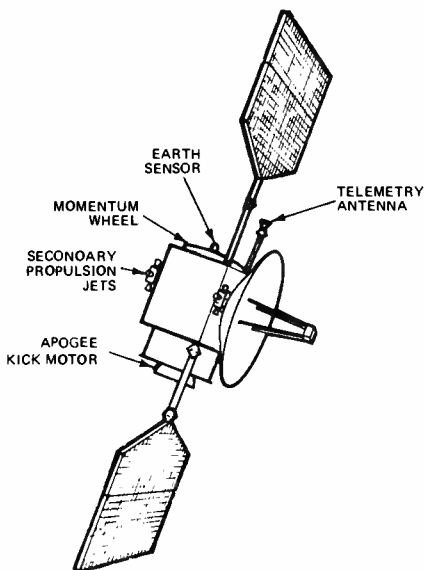


Fig. 4—Typical geostationary communications satellite showing thruster locations.

Table II—Weight comparison of propulsion systems

A. Characteristics						
		Type of propulsion	Function		Steady-state I_{sp} (s)	
System A		Catalytic hydrazine	Station acquisition and stationkeeping		230	
System B		(1) Hydrazine (2) Hydrazine Resistojet	Station acquisition stationkeeping		230 340	
System C		(1) Hydrazine (2) Ion	Station acquisition stationkeeping		230 3000	

B. Total system weight for different orbit lifetimes									
Spacecraft weight (lbs)	System type	Orbit lifetime (yrs)			Spacecraft weight (lbs)	System type	Orbit lifetime (yrs)		
		2	5	7			2	5	7
700	A	87	139	168	3000	A	255	491	654
	B	78	105	130		B	213	372	480
	C	99	105	110		C	269	291	306
1500	A	155	285	368	4500	A	360	531	684
	B	126	218	280		B	299	417	450
	C	168	187	200		C	364	417	450

configured from existing flight hardware. For the hydrazine resistojet system weights, power sharing is assumed for thruster operation because thruster duration for even the longest maneuvers (N-S station keeping) is relatively short. For example, at 10 millipounds thrust, firing times required twice daily at the nodes to null the solar-lunar perturbations at spacecraft masses of 1500, 3000, and 4500 lb are on the order of 17, 35, and 51 min, respectively. At this thrust level it is calculated that 75 W of additional power are required to achieve an I_{sp} of 340 s.

Ion engine system weights are based on existing, state-of-the-art cesium or mercury bombardment thrusters^{3,4} sized for the minimum thrust level to null mean station perturbations^{3,5} in order to minimize power requirements. At these thrust levels, however, thrusting is required 20 to 22 hours daily. Since this is beyond the capability of power sharing, power source weight has been charged to ion propulsion system weight.

Table II gives calculated propulsion system weights for 700, 1500, 3000, and 4500 lbm spacecraft for 1-, 5-, and 7-year orbital life. Fig. 5 compares total propulsion system weight as a function of years in orbit for 700 and 1500 lbm spacecraft. Similar graphs for 3000 and 4500 lbm spacecraft exhibit corresponding weight-orbital life crossover points. An interesting result of the comparisons is that although the hydrazine resistojet specific impulse is an order of magnitude below that obtainable from ion

engines (I_{sp} of 340 s vs 3000 s) the dual-thrust-level hydrazine combination is highly competitive in overall propulsion system weight. For lifetimes of 5 years, a requirement for many synchronous missions, the hydrazine/hydrazine resistojet system is lighter than, or weight competitive with a hydrazine/ion system. For longer mission life, say 7 years, the hydrazine/hydrazine resistojet is approximately 30% heavier than a hydrazine/ion system. For the 7-year life requirement with a 1500-lb spacecraft and 10 millipounds thrust, the hydrazine resistojet requires a total steady-state burn time of approximately 1450 hours to satisfy the mission demands. Six 10-millipound-force-level hydrogen fueled and ammonia fueled resistojets have completed 8000-hour endurance tests at 50% duty cycles with no degradation in any units at test termination.⁶ Ammonia, hydrogen, and nitrogen comprise the working fluids in a hydrazine resistojet. However, to satisfy a 7-year mission life,

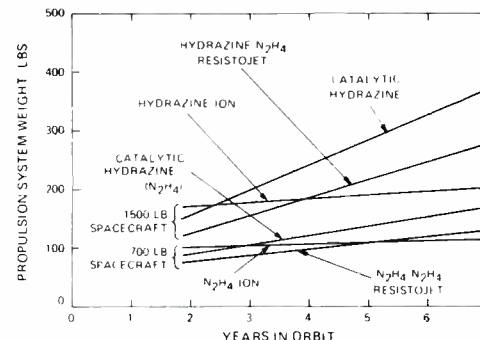


Fig. 5—Spacecraft propulsion system weight comparison for typical geostationary mission.

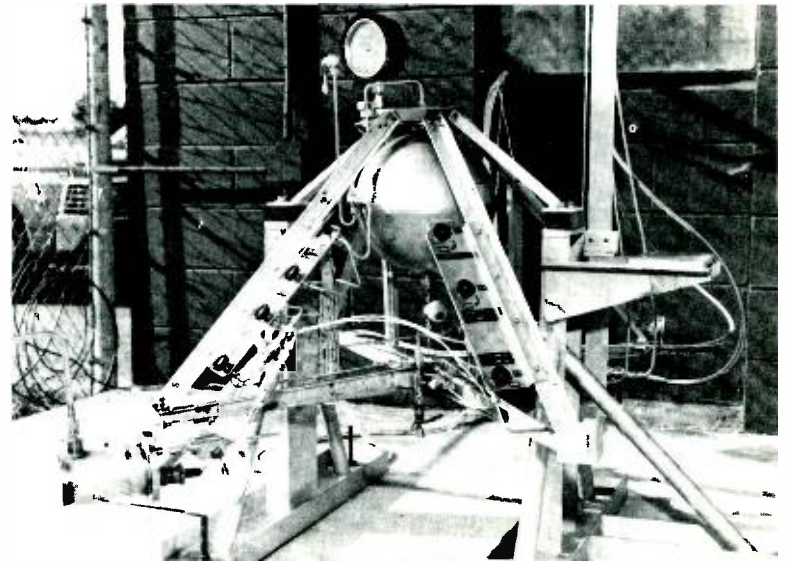
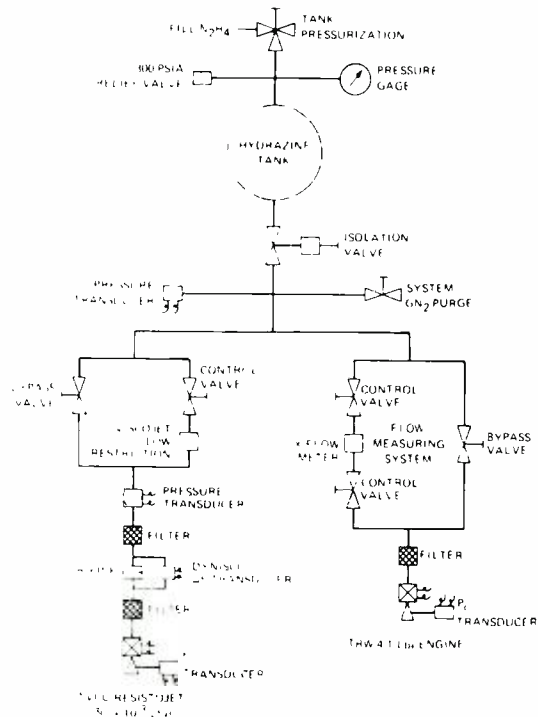


Fig. 6 (left)—Schematic of dual-thrust-level hydrazine propulsion subsystem. Fig. 7 (above)—Flight-type dual-thrust-level hydrazine propulsion system mounted on test stand.

an ion engine at 350 micropounds thrust, which represents the minimum station perturbation, requires a cumulative burn time of approximately 51,000 hours, which is considerably beyond the demonstrated state-of-the-art.

In addition to the reliability inherent in a monopropellant system, the hydrazine/hydrazine resistojet combination provides several unique advantages not available in hydrazine/ion propulsion systems. Any propellant not required in the initial phases of the mission to cancel booster dispersions or acquire station is available to the resistojet to extend orbital lifetime. Should the heaters which provide enhancement of the propulsive performance fail, a portion of the long-term station-keeping function can still be provided by the catalytic or thermal decomposition of hydrazine remaining in the propellant tanks.

The foregoing mission analysis establishes the utility of a dual-thrust-level hydrazine propulsion system. Catalytic hydrazine thrusters to fulfill mission high-impulse bit capability requirements are state-of-the-art and many nominal 5.0-lbf thrusters are operational in space. To satisfy the total mission requirement, then, what is the status of the hydrazine resistojet?

Status of hydrazine resistojet

Avco Corporation and TRW are pres-

ently engaged in research and advanced development of electrothermal hydrazine thrusters in the 5- to 55-millipound thrust range. These engines use thermal rather than catalytic decomposition of hydrazine with less than 5 W of power required to initiate thermal decomposition. For steady-state or duty cycles down to about 10%, the electric power need not be maintained as the engine is capable of self-sustaining operation. Current development emphasis is on improved pulse performance and characteristics for millipound-thrust-level hydrazine attitude control thrusters. The engines do not feature propulsive performance enhancement by supplemental resistojet type heating; however, Avco and TRW have demonstrated that the latter approach is feasible and Isp's above 300 s have been measured to date.

TRW is conducting additional design, development, and testing of a 20-millipound thruster under NASA Goddard Space Flight Center Contract No. NAS5-11477. Additional performance data on the Avco engine may be found in Refs. 7 and 8. An Avco engine was flown on the Navy SOL-RAD spacecraft in July 1971. A flight-type engine similar to that flown by the Navy is used in the model spacecraft propulsion system tests described next.

Model spacecraft propulsion system testing

Current research and advanced

development on electrothermal hydrazine thrusters substantiate the potential of this powerplant. To further characterize the performance of a developed electrothermal hydrazine thruster and experimentally demonstrate the adaptability of the resistojet to standard high thrust catalytic hydrazine systems, a test program on dual-thrust-level systems is in progress at Astro-Electronics Division.

Hardware description—The model spacecraft propulsion system, shown schematically in Fig. 6 and mounted on the test stand in Fig. 7, consists of a propellant feed system manifolded to a nominal 4.1 lbf-thrust-level catalytic hydrazine rocket engine assembly and a 30-millipound electrothermal decomposition hydrazine engine (resistojet).

The 11.5-in diameter, 803-in³ volume tank used to supply hydrazine to the thrusters was manufactured by ARDE, Inc. The tank is 304L stainless which is stretched to its final size at cryogenic temperatures (Ardéform process) to achieve a strength-to-weight ratio similar to that of a titanium vessel. Integral with the tank shell is a lightweight surface tension device, designed by Astro-Electronics Division, which provides propellant management control in a low-g orbital environment and during adverse disturbances from engine firings.

The high-thrust leg of the model system is a nominal 4.1-lbf-thrust catalytic hy-

Table III—Typical engine firing sequences

Test no.	Supply pressure (psia)	Engine	Thrust level (lbf)	Duty cycle on/off
1	300	TRW	2.8	1 min (Steady state)
2	200	TRW	1.8	1 min (Steady state)
3	75	TRW	0.75	30 min (Steady state)
Engines run simultaneously				
4	150	TRW	1.4	5 min (Steady state)
5	150	Avco	29×10^{-3}	0.20 s/0.80 s (Pulse 5 min)
6	100	Avco	21×10^{-3}	8 s/20 s (6 pulses)
7	75	Avco	17×10^{-3}	8 s/20 s (6 pulses)

drazine engine manufactured by TRW Systems Group. Identical engines are in operation on Intelsat III and several classified spacecraft. Nominal fuel flow at the 4.1-lb thrust-level is 0.02 lbf/s at a chamber pressure, P_c , of 250 psia. The thruster is capable of operation over a blowdown ratio of approximately 6:1 with a maximum inlet pressure of 550 psia.

The low-thrust leg of the model system is a nominal 30-millipound thruster manufactured by Avco, Lowell, Massachusetts. The thruster is capable of operation over a supply pressure range of 40 to 175 psia. The engine, pictured in Fig. 8, basically consists of a propellant injection system and thruster support, a heater section, a reaction chamber, and an exit nozzle.

Facilities and test equipment—All hot firings were done at the Sea Level Rocket Test Site which is located at the RCA Space Center, Princeton, New Jersey. Test operation was controlled from the blockhouse and monitored by simultaneous oscillograph display of chamber pressure, valve inlet pressure, fuel flow, and by TV observation of the rocket operations.

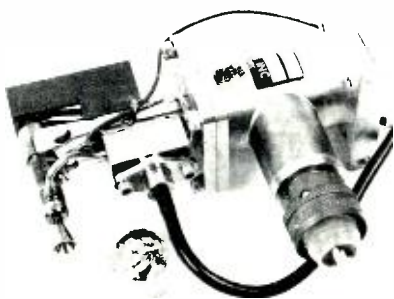


Fig. 8—Avco electrothermal hydrazine thruster.

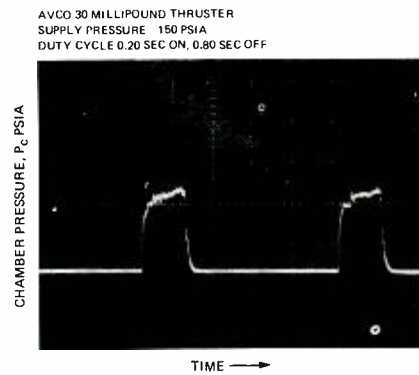


Fig. 9—Typical test trace for Avco electrothermal hydrazine engine.

Performance parameters recorded included propellant tank pressure, TRW and Avco engine valve inlet and chamber pressures, and TRW and Avco engine temperatures and propellant flows.

Test firings—Basepoint system performance was established for each thruster operating steady state and in pulse modes typical of synchronous propulsion system requirements. The thrusters were then fired sequentially and simultaneously to determine their compatibility with a common tankage propellant supply.

Test results—Table III lists the test sequences run. Typical pulse traces for the engines are shown in Figs. 9 and 10. Operation of the system proved stable and reproducible for all tests conducted. Results of firing both engines simultaneously indicated no feed system coupling and no discernable change in performance or pulse shape from the resistojet basepoint data.

Conclusions

The hydrazine/hydrazine resistojet propulsion system offers a relatively high-performance, simplified approach to meeting the propulsion requirements for geostationary missions. For long-life missions, the system weight is competitive with other techniques and has an inherent redundancy capability in its operating mode.

Advanced development electrothermal hydrazine engines indicate that near ideal performance at millipound thrust levels can be achieved without a catalyst and, depending on the duty cycle, without electric power after propellant ignition. Enhancement of propulsive performance of hydrazine by supple-

AVCO ENGINE PULSED AT RATE OF 1 CPS, 0.20 SEC ON, 0.80 SEC OFF DURING STEADY STATE OPERATION OF TRW ENGINE

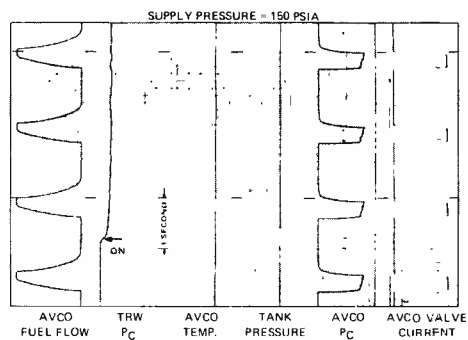


Fig. 10—Typical test traces.

mental resistojet type heating has been demonstrated and operating regimes are currently being defined.

Compatibility of millipound hydrazine thrusters with standard higher thrust catalytic hydrazine systems has been demonstrated. Testing of the model dual-thrust-level spacecraft propulsion system uncovered no significant problems and provides the confidence that such systems are ready for flight application.

Acknowledgments

Messrs. William Farrell, Oscar Gosman, and Richard Hartenbaum of RCA made contributions significant to the success of the test program. The rocket engine assemblies which were configured into the model spacecraft propulsion system were provided by Avco and TRW.

References

1. RCA Astro-Electronics Division. *Flywheel Stabilized Magnetically Torqued Attitude Control System for Meteorological Satellites*. Contract No. NASS-3886. NASA CR-232 (May 1965).
2. RCA Astro-Electronics Division. *Voice Broadcast Mission Study*. Final Report. Contract No. NASW-1476. NASA CR95491 (May 1967).
3. Duck, K. I., Bartlett, R. O., and Sullivan, R. J.. "Evaluation of an Ion Propulsion System for a Synchronous Spacecraft Mission." AIAA Paper No. 67-720. AIAA Electric Propulsion and Plasma-dynamics Conference (Sept. 11-13, 1967).
4. Kerslake, W. R., Byers, D. C., Rawling, V. K., Jones, S. G., and Berkopec, F. D.. "Flight and Ground Performance of the SERT II Thruster." AIAA Paper No. 70-1125. AIAA 8th Electric Propulsion Conference (Aug. 31-Sept. 2, 1970).
5. Molitor, J. H. and Kaplan, M. H.. "Optimization of Ion Engine Control Systems for Synchronous Satellites." *Journal of Spacecraft and Rockets*, Vol. 1, No. 5 (1964) pp. 557-559.
6. Yoshida, R. Y., Halback, C. R., and Hill, C. S.. "Life Test Summary and High Vacuum Test of 10 mlb Resistojets." AIAA Paper No. 70-1136. AIAA Electric Propulsion Conference (Aug. 31-Sept. 2, 1970).
7. Avco Corporation Final Report. *Hybrid Resistojet Development*. Report No. AVSD-0083-71-RR. Contract NAS 5-21080.
8. Pugmire, T. K., O'Connor, T., Shaw, R., and Davis, W.. "Electro-Thermal Hydrazine Engine Performance." AIAA Paper No. 71-760. AIAA/SAE 7th Propulsion Joint Specialists Conference (June 14-18, 1971).

High-performance television receiver experiment

D. H. Pritchard | A. C. Schroeder | W. G. Gibson

Alfred C. Schroeder, Consumer Electronics Research Laboratory, RCA Laboratories, Princeton, N.J., received the BSEE and MSEE from M.I.T. in 1937. In that year, he joined the RCA Victor Company in Camden, New Jersey, as a television research engineer. His research led to the development of the first commercial synchronizing generator for television signals. He was active in research on television cameras, receivers, and terminal equipment for black and white and color television systems. In 1942, he transferred to the RCA Laboratories as a Member of the Technical Staff. Here he has been engaged in the development of the NTSC (present standard) color television system, tricolor television reproducers. He is a Fellow of the IEEE and a member of the A.A.A.S., Sigma Xi, SMPTE, Opt. Soc. of America, Franklin Institute, and the Society for Social Responsibility in Science.

Dalton H. Pritchard, Consumer Electronics Research Laboratory, RCA Laboratories, Princeton, N.J., received the BSEE in 1943 from Mississippi State University. Upon graduation he entered the U.S. Army Signal Corps, receiving specialized radar training at Harvard University and at M.I.T. In 1946, Mr. Pritchard joined RCA Laboratories at Riverhead, N.Y. In 1950, he transferred to the Laboratories at Princeton. For a number of years, he was active in the field of color television. This work included the planning and testing of systems and circuits proposed for adoption by the National Television Systems Committee (NTSC). More recently, Mr. Pritchard, has been engaged in research in the field of information display systems and devices. He is also active in the related fields of vacuum preparation of materials, specialized electron devices, lasers, and the development of electro-optic materials and techniques for purposes of light control and display and color camera special systems development and evaluation. Mr. Pritchard is a Senior Member of the IEEE, SID, Sigma Xi, Tau Beta Pi, and Kappa Mu Epsilon and is listed in *American Men of Science* and *Who's Who in the East*.

Walter G. Gibson, Consumer Electronics Research Laboratory, RCA Laboratories, Princeton, N.J., received the BSEE from the University of California in 1948 and an MSEE from Newark College of Engineering in 1968. From 1946 to 1964 he was with the RCA Laboratories. During that time he was engaged in various phases of the development of color television, including work on color television cameras, vertical aperture equalization, color tape recording, color reproducers, and integrated electronics. From 1964 to 1967 he was at the Astro-Electronics Division where he worked on space sensors and TV scan converters. From 1967 to the present he has been at the Laboratories Division where he has worked on home communications' systems and SelectaVision. Mr. Gibson is a member of the IEEE and Sigma Xi and has published several papers in the television field.

Authors Schroeder, Pritchard and Gibson (left to right).



An experiment performed and demonstrated some years ago indicates the high degree of performance possible with a television receiver for both monochrome and color, while still being compatible with present color transmission methods. The three basic techniques of synchronous detection, sound cancellation, and comb filters were combined in the laboratory setup to obtain the desired performance. It was possible to remove the usual bandwidth restrictions in the receiving decoder and the resulting picture was free of cross-modulation components, free of color signal "dots", maintained full 400-line luminance-channel resolution, and had 2-MHz double-sideband color resolution without quadrature color edge distortion. Direct comparisons were made with the conventional methods as well as with direct simultaneous presentation. The results were such that the encoded, "high performance", pictures were subjectively comparable to those obtained by the direct simultaneous method. The advent of cablecasting has brought about renewed interest in the possibilities for new and improved performance in color TV systems and the techniques described fall into this category.

CABLECASTING has brought about renewed interest in the possibilities for new and improved performance in color television systems. The closed-circuit environment, new technology for wide-bandwidths, new large-area displays, and better signal transmission systems make it desirable to obtain the best possible performance from the NTSC system that is now serving very well for broadcast over-the-air transmissions.

This paper describes an experiment that has been performed indicating an approach to an improved, high performance, color-TV receiver which is completely compatible with broadcast standards. The original work was conducted some years ago and served at that time to prove the validity of the principles involved; however, the cost/performance tradeoffs at this early period discouraged development in the consumer

Reprint RE 18-3-8
Final manuscript received February 10, 1972

TV receiver product environment. The interim developments of integrated circuit technology and the growing availability of lower cost signal processing components may make the development of such a receiver both desirable and practical. This background, coupled with the growing interest in cable TV and high performance color television systems, make a review of the fundamentals worthwhile.

A properly operated color receiver of conventional design provides commercially satisfactory reproduction by excluding some picture detail that would otherwise give rise to undesirable color subcarrier dot patterns. It is possible to make improvements in the overall performance of a complete receiver by using techniques not normally employed in conventional design. The three basic techniques required are synchronous detection, sound cancellation, and comb filters. The results are such that the encoded high-performance pictures are essentially the same quality as those obtained by direct simultaneous viewing. The only bandwidth limitations imposed upon the receiver and decoder is the 6-MHz channel-spacing standards. The resulting picture is free of sound-versus-video and sound-versus-color cross-modulation components, free of color signal "dots", maintains full 400-line luminance-channel resolution, and allows the possibility of full-2 MHz double-sideband color-channel resolution without quadrature color-edge distortion. At the same time, such a system is somewhat susceptible to the effects of incidental phase modulation in the transmitted signal. The performance of the synchronizing functions is improved in the presence of impulse noise, although the visibility of white specks appearing in the picture may require special handling.

Conventional receiver limitations

In conventional television receiver design, there are several limitations on the quality of the reproduced image:

Composite video bandwidth is limited to approximately 4 MHz due to the presence of the sound carrier at 4.5 MHz. The removal of the sound carrier by means of rejection traps may introduce additional high frequency transients; this limits the double-sideband color-channel response to about 500 or 600 kHz. The necessity for operating the color channel as vestigial sideband above 600 kHz introduces

quadrature color distortion on edges that I-Q operation is intended to minimize; this limits the color resolution to 1.5 MHz in one channel and 600 kHz in the other channel.

Cross-modulation products between sound, video and color signal components become a problem, when a conventional envelope detector is used in a receiver. The sound-vs-color channel beats (920 kHz) are removed only by adequate rejection of the sound carrier by traps or by loss of high-frequency channel bandwidth.

Luminance channel bandwidth in a color receiver must be limited to 3.58 MHz or less to remove the color signal components to prevent rectification in the kinescope and the resulting luminance signal component errors.

Color signal sideband components still remain in the luminance signal and appear as "dot crawl" on edges. If the luminance signal response is not sufficiently reduced at 3.58 MHz the "dot" pattern exists in large color areas as well as on edges of colored objects.

High frequency luminance signal components, as well as *high frequency noise* in the region around 3.58 MHz, are fed to the color demodulators and are "beat down" to low frequency random color noise and edge beats which are added back to the composite color signal along with the desired color components.

In spite of the above limitations, a properly designed color receiver will provide commercially satisfactory picture reproduction.

High performance experiment

A composite color signal was supplied from a transmit encoder operating in accordance with broadcast standards except that the "I" and "Q" color bandwidth restrictions had been removed. The receiver is compatible with standard broadcast signals; but in the cable-cast type of closed circuit situation, the

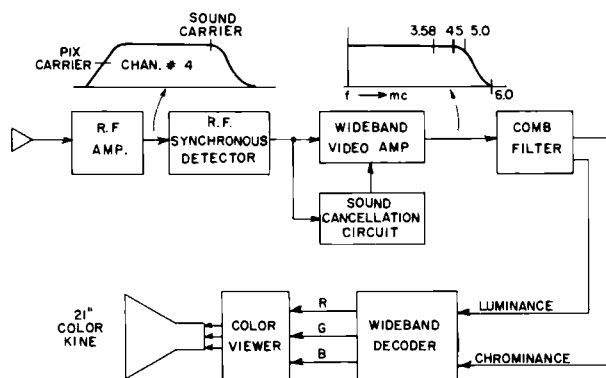


Fig. 1—Experimental receiver block diagram.

color bandwidth limitations were removed to demonstrate the maximum performance capability of the system.

The composite color signal was fed to an RF modulator, such as a Megapix, and then at RF level (channel 4), was fed to the antenna input of the experimental receiver. The RF portion of the receiver consists of a wideband amplifier containing the vestigial slope characteristic around the picture carrier and a synchronous detector operating at the RF level. The wideband (6 MHz) video output from the detector was fed to a sound cancellation circuit. This circuit selects the 4.5-MHz sound signals, passes it first through a limiter, then a circuit with the proper envelope delay characteristic over the FM deviation frequency range, and then adds the signal back to the composite video channel 180° out of phase and at the proper amplitude to provide cancellation of the sound signal in the video signal. The resulting video output signal is flat to 5 or 6 MHz with no "trap" at the sound frequency and is free of 4.5-MHz sound as well as the cross-modulation products between sound, video, and the color subcarrier. The synchronous detection process provides the freedom from intermodulation products, and the cancellation circuit removes the 4.5-MHz sound signal.

The resulting composite, wideband, video signal was fed to the input of a "comb" filter made possible by the use of a 1-H (one horizontal scanning line) delay line. One of the two outputs from the comb filter consists of the wideband (5 to 6 MHz) luminance signal from which the chrominance signal has been removed. No bandwidth limitations are imposed in the horizontal direction since the comb filter removes the color

signal "dots" by virtue of the frequency interleaving of the chrominance signal with the luminance signal. In the standard color signal this interlace condition is obtained by causing the color subcarrier frequency to be an odd multiple of one-half line frequency. This luminance signal was then fed to the luminance channel of a color decoder from which all passband restrictions had been removed (flat to at least 5 to 6 MHz).

The second output from the comb filter consists of a wideband chrominance signal from which the high frequency luminance components have been removed. Under these conditions the chrominance signal may be wideband, and double sideband, because the composite signal bandwidth was not restricted to frequencies below the sound carrier (4.5 MHz) by virtue of the synchronous detector and sound-cancellation process. This wideband chrominance signal was fed to the chrominance input of the color decoder from which all color bandpass limitations had been removed. The resulting red, green, and blue output signals from the wideband decoder were fed to a 21-inch color viewer and the results observed and compared with direct simultaneous signals as well as signals

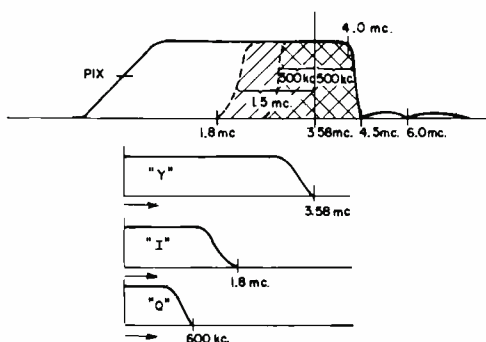


Fig. 2a—Conventional receiver passbands.

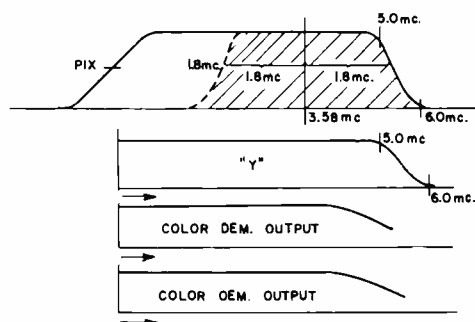


Fig. 2b—Experimental receiver passbands.

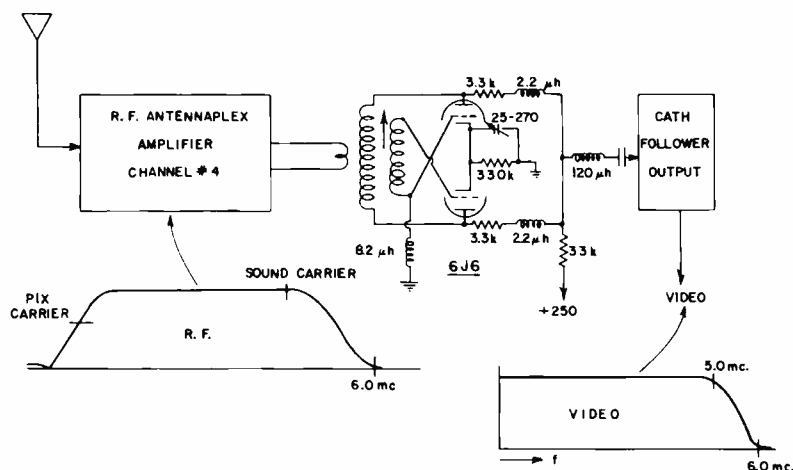


Fig. 3—RF and synchronous detector circuit.

passing through a conventional receiver and decoder. The results indicated that the "high performance" method provides color picture reproductions that are essentially the same as the simultaneous presentation even though the signal had passed through the encoding, RF transmission, and decoding processes.

Fig. 1 is a block diagram of the experimental receiver setup. Fig. 2 indicates the RF, IF, and color passbands in a conventional color receiver using I, Q color demodulation. Fig. 2 indicates the wideband characteristics of the experimental high-performance receiver.

Details of experimental apparatus

Since the primary purpose of the experiment was to investigate and observe the degree of improvement in performance possible with the techniques described, a semi-detailed description of the particular apparatus involved is included as an example rather than an indication of possible practical circuitry.

Synchronous detector

Any properly operating synchronous detector, such as the integrated circuit units including bridge-circuit balanced diodes with an associated AFC loop, will meet the requirements.¹ However, the particular unit available for test consisted of 6J6, injection locked, product detector operating at the RF level on Channel 4 frequency. Fig. 3 is a diagram of the RF and detector portion of the complete receiver.

The passband characteristic of the RF amplifier was adjusted to provide the

desired vestigial slope at the picture carrier frequency. The video output was adjusted to maintain flat response to at least 5 MHz.

The basic properties of synchronous detection are such that no cross-modulation products are contained in the video output. The sound carrier exists as a 4.5-MHz signal without the usual "herringbone" beats between sound and picture, and without the 920-kHz beat between sound and the chrominance signal. It is therefore not necessary to provide rejection at the sound frequency, and the overall passband is limited only by the adjacent picture signal (6 MHz) spacing in the standard broadcast situation. Also, the chrominance signal passband is not limited to 600 kHz, but may retain the double sideband characteristic to at least 1.8 MHz on either side of the 3.58-MHz subcarrier. If the sound signal is then removed by cancellation rather than by rejection traps, the conventional I and Q color bandwidth restrictions may be removed and color signals maintain at least 1.8-MHz bandwidth with no quadrature color-edge distortions.

Sound cancellation

Fig. 4 is a diagram of the sound-cancellation circuit available for the test. Since no cross modulation products exist in the synchronous-detector video output, it is possible to cancel the 4.5-MHz sound signal to a satisfactory degree without introducing bandwidth restrictions in the composite video channel. The sound signal is first amplified and then fed to a limiter which

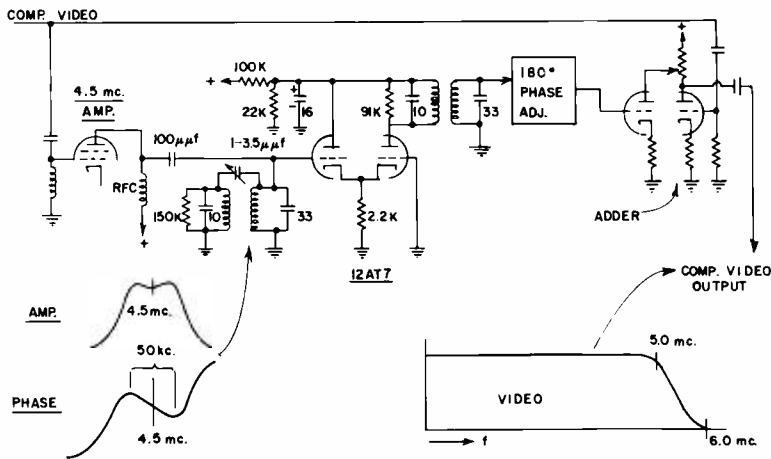


Fig. 4—Sound cancellation circuit.

removes the amplitude-modulated video components. Since the sound channel suffers time delay, an appropriate amount of delay must be introduced in the composite signal channel, prior to cancellation, so that the envelope delay characteristics match at 4.5-MHz over a bandwidth at least equivalent to that of the sound frequency deviation range. A simple method for obtaining this envelope delay match is to introduce a network in the sound channel that has a sufficiently "negative slope" characteristic. This may be accomplished, as in Fig. 4, by means of a two terminal, over-coupled, transformer adjusted to have a negative slope phase characteristic over the deviation frequency range. The sound signal is then added to the composite signal in the proper phase relationship (180°) and amplitude to obtain cancellation. In the test setup, a variable delay line was used to adjust the

180° relationship. Thus, the output from the linear adder consists of a wideband video signal from which the sound has been removed without introducing bandwidth restrictions. The 4.5-MHz signal from the limiter was also fed to a conventional ratio detector and audio-output circuit.

Comb filter

Comb filter techniques using 1-H delay lines for separation of interleaved signal components are well-known in the art and are being employed in practical circuitry, for example, color-TV receivers in Europe operating in accordance with PAL standards, vertical aperture corrector circuits in color cameras, etc.^{2,3} The comb filter used for the tests is made in two parts (see Fig. 5). These two delay units supply three signals differing in time delay by 1H (one horizontal scanning line). The matrix circuit manipulates these three signals so as

to produce the frequency responses as shown in Fig. 6. Comb filters may be and have been constructed employing only one 1-H delay line that operate satisfactorily.

The formation of the comb filter characteristic can be explained briefly as follows: non-interlaced frequencies are those that have the same phase on succeeding lines and interlaced frequencies are those that are exactly 180° out of phase on succeeding lines. Non-interlaced frequencies are integral multiples of line frequency, and interlaced frequencies are integral plus 1/2 multiples of line frequency and, in the standard color system, are those frequencies that contain the color subcarrier and its sidebands (odd multiple of 1/2 line frequency). In a comb-filter circuit employing 1-H delay elements to compare one line with the adjacent lines, the addition of the signals from one line to the signals from the two adjacent lines results in the cancellation of the interlaced frequencies while the non-interlaced frequencies reinforce each other. Subtracting the signals from the two adjacent lines, the non-interlaced frequencies cancel and the interlaced frequencies remain. This is the basic function of the matrix in Fig. 5. The interlaced frequencies from the matrix are split into two paths by conventional filters since the "comb" effect is desired only in the upper half of the frequency band (the color components do not extend appreciably into the lower half of the frequency band and these lower frequencies are necessary for vertical detail). Thus, one output contains the luminance signal information free of interference (dots) from the

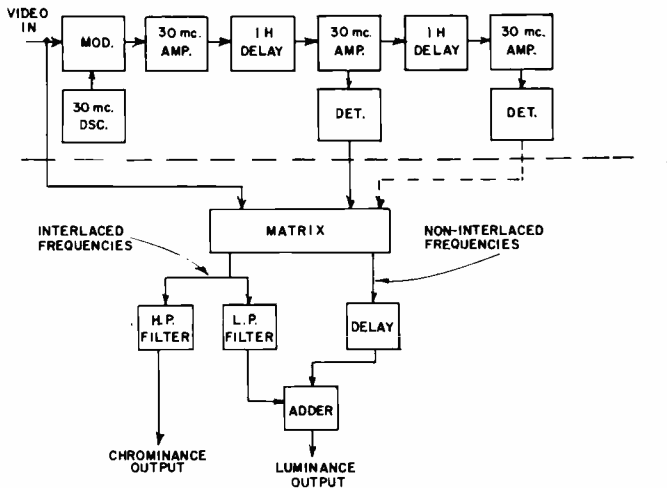


Fig. 5—Comb filter block diagram.

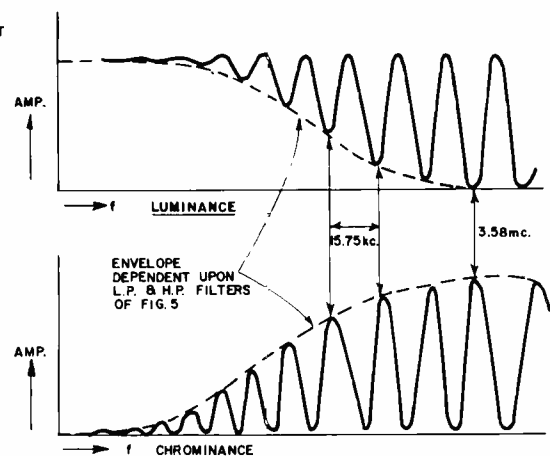


Fig. 6—Comb filter frequency characteristics.

color signals, and the other output consists of the wideband chrominance signal free of cross-modulation from high frequency luminance detail.

This discussion of comb filters has ignored the use of field-delay lines, effects of motion, resolution effects of 45°, etc., since a complete review of comb filter techniques is not the intention of this paper.

Decoder and viewing unit

The two outputs from the comb filter unit (luminance signal and chrominance signal) are fed to the appropriate inputs of a color decoder. The decoder is a laboratory unit in which it is possible to remove all passband filter limitations from both the luminance and chrominance channels. The overall bandwidth of the system is flat to at least 5 MHz. The red, green, and blue output signals are fed to a three-channel simultaneous color viewer employing a 21-inch shadow-mask color kinescope. Provisions were made for switching the viewing unit from direct simultaneous signals, to signals from a standard I, Q decoder and receiver, and to signals from the high-performance receiver and decoder.

Conclusions

The results possible are illustrated in Figs. 7 through 12. The experiment indicates the improvements possible in the performance of a color-TV receiver that makes use of synchronous detection, sound cancellation, and comb filters. The overall results, after encoding, RF transmission, and decoding provides picture reproductions that are subjectively the same as those obtained by a direct simultaneous method. Therefore, a high performance receiver could be developed which would make optimum use of the present method of color-TV transmission while still being compatible with it, or be extended into even higher performance levels in cablecasting or special closed-circuit environments.

References

1. Iunn, Gerald. "A Monolithic Wideband Synchronous Video Detector for Color TV". *IEEE Transactions on Broadcast and TV Receivers*, Volume BTR-15, No. 2 (July, 1969).
2. Gibson, W. G. and Schroeder, A. C., "A Vertical Aperture Equalizer for Television". *Journal of the Society of Motion Picture and TV Engineers*, Volume 69, No. 6 (June, 1960).
3. Parker, N., "The Cost of Using PAL or SECAM and Possible Improvements in NTSC Receivers". *IEEE Transactions on Broadcast and TV Receivers*, Volume BTR-12, No. 3 (July, 1966).

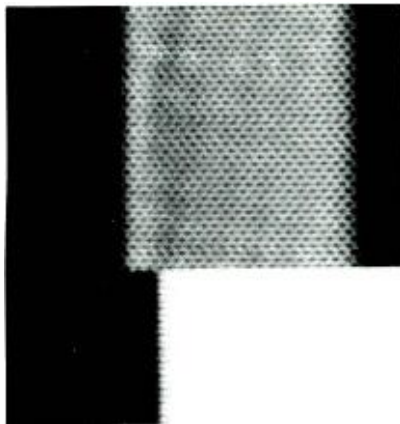


Fig. 7—Close-up portion of the color-bar signal after passing through the conventional system indicating the visible 3.58-MHz dot pattern.

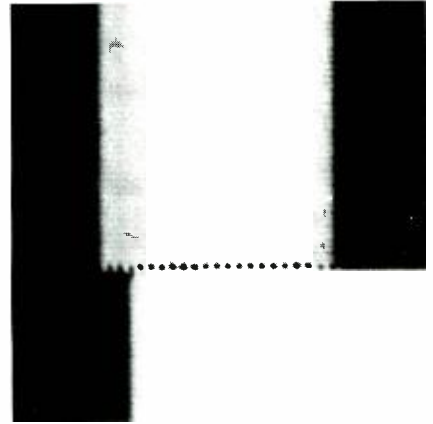


Fig. 8—Same portion of the color bar signal as in Fig. 7 after passing through the experimental receiver. Note the removal of the dot pattern from the luminance channel.

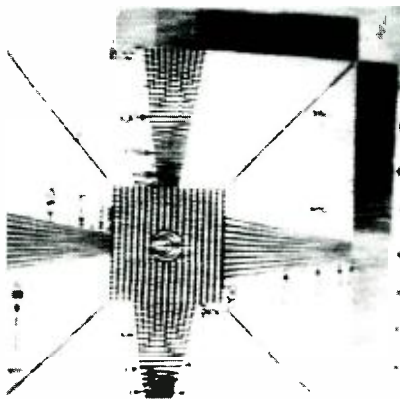


Fig. 9—Critical portion of the RMA test pattern after passing through the conventional system. The beats, cross-modulation products, moiré pattern, and limited resolution of the luminance channel are shown.

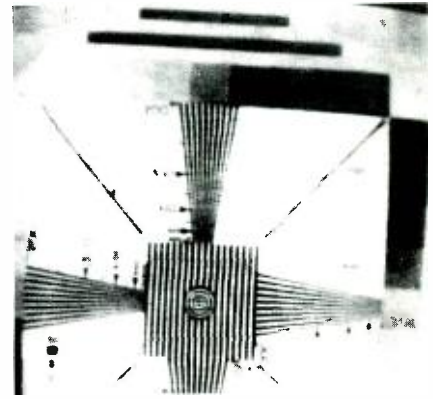


Fig. 10—Same test pattern as in Fig. 9 after being passed through the experimental system. The reduction of edge beats, moiré effects, noise, and increase in luminance channel resolution are evident.

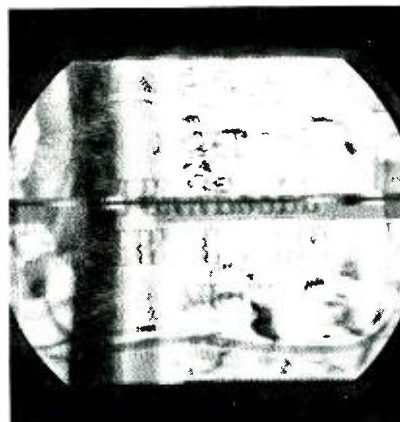
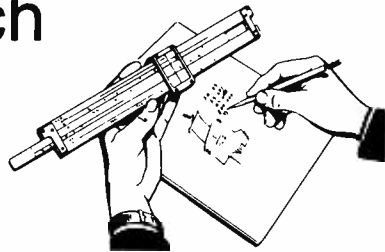


Fig. 11—A conventional receiver off-the-air signal using an envelope detector with severe adjacent-channel TV interference.



Fig. 12—Same receiver under the same conditions of excessive adjacent-channel signal as in Fig. 11, but using a synchronous detector indicating the excellent rejection of cross-modulation effects afforded by a synchronous detector.

Engineering and Research Notes



Brief Technical Papers
of Current Interest

Scrubbing and dicing of processed silicon-on-sapphire wafers

R. L. Loper
Advanced Technology Laboratories—West
Van Nuys, California



Difficulties encountered in successfully scribing and dicing processed silicon-on-sapphire wafers have led to the consideration of sophisticated laser-scribing techniques. For nonproduction applications, this level of sophistication is unnecessary. Although crystalline in nature, sapphire behaves as a glass during scribing. Experiments at Advanced Technology Laboratories-West have demonstrated that careful glass-cutting techniques applied to the scribing and dicing of silicon-on-sapphire wafers produce an acceptably high yield of cleanly diced chips.

First, and most obviously, the scribe must be harder than the material to be scribed. A number of materials are available; however, the experiments performed at ATL-W were accomplished using a diamond scribe.

The angle between the scribe and the work surface should be approximately 10 to 15° as shown in Fig. 1. The pressure applied to the scribe is most important and difficult to describe quantitatively. The most convenient method for determining the correct pressure is to observe the amount of residue produced by the scribing process. A binocular Bausch and Lomb microscope, with a half-power lens added to the bottom, is useful for viewing this. The microscope should be mounted at an angle of about 20° to the plane of the wafer at any convenient position around it, as shown in Fig. 2.

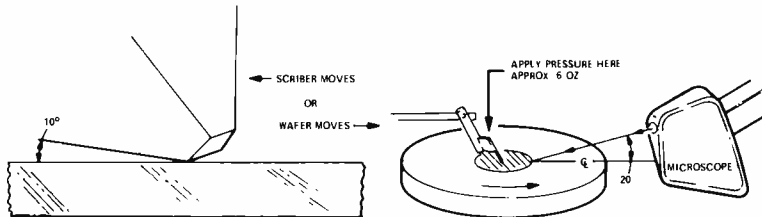


Fig. 1—Angle between scribe and work surface must be 10 to 15°.

Fig. 2—Microscope arrangement for observing the scribing process.

Unfortunately, the pressure required (6 to 8 oz.) is beyond the capabilities of many of the automated scribing machines, which also advance the scribe too quickly across the wafer. One quarter inch per second is approximately the correct speed. With pressure applied manually to the scribe, start to scribe in the direction of the 10° angle. If there is no crystalline residue in, or adjacent to, the cut, increase the pressure slightly. The proper pressure will scribe a line which is barely visible, with small amounts of residue. A line

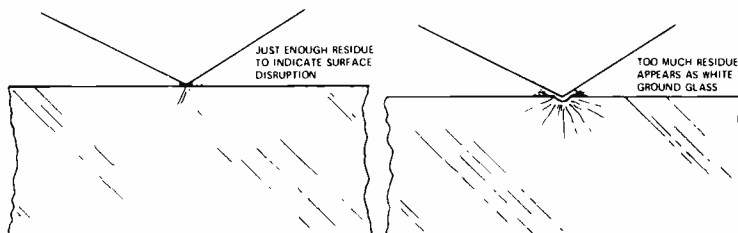


Fig. 3—Proper amount of pressure is critical in the scribing process.

which is white and clearly visible indicates too much pressure (see Figure 3). Start and finish the scribe as close to the edges as possible without running over the edge. The line should be scribed in one stroke on only one side of the wafer.

If the lines are properly scribed, nearly any dicing technique will work. Placing scribed-side down between two pieces of thick felt and rolling back and forth and from side to side with a 1-inch-diameter roller works well. In fact, it is not uncommon for the wafer to start falling apart before the scribing is completed.

Reprint RE-18-3-21 | Final manuscript received July 5, 1972.

Magnetic tweezers

Warren A. Mulle
Missile and Surface Radar Division
Moorestown, New Jersey



Ordinary tweezers or long-nose pliers are often used to position or insert small parts in optical, electrical, or mechanical assemblies having restricted openings. A high degree of manual dexterity is required and, in the case of small flat washers and round-head screws, it is often almost impossible to pick the part up from a flat surface with the proper orientation for the next operation. Magnetic tweezers provide a convenient means for controlling a magnetic field with one finger while using the force of the field to hold small magnetic parts during transfer and positioning operations.

A magnetic field is established with a slight finger motion and holds the part in position against the tool until the magnetic field is disabled. Slight finger pressure will open the magnetic field produced by the tweezers releasing the part, thus providing minimum fatigue in repetitive operations. In these tweezers there are no power supplies, wires, or switches.



Fig. 1—Tweezer construction.

Tweezer construction

Fig. 1 shows that the magnetic tweezers consist of rigidly mounted elongated finger-like magnetic member (10) and a pivotally mounted finger-like magnetic member (12) which are press-fitted in a corresponding recess (14) of a plastic handle or other holding device (16). The finger (12) is pivotally mounted to finger (10) by way of pivot pin (18). The ends (20) and (20') are suitably shaped as in conventional tweezers. Preferably, the end of finger (20) may be bent as shown to provide a positive electrical connection with end (20') as will be described. Spring (22) biases fingers (12) and (10) away from one another maintaining a gap between ends (20) and (20'). Handle (16) serves as a stop against which spring (22) biases fingers (10) and (12). Fingers (10) and (12) are preferably made of an iron alloy that readily is permanently magnetized with a relatively weak field. Adjacent to finger (12) is a resiliently mounted button (24) which, when forced against finger (12), closes the fingers. Button (24) may be conveniently formed from and be part of handle 16 by slotting the handle 16 at areas 26 as shown in Fig. 2.]

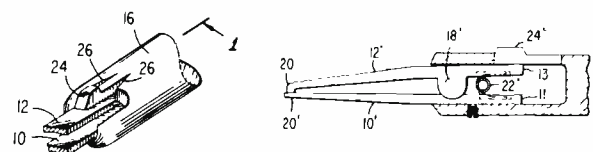


Fig. 2—(left) Integral control button and handle. Fig. 3—(right) Alternative construction.

Suitable fastening means, such as screw (32), may be provided to positively lock the assembled fingers (10) and (12) in recess (14).

When ends (20) and (20') are separated, a magnetic field (28) is present between and around the ends of fingers 12 and 10. When button 24 is depressed, the magnetic field is offered a low reluctance path through the electrically contacting fingers and the field in the

space around the fingers is effectively reduced to a very low value. Thus a steel part, such as a screw (30), will be readily picked up and held to the tweezers, the operator holding the tweezers in one hand. For the operator to release the part, button (24) is merely depressed so that the ends are connected. At this time, the magnetic field is reduced and the part is released.

An alternative construction is shown in Fig. 3. Spring (22) may be provided so as to resiliently bias fingers (10) and (12) against each other so that ends (20) and (20') are always in contact with each other.

In Fig. 3, fingers (12') and (10') each have an overhanging extending rear portion (13) and (11), respectively. In this case, spring (22') biases end portions (11) and (13) away from each other and end portions (20) and (20') against each other. Resiliently mounted button (24') when depressed against portion 13 opens up ends 20 and 20' providing a gap therebetween and producing a magnetic field. In this case, there is no gap between ends (20) and (20') and thus no effective magnetic field except when button (24') is depressed and thus momentary grasping action for the part is provided by the tweezers of Fig. 3. By contrast, the tweezers of Fig. 1 provide momentary release of the part.

Reprint RE-18-3-21 Final manuscript received June 21 9172

The meaning of crosscorrelation functions

Murlan S. Corrington
Computer Applications
Applied Computer Systems
Advanced Technology Laboratories
Camden, N.J.



Suppose two single-valued functions $f(x)$ and $g(x)$ are given, as shown by Fig. 1, and one wants to find out how much of the waveform $g(x)$ is contained in $f(x)$, over the range $0 \leq x \leq T$. To answer this question it is necessary to find a "best fit" of $g(x)$ to $f(x)$.

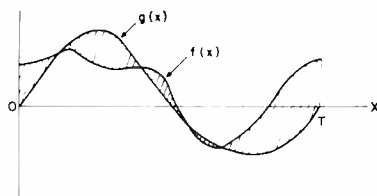


Fig. 1—Difference between two functions.

Best-fit criterion

There are many ways to define best fit, but a common way is to minimize the integral of the square of the difference of the two functions. The shaded area of Fig. 1 is the difference, and the best fit is obtained for that value of a which gives the minimum value for

$$\begin{aligned} I(a) &= \int_0^T [f(x) - ag(x)]^2 dx \\ &= \int_0^T [f(x)]^2 dx - 2a \int_0^T f(x) g(x) dx \\ &\quad + a^2 \int_0^T [g(x)]^2 dx. \end{aligned} \quad (1)$$

To find the best value for a , differentiate the integral for $I(a)$ with respect to a , and set the derivative equal to zero. This gives

$$\frac{dI}{da} = -2 \int_0^T f(x) g(x) dx + 2a \int_0^T [g(x)]^2 dx = 0 \quad (2)$$

so

$$a = \frac{\left[\int_0^T f(x) g(x) dx \right]}{\left[\int_0^T [g(x)]^2 dx \right]} \quad (3)$$

Meaning of crosscorrelation

The integral in the numerator of Eq. 3 is the crosscorrelation function of $f(x)$ and $g(x)$ over the range 0 to T . The integral in the denominator is a normalizing factor that makes $a=1$, if $f(x)=g(x)$. The crosscorrelation of $f(x)$ and $g(x)$ determines how much of the waveform $g(x)$ is in $f(x)$, using the integral-square-error criterion for best fit.

Fourier series

Example: The function $f(x)$ of Fig. 2 is periodic with period $T=2\pi$. Find how much of the sinewave, $\sin(nx)$, is contained in $f(x)$, using the integral-square-error criterion.

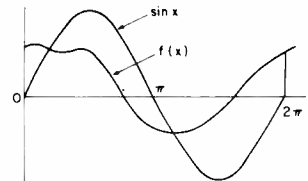


Fig. 2—Finding best fit of two waveforms by crosscorrelation

Solution: Let the amplitude of $g(x)=\sin(nx)$ in $f(x)$ be a_n . Then by Eq. 3:

$$a_n = \frac{\int_0^{2\pi} f(x) \sin(nx) dx}{\int_0^{2\pi} \sin^2(nx) dx} = \frac{1}{\pi} \int_0^{2\pi} f(x) \sin(nx) dx \quad (4)$$

since

$$\begin{aligned} \int_0^{2\pi} \sin^2(nx) dx &= \left[\frac{1}{2}x - \frac{1}{4n} \sin(2nx) \right]_0^{2\pi} \\ &= \pi \quad (n=1, 2, 3, \dots) \end{aligned} \quad (5)$$

This is the usual integral for the Fourier coefficient of the n th harmonic sine component of $f(x)$. A similar result is obtained if $g(x)=\cos(nx)$.

This shows that when one expands a function in a Fourier series, using the integrals for the Fourier coefficients, it is really a crosscorrelation operation using the least-square-error criterion to find the best fit.

Any frequency can be found

The solution (Eq. 3) is a general one and can be used to determine the amplitude of any desired frequency in $f(x)$. It is not necessary that the frequencies be harmonically related, as in a Fourier series, if the range of integration covers the entire period of the waveform. The range of integration may be infinite, as in a Fourier integral, if the integrals exist.

Time shift in correlator

It may be that one is not sure about the relative time delay between $f(x)$ and $g(x)$ that gives the best match. In this case, it is often useful to try different relative delays. The normalized crosscorrelation function is then defined as

$$\phi(\tau) = \frac{\left[\int_0^T f(x+\tau) g(x) dx \right]}{\left[\int_0^T [g(x)]^2 dx \right]} \quad (6)$$

where τ is the amount $f(x)$ is shifted with respect to $g(x)$. Often a specific value of τ will give the largest value of the crosscorrelation function, $\phi(\tau)$. This value of τ tells how much lead or lag has occurred in $f(x)$ with respect to $g(x)$, and is useful in determining arrival times of incoming waveforms.

Conclusions

The crosscorrelation function of two waveforms is a measure of how much of one waveform is contained in the other, using a least-square-error criterion for the best fit. Any two waveforms may be compared, so long as the functions are single valued and the integrals exist.

Reprint RE-18-3-21 | Final manuscript received July 20, 1972.



Pen and Podium

Recent
RCA
technical papers
and presentations

Both published papers and verbal presentations are indexed. To obtain a published paper, borrow the journal in which it appears from your library, or write or call the author for a reprint. For information on unpublished verbal presentations, write or call the author. (The author's RCA Division appears parenthetically after his name in the subject-index entry.) For additional assistance in locating RCA technical literature, contact: **RCA Staff Technical Publications, Bldg. 2-8, RCA, Camden, N.J. (Ext. PC-4018).**

This index is prepared from listings provided bimonthly by RCA Division Technical Publications Administrators and Editorial Representatives—who should be contacted concerning errors or omissions (see inside back cover).

Subject index categories are based upon standard announcement categories used by Technical Information Systems, Corporate Engineering Services, Bldg. 2-8, Camden, N.J.

Subject Index

Titles of papers are permuted where necessary to bring significant keyword(s) to the left for easier scanning. Authors' division appears parenthetically after his name.

SERIES 100 BASIC THEORY & METHODOLOGY

105 Chemistry

... organic, inorganic, & physical.

ELECTROCHEMILUMINESCENT PROCESS, Efficiency of the—P. M. Schwartz, R. A. Blakeley, B. B. Robinson (Labs, Pr) *J. of Physical Chemistry*, Vol. 76, No. 13, pp. 1868-1871; 6/22/72

VAPOR PHASE EPITAXY by Reactions Involving Organometallics—C. C. Wang (Labs, Pr) Second National Conf. on Crystal Growth, Princeton, N.J.; 7/30-8/5/72

125 Physics

... electromagnetic field theory, quantum mechanics, basic particles, plasmas, solid state, optics, thermodynamics, solid mechanics, fluid mechanics, acoustics.

POLING-DEPENDENCE of the Surface Wave Frequency Generated on PZT—K. Suzuki, K. Yoshikawa (Labs, Pr) Joint Mtg. of Electrical Institutes, Tohoku Univ., Japan; 8/31-9/2/72

ULTRASONIC ATTENUATION in Dielectric Materials on Structural Parameters, Dependence of the—W. Rehwald (Labs, Pr) Int'l Conf. on Phonon Scattering in Solids, Paris, France; 7/3-6/72

130 Mathematics

... basic & applied mathematical methods.

NUMERICAL DIFFERENTIATION (N.D.) Formulas, Minimal Error Constant—A. Pelios, R. W. Klopfenstein (Labs, Pr) *Mathematics of Computation*, Vol. 26, No. 118, pp. 467-475; 4/72

160 Laboratory Techniques & Equipment

... experimental methods & equipment, lab facilities, testing, data measurement, spectroscopy, electron microscopy, dosimeters.

RAMAN SCATTERING, Investigation of Nematic Ordering Using—E. Priestley (Labs, Pr) Fourth Int'l Liquid Crystal Conf., Kent State Univ., Kent, Ohio; 8/21-25/72

SCANNING ELECTRON MICROSCOPY IMAGES, Analysis of Contrast Reversal in—M. D. Coutts (Labs, Pr) Electron Microscopy Soc. of America, Los Angeles, Calif.; 8/14/72

SPECTROSCOPIC ANALYSIS of Trace Rare Earths, Cathode-Ray-Excited Emission (CREE)—S. Larach (Labs, Pr) NATO Advanced Study Institute, OSLO, Norway; 8/23-29/72

170 Manufacturing & Fabrication

... production techniques for materials, devices & equipment.

DATA COLLECTION SYSTEM for Control and Definition of Integrated Circuit Processes, with Application to Silicon on Sapphire, An Automatic—W. E. Ham, P. A. Corssley (Labs, Pr) Metallurgical Soc. of AIME, Boston, MA; 8/28-30/72

ELECTROLESS NICKEL PLATING, Recent Advances in the Elucidation of the Mechanism of—N. Feldstein (Labs, Pr) Frankford Arsenal, Philadelphia, PA; 7/14/72

EPITAXIAL GROWTH of Silicon Using Dichlorosilane Part I—Growth on Single Crystal Hemispheres—N. Goldsmith, P. H. Robinson (Labs, Pr) Second Nat'l Conf. on Crystal Growth, Princeton, N.J.; 7/30-8/4/72

EXPITAXIAL GROWTH, "Small" Misfit and "Large" Strain in—J. Blanc (Labs, Pr) Second Nat'l Conf. on Crystal Growth, Princeton, N.J.; 7/30-8/4/72

EVAPORATION AND SPUTTERING PROCESSES, Survey of the State of the Art of—J. L. Vossen (Labs, Pr) Symp. on Optical Thin Films for Laser Applications, Centerville, MA; 7/5-7/72

MULTIPLE LAYER EPITAXY, Thin Solution—H. F. Lockwood, M. Ettenberg (Labs, Pr) *J. of Crystal Growth*, Vol. 15, pp. 81-83; 1972

175 Reliability, Quality Control & Standardization

... value analysis, reliability analysis, standards for design & production.

INTEGRATED CIRCUIT Reliability—G. L. Schnable (Labs, Pr) Solid State Device Reliability Workshop, Warrenton, VA.; 7/27/72

MNOS MEMORY TRANSISTOR Characteristics and Failure Mechanism Model—J. W. Tuska, M. H. Woods (Labs, Pr) Gordon Research Conf., Tilton, N.H.; 8/28-9/1/72

SILICON, The Quality of Starting—A. Mayer (Labs, Pr) Solid State Device Reliability Workshop, Warrenton, VA.; 7/27/72

180 Management & Business Operations

... organization, scheduling, marketing, personnel.

M&SR TODAY—D. M. Cottler (M&SR, Mrstn) RCA, Camden; 4/11/72; RCA, Moorestown; 4/72; ASD, Burlington; 6/22/72

SERIES 200 MATERIALS, DEVICES, & COMPONENTS

205 Materials (Electronic)

... preparation & properties of conductors, semiconductors, dielectrics, magnetic, electro-optical, recording, & electromagnetic materials.

ALLOY SINGLE CRYSTALS, Melt Growth of—J. P. Dismukes, W. M. Yim (Labs, Pr) Second Nat'l Conf. on Crystal Growth, Princeton, N.J.; 7/30-8/4/72

ALUMINUMARSENIDE, Properties of Vapor-Deposited—A. G. Sigai, M. S. Abrahams, J. Blanc (Labs, Pr) *J. of Electrochemical Soc.*, Vol. 119, No. 7, pp. 952-956; 7/72

BENZENE DERIVATIVES, Second-Harmonic Generation and Miller's Delta Parameter in a Series of—P. D. Southgate, D. S. Hall (Labs, Pr) *J. of Applied Physics*, Vol. 43, No. 6, p. 2765; 6/72

CADMIUM SELENIDE POWDER—Comparison of Experiment and Theory, Negative Resistance in—L. J. Nicastro (ATL, Cam) *RCA Review*, Vol. 33, No. 2 pp. 357-576; 6/72

CdCr₂Se₄ and CdCr₂S₄, Optical Properties of Impurity Levels in—K. Miyatani, F. Okamoto, P. K. Baltzer, S. Osaka, T. Oka (Labs, Pr) *Proc. of the Conf. on Magnetism and Magnetic Materials* (Chicago, Illinois, Nov. 1971) pp. 285-289; 1972

DIELECTRIC CRYSTALS, Phonon-Phonon Collisions and Entropy Fluctuations in—R. Klein, R. K. Wehner (Labs, Pr) Int'l Conf. on Phonon Scattering in Solids, Paris, France; 7/3-6/72

EPITAXIALLY GROWN ALN and its Optical Bandgaps—W. M. Yim, E. J. Stofko, P. J. Zanuzchii, J. I. Pankove, M. Ettenberg, S. L. Gilbert (Labs, Pr) Second Nat'l Conf. on Crystal Growth, Princeton, N.J.; 7/30/72-8/4/72

GaAs_xP_{1-x} LAYERS, Influence of Deposition Temperature on Composition and Growth Rate of—V. S. Ban, H. F. Gossenberger, J. J. Tietjen (Labs, Pr) *J. of Applied Physics*, Vol. 43, No. 5, pp. 2471-2472; 5/72

GaN, Electrolytic Etching of—J. I. Pankove (Labs, Pr) *J. of the Electrochemical Soc.*, Vol. 119, No. 8, pp. 1118-1119; 8/72

GaN, Luminescence in—J. I. Pankove (Labs, Pr) Int'l Conf. on Luminescence, Leningrad, USSR, 8/17-22/72

GaN, Luminescence in—J. I. Pankove (Labs, Pr) 11th Int'l Conf. on the Physics of Semiconductors, Warsaw, Poland; 7/25-29/72

GARNET FILMS, Control of Product Phases in the Chemical Vapor Deposition of—S. T. Opreko, Jr. H. L. Pinch (Labs, Pr) *Materials Research Bulletin*, Vol. 7, No. 7, pp. 685-690; 1972

GARNET FILMS, Control of Product Phases in the Chemical Vapor Deposition of—S. T. Opreko, H. Pinch (Labs, Pr) Second National Conf. on Crystal Growth, Princeton, N.J.; 7/30/72-8/4/72

GRANULAR METALS, Electron Localization In—B. Abeles, P. Sheng (Labs, Pr) Low Temperature Conf., Boulder, CO.; 8/21/72

GRANULAR NICKEL/SiO₂ CERMET FILMS, Transmission Electron Microscopy of—M. S. Abrahams, C. J. Buiocchi, M. Rayl, P. J. Wojtowicz (Labs, Pr) *J. of Applied Physics*, Vol. 43, No. 6, p. 2537; 6/72

LIQUID-CRYSTAL MIXTURES, Equilibrium Properties of Schiff-Base—H. Sorokin (SSD, Som) Symp. on Liquid Crystals, Kent State Univ.; 8/72

LIQUID HELIUM, Non-Ohmic Electron Transport—R. S. Crandall (Labs, Pr) *Physical Review A*, Vol. 6, No. 2 pp. 790-795; 8/72

METEROEPITAXIAL SILICON ON SAPPHIRE and Spinel, A Comparison of the Semiconducting Properties of—G. W. Cullen J. F. Corboy, W. W. Claugs (Labs, Pr) Metallurgical Soc. of AIME, Boston, MA; 8/28-30/72

MONOCRYSTALLINE Nb₃Sn, Elastic Moduli and Magnetic Susceptibility of—W. Rehwald, M. Rayl, R. W. Cohen, G. D. Cody (Labs, Pr) *Physical Review B*, Vol. 6, No. 2, pp. 363-371; 7/15/72

n-Type CdCr₂S₄, A Magnetically Susceptible, Highly Resistive Surface Layer in—M. Toda, (Labs, Pr) Oyo Buturi Supplement, Vol. 41, pp. 183-190, 1972 (*Proc. of the 3rd Conf. on Solid State Devices, Tokyo, 1971*)

PbI₂, Band Edge Excitons in—G. Harbeke (Labs, Pr) 11th Int'l Conf. on the Physics of Semiconductors, Warsaw, Poland; 7/25-29/72

PIEZOELECTRIC III-V COMPOUNDS ON Dielectric Substrates, Epitaxial Growth and Properties of—M. T. Duffy, C. C. Wang, (Labs, Pr) G. D. O'Clock, Jr. (ATL, Van Nuys) Metallurgical Soc. of AIME, Boston, MA; 8/28-30/72

RARE EARTH MATERIALS, Analysis and Application of—P. N. Yocom (Labs, Pr) NATO Advanced Study Institute, Oslo, Norway; 8/23-29/72

SILICON FILMS ON SAPPHIRE using the MOS Hall Technique, Electrical Properties of—A. C. Iprì (Labs, Pr) *J. of Applied Physics*, Vol. 43, No. 6, p. 2770; 6/72

SILICON ON INSULATING SUBSTRATES: The Relationship Between the Density of Early Growth Islands and Semiconducting Properties—G. W. Cullen, J. F. Corboy, H. E. Temple (Labs, Pr) Second Nat'l Conf. on Crystal Growth, Princeton, N.J.; 7/30-8/4/72

SILICON-SAPPHIRE INTERFACE As a Function of the Film Deposited Conditions—G. E. Gottlieb (Labs, Pr) Second Nat'l Conf. on Crystal Growth, Princeton, N.J.; 7/30-8/4/72

210 Circuit Devices & Microcircuits

... electron tubes & solid-state devices (active & passive), integrated, array, & hybrid microcircuits, field-effect devices, resistors & capacitors, modular & printed circuits, circuit interconnection, waveguides & transmission lines.

AVALANCHING SILICON-ON-SAPPHIRE DIODES, Second-Breakdown Phenomena in—R. A. Sunshine, M. A. Lampert (Labs, Pr) IEEE Trans. on Electron Devices, Vol. ED-19, No. 7, p. 873; 7/72

CHARGE-COUPLED DEVICES, Free Charge Transfer in—J. E. Carnes, W. F. Kosonocky, E. G. Ramberg (Labs, Pr) IEEE Trans. on Electron Devices, Vol. ED-19, No. 6, pp. 798-808; 6/72

CMOS CIRCUITS, Hardening Techniques for—K. M. Schlesier, P. E. Norris (Labs, Pr) 1972 IEEE Nuclear & Space Radiation Effects Conf., Seattle, Washington; 7/24-27/72

DIGITAL INTEGRATED CIRCUITS for Consumer Applications—D. R. Carley (SSD, Som) WESCON, Los Angeles, Calif.; 9/72

HYBRID CIRCUITS for Microwave Applications, a Review of the Technological and Electromagnetic Limitations—H. Sobol (Labs, Pr) IEEE Trans. on Parts, Hybrids, and Packaging, Vol. PHP-8, No. 2, pp. 58-66; 6/72

IMPATT DIODES, Multilayer Vapor-Phase Epitaxial Silicon Millimeter-Wave—C. P. Wen, K. P. Weller, A. F. Young (Labs, Pr) IEEE Trans. on Electron Devices, Vol. ED-19, No. 7, p. 891; 7/72

SILICON ON SAPPHIRE Integrated Circuit Processes, Test Structure Design Criteria and Results of Electrical Tests—W. E. Ham, P. A. Crossley (Labs, Pr) Metallurgical Soc. of AIME, Boston, Ma.; 8/28-30/72

215 Circuit & Network Designs

... analog & digital functions in electronic equipment: amplifiers, filters, modulators, microwave circuits, A-D converters, encoders, oscillators, switches, masers, logic networks, timing & control functions, fluidic circuits.

ADAPTIVE CONTROL VOLTAGE MODULES, Analog Memory Devices Employing PE-FE Interactions for—S. S. Perlman, J. H. McCusker, S. M. Broadman (Labs, Pr) Ferroelectrics, Vol. 3, Nos. 2/3/4, pp. 239-245; 2/72

OPERATIONAL TRANSCONDUCTANCE AMPLIFIER (OTA) with Power Capability, An IC—L. Kaplan, H. Wittlinger (SSD, Som) Chig. Spring Conf.; 1972; Conf. Proc.

POWER SWITCH/AMPLIFIER IC for Industrial Applications, Programmable—G. J. Granier (SSD, Som) Mid-American Electronics Conf., Kansas City, Mo.; 10/72

SCR REGULATOR for SCR Deflection—W. Dietz (SSD, Som) Fernseh Technische Tagung 1972 (TV Broadcast-Receiver Seminar), Braunschweig, Germany; 10/72

VOLTAGE DETECTOR on Single IC, COS/MOS Fuze Timer Combines SCR and Analog—R. P. Fillmore, N. Cuttillo (SSD, Som) 1972 Government Microcircuit Applications Conf., San Diego, Calif.; 10/72

220 Energy & Power Sources

... batteries, solar cells, generators, reactors, power supplies.

MICROWAVE POWER Sources—H. Sobol, F. Sterzer (Labs, Pr) IEEE Spectrum, Vol. 9, No. 4, pp. 20-33; 4/72

225 Antennas & Propagation

... antenna design & performance, feeds & couplers, phased arrays, radomes & antenna structures, electromagnetic wave propagation, scatter, effects of noise & interference.

PHASED ARRAY for AN/SPY-1, Compact, Constrained Feed—W. Patton, R. Scudder, N. Landry, H. Goodrich (M&SR, Mrstn) Repeat of Tri-Service Symp. in Arlington, "Presentations on AEGIS"; 7/11/72

240 Lasers, Electro-Optical & Optical Devices

... design & characteristics of lasers, components used with lasers, electro-optical systems, lenses, etc. (excludes: masers).

ELLIPTIC CROSS SECTION, Efficient Generation of Laser Beams with an—A. H. Firester, T. E. Gayeski, M. E. Heller (Labs, Pr) Applied Optics, Vol. 11, No. 7, p. 1648; 7/72

GaAs ILLUMINATORS, New Developments in High Power Liquid-Nitrogen-Cooled—L. O'Hara (ATL, Cam) Fifth DoD Conf. on Laser Technology, Monterey, Calif.; 4/25-27/72

LASING OF CdS at Atmospheric Pressure, Low-Voltage Electron-Beam-Pumped—F. H. Nicoll (Labs, Pr) IEEE Trans. on Electron Devices, Vol. ED-19, No. 6, pp. 838-839; 6/72

POINTER TRACKER for a Laser Weapon System—D. G. Herzog (ATL, Cam) Missile Command Conf., Huntsville, Ala.; 7/25/72

VAPOR-GROWN GaAs p-n JUNCTIONS, Influence of Gas-Phase Stoichiometry on Defect Morphology and Electroluminescent Properties of—R. E. Enstrom, C. J. Nuese, J. R. Appert (Labs, Pr) Second National Conf. on Crystal Growth, Princeton, N.J.; 7/30-8/4/72

245 Displays

... equipment for the display of graphic, alphanumeric, & other data in communications, computer, military, & other systems, CRT devices, solid state displays, holographic displays, etc.

DIGITAL DISPLAY Systems, Liquid Crystal Driven by "CMOS" Offer Minimal Power—R. C. Heuner (SSD, Som) NEREM 72, Boston, Mass.; 11/72

DISPLAY for Use in Watches Calculators, and General Instrumentation, Liquid-Crystal Readout—H. C. Schindler (SSD, Som) Mid-American Electronics Conf., Kansas City, Mo.; 10/72

MATRIX DISPLAY Techniques—B. J. Lechner (Labs, Pr) Univ. of Wisconsin, Madison, Wisconsin; 7/20-21/72

250 Recording Components & Equipment

... disk, drum, film, holographic & assemblies for audio, image, & data systems.

VIDEO RECORDING and Playback—R. E. Flory (Labs, Pr) McGraw-Hill Yearbook of Science and Technology; 1972

SERIES 300 SYSTEMS, EQUIPMENT, & APPLICATIONS

305 Aircraft & Ground Support

... airborne instruments, flight control systems, air traffic control, etc.

SECANT - A Solution to the Problem of Mid-air Collisions—W. B. Miles (EASD, Van Nuys) Institute of Navigation (ION) Mtg.; West Point, N.Y.; 6/27/72

SECANT - A Solution to the Problem of Mid-air Collisions—J. L. Parsons (EASD, Van Nuys) 14th Guidance and Control Panel Symp.; AGARD/NATO: Edinburgh, Scotland; 6/26-29/72

320 Radar, Sonar, & Tracking Systems

... microwave, optical, & other systems for detection, acquisition, tracking, & position indication.

CSTCS IMPLEMENTATION on the AEGIS Development Program—J. M. Apgar (M&SR, Mrstn) American Institute of Industrial Engineers Seminar, Wash., D.C.; 3/23/72

RADAR CONTROL Architecture, AEGIS—R. Baugh, R. Ottinger, E. Prettyman (M&SR, Mrstn) Repeat of Tri-Service Symp. in Arlington, Va. "Presentations on AEGIS"; 7/11/72

TRANSMITTER Design Considerations, AN/SPY-1—I. Schottenfeld, C. Lorant, W. Zinger (M&SR, Mrstn) Repeat of Tri-Service Symp. in Arlington, Va. "Presentations on AEGIS"; 7/11/72

325 Checkout, Maintenance, & User Support

... automatic test equipment, maintenance & repair methods, installation & user support.

DIAGNOSIS BY FUNCTION, Central Processor Unit—M. E. Fohl (CSD, Camden) 1972 Int'l Symp. on Fault Tolerant Computing, Boston, Mass.; 6/19-21/72; Digest of Papers; 6/19-21/72

340 Communications Equipment & Systems

... industrial, military, commercial systems, telephony, telegraphy, & telemetry, (excludes: television & broadcast radio).

PHASE-LOCK LOOP RECEIVERS, Phase Detector Data Distortion In—G. D. O'Clock, Jr. (ATL, Camden) IEEE Trans. on Aerospace & Electronic Systems, Vol. AES-8, No. 3, pp. 391-393; 5/72

TIME DIVISION DIGITAL SWITCH Matrix Technique Evaluation—A. Mack, B. Patrusky (Labs, Pr) IEEE Int'l Conf. on Communications Phila., Pa.; 6/19-21/72; ICC 1972 Conf. Proc.

VOICE COMMUNICATIONS Systems, LHA Interior—W. J. Lawrence (CSD, Camden) IEEE Symp. on Computers & Comm., Cherry Hill, N.J.; 6/14/72

Author Index

Subject listed opposite each author's name indicates where complete citation to his paper may be found in the subject index. An author may have more than one paper for each subject category.

Advanced Technology Laboratories

Herzog, D. G., 240
Nicasro, L. J., 205
O'Clock, G. D., 340
O'Hara, L., 240

Communications Systems Division

Fohl, M. E., 325
Lawrence, W. J., 340

Electromagnetic and Aviation Systems Division

Miles, W. B., 305
Parsons, J. L., 305

Missile and Surface Radar Division

Apgar, J. M., 320
Baugh, R., 320
Cottler, D. M., 180
Goodrich, H., 225
Landry, N., 225
Lorant, C., 320
Ottinger, R., 320

Patton, W., 225
Prettyman, E., 320
Robinson, A. S., 180
Schottenfeld, I., 320
Scudder, R., 225
Zinger, W., 320

Solid State Division

Carley, D. R., 210
Cuttillo, N., 215
Dietz, W., 215
Fillmore, R. P., 215
Granier, G. J., 215
Heuner, R. C., 245
Kaplan, L., 215
Schindler, H. C., 245
Sorkin, H., 205
Wittlinger, H., 215

RCA Laboratories

Abeles, B., 205
Appert, J. R., 240
Abrahams, M. S., 205
Baltzer, P. K., 205
Ban, V. S., 205
Blakeley, R. A., 105
Blanc, J., 170, 205
Broadman, S. M., 215
Bulocchi, C. J., 205
Carnes, J. E., 210
Claugs, W. W., 205
Coldy, G. D., 205
Cohen, R. W., 205
Corboy, J. F., 205
Coutts, M. D., 160
Crandall, R. S., 205

Crossley, P. A., 170, 210
Cullen, G. W., 205
Dismukes, J. P., 205
Duffy, M. T., 205
Enstrom, R. E., 240
Ettenberg, M., 170, 205
Feldstein, N., 170
Firester, A. H., 240
Flory, R. E., 250
Gayeski, T. E., 240
Gilbert, S. L., 205
Goldsmith, N., 170
Gossenberger, H. F., 205
Gottlieb, G. E., 205
Hall, D. S., 205
Ham, W. E., 170, 210
Harbeck, G., 205
Heller, M. E., 240
Iprl, A. C., 205
Klein, R., 205
Klopfenstein, R. W., 130
Kosonocky, W. F., 210
Lampert, M. A., 210
Larach, S., 160
Larach, S., 160
Lechner, B. J., 245
Lockwood, H. F., 170
Mach, A., 340
Mayer, A., 175
McCusker, J. H., 215
Miyatani, K., 205
Nicoll, F. H., 240
Norris, P. E., 210
Nuese, C. J., 240
Oka, T., 205
Okamoto, F., 205
Opresko, Jr., S. J., 205
Oska, S., 205

Pankove, J. I., 205
Patrusky, B., 340
Pellos, A., 130
Perlman, S. S., 215
Pinch, A., 205
Priestley, E., 160
Ramberg, E. G., 210
Rayl, M., 205
Rehwald, W., 125, 205
Robinson, B. B., 105
Robinson, P. H., 170
Schlesier, K. M., 210
Schnable, G. L., 175
Schwartz, P. M., 105
Sheng, P., 205
Sigal, A. G., 205
Sobol, H., 210, 220
Southgate, P. D., 205
Sterzer, F., 220
Stofko, E. J., 205
Sunshine, R. A., 210
Suzuki, K., 125
Temple, H. E., 205
Tietjen, J. J., 205
Toda, M., 205
Tuska, J. W., 175
Vossen, J. L., 170
Wang, C. C., 105, 205
Wehner, R. K., 205
Weller, K. P., 210
Wen, C. P., 210
Sojtowicz, P. J., 205
Woods, M. H., 175
Yim, W. M., 205
Yocum, P. N., 205
Yoshikawa, K., 125
Young, A. F., 210
Zanzucchi, P. J., 205

Dates and Deadlines



As an industry leader, RCA must be well represented in major professional conferences . . . to display its skills and abilities to both commercial and government interests.

How can you and your manager, leader, or chief-engineer do this for RCA?

Plan ahead! Watch these columns every issue for advance notices of upcoming meetings and "calls for papers". Formulate plans at staff meetings—and select pertinent topics to represent you and your group professionally. Every engineer and scientist is urged to scan these columns; call attention of important meetings to your Technical Publications Administrator (TPA) or your manager. Always work closely with your TPA who can help with scheduling and supplement contacts between engineers and professional societies. Inform your TPA whenever you present or publish a paper. These professional accomplishments will be cited in the "Pen and Podium" section of the *RCA Engineer*, as reported by your TPA.

Calls for papers—be sure deadlines are met

Date	Conference	Location	Sponsors	Deadline Date	Submit	To
APR. 30- MAY 2, 1973	IEEE Region III Conference	Galt House Louisville, Ky.	IEEE	10/1/72 2/1/73	prel. papers final paper	R. D. Shelton, Dept. of Electrical Engineering, Speed Scientific School University of Louisville Louisville, KY 40208
MAY 15-17, 1973	1973 Electrical & Electronic Measurement & Test Instrument	Skyline Hotel Ottawa, Canada	Ottawa Section Group on I & M	12/31/72	abst	Chairman of the Technical Program Committee, Dr. Pieter G. Cath, Keithley Instruments, Inc., 28775 Aurora Road, Cleveland, Ohio 44139
MAY 21-23, 1973	Joint Life Sciences and Systems Specialist Meeting	International Hotel Las Vegas, Nev.	ASMA/ AIAA	11/24/72	abst	General Program Chairman: Col. Carl Weinberg (USAF) HQ - USAF (RDPS) Dept. of the Air Force, Washington, DC 20330 Technical Program Chairman: James A. Green, Life Sciences (FA45), Space Div., North American Rockwell Corp., Downey, Calif. 90241
JUNE 25-29, 1973	1973 IEEE International Symposium on Information Theory	Ashkelon, Israel	Group on IT	2/1/73	papers	Dr. N. J. A. Sloane, Room 2C-363, Bell Laboratories Murray Hill, NJ 07974
SEPT. 16-20, 1973	Jt. Power Generation Technical Conference	Mariott Hotel, New Orleans, La.	S-PE, ASME	5/4/73	ms	L. C. Grundmann, New Orleans Public Service Inc., 317 Baronne St., New Orleans, La 70160
SEPT. 30- OCT. 4, 1973	Electrical/Electronics Insulation Conference	Palmer House Chicago, Illinois	G-EI, NEMA	9/1/72 2/1/73	abst ms	NEMA, 155 E. 44th St., New York, NY 10017
OCT. 2-5, 1973	Automatic Control in Glass Manufacturing Conference	Purdue Univ., Lafayette, Ind.	S-IA, IFAC, AACC, ISA, Purdue Univ.	10/1/72 2/1/73	abst ms	IEEE Headquarters 345 E. 47th St., New York, NY 10017
APRIL 1-5, 1974	1974 IEEE Power Engineering Society Underground Transmission and Distribution Conference	Convention Center Dallas, Texas	Power (IEEE) Engineering Society	5/1/73	abst	Program Chairman: N. E. Piccione Long Island Lighting Company, 175 Old Country Road, Hicksville, NY 11801

Dates of upcoming meetings—plan ahead.

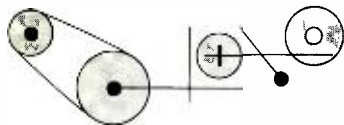
Date	Conference	Location	Sponsors	Program Chairman
NOV 1-3, 1972	Northeast Electronics Research & Engineering Meeting (NEREM)	Boston, Mass	New England Section	IEEE Boston Office, 31 Channing St., Newton, Mass. 02158
NOV. 9-10, 1972	Canadian Communications & EHV Conference	Queen Elizabeth Hotel Montreal, Quebec, Canada	Canadian Region, Montreal Section	Dinkar Mukhedkar, Ecole Polytechnique, 2500 Marie Guyard, Montreal 250 PQ Canada
NOV. 13-15, 1972	Conf. on Automatic Support Systems for Advanced Maintain- ability	Holiday Inn, Phila., Penna.	G-AES, Phila. Section	Fred Liguori, Naval Air Engrg. Ctr., Phila., Penna. 19112
NOV. 26-30, 1972	1972 Winter Annual Meeting and Energy Crises Forum	Statler Hilton Hotel New York City	ASME	Maurice Jones, Mgr. Information Services, ASME, United Engineer- ing Center, 345 E. 47th St., New York, NY 10017

Dates of upcoming meetings—plan ahead.

Date	Conference	Location	Sponsors	Program Chairman
NOV. 29- DEC. 1, 1972	AIAA/SAE 8th Joint Propulsion Specialist Conference	New Orleans, La.	AIAA SAE	AIAA, 1290 Ave. of the Americas, New York, NY 10019
NOV. 28- DEC. 1, 1972	Conference on Magnetism and Magnetic Materials	Denver Hilton Hotel Denver, Colorado	S-MAG, AIP	A. E. Berkowitz, Gen'l Elec. Co., POB 8, Schenectady, NY 12301
DEC. 4-5, 1972	Chicago Fall Conference on Broadcast & Television Receivers	Sheraton O'Hare Motor Hotel Rosemont, Ill.	G-BTR	W. C. Luplow, Zenith Radio Corp., 1851 Arthur Ave., Elk Grove, Ill. 60007
DEC. 4-6, 1972	Int'l. Electron Devices Meeting	Washington Hilton Hotel, Washington, D.C.	G-ED	R. W. Haitz, Hewlett-Packard, 620 Page Mill Road, Palo Alto, Calif. 94309
DEC. 4-6, 1972	Nat'l. Telecommunications Conference	Astroworld Hotel, Houston, Texas	G-AES, S-Comm., G-GE	R. S. Simpson, Dept. of EE, Univ. of Houston, Houston, Texas 77004
DEC. 5-7, 1972	Fall Joint Computer Conference	Convention Ctr., Anaheim, Calif.	S-C, AFIPS	D. A. Meier, P. O. Box 835, Hawthorne, Calif. 90250
DEC. 6-8, 1972	Nuclear Science Symposium	Deauville Hotel Miami Beach, Florida	G-NS, NASA, AEC	J. H. Trainor, Code 663, NASA/Goddard Space Flight Ctr., Greenbelt, Maryland 20771
DEC. 6-8, 1972	Vehicular Technology Conference	Dallas, Texas	G-VT	Nick Gorham, Motorola, Inc. POB 34290, Dallas, Texas 75234
DEC. 8-9, 1972	AIAA/NABE Seminar—Orienting the Aerospace Industry to Changing Priorities	Los Angeles, Calif.	AIAA NABE	AIAA, 1290 Ave. of the Americas, New York, NY 10019
DEC. 11-15, 1972	G-AP Int'l. Symposium & Fall USNC/URSI Meeting	William & Mary College, Williamsburg, Virginia	G-AP, USNC/ URSI	C. T. Swift, NASA, 168 Deane Dr., Newport News, Virginia 23602
DEC. 13-15, 1972	Conf. on Decision and Control (Inc. 11th Symp. on Adaptive Processes)	Fontainebleau Motor Hotel, New Orleans, La.	S-CS, G-IT, S-SMC	Y. C. Ho, Pierce Hall, Harvard Univ., Cambridge, Mass. 02138
JAN. 8-10, 1973	AIAA 9th Annual Meeting and Technical Display	Washington, D.C.	AIAA	AIAA, 1290 Ave. of the Americas, New York, NY 10019
JAN. 10-12, 1973	AIAA 11th Aerospace Sciences Meeting	Washington, D.C.	AIAA	AIAA, 1290 Ave. of the Americas, New York, NY 10019
JAN. 23-25, 1973	1973 Annual Reliability and Maintainability Symposium	Philadelphia, Pa.		AIAA, 1290 Ave. of the Americas, New York, NY 10019
JAN. 28- FEB. 2, 1973	IEEE Power Engineering Society Winter Meeting	Statler Hilton Hotel New York, New York	G-R, ASOC, IES et al	L. R. Webster, Radiation Inc. POB 37, Melbourne, Fla. 32901
FEB. 1-2, 1973	1973 Micrographic Science Seminar	New Orleans, La	SPSE	Mr. Russell P. Cook Polaroid Corporation 730 Main Street Cambridge, Mass. 02139
FEB. 13-15, 1973	Aerospace & Electronic Systems Winter Convention (WINCON)	Biltmore Hotel, Los Angeles, Calif.	G-AES, L.A. Council	IEEE L. A. Council Office, 3600 Wilshire Blvd., Los Angeles, Calif. 90010
FEB. 14-16, 1973	Int'l. Solid State Circuits Conference	Univ. of Penna. Sheraton Hotel, Phila., Penna.	SSC Council Phila. Section, Univ. of Penna.	Soi Triebwasser, T. J. Watson Res. Ctr., IBM Corp., Yorktown Heights, NY 10598
MARCH 5-7, 1973	Particle Accelerator Conference	Sheraton Palace Hotel, San Francisco, Calif	G-NS, NBS et al	R. B. Neal, Stanford Linear Accelerator Ctr., Stanford, Calif. 94305
MARCH 6-8, 1973	Diagnostic Testing of High Power Apparatus In Service	London, England	IEE, IEEE UKRI Section	IEE, Savoy Place, London, W. C. 2R OBL, England
MARCH 7-9, 1973	3rd Sounding Rocket Technology Conference	Albuquerque, N. Mex	AIAA	AIAA, 1290 Ave. of the Americas, New York, NY 10019
MARCH 20-22, 1973	14th Structures, Structural Dynamics and Materials Conference	Williamsburg, Va.	AIAA/ASME/ SAE	AIAA, 1290 Ave. of the Americas, New York, NY 10019
MARCH 26-29, 1973	IEEE International Convention (INTERCON)	Coliseum & N.Y. Hilton Hotel, New York, NY	IEEE	J. H. Schumacher, IEEE, 345 E. 47th St., New York, NY 10017
MARCH 28-30, 1973	Tactical Missile Meeting	Orlando, Fla	AIAA/ AOA	AIAA, 1290 Ave. of the Americas, New York, NY 10019

Patents Granted

to RCA Engineers



As reported by RCA Domestic Patents,
Princeton

Aerospace Systems Division

Low Level DC Amplifier with Automatic Zero Offset Adjustment—D. A. Johnson (ASD, Burl.) U.S. Pat. 3681703, August 1, 1972

Electromagnetic and Aviation Systems Division

Servo System with Noise Cancellation—M. S. Masse, J. P. McDowell (Aviation Equip., Los Angeles) U.S. Pat. 3683254, August 8, 1972

High Voltage Pulse Generator—R. N. Guadagnolo (EASD, Van Nuys) U.S. Pat. 3686516, August 22, 1972

Astro-Electronics Division

Bookbinding—E. W. Schlieben (AED, Hstn.) U.S. Pat. 3685857, August 22, 1972

Missile & Surface Radar Division

COS/MOS Phase Comparator for Monolithic Integration—W. J. Donoghue (M&SR, Mrstn.) U.S. Pat. 3673430, June 27, 1972; Assigned to U.S. Government

Advanced Technology

High Speed Tunable Maser for Use in Radar and Communication Receivers—L. C. Morris (ATL, Cam.) U.S. Pat. 3688207, August 29, 1972

Waveform Generator—J. G. Butler (ATL, Cam.) U.S. Pat. 3689914, September 5, 1972

Communications Systems Division

Measurement of Maximum Dynamic Skew in Parallel Channels—C. Y. Hsueh (CSD, Cam.) U.S. Pat. 3681693, August 1, 1972

Sheet Metal Waveguide Constructed of a Pair of Interlocking Sheet Metal Channels—W. A. Dischert (CSD, Cam.) U.S. Pat. 3686590, August 22, 1972

Conversion to a Digital Code Which is Self-clocking and Absolute Phasing—G. S. Newcomb (CSD, Cam.) U.S. Pat. 3689913, September 5, 1972

System for Record Medium Control and Editing—R. N. Hurst (CSD, Cam.) U.S. Pat. 3684826, August 15, 1972

Special Effects Generator—L. J. Thorpe (CSD, Cam.) U.S. Pat. 3689694, September 5, 1972

Contrast Compression Circuits—R. A. Dischert, J. F. Monahan (CSD, Cam.) U.S. Pat. 3684825, August 15, 1972

Laboratories

Method of Pressure Treating Electrophotographic Recording Elements to Change Their Sensitivity to Light—P. J. Donald (Labs., Pr.) U.S. Pat. 3681071, August 1, 1972

Method of Producing a Luminescent-Screen Structure Including Light-Emitting and Light-Absorbing Areas—N. Feldstein (Labs., Pr.) U.S. Pat. 3681110, August 1, 1972

Bucket Brigade Scanning of Sensor Array—P. K. Weimer (Labs., Pr.) U.S. Pat. 3683193, August 8, 1972

Ferro-Electric Transformers with Means to Suppress or Limit Resonant Vibrations—S. S. Periman, J. H. McCusker (Labs., Pr.) U.S. Pat. 3683211, August 8, 1972

Electroluminescent Semiconductor Device of GaN—J. I. Pankove (Labs., Pr.) U.S. Pat. 3683240, August 8, 1972

GaS Laser Discharge Tube—K. G. Herrngvist (Labs., Pr.) U.S. Pat. 3683295, August 8, 1972

Microwave Apparatus Using Multiple Avalanche Diodes Operating in the Anomalous Mode—H. Kawamoto (Labs., Pr.) U.S. Pat. 3683298, August 8, 1972

Doped Calcium Fluoride and Strontium Fluoride Photochromic Compositions—W. Phillips (Labs., Pr.) U.S. Pat. 3684727, August 15, 1972

Capacitive Steering Networks—Y. Yao (Labs., Pr.) U.S. Pat. 3684899, August 15, 1972

Coax Line to Strip Line End Launcher—L. S. Napoli, J. J. Hughes (Labs., Pr.) U.S. Pat. 3686624, August 22, 1972

Method of Coating Selective Areas of the Surface of a Body—A. N. Saxena (Labs., Pr.) U.S. Pat. 3687722, August 29, 1972

Synchronizing System—A. C. Iprì (Labs., Pr.) U.S. Pat. 3688037, August 29, 1972

Time Delay Device—C. J. Hirsch (Labs., Pr.) U.S. Pat. 3688131, August 29, 1972

High Resolution, Redundant Coherent Wave Imaging Apparatus Employing Pinhole Array—M. J. Lurie (Labs., Pr.) U.S. Pat. 3689129, September 5, 1972

Sound Records and Reproducing Apparatus—C. C. Ih (Lab. Pr.) U.S. Pat. 3689692, September 5, 1972

Electronic Components

Electron Tube Having Tamper-Detectable Label Attached Thereto—S. B. Deal, D. W. Barch (EC, Lanc.) U.S. Pat. 3680236, August 1, 1972

Photographic Method for Printing a Screen Structure for a Cathode-Ray Tube—H. R. Frey (EC, Lanc.) U.S. Pat. 3685994, August 22, 1972

Angled Array Semiconductor Light Sources—P. Nyul (EC, Lanc.) U.S. Pat. 3686543, August 22, 1972

Stabilized Transferred Electron Amplifier—C. L. Upadhyayula, B. S. Periman (EC, Pr.) U.S. Pat. 3686578, August 22, 1972

Spray Method for Producing a Glare-Reducing Coating—G. E. Long, III, D. W. Barch (EC, Lanc.) U.S. Pat. 3689312, September 5, 1972

Solid State Division

Method of Fabrication of Semiconductor Devices—J. H. Banfield, S. Y. Husni, W. J. Greig (SSD, Som.) U.S. Pat. 3686080, August 22, 1972

Gallium Arsenide Semiconductor Device with Improved Ohmic Electrode—S. Shwartzman (SSD, Som.) U.S. Pat. 3686539, August 22, 1972

Deflection Circuit—C. F. Wheatley, Jr. (SSD, Som.) U.S. Pat. 3686153, August 29, 1972

Operation of Field-Effect Transistor Circuits Having Substantial Distributed Capacitance—A. G. F. Dingwall (SSD, Som.) U.S. Pat. 3686264, August 29, 1972

Liquid Crystal Display Device—R. I. Klein, S. Caplan, R. T. Hansen (SSD, Som.) U.S. Pat. 3689131, September 5, 1972

Integrated Circuit Biasing Arrangements—L. A. Harwood (SSD, Som.) U.S. Pat. RE27454, August 1, 1972

Method for Manufacturing Wire Bonded Integrated Circuit Devices—A. N. Gardiner (SSD, Som.) U.S. Pat. 3685137, August 22, 1972

Consumer Electronics

High Q Circuits on Ceramic Substrates—R. S. Degenkolb, E. R. Skaw (CE, Indpls.) U.S. Pat. 3681713, August 1, 1972

Process for Forming a Conductive Coating on a Substrate—R. J. Ryan, S. F. Burtis, J. T. Grogan (CE, Indpls.) U.S. Pat. 3682784, August 8, 1972

Process for Forming an Isolated Circuit Pattern on a Conductive Substrate—R. R. Russo (CE, Indpls.) U.S. Pat. 3682785, August 8, 1972

Transistorized Vertical Deflection Circuit—L. E. Smith (CE, Indpls.) U.S. Pat. 3684920, August 15, 1972

Horizontal Oscillator Disabling—W. V. Fitzgerald, Jr., P. C. Willmarth (CE, Indpls.) U.S. Pat. 3688025, August 29, 1972

VHF and UHF Automatic Gain Control Circuitry Derived from a Single Control Voltage—J. B. George (CE, Indpls.) U.S. Pat. 3688198, August 29, 1972

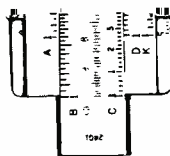
Astable Multivibrator Circuit with Means for Ensuring Proper Starting of Oscillations—T. J. Christopher (CE, Indpls.) U.S. Pat. 3688154, August 29, 1972

RCA Records

Recorder and Playback Apparatus for Pulse Width Modulated Record—M. J. Whittemore, Jr. (Rec., Indpls.) U.S. Pat. 3688025, August 29, 1972

Parts and Accessories

Antenna System for Television Reception within Both the UHF and VHF Television Band of Frequencies—J. D. Callaghan (P&A, Depford) U.S. Pat. 3683391, August 8, 1972



Rosenthal named Staff V.P.

Dr. James Hillier, Executive Vice President, Research and Engineering has appointed **Howard Rosenthal** Staff Vice President, Engineering. Mr. Rosenthal had been Director of Engineering. In his new position he will continue his responsibility for coordinating the engineering activities of RCA's product divisions. In addition, he will assume responsibility for Corporate Engineering Services, which includes the RCA Frequency Bureau, Corporate Standards Engineering, and Engineering Education and Technical Publication groups.

Mr. Rosenthal received the BSCE from the City College of New York in 1944. After two years in the Navy as a Radar Technician during World War II, he did graduate work at New York University, receiving the MS in Chemical Engineering in 1949. During the same year, he joined RCA Laboratories as a Member of the Technical Staff. He has received three RCA Laboratories Achievement Awards for his research on the application of phosphors in color TV display tubes. In 1959, he was appointed to the first of a series of Technical Administration positions at the Laboratories that led to his appointment in 1968 as Administrator, Staff Services, RCA Research and Engineering. He was named Director of Engineering in 1970. Mr. Rosenthal is a Member of the American Chemical Society, Phi Lambda Upsilon and the IEEE.

Degree granted

John E. Schoen, of Commercial Engineering Department, Solid State Division, has received the MA in English Literature from Fairleigh Dickinson University in May 1972.



Biewener named Staff V.P.

Dr. James Hillier, Executive Vice President, Research and Engineering has appointed **John F. Biewener**, Staff Vice President, Finance and Administrative Services. Formerly Director, Finance and Administrative Services, Research and Engineering. Mr. Biewener in his new position is responsible for the business and administrative functions of RCA's David Sarnoff Research Center in Princeton, N.J.

Since joining RCA in 1950, Mr. Biewener has held positions of increasing responsibility in engineering, administration, and finance at RCA activities in Moorestown, Camden, and Princeton, N.J., and Cambridge, Ohio. He also served on the RCA Corporate Staff in New York City from 1967 to 1970. He was appointed Controller at the David Sarnoff Research Center in 1970 and Director, Finance and Administrative Services in 1971. Mr. Biewener received the BSEE from Carnegie-Mellon University in 1950. In 1963, as an RCA employee, he attended the four-month Program for Management Development at the Harvard Business School.

Licensed engineers

When you receive a professional license, send your name, PE number (and state in which registered), RCA division, location and telephone number to: *RCA Engineer*, Bldg. 2-8, RCA, Camden, N. J. As new inputs are received they will be published.

Missile and Surface Radar Division

A. P. Moll, M&SR, Moorestown, PE—19538, New Jersey.

RCA Records

G. Nelson, Records Div., Rockaway, PE—19615, New Jersey.

Staff announcements

Cushman and Wakefield, Inc.

Anthony L. Conrad, President and Chief Operating Officer has announced that the Real Estate and Architecture and Construction activities in the RCA Staff Manufacturing Services and Materials organization are transferred to Cushman & Wakefield, Inc. **Leone J. Peters**, Chairman and Chief Executive Officer of Cushman & Wakefield, has advised that **Herbert A. Semler**, Senior Vice President, Finance and Administration, will assume responsibility for these activities.

Research and Engineering

James Hillier, Executive Vice President, Research and Engineering has appointed **John F. Biewener**, Staff Vice President, Finance and Administrative Services and **Howard Rosenthal**, Staff Vice President, Engineering.

James Hillier announced the Research and Engineering organization as follows: **John F. Biewener**, Staff Vice President, Finance and Administrative Services; **Edward W. Herold**, Director, Technology; **Howard Rosenthal**, Staff Vice President, Engineering; **A. Robert Trudel**, Director, Special Projects; and **William M. Webster**, Vice President, Laboratories.

Laboratories

Jan Rajchman, Staff Vice President, Information Sciences, has appointed **Bernard Hershenov** as Director of Research of RCA Research Laboratories, Inc. (Tokyo).

Kerns H. Powers, Director of the Communications Research Laboratory, has appointed **Harold Sobol** as Head of Communications Technology Research.

Solid State Division

William C. Hittinger, Vice President and General Manager, Solid State Division has announced the following appointments: **Daniel P. Del Frate**, Division Vice President, Solid State Marketing; **Joseph W. Karoly**, Division Vice President, Finance; **Donald W. Ponturo**, Division Vice President, Industrial Relations; and **William E. Wagner**, Manager, Marketing.

Electronic Components

John B. Farese, Executive Vice President, Electronic Components has appointed **Thomas I. Peters**, Director, Materials.

Joseph H. Colgrove, Division Vice President and General Manager, Entertainment Tube Division, has announced his organization as follows: **Donald R. Bronson**, Director, International Operations; **Gor-**

don W. Farmer, Director, Receiving Tube Operations Department; **Leonard Gillon**, Division Vice President; and **William G. Hartzell**, Director, Television Picture Tube Operations Department.

Carlos E. Burnett, Division Vice President and General Manager, Industrial Tube Division, has appointed **C. Price Smith**, Director, Industrial Tube Operations Department.

Gene W. Duckworth, Division Vice President, Equipment Marketing and Distributing, has announced the following appointments: **Joseph M. Cleary**, Director, Tube Equipment Sales and **Robert B. Means**, Division Vice President, Market Planning.

Government and Commercial Systems

Irving K. Kessler, Executive Vice President, Government and Commercial Systems has announced the appointment of **James H. Walker** as Division Vice President, Finance.

David Shore, Division Vice President, Government Plans and Systems Development, has appointed **F. P. Henderson** as Manager, Requirements Planning.

David A. Wilkinson, Manager, Marketing-Systems Development has appointed **Robert E. Coleman** as Manager, Systems Marketing.

Vernon H. Catron, Manager, Air Force and DCA Affairs has appointed **Leslie R. Long**, Administrator, Air Force Products.

M. L. Ribe, Manager, Eastern Field Office Operations has announced the appointment of **Irvin Guttman** as Manager, Rome (N.Y.) Region.

Warren E. Edwall, Manager, Navy and Marine Corps Affairs has announced the appointment of **Eugene C. Looney** as Administrator, Navy Products.

Palm Beach Division

James Vollmer, Division General Manager, Palm Beach Division has appointed **William J. Hannan**, Chief Engineer.

Aerospace Systems Division

Melvin E. Lowe, Acting Director, Marketing, Aerospace Systems Division has announced the appointment of **Claude M. Jones**, Manager, Air Force Affairs.

Patent Operations

John V. Regan, Staff Vice President, Patent Operations, has announced his organization as follows: **Glenn H. Burestle**, Director, Patents—Electronic Components; **Harold Christoffersen**, Director, Patents—Information Systems; **Philip G. Cooper**, Staff Patent Counsel; **Edward J. Norton**, Director, Patents—Engineering Products; **Albert Russinoff**, Staff Patent Counsel; **Eugene M. Whitacre**, Director, Patents—Consumer Electronics; and **Milton S. Winters**, Director, Patent Plans and Services.



Hannan is Chief Engineer for Palm Beach Division

Dr. James Vollmer, General Manager, Palm Beach Division, has appointed **William J. Hannan**, Chief Engineer. Mr. Hannan will direct the engineering organization at Palm Beach and its activities in connection with the Division's current and future product lines.

Mr. Hannan received the BSEE from Drexel University in 1954 and the MSEE from Brooklyn Polytechnic Institute in 1956. He has been with RCA since 1951 and previously was Head, Electro-optic Systems Research, RCA Laboratories, Princeton, N.J. Earlier, he held a number of engineering and engineering management positions at RCA's Princeton and Camden facilities. For nine years, Mr. Hannan was Engineering Project Leader in the development of magnetic tape, laser communications, and special television systems. He is noted for his work in the development of the holographic pre-recorded video system and the GT-7 laser transmitter, the first laser in space. He also developed the first laser cane for the blind. Mr. Hannan was a recipient of the David Sarnoff Fellowship in 1955 and the RCA Achievement Award in 1969 for his work in holography. Recently, he received the 1972 RCA David Sarnoff Outstanding Achievement Award for scientific research. Mr. Hannan holds membership in the Optical Society of America and is a Senior Member of the Institute of Electrical and Electronics Engineers where he has headed various committees on circuit theory.

Promotions

Electromagnetic and Aviation Systems Division

J. R. Hall from Staff Engr. Scientist, Electronic Warfare Engr. to Mgr., SE-CANT Engr. (F. C. Corey, Gov. Engr. Dept., Van Nuys)

R. W. McKelvy from Pr. Mbr. Design & Develop. Engr., Electronic Warfare Pro-

grams to Mgr., Design & Develop. Engr. (E. A. Cornwall, Electronic Warfare Engr., Van Nuys)

Communications Systems Division

J. J. Davaro from Ldr., Engr. Staff to Adm., Sys. Prod. Assurance (E. J. Westcott, Product Assurance, Camden)

A. C. Thompson from Ldr., Engr. Staff to Mgr., Sales (F. H. Stelter, Studio Equipment, Camden)

Electronic Components

R. D. McLaughlin from Sr. Engr., Prod. Develop. Thermoelectric Products to Engr. Ldr., Product Develop. (G. Silverman, Harrison)

Solid State Division

G. Waas from Ldr., Technical Staff to Mgr., MOS Integrated Circuit Design (D. R. Carley, Somerville)

Global Communications, Inc.

A. W. Brook from Staff Engr. to Mgr. Satellite Sys. Develop. (P. Schneider, Leased Facilities and Engr., New York)

M. ChaFong from Group Ldr. to Mgr., Message Switching Engr. (A. A. Avanesians, Computer Engr. Projects, New York)

L. Correard from Group Ldr., to Mgr., Computer Switching Engr. (A. A. Avanesians, Computer Engr. Projects, New York)

J. W. Cuddihy from Group Ldr., Mgr., Satellite Engr. (J. M. Walsh, Satellite Engr., New York)

E. F. Doherty from Group Ldr., to Mgr., Radio Engr. (J. M. Walsh, Engr., New York)

M. Fruchter from Group Ldr. to Ldr., Tech. Control and Transmission Engr. (A. A. Avanesians, Computer Engr. Projects, New York)

S. Latargia from Sr. Engr. to Mgr., Facilities Engr. (J. M. Walsh, Engr. New York)

J. H. Muller from Group Ldr. to Mgr., Videovoice Engr. (G. A. Shawy, New York)

E. Murphy from Group Ldr. to Ldr., Telephone Switching Engr. (A.A. Avanesians, Computer Engr., New York)

S. Nahum from Adm., Construction to Mgr., Construction (J. M. Walsh, Engr., New York)

S. Solomon from Group Ldr. to Ldr., Hot Line and Advanced Planning (S. Schadoff, Commercial Leased Channels, New York)

L. Spann from Group Ldr. to Mgr., Advanced Design and Development (J. M. Walsh, Engr., New York)



Sobol appointed research head

Dr. Kerns H. Powers, Director of the Communications Research Laboratory at RCA Laboratories in Princeton, N. J., recently appointed **Dr. Harold Sobol** as Head of Communications Technology Research. Formerly a Corporate Staff Engineer, Dr. Sobol now directs a research group concerned with the development of new microwave devices and technology for communication systems.

Dr. Sobol received the BSEE from the City College of New York in 1952. He then attended the University of Michigan, receiving the MS and his PhD in Electrical Engineering in 1955 and 1959, respectively. From 1952 to 1959, he did research

in the radar, weapon guidance, and microwave fields at the Willow Run and Electron Physics Laboratories of the University of Michigan. From 1960 to 1962, Dr. Sobol investigated superconducting films at the IBM Watson Research Center. He joined the Microwave Research Laboratory, RCA Laboratories, in Princeton, in 1962. A year later he was named Head of Power Generation Research and in 1965, Head, Microwave Integrated Circuits Research. In the latter position, he directed the research and development of microwave integrated circuits in RCA's corporate-wide Blue Chip Program.

He was Manager, Microwave Microelectronics, at the Solid State Division in Somerville, N. J., from 1968 to 1970. Under his direction, the basic technology for fabricating microwave integrated circuits was advanced from laboratory status to a pilot production. He then served as a Corporate Staff Engineer from 1970 until his present appointment.

Dr. Sobol is a Senior Member of the IEEE and a Member of the American Physical Society. He is also a Member of Eta Kappa Nu, Tau Beta Pi, Sigma Xi and Phi Kappa Phi. He held a Sperry Fellowship in Electron Physics during 1955-1956 and was the IEEE 1970 National Lecturer in Microwaves. Dr. Sobol is listed in *Who's Who in the East* and *American Men of Science*. He is author or co-author of 28 papers in technical journals and has presented more than 35 papers at technical meetings. He was an Adjunct Lecturer in the Graduate School at Drexel University during 1963 and 1964. He has lectured for several University of Michigan Summer Courses.



Corey named Chief Engineer at EASD

Frederick H. Krantz, Division Vice President and General Manager, Electromagnetic and Aviation Systems Division, has appointed **Frederick C. Corey**, Chief Engineer, Government Engineering Department. In his new post, Mr. Corey heads an engineering organization working in the areas of electronic warfare and ordnance systems and in data systems, including video displays, special purpose data terminals, memories and other devices.

Mr. Corey joined RCA recently after serving for two years as Chief Engineer, Avionics and Sensors in the Autonetics Division, North American Rockwell,

Awards

Aerospace Systems Division

The team of **D. W. Fogg**, **H. Honda**, **R. J. Kampf**, **M. J. Kurina**, **P. A. Michitson**, and **L. B. Wooten** led by **Bob Daly** and **Paul Seeley** received the Technical Excellence Engineering Award for September 1972 for their work on the design concept of the Missile Warning Radar System and presentation of its superior approach. The features developed by the team that sold the contract are: (1) A novel technique for reducing false alarms in clutter while providing broad azimuth coverage; (2) Maximum utilization of RCA's previously developed ALQ-127 system components; (3) Single antenna multi-function approach; (4) A cost effective design for future production; (5) A detailed program plan that provided a high degree of confidence in contract performance.

The team of **B. J. DiPalermo**, **J. L. Hall**, **R. E. Shupe**, and **J. C. Tranfaglia** of the Drafting Department was recognized for its work in implementing the PC and

Design Automation System. The team learned how to prepare input coding from logic designs and schematic interconnection data, mechanical limitations and component placement. In addition, it had to become familiar with an interactive computer/display installation utilized in displaying the computer routed board. They had to manually place wires not routed by the computer.

Communication Systems Division

Engineers **Bob Ernst** and **Ben Hitch** and technician **Arnis Mikelsons** of the Advanced Communication Laboratory located at Somerville, N.J., have been selected for a technical excellence team award. The team was cited for its outstanding accomplishment in successfully developing and integrating seven SHF microelectronic integrated circuit modules applicable to the SHF satellite communication product line. The modules are: 7500-to-700-MHz downconverter; 700-to-8150-MHz upconverter; 700-to-70-MHz downconverter; 70-to-700-MHz up-

converter; X-band frequency synthesizer mixer-coupler; 650-MHz power amplifier-power divider; and SHF power divider with monitoring detectors. These modules had more difficult performance requirements than the state-of-the-art discrete component versions.

Missile and Surface Radar Division

Six engineers have been cited for their second-quarter 1972 performance:

K. Berkowitz for his outstanding performance on the development of the precision guidance subsystem of the AN/TPA-27 system and his special contribution in a quick turnaround rework of guidance loops to accommodate unscheduled changes in aircraft performance.

E. Dixon for a unique personal contribution to the completion of the AN/SPY-1 radar beamformer waveguide assembly, in terms of both technical performance and timely completion.

Inc. He succeeds **Ramon H. Aires** who has been assigned full responsibility for two major programs in the RCA Division.

With Autonetics Mr. Corey was responsible for providing technical direction in such areas as navigation, communications, electronic warfare, systems avionics, digital computers, electro-optical, radar and sonar systems. Previously he was B-1 Proposal Program Manager, Deputy Program Manager for the F-15 Program, and F-111 Avionics Systems Program Manager, among other assignments with Autonetics. During 1957-64, Mr. Corey was with Nortronics, including two years as Director of Engineering at Nortronics Electronic Systems and Equipment Division. In addition he held engineering management positions on various space, missile and aircraft programs in which the company was involved. Mr. Corey was with Chance Vought for the five preceding years where he worked as an engineer and engineering supervisor in several missile and fighter aircraft programs.

Mr. Corey received the BSEE from Carnegie Institute of Technology and has completed course work for a master's degree at Southern Methodist University. During World War II he was with the Army Signal Corps and became a rated Army Aviator in 1951 when recalled to active duty during the Korean conflict. Mr. Corey is a member of the IEEE, American Association for the Advancement of Science, the Army Ordnance Association and Eta Kappa Nu.

J. Grabowski for outstanding technical contributions in the redesign of the TRADEX dual frequency L/S band antenna feed system.

D. Olivieri for his continuing contributions in the area of mechanical design studies related to solid-state transmit-receive module development.

D. V. Wylde for his demonstrated systems engineering excellence and ingenuity in helping M&SR develop a level of expertise required for a competitive position in the field of high energy laser devices.

L. O. Upton, Jr. for creativity and resourcefulness in developing high-density digital memory techniques employing MOS and PMOS devices, as well as an adaptive clutter-lock MTI cancellation system utilizing these techniques.

First Pratt Award presented to Goldsmith

The IEEE's first Haraden Pratt Award has been presented to **Alfred N. Goldsmith** in recognition of the more than 60 years he has devoted to the Institute and the electrical engineering profession. The new award, established in honor of Haraden Pratt, Director Emeritus of the Institute, will be given each year to a person performing an "outstanding service to the Institute."

Commenting on this year's presentation, IEEE President **Robert H. Tanner** said, "I know of no individual in our profession who better exemplifies the meaning and spirit of this award." He added that Dr. Goldsmith's service to IEEE "is matched by no other individual."

Dr. Goldsmith, a consulting engineer with a private practice, is an honorary vice president and senior technical consultant for RCA. From 1919 to 1951 he rose to vice president at RCA after holding such positions as Chief Broadcast Engineer and Director of Research. His career is studded with many technical contributions in the fields of radio, television, and motion pictures. He has also been active in biomedical engineering.

Dr. Goldsmith received the BS from the College of the City of New York in 1907 and the PhD from Columbia University in 1911. He has been associated with

C.C.N.Y. ever since his college days and holds life tenure as an associate professor of electrical engineering.

Dr. Goldsmith, who is 85, is a co-founder, Fellow, and Life Member of the IRE. He served as a Director ever since IRE's inception in 1912 and was President for one term and Secretary for ten years. In 1954 he was named Editor Emeritus, climaxing 41 years as the Institute's Editor. When IEEE was formed he was named Editor and Director Emeritus and the new Society and holds these appointments today.

A member or fellow in numerous engineering and scientific societies, Dr. Goldsmith is a former president of the Society of Motion Picture and Television Engineers and a former chairman of the board of the National Television Film Council.

He is the first holder of IRE's highest awards: the Founders Award and the Medal of Honor. His other honors include the Modern Pioneers Award from the National Association of Manufacturers, the Townsend Harris Medal from C.C.N.Y., and the Medal Award of the Television Broadcasters Association.

He is an honorary member of the New York Medico-Surgical Society and an honorary fellow of the International College of Surgeons.



President Tanner (left) presents Alfred N. Goldsmith with Haraden Pratt Award.



Higgs is TPA for Missile and Surface Radar

Donald R. Higgs has been appointed Technical Publications Administrator for the Missile and Surface Radar Division at Moorestown, New Jersey. In this capacity, Mr. Higgs is responsible for the review and approval of technical papers; for coordinating the technical reporting program; and for promoting the preparation of papers for the *RCA Engineer* and other journals, both internal and external.

Mr. Higgs joined RCA in 1960 as an engineer-writer on the Ballistic Missile Early Warning System program and spent three years on special assignment in the United Kingdom. He has been associated with proposals and technical reports since his return to Moorestown early in 1964. He was appointed Leader of the Contract Reports and Proposals organization in 1966, with overall responsibility for reports and proposals as well as publication production support. In September 1972 he assumed his present position of Manager, Technical Communication within the Engineering Department.

Prior to joining RCA, Mr. Higgs served five years as associate editor of a corporate technical journal. He received the BS from the U.S. Naval Academy in 1951; he has taken graduate work at the Polytechnic Institute of Brooklyn and has been active as an instructor in Effective Written Communications in the M&SR After Hours Study Program. He also served two years on the M&SR Chief Engineer's Technical Excellence Committee, including a one year term as Chairman.

Harvard and M.I.T. name first David Sarnoff professors in management of technology

Grants totaling \$2 million to endow two professorships—one at the Harvard Business School and one at the Sloan School of Management at the Massachusetts Institute of Technology—will be made by RCA as a tribute to David Sarnoff, long-time chairman of RCA, who died last December. The holders of the David Sarnoff professorship will collaborate in a

Contents

An Experimental Solid-State TV Camera Using a 32 x 44 Element Charge-Transfer Bucket-Brigade Sensor W. S. Pike | M. G. Kovac
F. V. Shallcross | P. K. Weimer

The Silicon Return-Beam Vidicon—A High-Resolution Camera Tube R. W. Engstrom | J. H. Sternberg

An Experimental Study of High-Efficiency GaP:N Green-Light-Emitting Diodes I. Ladany | H. Kressel

Non-Destructive Sheet-Resistivity Measurements with Two-Point Probes J. L. Vossen

Broad-Band Acousto-Optic Deflectors Using Sonic Gratings for First-Order Beam Steering G. A. Alphonse

The *RCA Review* is published quarterly. Copies are available in all PCA libraries. Subscription rates are as follows (rates are discounted 20% for RCA employees)

	DOMESTIC	FOREIGN
1-year.....	\$6.00	\$6.40
2-year.....	10.50	11.30
3-year.....	13.50	14.70

joint program of teaching and research in the management of modern technology.

Announcement of the joint program was made by President **Derek C. Bok** of Harvard, President **Jerome B. Wiesner** of M.I.T., and **Robert W. Sarnoff**, Chairman and Chief Executive Officer of RCA. Also present for the announcement were Dean **Lawrence E. Fouraker** of the Harvard Business School, Dean **William F. Pounds** of the M.I.T. Sloan School of Management and the first two professors to be named to the David Sarnoff Chairs—**Dr. Richard S. Rosenbloom** of the Harvard Business School and **Dr. Donald G. Marquis** of M.I.T.'s Sloan School of Management.

The David Sarnoff Program on the Management of Technology will be jointly conducted by the two professional schools. It will include, besides an endowed chair in each school, a joint seminar open to students of both schools. The seminar will mark the first such cooperative teaching venture undertaken by the business and management schools.

Professor Rosenbloom, an authority on the management implications of social and technological change, is the Director of the Doctoral Program of the Harvard Business School. He was an active participant in Harvard's Program on Technology and Society. He is co-author of two recent books: *Technology and Information Transfer* and *New Tools for Urban Management*.

Professor Marquis, a noted psychologist who has been Professor of Organizational Psychology and Management at M.I.T., is the former chairman of psychology departments at Yale and the University of Michigan. Since 1961, he has headed M.I.T.'s Research Program on Management of Science and Technology. His

books include *Factors in the Transfer of Technology* (co-editor) and *Successful Industrial Innovations* (co-author).

The David Sarnoff Program is being launched with grants of \$100,000 each to the Harvard Business School and to the Sloan School of Management at M.I.T. during the current academic year. Thereafter, annual grants of \$100,000 will be made to each school until the David Sarnoff Professorships are fully endowed at a total of \$1 million apiece.

President Wiesner, speaking in behalf of M.I.T., paid tribute to the late General Sarnoff as a man who had "the vision to anticipate the practical potentialities inherent in new technology, the strength to build and lead a great modern organization without losing the capacity to foster continuing scientific and technical innovation, the skill to combine a variety of technical resources to form new systems of unprecedented technical competence and productivity, and an understanding of the larger social role which science must play in an advanced society and of the special responsibilities thus implied."

"I was privileged to know David Sarnoff," President Wiesner added, "and his life and philosophy exemplified the essential qualities of industrial and professional leadership which in three quarters of a century have brought technology's promise so rapidly into reality."

"These qualities should provide the basis for a program of teaching and research on the management of technology. They relate to the central educational concerns of the assessment of technological processes and transfer, the management of innovation, the creation of complex yet reliable systems, and the interaction of technology, business and society."

Robert Sarnoff explained why he believed the two schools are eminently qualified to undertake a broad and in-depth look at the management of technology.

"M.I.T.'s expertise in studying the processes involved in change and Harvard's in studying organizational patterns can be intermeshed to form a unique combination of existing skills and interests. These qualities have the momentum of years of rigorous intellectual exploration and on-going research and can focus on this topic of interest to the faculties of both institutions."

The program was recommended by RCA's Educational Aid Committee after studying some twenty different commemorative proposals submitted by leading American educational institutions.

An advisory committee will be appointed to provide counsel for the Sarnoff professors, who will be joint directors of the program. Committee members will be charged with keeping the program related to critical problems, and for ensuring that the project's resources, human and monetary, are used most effectively.

Editorial Representatives

The Editorial Representative in your group is the one you should contact in scheduling technical papers and announcements of your professional activities.

Government and Commercial Systems

Aerospace Systems Division

P. P. NESBEDA* Engineering, Burlington, Mass.
J. J. O'DONNELL Industry Systems, Burlington, Mass.

Electromagnetic and Aviation Systems Division

C. S. METCHETTE* Engineering, Van Nuys, Calif.
J. McDONOUGH Engineering, Van Nuys, Calif.

Astro-Electronics Division

I. M. SEIDEMAN* Engineering, Princeton, N.J.
S. WEISBERGER Advanced Development and Research, Princeton, N.J.

Missile & Surface Radar Division

D. R. HIGGS* Engineering, Moorestown, N.J.

Government Engineering

M. G. PIETZ* Advanced Technology Laboratories, Camden, N.J.
J. E. FRIEDMAN Advanced Technology Laboratories, Camden, N.J.
J. L. KRAGER Central Engineering, Camden, N.J.

Government Plans and Systems Development

E. J. PODELL* Engineering Information and Communications, Camden, N.J.

Communications Systems Division Commercial Systems

R. N. HURST* Studio, Recording, & Scientific Equip. Engineering, Camden, N.J.
A. M. MISSEDA Advanced Development, Meadow Lands, Pa.
R. E. WINN Broadcast Transmitter & Antenna Eng., Gilbertsboro, N.J.

Government Communications Systems

A. LIGUORI* Engineering, Camden, N.J.

Palm Beach Division

P. M. WOOLLEY* Palm Beach Product Laboratory, Palm Beach Gardens, Fla.

Research and Engineering

Laboratories

C. W. SALL* Research, Princeton, N.J.
I. H. KALISH Solid State Technology Center, Somerville, N.J.
M. R. SHERMAN Solid State Technology Center, Somerville, N.J.

Electronic Components

Entertainment Tube Division

C. A. MEYER* Chairman, Editorial Board, Harrison, N.J.
J. KOFF Receiving Tube Operations, Woodbridge, N.J.
J. H. LIPSCOMBE Television Picture Tube Operations, Marion, Ind.
E. K. MADENFORD Television Picture Tube Operations, Lancaster, Pa.

Industrial Tube Division

J. M. FORMAN Industrial Tube Operations, Lancaster, Pa.
H. J. WOLKSTEIN Microwave Tube Operations, Harrison, N.J.

Solid State Division

E. M. McELWEE* Chairman, Editorial Board, Somerville, N.J.
J. DIMAURO Solid State Division, Mountaintop, Pa.
S. SILVERSTEIN Power Transistors, Somerville, N.J.
E. M. TROY Integrated Circuits, Somerville, N.J.
J. D. YOUNG Solid State Division, Findlay, Ohio

Consumer Electronics

C. HOYT* Chairman, Editorial Board, Indianapolis, Ind.
R. BUTH Engineering, Indianapolis, Ind.
R. C. GRAHAM Audio Products Engineering, Indianapolis, Ind.
F. HOLT Advanced Development, Indianapolis, Ind.
E. JANSON Black and White TV Engineering, Indianapolis, Ind.
W. LIEDERBACH Ceramic Circuits Engineering, Rockville, Ind.
J. STARK Color TV Engineering, Indianapolis, Ind.
P. HUANG Engineering, RCA Taiwan Ltd., Taipei, Taiwan

Services

RCA Service Company

M. G. GANDER* Consumer Products Administration, Cherry Hill, N.J.
W. W. COOK Consumer Products Service Dept., Cherry Hill, N.J.
R. M. DOMBROSKY Technical Support, Cherry Hill, N.J.
R. I. COGHILL Missile Test Project, Cape Kennedy, Fla.

Parts and Accessories

C. C. REARICK* Product Development Engineering, Deptford, N.J.

RCA Global Communications, Inc.

W. S. LEIS* RCA Global Communications, Inc., New York, N.Y.
J. D. SELLERS RCA Alaska Communications, Inc., Anchorage, Alaska

National Broadcasting Company, Inc.

W. A. HOWARD* Staff Eng., New York, N.Y.

RCA Records

M. L. WHITEHURST Record Eng., Indianapolis, Ind.

RCA International Division

C. A. PASSAVANT* New York, N.Y.

RCA Ltd.

W. A. CHISHOLM* Research & Eng., Montreal, Canada

Patents and Licensing

J. EPSTEIN Staff Services, Princeton, N.J.

* Technical Publication Administrators listed above are responsible for review and approval of papers and presentations.

RCA Engineer

A TECHNICAL JOURNAL PUBLISHED BY CORPORATE ENGINEERING SERVICES
"BY AND FOR THE RCA ENGINEER"

Form No. RE-18-3

Printed in U.S.A.